2020 • 24 • 4

Print ISSN 2500-0462
Online ISSN 2500-3259

Научный рецензируемый журнал

ВАВИЛОВСКИЙ ЖУРНАЛ ГЕНЕТИКИ И СЕЛЕКЦИИ

Основан в 1997 г.
Периодичность 8 выпусков в год
DOI 10.18699/VJ20.624

Учредители

Федеральное государственное бюджетное научное учреждение «Федеральный исследовательский центр Институт цитологии и генетики Сибирского отделения Российской академии наук»

Межрегиональная общественная организация Вавиловское общество генетиков и селекционеров

Сибирское отделение Российской академии наук

2020 • 24 • 4

Print ISSN 2500-0462
Online ISSN 2500-3259

Scientific Peer Reviewed Journal

VAVILOV JOURNAL OF GENETICS AND BREEDING

VAVILOVSKII ZHURNAL GENETIKI I SELEKTSII

Founded in 1997
Published 8 times annually
DOI 10.18699/VJ20.624

Founders
Federal State Budget Scientific Institution "The Federal Research Center Institute of Cytology and Genetics of Siberian Branch of the Russian Academy of Sciences"
The Vavilov Society of Geneticists and Breeders
Siberian Branch of the Russian Academy of Sciences

ВАВИЛОВСКИЙ ЖУРНАЛ ГЕНЕТИКИ И СЕЛЕКЦИИ

СОДЕРЖАНИЕ • 2020 • 24 • 4

VAVILOV JOURNAL OF GENETICS AND BREEDING

CONTENTS • 2020 • 24 • 4

Вавиловский журнал генетики и селекции. 2020;24(4):331-339
DOI 10.18699/VJ20.625

A high coverage reference transcriptome assembly of pea (*Pisum sativum* L.) mycorrhizal roots

A.M. Afonin[1] ✉, I.V. Leppyanen[1], O.A. Kulaeva[1], O.Y. Shtark[1], I.A. Tikhonovich[1, 2], E.A. Dolgikh[1], V.A. Zhukov[1]

[1] All-Russia Research Institute for Agricultural Microbiology, Pushkin, St. Petersburg, Russia
[2] Faculty of Biology, St. Petersburg State University, St. Petersburg, Russia
✉ e-mail: afoninalexeym@gmail.com

Abstract. Arbuscular mycorrhiza (AM) is an ancient mutualistic symbiosis formed by 80–90 % of land plant species with the obligatorily biotrophic fungi that belong to the phylum Glomeromycota. This symbiosis is mutually beneficial, as AM fungi feed on plant photosynthesis products, in turn improving the efficiency of nutrient uptake from the environment. The garden pea (*Pisum sativum* L.), a widely cultivated crop and an important model for genetics, is capable of forming triple symbiotic systems consisting of the plant, AM fungi and nodule bacteria. As transcriptomic and proteomic approaches are being implemented for studying the mutualistic symbioses of pea, a need for a reference transcriptome of genes expressed under these specific conditions for increasing the resolution and the accuracy of other methods arose. Numerous transcriptome assemblies constructed for pea did not include mycorrhizal roots, hence the aim of the study to construct a reference transcriptome assembly of pea mycorrhizal roots. The combined transcriptome of mycorrhizal roots of *Pisum sativum* cv. Frisson inoculated with *Rhizophagus irregularis* BEG144 was investigated, and for both the organisms independent transcriptomes were assembled (coverage 177x for pea and 45x for fungus). Genes specific to mycorrhizal roots were found in the assembly, their expression patterns were examined with qPCR on two pea cultivars, Frisson and Finale. The gene expression depended on the inoculation stage and on the pea cultivar. The investigated genes may serve as markers for early stages of inoculation in genetically diverse pea cultivars.
Key words: RNAseq; transcriptomics; arbuscular mycorrhiza; garden pea.

For citation: Afonin A.M., Leppyanen I.V., Kulaeva O.A., Shtark O.Y., Tikhonovich I.A., Dolgikh E.A., Zhukov V.A. A high coverage reference transcriptome assembly of pea (*Pisum sativum* L.) mycorrhizal roots. *Vavilovskii Zhurnal Genetiki i Selektsii = Vavilov Journal of Genetics and Breeding*. 2020;24(4):331-339. DOI 10.18699/VJ20.625

Референсный транскриптом микоризованных корней гороха посевного (*Pisum sativum* L.) с высоким покрытием

А.М. Афонин[1] ✉, И.В. Леппянен[1], О.А. Кулаева[1], О.Ю. Штарк[1], И.А. Тихонович[1, 2], Е.А. Долгих[1], В.А. Жуков[1]

[1] Всероссийский научно-исследовательский институт сельскохозяйственной микробиологии, г. Пушкин, Санкт-Петербург, Россия
[2] Санкт-Петербургский государственный университет, факультет биологии, Санкт-Петербург, Россия
✉ e-mail: afoninalexeym@gmail.com

Аннотация. Арбускулярная микориза (АМ) – это древний мутуалистический симбиоз, который образуют 80–90 % видов наземных растений с облигатно биотрофными грибами, принадлежащими к филе Glomeromycota. Этот симбиоз является взаимовыгодным, поскольку грибы АМ питаются продуктами фотосинтеза растений, в свою очередь повышая эффективность поглощения питательных веществ растением из окружающей среды. Горох (*Pisum sativum* L.), широко распространенная сельскохозяйственная культура и важный модельный объект генетики, способен образовывать тройные симбиотические системы, состоящие из растения, грибов АМ и клубеньковых бактерий. По мере распространения транскриптомных и протеомных подходов в изучении мутуалистических симбиозов гороха, для повышения разрешающей способности и точности других методов возникла необходимость в референсном транскриптоме, т. е. в знании последовательностей генов, экспрессирующихся в различных экспериментальных условиях. Многочисленные транскриптомные сборки, сконструированные для гороха, не включали микоризованные корни, поэтому целью данного исследования было создание референсной транскриптомной сборки микоризованных корней. Было проведено глубокое РНК-секвенирование транскриптома микоризованных корней *Pisum sativum* сорта Frisson, инокулированных *Rhizophagus irregularis* BEG144, и для каждого из организмов получены независимые транскриптомные сборки (покрытие 177х для транскриптома гороха и 45х для транскриптома гриба). Качество сборки транскриптома гороха оценено путем сравнения с уже имеющимися сборками транскриптомов других тканей. Для дополнительной оценки качества сборки, у двух сортов гороха (Frisson и Finale) с помощью qPCR проведен анализ экспрессии генов, специфичных для микоризованных корней, последовательности которых были найдены в созданной сборке. Исследованные гены могут служить маркерами ранних стадий развития арбускулярной микоризы у генетически разнообразных сортов гороха.
Ключевые слова: РНК-секвенирование; транскриптомика; арбускулярная микориза; горох посевной.

Introduction

Plants are able to establish mutualistic association with the arbuscular mycorrhizal (AM) fungi that improve the efficiency of nutrient uptake from the environment. About 80–90 % of all land plant species may form mutually beneficial symbiosis with the obligatorily biotrophic AM fungi that belong to the phylum Glomeromycota (Kaschuk, 2009; Alizadeh, 2011; Tisserant et al., 2012; Gutjahr, Parniske, 2013; Manck-Götzenberger, Requena, 2016). The AM facilitates plant nutrition and increases plant tolerance to biotic and abiotic stresses, when AM fungi feed on photosynthesis products and utilize a considerable proportion of the assimilated carbon (Siddiqui et al., 2008; Solaiman et al., 2014).

The garden pea (*Pisum sativum* L.) is a widely cultivated crop plant and the first model object of genetics. Similarly to other legume plants belonging to the Fabaceae family, it is capable of forming triple symbiotic systems consisting of plant, AM fungi and nodule bacteria (Tikhonovich et al., 2015). The formation of symbioses increases yield and plant fitness in general (Jacobi et al., 1999; Borisov et al., 2004; Shtark et al., 2006; Zhukov et al., 2019), although the effect of inoculation is often dependent on experimental conditions and plant genotype (Shtark et al., 2006; Zhukov et al., 2017; Mamontova et al., 2019). During the last decade, transcriptomic and proteomic approaches had been implemented for studying the mutualistic symbioses of pea, which implied the need for a reference genomic or transcriptomic sequences required for proper annotation of transcripts/proteins under analysis. Although numerous transcriptome assemblies were constructed (Franssen et al., 2011; Alves-Carvalho et al., 2015; Sudheesh et al., 2015; Zhukov et al., 2015; Kerr et al., 2017), no samples containing mycorrhizal roots had been analysed. Moreover, the only available genomic sequence (Kreplak et al., 2019) is far from ideal and lacks sequences of many important genes (for example, short peptides of NCR and defensin families).

Thus, the present work aimed at obtaining the reference transcriptome assembly of pea mycorrhizal roots using RNA-seq. In order to validate the constructed assembly, which is destined for further analysis of the mycorrhization in pea with use of transcriptomics and/or proteomics, we designed the set of primers for qPCR expression analysis and successfully quantitated the expression level of 10 AM-specific genes in mycorrhizal roots of two pea cultivars.

Materials and methods

Plants and microorganisms used. The wild-type *Pisum sativum* L. cultivars Frisson (= JI2491 (Duc, Messager, 1989)) and Finale (= JI2678 (Engvild, 1987)) were used in this study. The fungal isolate *Rhizophagus irregularis* BEG144 was provided by the International Bank for the Glomeromycota (Dijon, France) as a substrate-root based inoculum for leek (*Allium porrum* L.) pot cultures. It was used to obtain nurse pots of chives (*Allium schoenoprasum* L.) for the *R. irregularis*-inoculated pea plants (according to (Shtark et al., 2016)).

Plant growth conditions and root sampling. In order to provide an efficient inoculation of *P. sativum* plants, nurse pots with established mycorrhiza were used. These were 300-ml ceramic flower pots filled with opoka-rock mineral substrate, which is silica rich marl (Krasnodar, Russia), supplemented with 1 $g \cdot L^{-1}$ calcium orthophosphate. Prior to nurse pots preparation, pots with substrate were sterilized by autoclaving for 60 min at 134 °C and 0.22 MPa. Procedures for the chive-based nurse pots are described by (Demchenko et al., 2004; Shtark et al., 2016).

Seeds of *P. sativum* were surface-sterilised for 10 minutes with 98 % sulphuric acid, rinsed with sterile deionised water five times, and then germinated for 3 days at 27 °C in the dark on sterile vermiculite in Petri dishes with 30 ml of water added to each one. Three *P. sativum* seedlings of similar size were planted into each nurse pot around a mycorrhizal chive plant. Plants were grown in a growth chamber (model VB 1514, Vötsch, Germany) under the following conditions: day/night, 16/8 h; temperature, 24/22 °C; relative humidity, 75; irradiation 10000 lux and were supplemented once a week with 1/2-x Hoagland's solution (Hoagland, Arnon, 1950) without phosphate (50 mL per pot), and watered as needed.

After several days of co-cultivation with chives in nurse pots *P. sativum* root samples were collected for transcriptome analyses and RT-qPCR (see relevant sections) and immediately frozen in liquid nitrogen and stored at –80 °C. Frozen root samples were ground in liquid nitrogen using pestle and mortar. Before collecting plant material for those analyses, several lateral roots (15 cm length) from each pea root system were randomly selected and frozen at –20 °C and then subjected to analysis of AM development as described by Shtark and colleagues (Shtark et al., 2016). The parameters of root colonization of these pea plants estimated according to (Trouvelot et al., 1986) were: *M %* (intensity of internal colonization of the root system), and *a %* (arbuscule abundance in mycorrhizal root fragments).

For transcriptome sequencing root samples were collected after 25 days of co-cultivation with chives. Three plants of cv. Frisson with $M\,\% = 68.6 \pm 2.6$, and $a\,\% = 50.9 \pm 1.2$ (this level of root colonization is common with this genotype (Morandi et al., 2000; Grunwald et al., 2004)), were chosen for the transcriptome analysis. The whole root systems were cut off directly below the cotyledons and frozen in liquid nitrogen in 50 mL Falcon tubes.

For RT-qPCR assays root samples were collected after 7, 14 or 28 days of co-cultivation with chives. Root samples of uninoculated plants grown under the same conditions during the same time periods were used as a control. Lateral roots were used, in which tips 1 cm long were removed. The collected samples were frozen in 2 mL Eppendorf™ tubes. The AM development was analysed at two time points (after 14 and 28 days of co-cultivation with chives). The parameters of cv. Finale root colonization were: $M\,\% = 17.5 \pm 2.3$, and 35.0 ± 4.7, respectively; $a\,\% = 29.4 \pm 5.7$, and 36.5 ± 5.7, respectively. This level of colonization is common with cv. Finale (Shtark et al., 2016; Leppyanen et al., 2018). The parameters of cv. Frisson root colonization were: $M\,\% = 44.6 \pm 4.7$, and 68.1 ± 5.4, respectively; $a\,\% = 62.6 \pm 3.5$, and 65.3 ± 4.4, respectively. This is also consistent with previous investigations; in particular it was shown that internal AM colonization and arbuscule development reaches higher values in cv. Frisson than in cv. Finale (Morandi et al., 2000; Grunwald et al., 2004).

Transcriptome sequencing. The RNA extraction, library construction and the sequencing on an Illumina 2500 HiSeq platform was carried out by GenXPro GmbH (Frankfurt-am-Main, Germany).

Read preparation. In order to remove possible human and bacterial contaminants from the raw data we used the method, devised by dr. Brian Bushnell and described in *removeHuman* tool from the *BBTools suite* (Bushnell, 2014). Additionally, reads belonging to bacteria and viruses were discarded using the databases provided by the author of the package. In order to separate fungal reads from those of pea, we first prepared the genome assembly of *Rhizophagus irregularis* strain DAOM197198 from (Tisserant et al., 2013) as described by the author of the bbmap package. The areas of genome, containing multiple tandem short k-mers, as well as windows of low entropy sequences, which were calculated using pentamer frequencies, were masked using the bbmask.sh script. In order to exclude the sequences, common between the *R. irregularis* genome and plant genomes, all the available non-draft plant genomes from the Phytozome V12 (Goodstein et al., 2012) were masked for repetitive sequences, and then used to exclude all the non-specific parts of the DAOM197198 genome as described for the bbmask.sh script. The resulting masked assembly was used for read mapping using the bbmap.sh script. All the mapped reads were considered to belong to the fungus, all the non-mapped reads were considered plant reads. The transcriptome completeness and assembly quality were assessed using BUSCO algorithm (Simão et al., 2015). Blast search was used for the comparison of the various transcriptomes.

Transcriptome assembly. The reads belonging to *Pisum* were then assembled using *Trinity* assembler (v2.6.6) (Grabherr et al., 2011) with default parameters, *rnaSPAdes* (v3.11.1) (Bankevich et al., 2012). *Corset/Lace* pipeline was used to assemble the SuperTranscriptome (Davidson et al., 2017).

The transcriptome shotgun assemblies (TSAs) from the following bioprojects were downloaded from the NCBI for comparison to current assembly: PRJNA277074 – cv. Kaspa (Sudheesh et al., 2015), PRJNA277076 – cv. Parafield (Sudheesh et al., 2015), PRJNA308776 – cv. Torsdag (Kerr et al., 2017). The assembly of the nodule transcriptome of cv. SGE (accession GDTM00000000.1) and the assembly of roots of cv. SGE (accession GDTL00000000.1) were also downloaded from the NCBI (Zhukov et al., 2015). Additionally, the assemblies from cv. Caméor (Alves-Carvalho et al., 2015) and cv. Little Marvel (Franssen et al., 2011) were downloaded from supplementary files for the respective articles. The CDS sequences from the *M. truncatula* v4.0v2 genome were used for benchmarking the assembled transcriptomes (Young et al., 2011).

The following accessions were downloaded from the NCBI in order to identify the *R. irregularis* strain closest to BEG144: GCA_000439145.3, GCA_000597565.1, GCA_000597585.1, GCA_000597605.1, GCA_000597625.1, GCA_000597645.1, GCA_000597665.1, GCA_000597685.1, GCA_001593125.1, GCA_001593145.1, GCA_001593155.1, GCA_001593205.1, GCA_002897155.1, GCA_003833045.1, GCA_003833115.1. The reads binned as belonging to the fungi were assembled de-novo using the *Trinity* assembler. *Cufflinks* (v2.2.1) (Trapnell et al., 2010) was used to build a genome-guided assembly.

Annotation. CDS discovery for both the organisms was performed using the *transdecoder* (v5.2.0) algorithm (https://github.com/TransDecoder/TransDecoder/). Both the hmm and the blast homology search options were used, according to the manual. The annotation was performed using the EggNOG 5.0 database using the *eggNOG-mapper* (v2.0.1) (Huerta-Cepas et al., 2016).

In order to determine the best overall assembly, the three transcriptomes were evaluated using the *BUSCO* tool (Simão et al., 2015).

Table 1. Constructed primers used for qPCR

Name	Sequence, 5′–3′
PsUbiquitin-F	ATGCAGATYTTTGTGAAGAC
PsUbiquitin-R	ACCACCACGRAGACGGAG
PsActin-F	CTCAGCACCTTCCAGCAGATGTG
PsActin-R	CTTCTTATCCATGGCAACATAGTTC
*Ps*AJ308147-F	TTAGGGGCTAGAAAATTTGGCATC
*Ps*AJ308147-R	AACATGGACCCTCTCCATTCAAC
*Ps*AJ308164-F	AAAGAAACTGAAAAGTTTGTGAGTATTC
*Ps*AJ308164-R	TCACTTCATTGCTTTTGGAGGC
*Ps*AJ308156-F	CAAAGCGTCTCTGTCACATCCG
*Ps*AJ308156-R	ATCTTCCTCATCAAGACCAGCACC
*Ps*AJ308170-F	GAAGGGAAGTAGGAAATGAAAAGTTG
*Ps*AJ308170-R	CCAGAAACTAGTCTCCAAACACTCAC
PsMAPK-F	TGCACTGGCACACCCTTACTTG
PsMAPK-R	CTGCTGGTACTCGGGGTTAAATG
PsPR6-F	CCCGTGTGGTTGACCTCATTG
PsPR6-R	GATCATAGTGTGGAAACTTGATTAGTACAG
PsRAD1-F	GAAAAGACCAACCGTAACTATCCC
PsRAD1-R	GAACTAGTCTCATTCCATCAGCACA
PsVPN-F	ATAGCAGCAGCCAATGGAGATG
PsVPN-R	CCACCACTTTCCAAAACCTTT

Note: Melting point (Tm) for every primer was 54 °C.

RT-qPCR. Total RNA was isolated using the TriZol reagent (ThermoScientific, USA). cDNA synthesis was performed with reverse transcriptase (ThermoScientific, USA) and oligo-dT primers (Evrogen, Russia; www.evrogen.com). RT-qPCR was performed on the CFX-96 C1000 thermocycler (Bio-Rad Laboratories, USA) with the double-stranded DNA dye SYBR Green (Bio-Rad Laboratories, USA). The data was analysed using the 2-ΔΔCt method (Livak, Schmittgen, 2001). PCR amplification was confirmed with the dissociation curve method (55 to 95 °C). mRNA levels were normalised in relation to the ubiquitin and actin reference genes. Three biological replicates were analysed. The primers were constructed using the Vector NTI suite (Lu, 2004) (Table 1). The expression levels of the genes of interest (GOI) relative to the reference genes *Ubiquitin* and *Actin* were calculated for each cDNA sample using the CFX Manager™ software version 2.1 (BioRad Laboratories, USA). The expression levels of GOI were calculated as ratio of treated samples to control samples. Statistical analysis was conducted by SIGMAPLOT 13 (Systat Software, Inc., San Jose California, USA).

Results and discussion

In order to obtain a reference transcriptome of the mycorrhizal roots of *P. sativum*, the RNA from this tissue was sequenced on an Illumina 2500 sequencing platform.

A total of 120 mln pairs of reads with average length of 150 bp were obtained. After quality trimming 119 mln reads remained. Since we knew, that *R. irregularis* transcripts are present in the tissues, we decided to remove all possible contaminants (as described in the Materials and methods section). Additionally, we masked low complexity regions and repetitive elements from *R. irregularis* genome. Of the 119 mln remaining reads 6.7 mln (approximately 5 %) of the paired reads were mapped onto the masked *Rhizophagus* genome.

The resulting reads belonging to *P. sativum* were then assembled using two assemblers: *Trinity* with default parameters and *rnaSPAdes* with default parameters. Afterwards, with use of *Corset*/*Lace* pipeline, a SuperTranscripts assembly was constructed using these two assemblies comprising 94360 supertranscripts (Table 2).

Transcriptome evaluation

In order to determine the best overall assembly, the three transcriptomes were evaluated using the *BUSCO* tool. Results of the analysis are presented in the Table 3.

As BUSCO tends to favor the number of transcripts, the Trinity assembly scored higher than the SuperTranscripts assembly, despite the latter containing the former. The other comparisons, such as N50 and the duplication numbers speak in favor of the SuperTranscripts assembly.

The resulting SuperTranscripts assembly, as well as the other two assemblies, the table of relation between the assemblies and the full results of are available at the (https://cloud.arriam.ru/s/RKD67CZak58BzzN).

Since the SuperTranscript assembly contains the two other assemblies, it was used to compare to all available pea transcriptome assemblies. The comparison was performed using the BLASTN algorithm (e-value < 10^{-10}, identity > 90 %, query coverage > 90 %), the results are presented in the Table 4.

The low numbers of query matches in the case of the cv. Caméor is most probably due to the fact, that the transcriptome in this study represents a single, rather than multiple, plant tissues.

All the available pea transcriptomes were compared to the latest *Medicago truncatula* Gaertn. transcriptome in order to determine the fullness of the transcriptomes and the number of novel transcripts (Table 5). Our assembly had an almost identical number of transcripts, homologous to those of *M. truncatula* as the more diverse transcriptomes of cv. Kaspa, cv. Parafield, and cv. Caméor, and also showed a large number of previously undiscovered transcripts.

Determining the specificity of inoculation

In order to check for possible rhizobial contamination and formation of nodules possibly missed during sample preparation we decided to search for nodule specific proteins. Since the expression counts for a single RNAseq analysis cannot be considered statistically significant, we chose instead to search for contigs, encoding proteins, specific to nodules – NCR peptides (Zorin et al., 2019). Using the approach from that article, we found only 28 genes of the NCR gene family in the newly assembled transcriptome, compared to 40 in the cv. SGE root tips and 425 in the cv. SGE nodules. Therefore, it is reasonable to assume that the plants were not accidentally infected with rhizobia, and thus are representative of a fungal monoinoculation.

Table 2. Comparison of transcriptome assemblies' parameters

Parameters	SPAdes	Trinity	SuperTranscripts
Identified "genes"	136817	71149	94360
Identified isoforms	139631	182345	190210
Longest isoform	16300	15688	16300
Average isoform length	812	1110	1277
Transcript n50	884	2168	4357

Note: The estimated coverage for the transcriptome was 177x.

Table 3. The comparison of the transcriptome assemblies using the BUSCO tool

Transcriptome assembly	Complete and single-copy	Complete and duplicated	Fragmented	Missing
SPAdes	852	284	119	185
SuperTranscripts	454	707	109	170
Trinity	597	665	63	115

Table 4. The results of comparison of the SuperTranscripts assembly to the other available transcriptome assemblies

Transcriptome	# of query matches	# of SuperTranscripts matches
cv. Kaspa	68210 (54 %)	51787 (54 %)
cv. Parafield	73966 (50 %)	52932 (56 %)
cv. Caméor	26734 (51 %)	42059 (44 %)
cv. SGE nodules	45081 (77 %)	40290 (42 %)
cv. SGE roots	32228 (86 %)	34739 (36 %)
cv. Torsdag	76244 (39 %)	41683 (43 %)
cv. Little Marvel	48964 (60 %)	25982 (27 %)

Table 5. The results of comparison of the pea transcriptome assemblies (query) to the *M. truncatula* transcriptome (reference)

Transcriptome	# of reference matches	# of query matches
cv. Kaspa	43772 (76 %)	62335 (49 %)
cv. Parafield	43931 (76 %)	67221 (46 %)
cv. Caméor	45004 (78 %)	35602 (68 %)
cv. SGE nodules	41639 (72 %)	40414 (69 %)
cv. SGE roots	39298 (68 %)	29188 (78 %)
cv. Torsdag	43914 (76 %)	117639 (60 %)
cv. Little Marvel	35048 (60 %)	59517 (73 %)
SuperTranscripts	44068 (76 %)	59029 (62 %)

Note: e-value < e^{-10}, query coverage > 80 %, identity > 60 %.

Table 6. The results of mapping of fungal reads onto the transcriptome assemblies of *R. irregularis* from the NCBI

The accession of *R. irregularis* genome assembly	The percentage of mapped reads
GCA_001593125.1 (A1)	84.99
GCA_000597645.1	82.73
GCA_000597665.1	73.00
GCA_000597685.1	70.37
GCA_001593205.1	69.84
GCA_003833045.1	68.33
GCA_001593145.1	66.08
GCA_002897155.1	65.93
GCA_001593155.1	65.02
GCA_003833115.1	62.08
GCA_000597625.1	61.37
GCA_000597605.1	47.71
GCA_000597565.1	44.23
GCA_000597585.1	37.80

Note: *BBmap.sh* tool was used to map the reads against the genomes.

Table 7. Comparison of *R. irregularis* transcriptome assemblies

Transcriptome assembler	Trinity	Cufflinks
Identified "genes"	17425	10488
Identified isoforms	28074	14561
Longest isoform	13072	13849
Average isoform length	1070.77	1451.65
Transcript n50	1861	1869

Novel transcripts of *Rhizophagus irregularis*

Since for now there is no published genome available for the strain BEG144 used in this study, we decided to determine the closest related strain in the NCBI database. To do this, we downloaded all the available *R. irregularis* genomes and mapped the filtered transcripts using bbmap.sh to the genomes. The best overall mapping was to the strain A1 of *R. irregularis* GCA_001593125.1 (registered bioproject url: https://www.ncbi.nlm.nih.gov/bioproject/PRJNA299202/). This genome was used for a genome-guided Cufflinks assembly. The mapping results are presented in the Table 6.

Genome guided Trinity assembly did not yield any assembled contigs, possibly due to the lower coverage of the fungal genome, so a de-novo assembly of the fungal transcriptome was performed. The results of the assemblies are present in the Table 7.

The likely protein-coding genes from the assemblies were identified by *transdecoder* (see Materials and methods section). The Cufflinks assembly contained 12036 (77.8 %) protein-coding genes, whereas the Trinity assembly contained 17909 (63.7 %). After comparing the assemblies with the blast algorithm we discovered that 8301 (68 %) of Cufflinks CDS-containing transcripts corresponded to 12036 (60.1 %) of CDS-containing transcripts of Trinity. The rest of the transcripts, unique to the Trinity assembly may represent the parts of genome different between the strain BEG144 and the strain used as the reference. The low coverage and the unavailability of the genome of the strain BEG144 make it harder to distinguish the real transcripts from the chimeric. The results, however, show the usability of proposed methods to assemble the transcriptomes of mixed samples, even in the absence of high-quality reference genomes.

RT-qPCR of AM-specific genes

In order to study the inoculation effects in detail and to monitor the AM development during the experiments, the set of marker genes with AM-specific expression pattern was required. In previous work by Grunwald et al. (2004), a set of 25 genes which were upregulated more than in 2.5 times in response to inoculation with AM fungus in roots of pea cultivar Finale was identified using suppressive subtractive hybridization. We selected eight of them for the present study and supplemented this list with the well-characterized mycorrhiza-related genes encoding the transcription factor RAD1 and the VAPYRIN protein for analysis (Pumplin et al., 2010; Murray et al., 2011; Park et al., 2015). In order to find the sequences of 10 AM-specific genes of cv. Frisson, a BLASTN search of corresponding genes was performed against the newly created SuperTranscripts transcriptome assembly. The accessions are presented in Table 8. We compared the RT-PCR expression

Table 8. Genes chosen according to (Grunwald et al., 2004) and their corresponding accessions in the SuperTranscripts assembly

Accession #	Encoded gene	SuperTranscripts	ID
AJ308129	Methallothionein	Cluster-40920.0	129
AJ308147	GDSL-motif lipase/acylhydrolase	Cluster-12403.0	147
AJ308148	MAP kinase	Cluster-38009.0	MAPK
AJ308156	Translation initiation factor 1α	Cluster-9362.0	156
AJ308158	Proteinase inhibitor PR6	Cluster-38215.1	PR6
AJ308163	Trypsin inhibitor	Cluster-56992.0	TI
AJ308164	Putative lipid-transfer protein	Cluster-57882.0	164
AJ308170	Polyphosphate inosite-binding protein	Cluster-48448.0	170
Medtr4g104020.1	Transcription factor RAD1	Cluster-11628.0	RAD1
Medtr6g027840.1	VAPYRIN	Cluster-42154.0	VPN

Note: "ID" column contains the chosen shorter names, used in the text and figures.

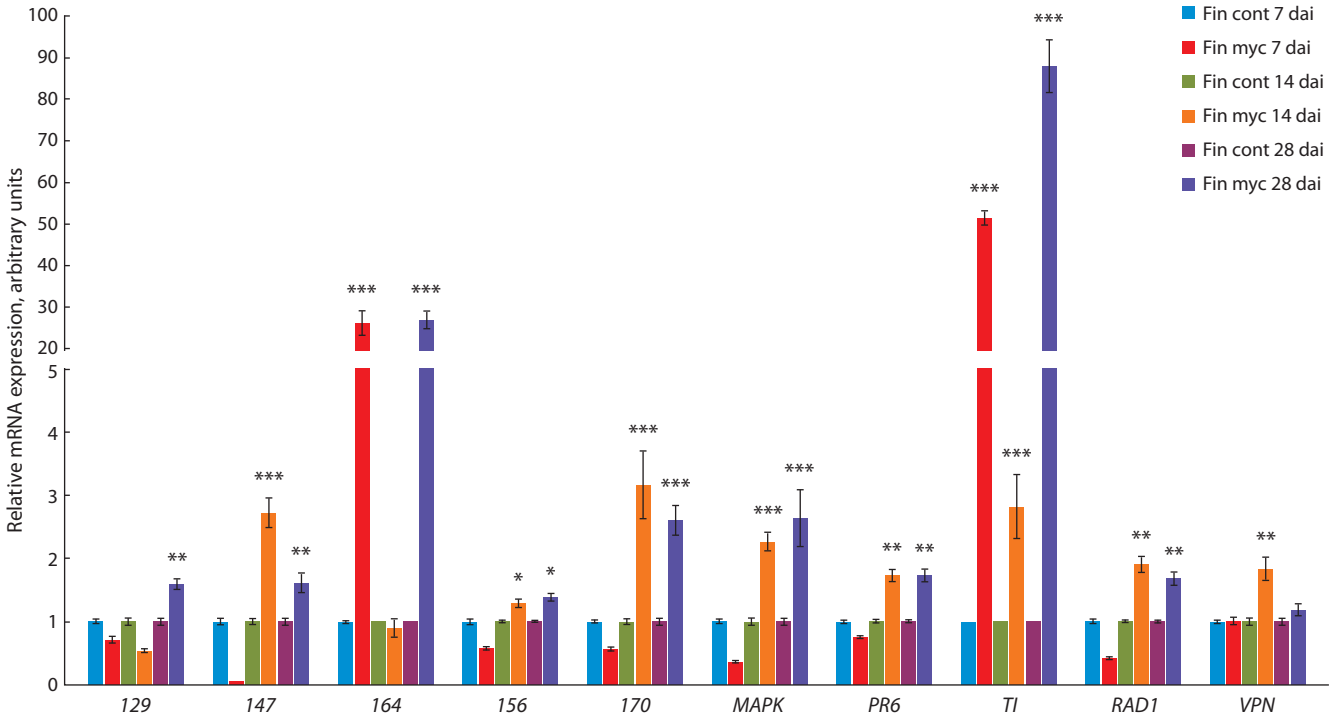

Fig. 1. Transcript levels of genes encoding markers of AM development in pea roots of cv. Finale infected with *R. irregularis* after 7, 14 and 28 days.

Here and in Figure 2: uninoculated plant roots were used as control (cont); the treatment was mycorrhization (myc). The relative expression was normalized against the constitutively expressed ubiquitin and actin genes. Values are means ± SEM of three technical repeats. The graphs show the results of one biological replication, representative of three biological independent experiments, the asterisks indicate the significant differences between control and treatment as analysed by Student's *t*-test ($^{***}p < 0.001$, $^{**}p < 0.01$, $^{*}p < 0.05$).

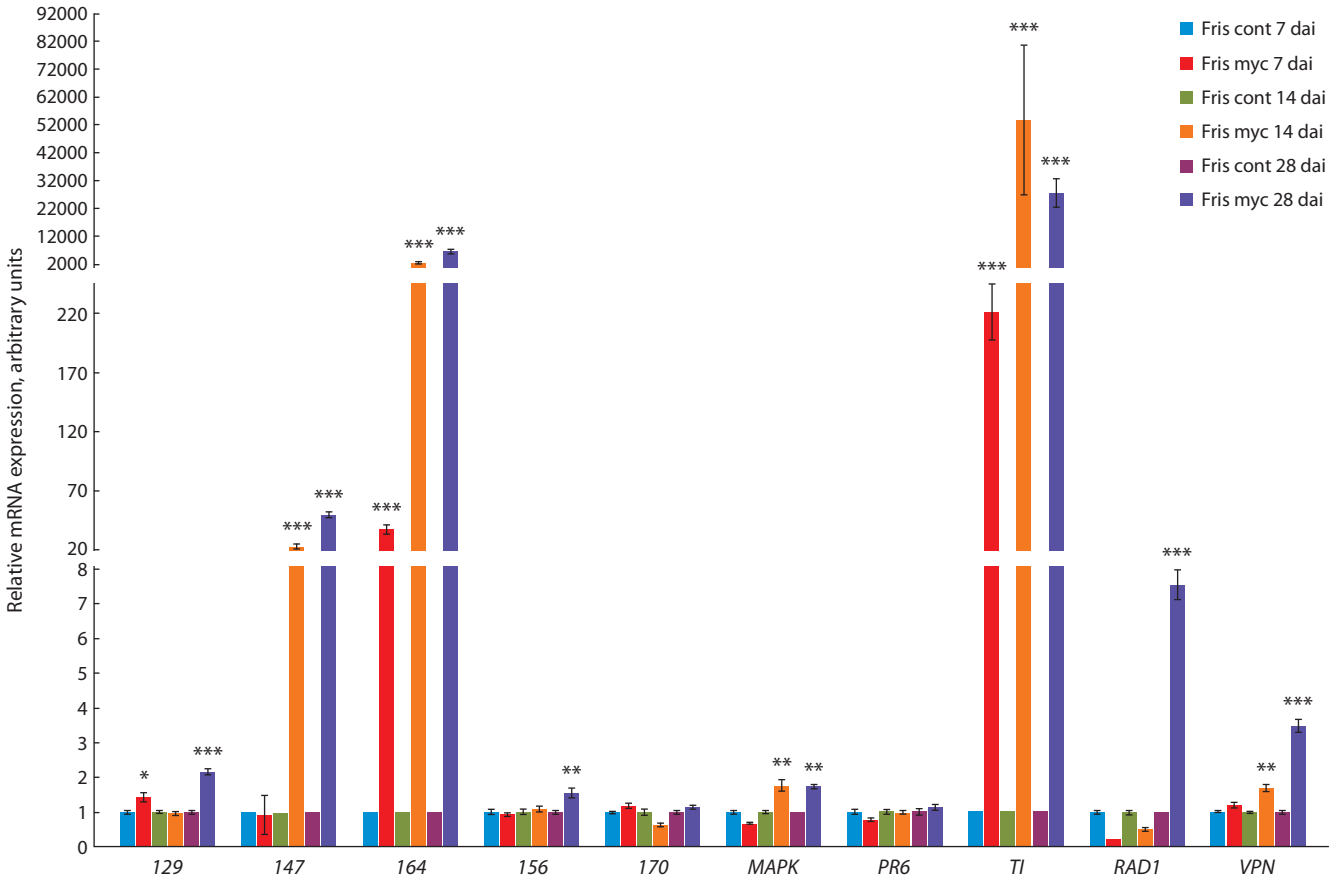

Fig. 2. Transcript levels of genes encoding markers of AM development in pea roots of cv. Frisson infected with *R. irregularis* after 7, 14, and 28 days.

patterns for chosen genes in cv. Finale as well as cv. Frisson pea plants (Grunwald et al., 2004). The used primers are presented in the Table 1.

This allowed the identification of predicted full-length sequences for genes of interest. The expression of 10 genes was investigated by RT-PCR using RNA from control and inoculated roots of cv. Finale and cv. Frisson on several days after inoculation (dai) (Figure 1, 2). The cv. Finale was chosen to compare the results with previously obtained data for this genotype, while cv. Frisson was used for analysis, because the newly created transcriptome was assembled for this cultivar. Indeed up-regulation of a number of genes was confirmed by RT-PCR using RNA from controls and mycorrhiza-inoculated pea roots of cv. Frisson and cv. Finale. The expression of RAD1 and VAPYRIN genes was mainly enhanced at stages of symbiosis development related to AM fungal colonization of root cells and arbuscules formation (14–28 dai). The similar results were previously obtained for model legume plant *M. truncatula* (Pumplin et al., 2010; Murray et al., 2011; Park et al., 2015).

The highest levels of expression were found for four genes encoding GDSL-motif lipase/acylhydrolase (*147*), MAP kinase (*MAPK*), trypsin inhibitor (*TI*) and putative lipid-transfer protein (*164*) in both genotypes (see Figures 1, 2). It is in a good agreement with previous results (Grunwald et al., 2004). It is interesting to note that activation of *TI* and *164* was connected with early stages of AM symbiosis development such as 7 dai. These markers may be helpful to estimate the inoculation effect, because usually visible signs of inoculation seem to be connected with later stages of symbiosis between pea plants and AM fungi like 14 dai. At the same time some cultivar-specific mycorrhiza-related pattern of expression was found in our experiments. It was shown for gene *170* with high level of expression in cv. Finale, but not in cv. Frisson (see Figure 1, 2). Moderate level of expression was shown for the stress-related genes like *129* and *PR6* in our experiments that may be due to differences in experimental conditions as compared to previous study (Grunwald et al., 2004).

Conclusion

Studies on model legume plants *M. truncatula* and *Lotus japonicus* (Regel.) K. Larsen resulted in the description of the molecular mechanisms underlying the formation and functioning of the symbioses (Gutjahr, Parniske, 2013; Gobbato, 2015; Pimprikar, Gutjahr, 2018). However, for the agriculturally important legume plants, the information regarding the molecular bases of AM and root nodule symbiosis (RNS) is still limited. As for the garden pea, about 40 regulatory symbiotic genes are known (Zhukov et al., 2016), of which about a half are attributed to the 'common' symbiotic genes needed for both AM and RNS (Borisov et al., 2007). The recent development of transcriptome sequencing technologies has made it possible to analyze the molecular machinery of symbiotic nodules and, in particular, to pinpoint the single nucleotide deletion mutation in important symbiotic gene *Sym33* (*IPD3*) (Zhernakov et al., 2019). Our first assembled transcriptome of mycorrhizal pea roots will help in characterization of the key plant genes involved in the regulation of mycorrhizal symbiosis and, therefore, will be a basis for the future advances in our understanding of plant-microbe interactions. The AM-specific genes that we selected on the base of this reference transcriptome may also serve as markers of successful colonisation in inoculation experiments, which is important for analysing the early stages of mycorrhization, when intraradical mycelium is almost invisible.

References

Alizadeh O. Mycorrhizal symbiosis. *Adv. Stud. Biol.* 2011;3(6):273-281.

Alves-Carvalho S., Aubert G., Carrère S., Cruaud C., Brochot A.L., Jacquin F., Klein A., Martin C., Boucherot K., Kreplak J., Da Silva C., Moreau S., Gamas P., Wincker P., Gouzy J., Burstin J. Full-length de novo assembly of RNA-seq data in pea (*Pisum sativum* L.) provides a gene expression atlas and gives insights into root nodulation in this species. *Plant J*. 2015;84(1):1-19. DOI 10.1111/tpj.12967.

Bankevich A., Nurk S., Antipov D., Gurevich A.A., Dvorkin M., Kulikov A.S., Lesin V.M., Nikolenko S.I., Pham S., Prjibelski A.D., Pyshkin A.V., Sirotkin A.V., Vyahhi N., Tesler G., Alekseyev M.A., Pevzner P.A. SPAdes: a new genome assembly algorithm and its applications to single-cell sequencing. *J. Comput. Biol*. 2012;19(5):455-477. DOI 10.1089/cmb.2012.0021.

Borisov A., Vasil'chikov A., Voroshilova V., Danilova T., Zhernakov A., Zhukov V., Koroleva T., Kuznetsova E., Madsen L., Mofett M., Naumkina T., Nemankin T., Ovchinnikova E., Pavlova Z., Petrova N., Pinaev A., Radutoiu S., Rozov S., Rychagova T., Solovov I., Stougaard J., Topunov A., Weeden N., Tsyganov V., Shtark O., Tikhonovich I. Regulatory genes of garden pea (*Pisum sativum* L.) controlling the development of nitrogen-fixing nodules and arbuscular mycorrhiza: a review of basic and applied aspects. *Appl. Biochem. Microbiol.* 2007;43(3):237-243. DOI 10.1134/S0003683807030027.

Borisov A.Y., Danilova T.N., Koroleva T.A., Naumkina T.S., Pavlova Z.B., Pinaev A.G., Shtark O.Y., Tsyganov V.E., Voroshilova V.A., Zhernakov A.I., Zhukov V.A., Tikhonovich I.A. Pea (*Pisum sativum* L.) regulatory genes controlling development of nitrogen-fixing nodule and arbuscular mycorrhiza: fundamentals and application. *Biologia* (*Bratislava*). 2004;59(13):137-144.

Bushnell B. BBMap. 2014. Available at: sourceforge.net/projects/bbmap/

Davidson N.M., Hawkins A.D.K., Oshlack A. SuperTranscripts: a data driven reference for analysis and visualisation of transcriptomes. *Genome Biol*. 2017;18:148. DOI 10.1186/s13059-017-1284-1.

Demchenko K., Winzer T., Stougaard J., Parniske M., Pawlowski K. Distinct roles of *Lotus japonicus SYMRK* and *SYM15* in root colonization and arbuscule formation. *New Phytol*. 2004;163(2):381-392. DOI 10.1111/j.1469-8137.2004.01123.x.

Duc G., Messager A. Mutagenesis of pea (*Pisum sativum* L.) and the isolation of mutants for nodulation and nitrogen fixation. *Plant Sci*. 1989;60(2):207-213. DOI 10.1016/0168-9452(89)90168-4.

Engvild K.C. Nodulation and nitrogen fixation mutants of pea, *Pisum sativum*. *Theor. Appl. Genet*. 1987;74(6):711-713. DOI 10.1007/BF00247546.

Franssen S.U., Shrestha R.P., Bräutigam A., Bornberg-Bauer E., Weber A.P. Comprehensive transcriptome analysis of the highly complex *Pisum sativum* genome using next generation sequencing. *BMC Genomics*. 2011;12(1):227. DOI 10.1186/1471-2164-12-227.

Gobbato E. Recent developments in arbuscular mycorrhizal signaling. *Curr. Opin. Plant Biol*. 2015;26:1-7. DOI 10.1016/j.pbi.2015.05.006.

Goodstein D.M., Shu S., Howson R., Neupane R., Hayes R.D., Fazo J., Mitros T., Dirks W., Hellsten U., Putnam N., Rokhsar D.S. Phytozome: a comparative platform for green plant genomics. *Nucleic Acids Res*. 2012;40(D1):D1178-D1186. DOI 10.1093/nar/gkr944.

Grabherr M.G., Haas B.J., Yassour M., Levin J.Z., Thompson D.A., Amit I., Adiconis X., Fan L., Raychowdhury R., Zeng Q., Chen Z., Mauceli E., Hacohen N., Gnirke A., Rhind N., di Palma F., Bir-

ren B.W., Nusbaum C., Lindblad-Toh K., Friedman N., Regev A. Full-length transcriptome assembly from RNA-Seq data without a reference genome. *Nat. Biotechnol*. 2011;29(7):644-652. DOI 10.1038/nbt.1883.

Grunwald U., Nyamsuren O., Tamasloukht M., Lapopin L., Becker A., Mann P., Gianinazzi-Pearson V., Krajinski F., Franken P. Identification of mycorrhiza-regulated genes with arbuscule development-related expression profile. *Plant Mol. Biol*. 2004;55(4):553-566. DOI 10.1007/s11103-004-1303-y.

Gutjahr C., Parniske M. Cell and developmental biology of arbuscular mycorrhiza symbiosis. *Annu. Rev. Cell Dev. Biol*. 2013;29(1):593-617. DOI 10.1146/annurev-cellbio-101512-122413.

Hoagland D.R., Arnon D.I. The water-culture method for growing plants without soil. *Circular. California Agric. Exp. Station*. 1950; 347(2).

Huerta-Cepas J., Szklarczyk D., Forslund K., Cook H., Heller D., Walter M.C., Rattei T., Mende D.R., Sunagawa S., Kuhn M., Jensen L.J., von Mering C., Bork P. eggNOG 4.5: a hierarchical orthology framework with improved functional annotations for eukaryotic, prokaryotic and viral sequences. *Nucleic Acids Res*. 2016;44(D1):D286-D293. DOI 10.1093/nar/gkv1248.

Jacobi L.M., Kukalev A.S., Ushakov K.V., Tsyganov V.E., Provorov N.A., Borisov A.Y., Tikhonovich I. Genetic variability of garden pea (*Pisum sativum* L.) for symbiotic capacities. *Pisum Genet*. 1999; 31:44-45.

Kaschuk G. Sink Stimulation of Leaf Photosynthesis by the Carbon Costs of Rhizobial and Arbuscular Mycorrhizal Fungal Symbioses. Wageningen, Wageningen Univ., S.n., 2009.

Kerr S.C., Gaiti F., Beveridge C.A., Tanurdzic M. *De novo* transcriptome assembly reveals high transcriptional complexity in *Pisum sativum* axillary buds and shows rapid changes in expression of diurnally regulated genes. *BMC Genomics*. 2017;18(1):221. DOI 10.1186/s12864-017-3577-x.

Kreplak J., Madoui M.A., Cápal P., Novák P., Labadie K., Aubert G., Bayer P.E., Gali K.K., Syme R.A., Main D., Klein A., Bérard A., Vrbová I., Fournier C., D'Agata L., Belser C., Berrabah W., Toegelová H., Milec Z., Vrána J., Lee H.T., Kougbeadjo A., Térézol M., Huneau C., Turo C.J., Mohellibi N., Neumann P., Falque M., Gallardo K., McGee R., Tar'an B., Bendahmane A., Aury J.M., Batley J., Le Paslier M.C., Ellis N., Warkentin T.D., Coyne C.J., Salse J., Edwards D., Lichtenzveig J., Macas J., Doležel J., Wincker P., Burstin J. A reference genome for pea provides insight into legume genome evolution. *Nat. Genet*. 2019;51(9):1411-1422. DOI 10.1038/s41588-019-0480-1.

Leppyanen I.V., Shakhnazarova V.Y., Shtark O.Y., Vishnevskaya N.A., Tikhonovich I.A., Dolgikh E.A. Receptor-like kinase LYK9 in *Pisum sativum* L. is the CERK1-like receptor that controls both plant immunity and AM symbiosis development. *Int. J. Mol. Sci*. 2018; 19:8. DOI 10.3390/ijms19010008.

Livak K.J., Schmittgen T.D. Analysis of relative gene expression data using real-time quantitative PCR and the 2-ΔΔCT method. *Methods.* 2001;25(4):402-408. DOI 10.1006/meth.2001.1262.

Lu G. Vector NTI, a balanced all-in-one sequence analysis suite. *Brief. Bioinformatics*. 2004;5(4):378-388. DOI 10.1093/bib/5.4.378.

Mamontova T., Afonin A.M., Ihling C., Soboleva A., Lukasheva E., Sulima A.S., Shtark O.Y., Akhtemova G.A., Povydysh M.N., Sinz A., Frolov A., Zhukov V.A., Tikhonovich I.A. Profiling of seed proteome in pea (*Pisum sativum* L.) lines characterized with high and low responsivity to combined inoculation with nodule bacteria and arbuscular mycorrhizal fungi. *Molecules*. 2019;24(8):1603. DOI 10.3390/molecules24081603.

Manck-Götzenberger J., Requena N. *Arbuscular mycorrhiza* symbiosis induces a major transcriptional reprogramming of the potato *SWEET* sugar transporter family. *Front. Plant Sci.* 2016;7:487. DOI 10.3389/fpls.2016.00487.

Morandi D., Sagan M., Prado-Vivant E., Duc G. Influence of genes determining supernodulation on root colonization by the mycorrhizal fungus *Glomus mosseae* in *Pisum sativum* and *Medicago truncatula* mutants. *Mycorrhiza*. 2000;10(1):37-42. DOI 10.1007/s005720050285.

Murray J.D., Muni R.R.D., Torres-Jerez I., Tang Y., Allen S., Andriankaja M., Li G., Laxmi A., Cheng X., Wen J., Vaughan D., Schultze M., Sun J., Charpentier M., Oldroyd G., Tadege M., Ratet P., Mysore K.S., Chen R., Udvardi M.K. *Vapyrin*, a gene essential for intracellular progression of arbuscular mycorrhizal symbiosis, is also essential for infection by rhizobia in the nodule symbiosis of *Medicago truncatula*. *Plant J.* 2011;65(2):244-252. DOI 10.1111/j.1365-313X.2010.04415.x.

Park H.J., Floss D.S., Levesque-Tremblay V., Bravo A., Harrison M.J. Hyphal branching during arbuscule development requires *Reduced Arbuscular Mycorrhiza1*. *Plant Physiol.* 2015;169(4):2774-2788. DOI 10.1104/pp.15.01155.

Pimprikar P., Gutjahr C. Transcriptional regulation of arbuscular mycorrhiza development. *Plant Cell Physiol*. 2018;59(4):876. DOI 10.1093/pcp/pcy024.

Pumplin N., Mondo S.J., Topp S., Starker C.G., Gantt J.S., Harrison M.J. *Medicago truncatula* Vapyrin is a novel protein required for arbuscular mycorrhizal symbiosis. *Plant J*. 2010;61(3):482-494. DOI 10.1111/j.1365-313X.2009.04072.x.

Shtark O.Y., Danilova T.N., Naumkina T.S., Vasilchikov A.G., Chebotar V.K., Kazakov A.E., Zhernakov A.I., Nemankin T.A., Prilepskaya N.A., Borisov A.U., Tikhonovich I.A. Analysis of pea (*Pisum sativum* L.) source material for breeding of cultivars with high symbiotic potential and choice of criteria for its evaluation. *Ecol. Genet*. 2006;4(2):22-28. DOI 10.17816/ecogen4222-28.

Shtark O.Y., Sulima A.S., Zhernakov A.I., Kliukova M.S., Fedorina J.V., Pinaev A.G., Kryukov A.A., Akhtemova G.A., Tikhonovich I.A., Zhukov V.A. Arbuscular mycorrhiza development in pea (*Pisum sativum* L.) mutants impaired in five early nodulation genes including putative orthologs of *NSP1* and *NSP2*. *Symbiosis*. 2016; 68(1-3):129-144. DOI 10.1007/s13199-016-0382-2.

Siddiqui Z.A., Akhtar M.S., Futai K. (Eds.). Mycorrhizae: Sustainable Agriculture and Forestry. Springer, 2008. DOI 10.1007/978-1-4020-8770-7.

Simão F.A., Waterhouse R.M., Ioannidis P., Kriventseva E.V., Zdobnov E.M. BUSCO: assessing genome assembly and annotation completeness with single-copy orthologs. *Bioinformatics*. 2015;31(19): 3210-3212. DOI 10.1093/bioinformatics/btv351.

Solaiman Z., Abbott L.K., Varma A. (Eds.). Mycorrhizal Fungi: Use in Sustainable Agriculture and Land Restoration. Springer, Berlin, Heidelberg, 2014. DOI 10.1007/978-3-662-45370-4.

Sudheesh S., Sawbridge T.I., Cogan N.O., Kennedy P., Forster J.W., Kaur S. *De novo* assembly and characterisation of the field pea transcriptome using RNA-Seq. *BMC Genomics*. 2015;16(1):611. DOI 10.1186/s12864-015-1815-7.

Tikhonovich I.A., Andronov E.E., Borisov A.Y., Dolgikh E.A., Zhernakov A.I., Zhukov V.A., Provorov N.A., Roumiantseva M.L., Simarov B.V. The principle of genome complementarity in the enhancement of plant adaptive capacities. *Russ. J. Genet*. 2015;51(9): 831-846. DOI 10.1134/S1022795415090124.

Tisserant E., Kohler A., Dozolme-Seddas P., Balestrini R., Benabdellah K., Colard A., Croll D., … Shachar-Hill Y., Tuskan G., Young J.P.W., Gianinazzi-Pearson V., Martin F. The transcriptome of the arbuscular mycorrhizal fungus *Glomus intraradices* (DAOM 197198) reveals functional tradeoffs in an obligate symbiont. *New Phytol*. 2012;193(3):755-769. DOI 10.1111/j.1469-8137.2011.03948.x.

Tisserant E., Malbreil M., Kuo A., Kohler A., Symeonidi A., Balestrini R., Charron P., … Rensing S.A., Grigoriev I.V., Corradi N., Roux C., Martin F. Genome of an arbuscular mycorrhizal fungus provides insight into the oldest plant symbiosis. *Proc. Natl. Acad. Sci. USA*. 2013;110(50):20117-20122. DOI 10.1073/pnas.1313452110.

Trapnell C., Williams B.A., Pertea G., Mortazavi A., Kwan G., Van Baren M.J., Salzberg S.L., Wold B.J., Pachter L. Transcript assem-

bly and quantification by RNA-Seq reveals unannotated transcripts and isoform switching during cell differentiation. *Nat. Biotechnol*. 2010;28(5):511-515. DOI 10.1038/nbt.1621.

Trouvelot A., Kough J.L., Gianinazzi-Pearson V. Mesure du taux de mycorhization VA d'un système radiculaire. Recherche de méthodes d'estimation ayant une signification fonctionnelle. *Mycorhizae: Physiologie et Génétique*. 1986;217-221.

Young N.D., Debellé F., Oldroyd G.E.D., Geurts R., Cannon S.B., Udvardi M.K., Benedito V.A., … Schwartz D.C., Rogers J., Quétier F., Town C.D., Roe B.A. The *Medicago* genome provides insight into the evolution of rhizobial symbioses. *Nature*. 2011;480:520-524. DOI 10.1038/nature10625.

Zhernakov A.I., Shtark O.Y., Kulaeva O.A., Fedorina J.V., Afonin A.M., Kitaeva A.B., Tsyganov V.E., Afonso-Grunz F., Hoffmeier K., Rotter B., Winter P., Tikhonovich I.A., Zhukov V.A. Mapping-by-sequencing using NGS-based 3′-MACE-Seq reveals a new mutant allele of the essential nodulation gene *Sym33* (*IPD3*) in pea (*Pisum sativum* L.). *PeerJ*. 2019;7. DOI 10.7717/peerj.6662.

Zhukov V.A., Akhtemova G.A., Zhernakov A.I., Sulima A.S., Shtark O.Yu., Tikhonovich I.A. Evaluation of the symbiotic effectiveness of pea (*Pisum sativum* L.) genotypes in pot experiment. *Sel'skokhozyaistvennaya Biologiya = Agricultural Biology*. 2017; 52(3):607-614. DOI 10.15389/agrobiology.2017.3.607eng.

Zhukov V.A., Shtark O.Y., Nemankin T.A., Kryukov A.A., Borisov A.Y., Tikhonovich I.A. Genetic mapping of pea (*Pisum sativum* L.) genes involved in symbiosis. *Sel'skokhozyaistvennaya Biologiya = Agricultural Biology*. 2016;51(5):593-601. DOI 10.15389/agrobiology.2016.5.593eng.

Zhukov V.A., Shtark O.Y., Puzanskiy R.K., Avdeeva G.S., Yurkov A.P., Smolikova G.N., Yemelyanov V.V., Kliukova M.S., Shavarda A.L., Kirpichnikova A.A., Zhernakov A.I., Afonin A.M., Tikhonovich I.A., Shishova M.F. Metabolic alterations in pea leaves during arbuscular mycorrhiza development. *PeerJ*. 2019; DOI 10.7717/peerj.7495.

Zhukov V.A., Zhernakov A.I., Kulaeva O.A., Ershov N.I., Borisov A.Y., Tikhonovich I.A. *De novo* assembly of the pea (*Pisum sativum* L.) nodule transcriptome. *Int. J. Genomics*. 2015:695947. DOI 10.1155/2015/695947.

Zorin E.A., Kliukova M.S., Kulaeva O.A., Afonin A.M., Tikhonovich I.A., Zhukov V.A. Identification of sequences encoding for NCR-peptides and defensins in the "meta-assembly" of transcriptome of pea (*Pisum sativum* L.) nitrogen-fixing nodules. *Ecol. Genet*. 2019;17(3):39-46. DOI 10.17816/ecogen17339-17346.

Data availability. All the data described in this project are available in the NCBI database under the Bioproject PRJNA592445. This Transcriptome Shotgun Assembly project has been deposited at DDBJ/EMBL/GenBank under the accession GICP00000000. The version described in this paper is the first version, GICP01000000. The additional transcriptome assemblies are available at https://cloud.arriam.ru/s/RKD67CZak58BzzN

Acknowledgements. The work of A.M. Afonin, O.A. Kulaeva, O.Y. Shtark, I.A. Tikhonovich and V.A. Zhukov on pea transcriptome sequencing, assembly and analysis was supported by the Russian Science Foundation grant # 16-16-00118. The work of I.V. Leppyanen and E.A. Dolgikh on primer design and analysis of expression of the marker genes was supported by the Russian Science Foundation grant # 16-16-10043.

Conflict of interest. The authors declare no conflict of interest.

Received December 5, 2019. Revised May 10, 2020. Accepted May 11, 2020.

Вавиловский журнал генетики и селекции. 2020;24(4):340-347
DOI 10.18699/VJ20.626

Analysis of color and texture characteristics of cereals on digital images

E.G. Komyshev[1, 2] ✉, M.A. Genaev[1, 2, 3], D.A. Afonnikov[1, 2, 3]

[1] Institute of Cytology and Genetics of Siberian Branch of the Russian Academy of Sciences, Novosibirsk, Russia
[2] Kurchatov Genomic Center of the Institute of Cytology and Genetics of Siberian Branch of the Russian Academy of Sciences, Novosibirsk, Russia
[3] Novosibirsk State University, Novosibirsk, Russia
✉ e-mail: komyshev@bionet.nsc.ru

Abstract. The color of the grain shell of cereals is an important feature that characterizes the pigments and metabolites contained in it. The grain shell is the main barrier between the grain and the environment, so its characteristics are associated with a number of important biological functions: moisture absorption, grain viability, resistance to pre-harvest germination. The presence of pigments in the shell affects various technological properties of the grain. Color characteristics, as well as the appearance of the grain shell are an important indicator of plant diseases. In addition, the color of the grains serves as a classifying feature of plants. Genetic control of the color formation of both grains and other plant organs is exerted by genes encoding enzymes involved in the biosynthesis of pigments, as well as regulatory genes. For a number of pigments, these genes are well understood, but for some pigments, such as melanin, which causes the black color of grains in barley, the molecular mechanisms of biosynthesis are still poorly understood. When studying the mechanisms of genetic control of grain color, breeders and geneticists are constantly faced with the need to assess the color characteristics of their shell. The technical means of addressing this problem include spectrophotometers, spectrometers, hyperspectral cameras. However, these cameras are expensive, especially with high resolution, both spatial and spectral. An alternative is to use digital cameras that allow you to get high-quality images with high spatial and color resolution. In this regard, recently, in the field of plant phenotyping, methods for evaluating the color and texture characteristics of cereals based on the analysis of two-dimensional images obtained by digital cameras have been intensively developed. This mini-review is devoted to the main tasks related to the analysis of color and texture characteristics of cereals, and to methods of their description based on digital images.

Key words: color; texture; digital images; image analysis; cereal grains.

For citation: Komyshev E.G., Genaev M.A., Afonnikov D.A. Analysis of color and texture characteristics of cereals on digital images. *Vavilovskii Zhurnal Genetiki i Selektsii = Vavilov Journal of Genetics and Breeding*. 2020;24(4): 340-347. DOI 10.18699/VJ20.626

Анализ цветовых и текстурных характеристик зерен злаков на цифровых изображениях

Е.Г. Комышев[1, 2] ✉, М.А. Генаев[1, 2, 3], Д.А. Афонников[1, 2, 3]

[1] Федеральный исследовательский центр Институт цитологии и генетики Сибирского отделения Российской академии наук, Новосибирск, Россия
[2] Курчатовский геномный центр Федерального исследовательского центра Институт цитологии и генетики Сибирского отделения Российской академии наук, Новосибирск, Россия
[3] Новосибирский национальный исследовательский государственный университет, Новосибирск, Россия
✉ e-mail: komyshev@bionet.nsc.ru

Аннотация. Цвет оболочки зерен злаков – важный признак, характеризующий содержащиеся в ней пигменты и метаболиты. Оболочка зерна служит основным барьером между зерном и внешней средой, поэтому с ее характеристиками связан ряд важных биологических функций: поглощение влаги, жизнеспособность зерна, устойчивость к предуборочному прорастанию. Наличие пигментов в оболочке влияет на различные технологические свойства зерна. Цветовые характеристики, как и внешний вид оболочки зерна, – важный индикатор заболеваний растений. Цвет зерна давно используется в систематике пшеницы для описания ее ботанических разновидностей, и для некоторых систем это одна из основных характеристик. Генетический контроль формирования окраски зерен и других органов растений осуществляется генами, кодирующими ферменты, вовлеченные в биосинтез пигментов, и регуляторными генами. Для ряда пигментов эти гены исследованы достаточно хорошо, однако для некоторых пигментов, например меланина, обусловливающего черную окраску зерен у ячменя, молекулярные

механизмы биосинтеза еще слабо изучены. При исследовании механизмов генетического контроля окраски зерен селекционеры и генетики постоянно сталкиваются с необходимостью оценки цветовых характеристик их оболочки. К техническим средствам решения этой задачи относятся спектрофотометры, спектрометры, гиперспектральные камеры. Однако эти камеры дорогостоящие, в особенности с высоким разрешением, как пространственным, так и спектральным. Альтернативой является использование цифровых фотокамер, позволяющих получать высококачественные изображения с высоким пространственным и цветовым разрешением. В связи с этим в последнее время в области фенотипирования растений интенсивно развиваются методы оценки цветовых и текстурных характеристик зерен злаков, основанные на анализе двумерных изображений, полученных цифровыми камерами. Данный мини-обзор посвящен основным задачам, связанным с анализом цветовых и текстурных характеристик зерен злаков, методам их описания на основе цифровых изображений.
Ключевые слова: цвет; текстура; цифровые изображения; анализ изображений; зерна злаков.

Introduction

The coloration of cereal grain shell is an important trait that characterizes the pigments and metabolites contained there. Violet and blue grain color is determined by anthocyans; yellow color, by carotenoids; and red brown or dark brown, by flavonoids, such as proanthocyanidins and phlobaphenes (Adzhieva et al., 2015; Lachman et al., 2017). The correlation between the shell color and content of the corresponding substances is experimentally demonstrated. Significant correlations of the kernel shell color and the content of phenols, flavonoids, and antioxidant capacity have been observed (Shen et al., 2009). The contents of phenols, flavonoids, anthocyans, β-carotenoids, and luteins significantly differ between the maize grains with different colors (Žilić et al., 2012). Flavonoids, anthocyans, and carotenoids possess several valuable properties. They are antioxidants, and influence the nutritional value. For example, addition of the wheat seed coats with a purple pericarp or blue aleurone layer to flour improves the quality of bakery products owing to flavor, texture, and color characteristics (Machálková et al., 2017). Correspondingly, the varieties and lines with different grain coloration recently cause a strong interest of the food industry (Khlestkina et al., 2017; Corrêa et al., 2019).

The kernel shell is the main barrier between the grain and environment; correspondingly, a set of important biological functions are associated with the shell properties, including, water absorption, grain viability, and resistance to pre-harvest sprouting (Souza, Marcos-Filho, 2001). The pigments in the grain shell influence manifold grain technological properties. In particular, phlobaphenes (condensed tannins), coloring the pericarp red, have a positive effect on the duration of grain dormancy, thereby preventing its pre-harvest sprouting (Flintham et al., 2002). That is why the wheat genotypes with red-colored kernels are used in breeding as a donor of the genes controlling the resistance to pre-harvest grain germination (Krupnov et al., 2012; Fakthongphan et al., 2016). The shell color of rice kernels (the intensities of red, green, and blue color components) correlates with the grain quality characteristics, such as kernel transparency and the share of broken kernels, in a statistically significant manner (Septiningsih et al., 2003).

The color characteristics and the external appearance of the kernel shell are important indicators of plant diseases. For example, fusariosis manifests as a pinky or bluish coloration on the wheat and barley kernel shell (McMullen et al., 1997). Characteristic of another disease, kernel black-point, is dark discoloration of the embryo side of grains (Draz et al., 2016).

Grain coloration may also serve as a trait in plant classification. As early as the late 19th century, F. Körnicke suggested using the grain color for description of wheat botanical varieties (Körnicke, Werner, 1885). The N.I. Vavilov All-Russian Institute of Plant Genetic Resources classifies the wheat botanical varieties using the system in which the grain color is one of the major traits (Dorofeev et al., 1979).

The coloration of both the kernels and other plant organs is controlled by the genes coding for the enzymes involved in biosynthesis of pigments, as well as by regulatory genes (Khlestkina, 2014; Lachman et al., 2017; Shoeva et al., 2018). The corresponding genes are well studied for several pigments, including even their complete nucleotide sequences and their positions in the genome. However, the molecular mechanisms of biosynthesis are still rather vague for some pigments, in particular, melanin, which determines black color of barley kernels (Glagoleva et al., 2017; Shoeva, 2018).

When studying the mechanisms underlying genetic control of grain color, breeders and geneticists constantly face the necessity of estimating the color characteristics of their shells. Several technical tools allow this problem to be solved, first and foremost, spectrophotometers, able to characterize both the chromatic and textural characteristics of kernels with a high accuracy. Spectrophotometers have been long and successfully used and serve as a standard for estimating the color of biological objects (Black, Panozzo, 2004; Garg et al., 2016; Machálková et al., 2017). Another approach is provided by spectrometers with the wavelength range covering both visible and near-

infrared regions (hyperspectral cameras of visible and near-infrared ranges) (Black, Panozzo, 2004; ElMasry et al., 2019). However, these cameras are very expensive, especially, with a high spatial and spectral resolution. An alternative is digital cameras capturing high-quality images with a high spatial and color resolution. The price of digital cameras are constantly decreasing and they are now widely available, while even an amateur camera allows for capturing high-resolution and high quality images. In this regard, the methods for evaluating the color and texture characteristics of cereal grains based on analysis of two-dimensional digital images have been intensively developed recently in the field of plant phenotyping.

This brief review focuses on the main problems related to the analysis of color and texture characteristics of cereals and methods of their description utilizing digital images.

The tasks associated with the analysis of color and texture characteristics in kernel images

One of the relevant problems in the analysis of digital images of grains is related to classification. The particular tasks of classification may be different. For example, it is necessary to classify grains according to their color and surface texture into several different genotypes (Pourreza et al., 2012; Olgun el al., 2016). Frequently, the characteristics of size and shape are added to the color and texture parameters (Majumdar, Jayas, 2000; Chaugule, Mali, 2014; Sabanci et al., 2016).

Another tightly associated problem is to assort the kernels according to color and surface texture (Pearson, 2010); in particular, sorters are designed for mass screening of a large number of grains to separate the sound grains from waste and damaged grains. M. Huang et al. (2015) reviewed the current developments on the seed quality and safety tests based on image analysis, including hyperspectral ones, and Z. Gong et al. (2015) briefly describe the approaches, engineering included, to the seed quality inspection.

Sometimes the grains are classified only by their color (red or white). In particular, M.S. Ram et al. (2002) used spectrophotometer and spectrometer to design a procedure for determining the color of kernel shell in red and white wheats. T.N. McCaig et al. (1993) classified the wheat into red-grained and white-grained cultivars using the spectrophotometry data for 262 genotypes of both soft and hard wheats. Analysis of the color characteristics also makes it possible to identify the kernels affected by pathogens (Ahmad, 1999; Goriewa-Duba et al., 2018) or mechanically damaged (Delwiche et al., 2013). Note that machine learning and artificial intelligence techniques are also frequently used along with the image analysis in solving the relevant problems (Patrício, Rieder, 2018); however, the description of these methods is beyond the area of our review.

Color coding systems

The color of the surface is a characteristic of its spectral reflectivity, which is determined by many factors, such as absorption of radiation of a light source at different wavelengths, its reflection, and scattering (Forsyth, Pons, 2004). Spectrometers give the fullest estimate of the reflection and absorption characteristics in different ranges of wavelengths. As for the most of the digital cameras, their sensors respond to reflected radiation in the visible wavelength range (400–780 nm). Note that the color perception by the human eye has its specific features associated with its structure: there is no one-to-one correspondence between the surface color perception by the eye and the spectral characteristics of this surface; for example, the same shade of gray can be reproduced by the reflected radiation with completely different intensities for different wavelengths.

When studying the human perception, it was found out that three main colors – red, green, and blue – are sufficient to get the overall set of colors perceived by humans by mixing them in different proportions (Forsyth, Pons, 2004). This inference is confirmed by the structure of the human eye itself since the eye retina comprises three types of receptors (retinal cones) responsible for color vision.

Different models (color spaces) have been elaborated to digitally represent colors. Color model specifies the system of coordinates that unambiguously determines colors. Several different color models have been developed to provide the best method of color description for TV, photo, video, and color printing. The following systems are most frequently used when analyzing digital images of plants.

The RGB color model is the most well known color space, encoding a broad array of colors by relative intensities of its three components: red (R), green (G), and blue (B). These components are described by integers, most frequently from 0 to 256. The higher the values, the higher is the intensity of color (luminance). The colors with equal values of the components are the shades of gray. This representation is used mainly in computer screens and digital cameras.

The HSV (HSB) model is a color space also using three color components, proposed in the mid-1970s. The hue component (H) varies from 0 to 360; the values close to 0 and 360 correspond to red; close to 60, to yellow; 120, to green; 180, to cyan; 240, to blue; and 300, to magenta. Saturation (S) is the larger, the more saturated is the color tone, while small values of this parameter correspond to the shades of gray. Brightness (value, B/V) takes on the smaller values for the dark colors and larger, for bright

ones. One of the shortcomings of the HSV and RGB consists in that the number of saturation and color tint levels perceptible to eye in these spaces decreases when brightness approaches zero.

The CIE L*a*b* space, proposed in 1976 by the International Commission on Illumination (CIE), was designed to approximate the human vision and to provide perceptual uniformity. Similar to HSV, the brightness component in CIE L*a*b* (L* component) is separated from the chromatic component of color (Pathare et al., 2013) and is an approximate estimate of brightness. The a* parameter takes on the positive values for reddish tints and negative values for greenish ones; the b* parameter is positive for the yellowish tints and negative for the bluish ones. This color model is widely used in software solutions for image processing and color correction. The CIE L*a*b* space is used for assessing the color characteristics in spectrophotometers.

The characteristics of other color spaces with their description are available in specialized literature on image analysis (Fisenko V.T., Fisenko T.Yu., 2008; Domasev, Gnatyuk, 2009). The components of the same color in different systems are linked by transformation rules, so that knowing the values of the chromatic components for a color tint in one space, the corresponding values for another space are obtainable. For example, the values for the RGB components make it possible to compute the values for the HSV components and vice versa. This allows the color representation for a particular image to be selected depending on the particular task.

When solving a problem of machine vision and analysis of chromatic characteristics, the HSV and L*a*b* color models are of the principal interest since these systems represent colors in the same terms as a human does when describing a color, namely, hue, saturation, and brightness (lightness).

Analysis of color characteristics of kernels

The images used for analyzing kernels are as a rule captured by digital cameras in the RGB space shot under laboratory conditions using a controlled illumination. The kernels in images are typically placed onto a contrast background at a distance from one another (Sabanci et al., 2017; Goriewa-Duba et al., 2018). This protocol makes it possible to analyze not only the color and surface texture characteristics, but also the kernel shape and size. Moreover, bulk specimens are used in some studies (Pourreza et al., 2012; Olgun et al., 2016) in which the kernels lie in a dense grain touching one another. As a rule, the textural and chromatic characteristics of the bulk specimen are assessed in this approach rather than individual kernels.

In the case the individual kernels are analyzed, first, their local images are isolated in the integral image. For this purpose, the images are preprocessed (using despeckle and removal of noise and foreign objects) and segmented to identify the regions of the image that correspond to individual kernels. Then, the quantitative traits available from images are extracted from these regions. Note that it is rather difficult to control the illumination conditions, especially when the images are captured outside laboratory (Berry et al., 2018). Correspondingly, color correction procedure using color patterns (a set of cards with cells of specified standard colors) is helpful (Berry et al., 2018; Genaev et al., 2019; Alemu et al., 2020).

In an image, the regions corresponding to individual kernels comprise hundred of pixels, each displaying its own color characteristics in a selected color space (for example, three values of the R, G, and B components). That is why statistical characteristics of color components are most frequently used for description of the color of these objects. First and foremost, the histograms of pixel distribution according to the intensity of each color component independently of the other components and the location of pixels in the image are computed. The histograms are used to calculate the other parameters, such as the mean value, variance, asymmetry, and the kurtosis of pixel intensities for each color component (Ahmad et al., 1999; Majumdar, Jayas, 2000). These values are further utilized to describe the color properties of kernels.

In particular, T. Pearson and D. Brabec (2008) developed a system of machine vision for an automated estimation and sorting of the kernels of wheat and other cereals in a real-time mode. The images with a resolution of 640 × 480 pixels were captured with a digital camera and transferred to a PC, which, after classification, output a signal to an air valve to correspondingly sort the kernels. The intensity histograms as well as the mean and standard deviations of the RGB channel intensities (in total, 198 characteristics for each kernel) were used for classification by linear discriminant analysis. The accuracy of the system when classifying red and white kernels of hard wheat was 94 to 99 % depending on the wheat cultivar, feeding rate, and number of classification characteristics.

N.S. Visen et al. (2002) compared the accuracy of different architectures of simple and specialist neural networks in the classification of cereals. Morphological and chromatic characteristics of wheat, barley, oat, and rye kernels calculated using color images captured with a CCD camera were used as the input data. The gray features: mean, median, mode, and standard deviation of gray-level values of the objects in the image – were extracted and used as the input data. The best mean classification accuracy of 98 % was obtained using specialist probabilistic neural networks.

K. Goriewa-Duba et al. (2018) used the digital images of the kernels of six wheat species acquired with a flatbed

CCD scanner to analyze the shape and color. They assessed the effect of grain colonization by endophytic fungi on the color of the seed coat as well as estimated the wheat subspecies with a high genetic variation. The images were analyzed using the ImageJ software to assess the shape characteristics, such as area, perimeter, Feret diameter, circularity, aspect ratio, roundness, and solidity. The color descriptors included the mean values for the RGB, HSI, and L*a*b* channels. The principal component analysis of the kernels with different genotypes has shown that their color characteristics significantly contribute to the first variance component and are among the most important when classifying wheats into different genotypes.

A. Alemu et al. (2020) analyzed the genome-wide associations of nucleotide substitutions (GWAS) in the population of 192 hard wheat (*Triticum durum*) genotypes from Ethiopia with grain shape and color traits. Grain length and width were used to describe the kernel shape and the mean values of the L*a*b* components to describe the color. In total, 11 quantitative trait loci (QTLs) were detected for the color characteristics; the locus for the a* component resides on chromosome 2A; five loci for the b* component, on chromosomes 1B, 3A, 4B, 5A, and 7B; and five for the L* component, on chromosomes 1A, 2A, 7A, and 7B.

Characteristics of the image texture used when analyzing kernels

Another characteristic of the surface is its texture, which is the image component that reflects the visual properties of these surfaces or objects (bumpiness and the presence of regular patterns). The concept of texture is difficult to formalize since it to a considerable degree depends on the scale and has not any limitations on the basis of which it is formed. A leaf in an image is an object and the foliage is a texture. It is possible to separate simple textures that are formed of ordered patterns or textons (Forsyth, Pons, 2004). A distinctive feature of a simple texture is its regularity and repeated or partially reproduced elements on a certain surface or object. Other textures may have a considerably more complex structure.

The approaches more intricate as compared with the color analysis are used to describe textures since the texture is characterized by mutual spatial arrangement of pixels with different intensities of their color components. Both the color and texture characteristics can be determined utilizing statistical methods to assess the parameters of the histograms of the initial image, such as, the mean, variance, asymmetry, and kurtosis. For simplicity, the images are described in the gray scale, i. e., the description is reduced from pixel color characteristics (three components) to its total intensity alone (one component, $I(x, y)$, where x and y are the coordinates of pixel). The gray level co-occurrence matrix (GLCM) is used for this purpose (Supplementary Materials, Table 1, Eq. (1))[1], which is a second order histogram (Haralick et al., 1973). The second order means that the matrix describes the distribution of intensities for the pairs of pixels of an image with specific values. Thus, the combinations of intensities for these pairs are taken into account. See V.G. Astafurov et al. (2014) for an example of computation of a GLCM. The GLCM is then used to extract the statistics for the distribution of its elements, such as uniformity, homogeneity, moments of inertia, correlation, different mean values, variance, and entropy (see Supplementary Materials, Table 2) (Majumdar, Jayas, 1999).

The gray level run length matrix (GLRM; see Supplementary Materials, Table 1, Eq. (2)) is constructed based on the information about the run length of the pixels with equal intensity (Galloway, 1975). These run lengths can be specified by different levels of intensities and the traversal direction from one pixel to another. GLRM allows for computation of the statistics, such as inhomogeneity of gray level, inhomogeneity of run lengths, coefficient of runs, entropy, inverse moment of short runs, moment of long runs, and other characteristics (Haralick et al., 1979).

The third approach relies on the model-based interpretation of texture, for example, a method based on autoregressive model parameters in which the intensity of a pixel is predicted as the weighted sum of four intensities of the neighboring pixels (Szczypiński et al., 2015). Several methods for texture description utilize Fourier, Gabor, or wavelet transform to characterize the spatial arrangement of the pixels of different intensities in the image from its frequency characteristic or wavelet components (Szczypiński et al., 2009). In general, the above briefed characteristics make it possible to form over a hundred of digital traits of image textures. As a rule, only part of these characteristics is used in the relevant literature.

An example of the use of texture characteristics in kernel analysis is the study by A. Pourreza et al. (2012). Images of nine wheat cultivars in a container illuminated with a fluorescent lamp were analyzed. The matrices (GLCM and GLRM) were computed for the gray scale images. Three additional characteristics were used; these characteristics are determined by the difference between the intensity of the central pixel from the intensities of the neighboring pixels in a 3×3 matrix. The local similarity patterns (LSPs; see Supplementary Materials, Table 1, Eq. (3)) are calculated from the difference in the intensities between the central and neighboring pixels. If the difference is below the SRR threshold, the LSP of the neighboring pixel is set equal to unity; otherwise, zero. A clockwise traversal of eight pixels gives a vector of zeros and unities, which characterizes the correspondence

[1] Supplementary Materials are available in https://vavilov.elpub.ru/jour/manager/files/SupplKomyshev_engl.pdf

of the intensity of the central pixel and all its neighbors. Another parameter in this work is local binary patterns (LBPs; see Supplementary Materials, Table 1, Eq. (4)), which were computed taking into account the weight coefficients of the neighboring pixels multiplied by LSP vector components. Finally, one more texture characteristics was the local similarity number (LSN; see Supplementary Materials, Table 1, Eq. (5)), which is the number of pixels with an intensity similar to that of the central pixel in the square of N × N.

Then, different statistics were calculated for the above textural features (mean, standard deviation, entropy, etc.; in total, 131 features). Some of them were based on the histogram gray level quantification (25 histogram bands). As was demonstrated, the textural features were most effective in classifying the cultivars as compared with the other characteristics. Six of the nine cultivars were identified with a 100 % accuracy; two of the remained cultivars were identified with 96 % accuracy. The use of the characteristics obtained from the LBP, LSP, and LSN matrices improved the classification accuracy as compared with the earlier studies. In total, 54 % of the 50 main textural features were selected from LBP, LSP, and LSN groups. The authors also conclude that the characteristics of feature distribution considerably contributed to identification of wheat cultivars.

K. Sabanci et al. (2017) describes a machine vision system for distinguishing of kernels between the durum and bread wheats. The used visual characteristics include size (length, width, perimeter, and area), color (R, G, and B), and texture (contrast, correlation, energy, homogeneity, and entropy); in addition, nine characteristics were calculated from the main ones. In tests, the simplified classifier identifies the grain type with an accuracy of 99.46 % and sorts the wheat kernels with an accuracy of 100 %. For training and verification, images of 200 wheat kernels (100 of bread wheat and 100 of durum wheat) were captured by a high-resolution camera.

Conclusions

Spectrophotometers, spectrometers, and hyperspectral cameras are efficient and reliable tools for analysis and estimation of cereal kernels. However, they are expensive, especially those with a high resolution, both spatial and spectral. An alternative is digital cameras capturing high-quality images with a high spatial and color resolution. Although the precieved spectrum of the currently available digital cameras is limited, the studies have shown that they can be effectively used as a reliable and precise tool for solving manifold applied problems. A high spatial and color resolution of such cameras makes it possible to analyze the textural characteristics of cereal kernels in detail. The textural characteristics are supplemented with color characteristics represented in different color models.

Thus, the use of color and textural characteristics in the analysis of digital images of cereal kernels allow for an efficient resolution of several important problems in their classification, sorting, and identification of diseases.

References

Adzhieva V.F., Babak O.G., Shoeva O.Yu., Kilchevsky A.V., Khlestkina E.K. Molecular-genetic mechanisms underlying fruit and seed coloration in plants. *Vavilovskii Zhurnal Genetiki i Selektsii = Vavilov Journal of Genetics and Breeding*. 2015;19(5): 561-573. DOI 10.18699/VJ15.073. (in Russian)

Ahmad I.S., Reid J.F., Paulsen M.R., Sinclair J.B. Color classifier for symptomatic soybean seeds using image processing. *Plant Dis*. 1999;83(4):320-327. DOI 10.1094/PDIS.1999.83.4.320.

Alemu A., Feyissa T., Tuberosa R., Maccaferri M., Sciara G., Letta T., Abeyo B. Genome-wide association mapping for grain shape and color traits in Ethiopian durum wheat (*Triticum turgidum* ssp. *durum*). *Crop. J*. 2020. DOI 10.1016/j.cj.2020.01.001.

Astafurov V.G., Evsyutkin T.V., Kuriyanovich K.V., Skorokhodov A.V. Statistical model of cirrus cloud textural features based on MODIS satellite images. *Optika Atmosphery i Okeana = Atmospheric and Oceanic Optics.* 2014;27(07):640-646. (in Russian)

Berry J.C., Fahlgren N., Pokorny A.A., Bart R.S., Veley K.M. An automated, high-throughput method for standardizing image color profiles to improve image-based plant phenotyping. *PeerJ.* 2018;6:5727. DOI 10.7717/peerj.5727.

Black C.K., Panozzo J.F. Accurate technique for measuring color values of grain and grain products using a visible-NIR instrument. *Cereal Chem*. 2004;81(4):469-474. DOI 10.1094/CCHEM.2004.81.4.469.

Chaugule A., Mali S.N. Evaluation of texture and shape features for classification of four paddy varieties. *J. Engineer*. 2014. DOI 10.1155/2014/617263.

Corrêa R.C.G., Garcia J.A.A., Correa V.G., Vieira T.F., Bracht A., Peralta R.M. Pigments and vitamins from plants as functional ingredients: Current trends and perspectives. *Adv. Food Nutr. Res.* 2019; 90:259-303. DOI 10.1016/bs.afnr.2019.02.003.

Delwiche S.R., Yang I.C., Graybosch R.A. Multiple view image analysis of freefalling US wheat grains for damage assessment. *Comput. Electron. Agr*. 2013;98:62-73. DOI 10.1016/j.compag.2013.07.002.

Domasev M.V., Gnatyk S.P. Color, Color Management, Color Calculations and Measurements. St. Petersburg: Piter Publ., 2009. (in Russian)

Dorofeev V.F., Filatenko A.A., Migushova E.F., Udachin R.A., Yakubtsiner M.M. The Cultural Flora of the USSR. Vol. 1. Wheat. Leningrad: Kolos Publ., 1979. (in Russian)

Draz I.S., El-Gremi S.M., Youssef W.A. Response of Egyptian wheat cultivars to kernel black point disease alongside grain yield. *Pak. J. Phytopathol*. 2016;28(1):15-17.

ElMasry G., Mandour N., Al-Rejaie S., Belin E., Rousseau D. Recent applications of multispectral imaging in seed phenotyping and quality monitoring – An overview. *Sensors*. 2019;19(5):1090. DOI 10.3390/s19051090.

Fakthongphan J., Graybosch R.A., Baenziger P.S. Combining ability for tolerance to pre-harvest sprouting in common wheat (*Triticum aestivum* L.). *Crop Sci.* 2016;56(3):1025-1035. DOI 10.2135/cropsci 2015.08.0490.

Fisenko V.T., Fisenko T.Yu. Computer Processing and Image Recognition: Tutorial. St. Petersburg, 2008. (in Russian)

Flintham J., Adlam R., Bassoi M., Holdsworth M., Gale M. Mapping genes for resistance to sprouting damage in wheat. *Euphytica*. 2002;126:39-45. DOI 10.1023/A:1019632008244.

Forsyth D., Ponce J. Computer Vision: A Modern Approach. Prentice Hall, 2003. (Russ. ed. Forsayt D., Pons Zh. Komp'yuternoe Zrenie. Sovremennyy Podkhod. Moscow: Williams, 2004.)

Galloway M.M. Texture analysis using grey level run lengths. C*omput. Graphics Image Process*. 1975;4:172-179.

Garg M., Chawla M., Chunduri V., Kumar R., Sharma S., Sharma N.K., Kaur N., Kumar A., Mundey J.K., Saini M.K., Singh S.P. Transfer of grain colors to elite wheat cultivars and their characterization. *J. Cereal Sci*. 2016;71:138-144. DOI 10.1016/j.jcs.2016.08.004.

Genaev M.A., Komyshev E.G., Smirnov N.V., Kruchinina Y.V., Goncharov N.P., Afonnikov D.A. Morphometry of the wheat spike by analyzing 2D images. *Agronomy*. 2019;9(7):390.

Glagoleva A.Y., Shmakov N.A., Shoeva O.Y., Vasiliev G.V., Shatskaya N.V., Börner A., Afonnikov D.A., Khlestkina E.K. Pleiotropic effect of barley Blp locus: metabolic pathways and genes identified by RNA-seq analysis of near-isogenic lines. *BMC Plant Biol*. 2017;17(Suppl.1):182. DOI 10.1186/s12870-017-1124-1.

Gong Z., Cheng F., Cheng F., Liu Z., Yang X., Zhai B., You Z. Recent developments of seeds quality inspection and grading based on machine vision. ASABE Annual International Meeting. 2015;1. DOI 10.13031/aim.20152188378.

Goriewa-Duba K., Duba A., Wachowska U., Wiwart M. An evaluation of the variation in the morphometric parameters of grain of six *Triticum* species with the use of digital image analysis. *Agronomy*. 2018;8(12):296. DOI 10.3390/agronomy8120296.

Haralick R.M. Statistical and structural approaches to texture. *Proc. IEEE*. 1979;67(5):786-804.

Haralick R.M., Shanmugam K., Dinstein I.H. Textural features for image classification. *IEEE Trans. Syst. Man Cybern.* 1973;6: 610-621.

Huang M., Wang Q.G., Zhu Q.B., Qin J.W., Huang G. Review of seed quality and safety tests using optical sensing technologies. *Seed Sci. Technol*. 2015;43(3):337-366.

Khlestkina E.K. Genes determining coloration of different organs in wheat. *Vavilovskii Zhurnal Genetiki i Selektsii = Vavilov Journal of Genetics and Breeding.* 2014;16(1):202-216. (in Russian)

Khlestkina E.K., Pshenichnikova T.A., Usenko N.I., Otmakhova Yu.S. Promising opportunities of using molecular genetic approaches for managing wheat grain technological properties in the context of the "grain–flour–bread" chain. *Russ J. Genet.: Appl. Res.* 2017;7(4):459-476. DOI 10.1134/S2079059717040037.

Körnicke F., Werner H. Die Arten und Varietäten des Getreides. In: Handbuch des Getreidebaus. Vol. 1. Berlin, 1885.

Krupnov V.A., Antonov G.Yu., Druzhin A.E., Krupnova O.V. Preharvest sprouting resistance in spring bread wheat carrying chromosome *6Ag^{i}*(*6D*) from *Agropyron intermedium*. *Vavilovskii Zhurnal Genetiki i Selektsii = Vavilov Journal of Genetics and Breeding.* 2012;16(2):444-450. (in Russian)

Lachman J., Martinek P., Kotíková Z., Orsák M., Šulc M. Genetics and chemistry of pigments in wheat grain – A review. *J. Cereal Sci*. 2017;74:145-154. DOI 10.1016/j.jcs.2017.02.007.

Machálková L., Janečková M., Hřivna L., Dostálová Y., Hernandez J., Mrkvicová E., Vyhnánek T., Trojan V. Impact of added colored wheat bran on bread quality. *Acta Univ. Agric. Silvic.* 2017;65(1):99-104. DOI 10.11118/actaun201765010099.

Majumdar S., Jayas D.S. Classification of bulk samples of cereal grains using machine vision. *J. Agric. Eng. Res*. 1999;73(1):35-47. DOI 10.1006/jaer.1998.0388.

Majumdar S., Jayas D.S. Classification of cereal grains using machine vision: IV. Combined morphology, color, and texture models. *Trans. ASAE*. 2000;43(6):1689. DOI 10.13031/2013.3069.

McCaig T.N., DePauw R.M., Williams P.C. Assessing seed-coat color in a wheat breeding program with a NIR/VIS instrument. *Can. J. Plant Sci*. 1993;73(2):535-539. DOI 10.4141/cjps93-073.

McMullen M., Jones R., Gallenberg D. Scab of wheat and barley: a re-emerging disease of devastating impact. *Plant Dis*. 1997; 81(12):1340-1348. DOI 10.1094/PDIS.1997.81.12.1340.

Olgun M., Onarcan A.O., Özkan K., Işik Ş., Sezer O., Özgişi K., Ayter N.G., Başçiftçi Z.B., Ardiç M., Koyuncu O. Wheat grain classification by using dense SIFT features with SVM classifier. *Comput. Electron. Agric*. 2016;122:185-190. DOI 10.1016/j.compag.2016.01.033.

Pathare P.B., Opara U.L., Al-Said F.A.J. Colour measurement and analysis in fresh and processed foods: A review. *Food Bioprocess Technol*. 2013;6(1):36-60. DOI 10.1007/s11947-012-0867-9.

Patrício D.I., Rieder R. Computer vision and artificial intelligence in precision agriculture for grain crops: A systematic review. *Comput. Electron. Agric*. 2018;153:69-81. DOI 10.1016/j.compag.2018.08.001.

Pearson T. High-speed sorting of grains by color and surface texture. *Appl. Eng. Agric*. 2010;26(3):499-505. DOI 10.13031/2013.29948.

Pearson T., Brabec D., Haley S. Color image based sorter for separating red and white wheat. *Sens. Instrum. Food Qual. Saf*. 2008; 2(4):280-288. DOI 10.1007/s11694-008-9062-0.

Pourreza A., Pourreza H.R., Abbaspour-Fard M.H., Sadrnia H. Identification of nine Iranian wheat seed varieties by textural analysis with image processing. *Comput. Electron. Agric*. 2012; 83:102-108. DOI 10.1016/j.compag.2012.02.005.

Ram M.S., Dowell F.E., Seitz L., Lookhart G. Development of standard procedures for a simple, rapid test to determine wheat color class. *Cereal Chem*. 2002;79(2):230-237. DOI 10.1094/CCHEM.2002.79.2.230.

Sabanci K., Ekinci S., Karahan A.M., Aydin C. Weight estimation of wheat by using image processing techniques. *J. Image Graph*. 2016;4(1):51-54. DOI 10.18178/joig.4.1.51-54.

Sabanci K., Toktas A., Kayabasi A. Grain classifier with computer vision using adaptive neuro-fuzzy inference system. *J. Sci. Food Agric*. 2017;97(12):3994-4000. DOI 10.1002/jsfa.8264.

Septiningsih E.M., Prasetiyono J., Lubis E., Tai T.H., Tjubaryat T., Moeljopawiro S., McCouch S.R. Identification of quantitative trait loci for yield and yield components in an advanced backcross population derived from the *Oryza sativa* variety IR64 and the wild relative *O. rufipogon*. *Theor. Appl. Genet*. 2003;107(8): 1419-1432. DOI 10.1007/s00122-003-1373-2.

Shen Y., Jin L., Xiao P., Lu Y., Bao J. Total phenolics, flavonoids, antioxidant capacity in rice grain and their relations to grain color, size and weight. *J. Cereal Sci*. 2009;49(1):106-111. DOI 10.1016/j.jcs. 2008.07.010.

Shoeva O.Yu., Strygina K.V., Khlestkina E.K. Genes determining the synthesis of flavonoid and melanin pigments in barley. *Vavilovskii Zhurnal Genetiki i Selektsii = Vavilov Journal of Genetics and Breeding*. 2018;22(3):333-342. DOI 10.18699/VJ18.369. (in Russian)

Souza F.H., Marcos-Filho J.Ú.L.I.O. The seed coat as a modulator of seed-environment relationships in Fabaceae. *Braz. J. Bot*. 2001; 24(4):365-375. DOI 10.1590/S0100-84042001000400002.

Szczypiński P.M., Klepaczko A., Zapotoczny P. Identifying barley varieties by computer vision. *Comput. Electron. Agric*. 2015; 110:1-8. DOI 10.1016/j.compag.2014.09.016.

Szczypiński P.M., Strzelecki M., Materka A., Klepaczko A. MaZda – a software package for image texture analysis. *Comput. Methods Prog. Biomed*. 2009;94(1):66-76. DOI 10.1016/j.cmpb.2008.08.005.

Visen N.S., Paliwal J., Jayas D.S., White N.D.G. Ae – automation and emerging technologies: specialist neural networks for cereal grain classification. *Biosyst. Eng.* 2002;82(2):151-159. DOI 10.1006/bioe.2002.0064.

Žilić S., Serpen A., Akıllıoğlu G., Gökmen V., Vančetović J. Phenolic compounds, carotenoids, anthocyanins, and antioxidant capacity of colored maize (*Zea mays* L.) kernels. *J. Agric. Food Chem.* 2012;60(5):1224-1231. DOI 10.1021/jf204367z.

ORCID ID

D.A. Afonnikov orcid.org/0000-0001-9738-1409

Acknowledgements. The work was funded by the Kurchatov Genomic Center of the Institute of Cytology and Genetics of Siberian Branch of the Russian Academy of Sciences (Novosibirsk, Russia) according to the agreement with the Ministry of Education and Science RF, No. 075-15-2019-1662.

Conflict of interest. The authors declare no conflict of interest.

Received December 27, 2019. Revised April 03, 2020. Accepted April 07, 2020.

Вавиловский журнал генетики и селекции. 2020;24(4):348-355
DOI 10.18699/VJ20.627

NGS-секвенирование в селекционно-генетических исследованиях ячменя

И.В. Розанова[1, 2] ✉, Е.К. Хлесткина[1, 2]

[1] Федеральный исследовательский центр Всероссийский институт генетических ресурсов растений имени Н.И. Вавилова (ВИР), Санкт-Петербург, Россия
[2] Федеральный исследовательский центр Институт цитологии и генетики Сибирского отделения Российской академии наук, Новосибирск, Россия
✉ e-mail: i.rozanova@vir.nw.ru

Аннотация. Ячмень (*Hordeum vulgare* L.) – один из важнейших видов злаковых растений, используемых в качестве продовольственной и кормовой культуры, а также для пивоварения и производства спирта. В конце прошлого столетия к традиционным методам селекции прибавились методы, основанные на применении ДНК-маркеров. Молекулярные маркеры также активно вовлекаются в процессы молекулярно-генетического картирования и анализа QTL (quantitative trait loci). В 2012 г. было завершено секвенирование генома ячменя, что выявило целый спектр новых возможностей – от более эффективного поиска генов-кандидатов хозяйственно ценных признаков до геномной селекции. В обзоре обобщены результаты работ периода после секвенирования генома ячменя, открывшего новые направления генетики и селекции этой культуры с применением высокопроизводительных методов секвенирования и генотипирования. В рассматриваемый период ведутся интенсивные исследования по идентификации геномных локусов ячменя, ассоциированных с хозяйственно ценными признаками, появились и пополняются ресурсы для работы с геномными данными ячменя и для их депонирования. В последние годы для массового поиска ассоциаций между фенотипом и генотипом используется анализ GWAS (genome wide association studies), широкое применение которого на ячмене стало возможным с 2010 г. благодаря разработанным SNP-чипам, а также методам генотипирования, основанным на прямом NGS-секвенировании (next generation sequencing) выборочных фракций генома. К настоящему времени опубликовано более 80 работ, описывающих результаты GWAS-анализа на ячмене. Идентификация SNP, ассоциированных с хозяйственно ценными признаками, и их преобразование в удобные для скрининга селекционного материала CAPS или KASP-маркеры существенно расширяют возможности маркер-ориентированной селекции ячменя. Кроме того, имеющаяся информация о потенциальных генах-мишенях и качество полногеномной последовательности ячменя представляют достаточную базу для применения технологий геномного редактирования с целью создания исходного материала для селекции сортов с заданными свойствами.
Ключевые слова: *Hordeum vulgare*; SNP; ячмень; геном; секвенирование; высокопроизводительное генотипирование; геномное редактирование.

Для цитирования: Розанова И.В., Хлесткина Е.К. NGS-секвенирование в селекционно-генетических исследованиях ячменя. *Вавиловский журнал генетики и селекции*. 2020;24(4):348-355. DOI 10.18699/VJ20.627

NGS sequencing in barley breeding and genetic studies

I.V. Rozanova[1, 2] ✉, E.K. Khlestkina[1, 2]

[1] Federal Research Center the N.I. Vavilov All-Russian Institute of Plant Genetic Resources (VIR), St. Petersburg, Russia
[2] Institute of Cytology and Genetics of Siberian Branch of the Russian Academy of Sciences, Novosibirsk, Russia
✉ e-mail: i.rozanova@vir.nw.ru

Abstract. Barley (*Hordeum vulgare* L.) is the one of the most important cereal species used as food and feed crops, as well as for malting and alcohol production. At the end of the last century, traditional breeding techniques were complemented by the use of DNA markers. Molecular markers have also been used extensively for molecular genetic mapping and QTL analysis. In 2012, the barley genome sequencing was completed, which provided a broad range of new opportunities – from a more efficient search for candidate genes controlling economically important traits to genomic selection. The review summarizes the results of the studies performed after barley genome sequencing, which discovered new areas of barley genetics and breeding with high throughput screening and genotyping methods. During this period, intensive studies aimed at identification of barley genomic loci associated with economically important traits have been carried out; online databases and tools for working with barley genomic data and their deposition have appeared and are being replenished. In recent years, GWAS analysis has been used for large-scale phenotype-genotype association studies, which has been widely used in barley since 2010 due to the developed SNP-arrays, as well as genotyping methods based on direct NGS sequencing of selected fractions of the genome. To date, more than 80 papers have been published that describe the results of the GWAS analysis in barley. SNP identification associated with economically important traits and their transformation into CAPS or KASP markers convenient for screening

selection material significantly expands the possibilities of marker-assisted selection of barley. In addition, the currently available information on potential target genes and the quality of the whole barley genome sequence provides a good base for applying genome editing technologies to create material for the creation of varieties with desired properties.
Key words: *Hordeum vulgare*; SNP; barley; genome; sequencing; throughput genotyping; genomic editing.

For citation: Rozanova I.V., Khlestkina E.K. NGS sequencing in barley breeding and genetic studies. *Vavilovskii Zhurnal Genetiki i Selektsii = Vavilov Journal of Genetics and Breeding*. 2020;24(4):348-355. DOI 10.18699/VJ20.627 (in Russian)

Введение

Ячмень (*Hordeum vulgare* L.) – одна из важнейших сельскохозяйственных культур, занимающая пятое место в мире после пшеницы, кукурузы, риса и сои по площади посевов (47 млн га), согласно данным 2017 г. (http://www.fao.org/faostat/ru/). Зерно ячменя идет в основном на кормопроизводство (до двух третей от всего урожая), пивоваренную промышленность и производство спирта (около одной трети) и лишь небольшой процент приходится на долю продовольственного, т. е. применяемого для пищи человека (в Российской Федерации, по данным 2017 г., – 0.12 %, http://www.fao.org/faostat/ru/). Кроме того, отмечен рост значимости ячменя как источника сырья для производства крахмала и крахмалопродуктов пищевого и технического назначения (Blennow et al., 2013).

По сравнению с основным хлебным злаком – пшеницей – ячмень неприхотлив, легче адаптируется к неблагоприятным условиям окружающей среды – холоду, засухе, лучше переносит защелачивание и засоление почвы, недостаток питательных веществ в ней. Раннее созревание в сочетании с высокой адаптивностью позволили ячменю как сельскохозяйственной культуре распространиться по всему миру – от экватора до северных и южных широт – более чем в 100 странах мира (http://www.fao.org/faostat/ru/). Благодаря ряду биологических особенностей ячменя (относительно короткий жизненный цикл, самоопыление, диплоидный геном) современные молекулярно-генетические и геномные исследования этой культуры продвигаются динамичнее, чем в случае других представителей Triticeae, в частности пшеницы и ржи (Hayes, Szucs, 2006; Schulte et al., 2009). Вследствие этого ячмень служит модельным растением, а полученные данные о его генах и геноме используются для продолжения генетических исследований на других представителях трибы Triticeae.

Развитие методов NGS-секвенирования позволило получить качественные полногеномные последовательности многих видов растений (Брагина и др., 2019), включая ячмень (International Barley Genome Sequencing Consortium, 2012) и пшеницу (Appels et al., 2018). Секвенирование геномов, а вслед за этим секвенирование транскриптомов и микроРНКомов вывели на новый этап исследования о функционировании наследственного материала. Получаемые сведения применяются для маркер-контролируемого отбора в селекционном процессе, а также для разработки принципиально новых технологий создания исходного селекционного материала с заданными свойствами на основе геномного редактирования (Хлесткина, Шумный, 2016; Korotkova et al., 2019).

Цель настоящего обзора – обобщить результаты генетико-селекционных работ, базирующихся на применении методов NGS-секвенирования.

Секвенирование генома ячменя и его структурная организация

Для секвенирования генома ячменя в 2006 г. был сформирован Международный консорциум (International Barley Genome Sequencing Consortium…, 2012), который изначально включал в себя исследователей из восьми научных организаций шести стран: Германии, США, Австралии, Японии, Финляндии и Шотландии. Позднее к консорциуму присоединились группы ученых из Великобритании, Израиля, Франции и Италии.

К 2009 г. был собран первый вариант последовательности генома ячменя (сорт Morex), которая была необходима для дальнейшего секвенирования генома, но вместе с тем оказалась полезной и широкому кругу исследователей, нацеленных на выделение отдельных генов, контролирующих хозяйственно ценные признаки (Schulte et al., 2009). Основу физической карты составили более 83 тыс. ген-содержащих BAC-клонов (bacterial artificial chromosome, бактериальных искусственных хромосом), которые исследовались методом гибридизации с применением избыточных зондов (метод overgo) (Madishetty et al., 2007). Данные были получены с помощью высокопроизводительного фингерпринтинга (fingerprinting) (Luo et al., 2003).

В 2012 г. создана референсная карта генома ячменя (International Barley Genome Sequencing Consortium…, 2012). Для этого были секвенированы и проанализированы последовательности 571 тыс. ген-содержащих BAC-клонов из шести независимых геномных библиотек.

В дальнейшем работы по уточнению полногеномной физической карты были продолжены. В частности, использован метод MTP (minimum tiling path), основанный на принципе минимального количества составных частей карты при максимальной плотности покрытия (Ariyadasa et al., 2014). Кроме того, разработана ультраплотная генетическая карта. Для этого было проведено генотипирование на основе высокопроизводительного секвенирования потомства из 90 рекомбинантных инбредных линий (RILs) от скрещивания Morex*Barke (M × B) и 82 дигаплоидных линий (DH) из картирующей популяции Oregon Wolfe Barley (Cistué et al., 2011). Сконструированные генетические карты были соотнесены с физической картой сорта Morex, полученной в результате работы Консорциума (Mascher et al., 2013). Таким образом, генетические локусы были сопоставлены с положением на физической карте. Суммарная длина прочитанного и собранного генома ячменя составила 4.98 Гб – более 95 % генома, если учесть, что, согласно имеющимся оценкам, 100 % – это 5.1 Гб.

Полученный материал позволил создать ресурсы (Приложение 1)[1], ценные для дальнейших исследований, на-

[1] Приложения 1 и 2 см. по адресу:
http://www.bionet.nsc.ru/vogis/download/pict-2020-24/appx4.pdf

правленных на изучение функциональной организации генов и генома ячменя, и для прикладных работ, нацеленных на выведение новых улучшенных сортов, в том числе с применением методов селекции следующего поколения (next-generation breeding), а именно систем генетического редактирования.

Структурная организация генома ячменя

Согласно распределению уникальных последовательностей и повторов в хромосомах ячменя, выделяют три зоны. Зона 1 – дистальная – характеризуется большим количеством низкокопийных элементов (low-copy regions, LCRs), высоким содержанием генов и высокой частотой мейотических рекомбинаций. Зона 2, занимающая промежуточное положение на хромосомах, обладает средней плотностью генов. В третьей зоне, проксимальной, количество генов минимальное (Mascher et al., 2017).

Выделенные зоны различаются не только по количеству генов, но и по их специализации. Так, в проксимальных (прицентромерных) участках хромосом, расположены главным образом «гены домашнего хозяйства» – консервативные гены, важные для жизнедеятельности клетки, мутации по которым, как правило, летальные. Эта фракция генома не является материалом для искусственного отбора. Гены, потенциально интересные для селекционеров, например участвующие в защитном ответе и репродуктивных процессах, расположены преимущественно в дистальных районах (концевые участки хромосом), которые, в противоположность проксимальным, характеризуются высокой частотой рекомбинации (Mascher et al., 2017).

Большая часть генома растений состоит в основном из очень похожих копий повторяющихся элементов, таких как ДНК-транспозоны (MITE, miniature inverted-repeat transposable elements, CACTA-элементы) и ретротранспозоны, включая LTR (long terminal repeats – ретротранспозоны с длинными концевыми повторами) и LINE (long interspersed nuclear element – подтип с длинными диспергированными повторами). В настоящее время считается, что эти элементы играют значительную роль в функциональной организации и эволюции геномов растений. Сравнение с библиотекой повторов, специфичной для Triticeae, выявило, что 3.7 Гб (80.8 %) от собранного генома ячменя относится к мобильным элементам, причем только 10 % этих элементов потенциально активны (Mascher et al., 2017). Повторы MITEs и LINEs в основном представлены в богатых генами дистальных районах в зоне 1. Локализация LTR-ретротранспозонов зависит от их типа: *Ty3-Gypsy*-ретротранспозоны обнаружены в зоне 3, тогда как *Ty1-Copia* преимущественно располагаются в зонах 1 и 2.

Для генома ячменя характерно распределение разных мобильных элементов в зависимости от положения относительно генов. Мобильные элементы небольшого размера (например, транспозоны *Mariner*, относящиеся к семейству MITE) предпочтительно находятся в пределах 1 Кб, фланкируя кодирующие области генов, в то время как мобильные элементы более крупного размера (например, Harbinger, второе семейство MITE и LINEs) находятся на значительно более удаленном расстоянии от генов. Полученное распределение различных типов мобильных элементов среди генов может отражать давление отбора, которое позволяет только небольшим элементам, а именно транспозонам *Mariners*, находиться ближе всего к генам (Mascher et al., 2017). На большем расстоянии от генов доминируют мобильные элементы большого размера, такие как LTR-ретротранспозоны и транспозоны семейства CACTA.

Пространственная организация генома ячменя

Полученная референсная последовательность генома ячменя также позволила исследовать пространственную организацию хроматина в ядре при помощи метода Hi-C (Mascher et al., 2017). Результаты подтвердили заключения, сделанные на основе более ранних исследований с применением методов микроскопии (Щапова, 1971; Künzel et al., 2000), о том, что хромосомы в ядрах ячменя принимают положение, известное в литературе под термином “Rabl orientation” (Cowan et al., 2001). Это конфигурация, при которой каждая хромосома в интерфазном ядре занимает место, во многом задаваемое позицией в анафазе предшествующего митоза. При этом хромосомы располагаются следующим образом: центромеры хромосом находятся на одном полюсе ядра, а теломеры ориентированы к противоположному.

После основополагающей работы А.И. Щаповой (1971) было уточнено, что описанная конфигурация сохраняется у таких видов растений, как ячмень, пшеница, рожь и овес, во всех клетках растения (Anamthawat-Jónsson, Heslop-Harrison, 1990), у риса – только в клетках ксилемы корня и в недифференцированных клетках пыльника (Prieto et al., 2004), у кукурузы и сорго подобной конфигурации хромосом не обнаружено (Dong, Jiang, 1998).

Ранее было также установлено (Щапова, 1971), что ячмень обладает сходными по размеру плечами хромосом, тогда как у большинства видов эукариот все плечи по длине различаются и местоположение каждой хромосомы определено размерами ее плеч. Благодаря поляризации хромосомы складываются, как книжка, сопоставляя длинные и короткие плечи, в результате чего короткое плечо одной хромосомы имеет возможность взаимодействовать с локусами, расположенными на относительно таком же расстоянии от центромеры на длинном плече. Была отмечена также более высокая частота контактов между прителомерными регионами. При этом не имеет значения, гомологичны хромосомы или нет, контакты между материнской и отцовской хромосомами имеют место так же часто, как и между негомологами (Mascher et al., 2017).

Методы NGS-секвенирования для анализа полиморфизма ДНК как инструмента повышения эффективности маркер-ориентированной селекции

В основе картирования и маркирования генов и идентификации различных аллельных вариантов и в разработке технологий ускоренного и направленного отбора селекционного материала (маркер-ориентированная и геномная селекция) лежит анализ полиморфизма ДНК. Методы анализа полиморфизма ДНК «эволюционировали» от трудоемких подходов, основанных на блот-гибридизации (например, restriction fragment length polymorphism,

RFLP – полиморфизм длины рестрикционных фрагментов) (Botstein et al., 1980) до гораздо менее трудоемких методов, основанных на полимеразной цепной реакции (ПЦР). Среди последних можно выделить такие ДНК-маркеры, как SSR – simple sequence repeats – простые повторяющиеся последовательности (Tautz, Renz 1984), STS – sequence tagged site – последовательности, характеризующие локус (Olson et al., 1989), и другие (Хлесткина, 2011). Позже появились высокопроизводительные методы с возможностью полной автоматизации процесса, такие как анализ SNP – single-nucleotide polymorphism – однонуклеотидный полиморфизм (Wang et al., 1998). Выявление SNP – результат работ по секвенированию и ресеквенированию сначала отдельных фракций, а затем и полных геномов.

Появление, быстрое развитие и удешевление технологий секвенирования нового поколения (next generation sequencing, NGS) не только позволили секвенировать один за другим геномы хозяйственно значимых видов растений и животных (Хлесткина, 2013; Брагина и др., 2019), но и сделали возможными быстрое определение полиморфизма тысяч генов и разработку SNP-чипов для анализа генетического и селекционного материала. Для выявления SNP достаточно ресеквенировать небольшую выборку образцов. Полученные данные могут быть использованы для разработки SNP-чипов, пригодных к генотипированию больших выборок растений в относительно экономном режиме с большой пропускной способностью анализа.

Позже на основе NGS-секвенирования были разработаны методы высокопроизводительного генотипирования, основанные на прямом секвенировании выборочных фракций генома изучаемых образцов. Один из них – метод GBS (genotyping-by-sequencing), впервые описанный в 2011 г. (Elshire et al., 2011), был успешно применен для генотипирования 276 рекомбинантных инбредных линий кукурузы и 43 дигаплоидных линий ячменя из картирующей популяции Oregon Wolfe Barley. В настоящее время термин “GBS” используется уже как обобщающий для различных разрабатываемых методов высокопроизводительного генотипирования, основанного на NGS-секвенировании (Rasheed et al., 2017). Геномная ДНК при этом обрабатывается эндонуклеазами рестрикции, далее создается библиотека фрагментов, при секвенировании их получают короткие прочтения (~100 пар нуклеотидов), объединяемые в контиги, выравнивание которых позволяет обнаружить SNP (Davey et al., 2011). Преимущество метода заключается в том, что его можно применять для анализа образцов не только видов с уже расшифрованным геномом, но и менее изученных видов, для которых еще не выполнена полногеномная сборка. Похожий на GBS метод RAD-seq (restriction-site-associated DNA sequencing), схожий в основе с методом GBS (используется подобный протокол секвенирования, основанный на присутствии в геноме сайтов узнавания эндонуклеазами рестрикции), но отличающийся протоколом подготовки библиотек (Chutimanitsakun et al., 2011; Andrews et al., 2016).

Метод GBS применяется для выявления взаимосвязи между фенотипом и генотипом на основе анализа двуродительских картирующих популяций (QTL-анализ – quantitative trait loci) или выборок сортообразцов (GWAS-анализ – genome wide association studies). Выявленные в результате этих работ геномные районы, ассоциированные с проявлением того или иного селекционно значимого свойства, сразу маркированы SNP-маркером. Если геном изучаемого вида уже секвенирован, то информация об обнаруженном районе генома, ассоциированного с признаком, может быстро привлекаться для поиска гена-кандидата, влияющего на изменчивость по данному признаку. Метод GBS только начинает применяться на ячмене (Fan et al., 2017; Darrier et al., 2019; Goddard et al., 2019), а результаты использования SNP-чипов уже применяются более 10 лет.

Высокопроизводительное генотипирование ячменя впервые апробировано в 2005 г. (Rostoks et al., 2005) на основе технологии Illumina GoldenGate (Fan et al., 2003). Первые коммерчески доступные чипы для генотипирования ячменя появились в 2009 г. (Close et al., 2009). Для его создания было выбрано и протестировано 4596 SNP на 576 ДНК-образцах для двух пилотных чипов OPA, POPA1 и POPA2, и на 480 ДНК-образцах для третьего пилотного чипа – POPA3. Далее было выбрано 3072 SNP, которые прошли качественный контроль и были генетически информативны. Они составили две производные OPA – BOPA1 и BOPA2, которые планировалось использовать для дальнейших исследований генофонда ячменя. Из 3072 SNP, выбранных для изучения, 2279 были получены из библиотек EST, а 793 – путем секвенирования ПЦР-ампликонов. В результате в платформу для генотипирования, содержащую 3072 маркера, вошли два чипа, BOPA1 и BOPA2, каждый из которых содержал по 1536 маркеров SNP, и они имели различные дизайны генотипирования (Close et al., 2009). Следующий чип был разработан Illumina Infinium iSelect 9K Custom Genotyping BeadChip (Comadran et al., 2012) и включал в себя 2832 маркера, разработанных для предыдущей технологии GoldenGate, и 5010 дополнительных маркеров, основанных на обнаружении маркеров SNP в данных Illumina RNA-seq из 10 элитных сортов Великобритании (Bayer et al., 2017).

По мере снижения затрат на секвенирование постоянно росло число обнаруживаемых SNP. Поэтому на следующем этапе платформа 9K Infinium iSelect была расширена до 50K. Чип 50K включил около 6000 SNP из предыдущего чипа 9K и новые SNP, выявленные для ячменя на основе захвата экзома. Это эффективный метод, позволяющий проводить исследования генома по выбранным локусам, которые с большей вероятностью будут содержать полиморфизмы, сцепленные с интересуемыми признаками фенотипа (https://ics.hutton.ac.uk/50k; Bayer et al., 2017).

Методы анализа ассоциаций между геномными вариантами и фенотипическими признаками: QTL-анализ и GWAS

Первым методом поиска взаимосвязи генотипа с фенотипом, получившим широкое распространение, стал QTL-анализ, или метод анализа локусов количественных признаков при использовании двуродительских популяций. При этом для изучения признака исследуется популяция потомства от контрастных по признаку родителей (Kearsey, Farquhar, 1998). Такой анализ на ячмене осуществляется с 1989 г. (Jensen, 1989), для него применялись раз-

личные типы маркеров, начиная с RFLP. В 2003–2010 гг. преобладали исследования, в которых QTL-анализ двуродительских популяций ячменя проводился на основе данных генотипирования, полученных при помощи SSR-маркеров. С 2010 г. для QTL-анализа ячменя преимущественно применялись популяции, генотипированные с помощью SNP-маркеров. С 2014 г. начали использоваться методы прямого секвенирования: GBS и RAD (Andrews et al., 2016; Darrier et al., 2019). Картирование значимых локусов с применением QTL-анализа дает высокую статистическую значимость для определяемого QTL, но в то же время имеет низкое разрешение. Существенный недостаток метода – ограничение генетического разнообразия родителей выбранной популяции (Hyne, Kearsey, 1995).

В последние годы для массового поиска ассоциаций между фенотипом и генотипом используется GWAS-анализ. На ячмене он применяется с 2010 г. (Lorenz et al., 2010). Сравнительный анализ работ показывает, что на основе GWAS обнаруживается больше новых локусов, по сравнению с QTL-анализом двуродительских популяций (Pauli et al., 2014). Преимущество метода заключается в высоком разрешении, вплоть до одного нуклеотида. Ассоциированный с признаком аллель детектируется частотой его наличия в популяции. Однако в этом случае можно упустить редкий аллель, так как значимость определения локуса будет зависеть от той же частоты аллеля. Для выявления локусов методом GWAS изучаемая популяция должна быть как можно более разнородна. Метод чувствителен к структуре популяции. Неправильно сформированная популяция может привести к установлению ложноположительных ассоциаций.

Метод GWAS – достаточно новый, и, как видно по данным анализа публикаций, индексируемых в базе данных Scopus (рис. 1), в течение последних лет количество работ, выполненных с применением GWAS на ячмене, неуклонно возрастает. В настоящее время благодаря этому подходу обнаружены геномные районы, ассоциированные со многими признаками ячменя. Для нахождения компонентов урожайности и качества зерна ячменя с помощью GWAS изучаются агрономические признаки: высота растения, длина колоса, количество зерен в колосе, масса 1000 зерен, количество продуктивных побегов. Существует ~40 работ по исследованиям с использованием GWAS устойчивости ячменя к различным болезням и ~25 работ – по устойчивости к абиотическому стрессу – засухоустойчивости, устойчивости к засолению и др. Помимо этого, выполнены работы по изучению свойств крахмала, содержания белка, β-глюкана и микроэлементов в зерне. (Более подробно обзор работ представлен в Приложении 2.)

Таким образом, для метода GWAS чаще всего используются SNP-чипы; SSR и DArT применяются редко, они были актуальны до разработки SNP-чипов и GBS (DArT – это, по сути, аналог GBS, но с применением чипов, а не прямого секвенирования). Метод GBS только начинает применяться для анализа полиморфизмов ДНК ячменя, ожидается, что он получит дальнейшее распространение.

Как можно судить по публикациям, индексируемым в базе данных Scopus (рис. 2), работы по GWAS-анализу в равной мере направлены на проблемы устойчивости к фитопатогенам и вредителям (биотический стресс), толерантности к неблагоприятным абиотическим факторам окружающей среды и на повышение продуктивности растений.

Селекция на устойчивость позволяет сокращать потери урожая, вызываемые фитопатогенами и вредителями. В настоящее время бóльший успех наблюдается в идентификации генетических маркеров для признаков

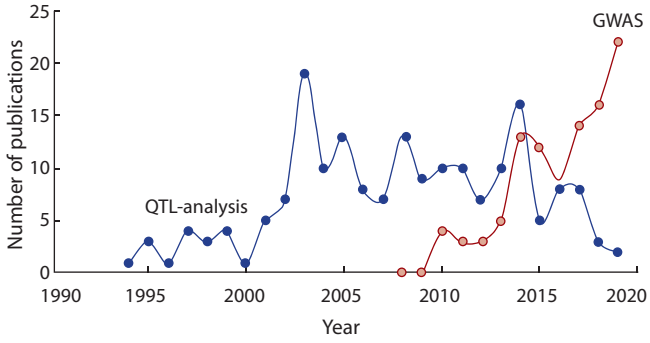

Fig. 1. The numbers of publications on QTL and GWAS in barley revealed by queries "barley + genome-wide-association" and "barley + QTL-analysis" in the Scopus database (Website: http://scopus.com as to August 28, 2019).

The summary on different techniques of DNA polymorphism analysis and different approaches (QTL and GWAS) to the identification of loci associated with commercially important barley traits

DNA polymorphism analysis technique	QTL-analysis	GWAS
RFLP	56	0
SSR	83	5
DArT	41	16
SNP-chip	78	58
GBS	7	2
RAD	4	0

Note: The numbers of articles found in the Scopus database as to August 29, 2019 are indicated.

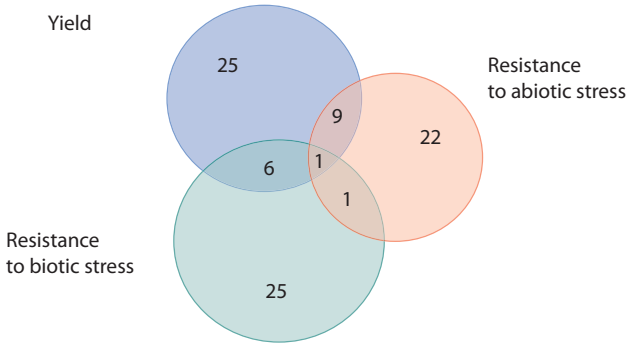

Fig. 2. The genome-wide association (GWAS) in barley: number of publications revealed in the Scopus database as to August 29, 2019 by keyword intersection queries.

устойчивости к болезням, имеющих моно- или олигогенный контроль (ржавчинные болезни, головня, мучнистая роса). Сложнее идентифицировать генетические маркеры для устойчивости зерновых культур к фузариозу колоса, септориозам, гельминтоспориозным пятнистостям, корневым гнилям и другим болезням (Афанасенко, 2016). Часто уровень фенотипического проявления устойчивости зависит не от одного гена, а от суммарного эффекта всех генов устойчивости. Это ведет к постановке задачи перед исследователями – создать сорта с полигенной устойчивостью, обеспечивающей средний уровень устойчивости, что выражается в замедленном развитии болезней. Эта задача отягощается тем, что возникают новые патотипы (Ghazvini, Tekauz, 2007; Leng et al., 2016).

Как использовать данные, полученные с помощью GWAS, в дальнейших программах селекции? Исследования установленных геномных районов позволяют идентифицировать, валидировать и маркировать гены-кандидаты. Можно и без поиска генов-кандидатов преобразовать выявленные SNP в удобные KASP- или CAPS-маркеры (Konieczny, Ausubel, 1993; Kumpatla et al., 2012; Semagn et al., 2014; Shavrukov, 2015), проверить их на независимых выборках и, при успешной валидации, рекомендовать применять эти маркеры для отбора селекционного материала. Этот подход может быть эффективен в случае локусов, существенно влияющих на изменение фенотипа. Полученная в результате GWAS-анализа информация о локусах с малым эффектом или локусах, эффект которых существенно зависит от генотипа, не будет играть роли для программ по маркер-ориентированной селекции, однако она является основой для развития работ по геномной селекции.

Геномное редактирование

Наличие полногеномных последовательностей и известных последовательностей-мишеней для внесения заданных мутаций позволяет осуществлять редактирование целевых генов на основе систем ZFNs, TALENs и CRISPR/Cas, изменяя тем самым свойства растений (Хлесткина, Шумный, 2016). Системы ZFNs и TALENs не получили широкого распространения из-за сложности исполнения. Система геномного редактирования CRISPR/Cas наоборот оказалась достаточно простой и значительно способствовала развитию геномного редактирования растений. Система CRISPR/Cas применяется на растениях более пяти лет. За это время она успешно апробирована на 24 культурах, для 16 из них, включая ячмень, получены модификации более 80 селекционно значимых генов (Короткова и др., 2017; Korotkova et al., 2019). Работы по редактированию генов ячменя ведутся преимущественно на модельном сорте Golden Promise. Редактированы несколько селекционно значимых генов ячменя. Так, в 2015 г. T. Lawrenson с коллегами (2015) сделали неработоспособными две копии гена *HvPM19*, кодирующего ABA-индуцируемый белок плазматической мембраны, что привело к сокращению продолжительности периода покоя семян. Полученные растения несут мутантные копии гена-мишени, но не являются при этом трансгенными. В 2018 г. N. Kumar с коллегами (2018) нокаутировали ген *MORC1* – негативный регулятор устойчивости к грибным патогенам, а S.V. Gerasimova с коллегами (2018a) получили голозерные растения из пленчатых растений сорта Golden Promise, выведя из строя ген *Nud1*. Кроме того, при использовании метода трансфекции протопластов была впервые показана возможность успешной модификации генома немодельного сорта ячменя – сибирского сорта Алей (Gerasimova et al., 2018b).

Таким образом, существующая на сегодняшний день информация о потенциальных генах-мишенях и качество полногеномной последовательности ячменя представляют хорошую базу для применения технологий геномного редактирования с целью создания исходного материала для селекции сортов с заданными свойствами. Лимитирующим фактором для развития этого направления служит проблема получения растений-трансформантов других сортов ячменя, кроме модельного.

Изучение потомства от скрещивания сорта Golden Promise с сортами, обладающими низкой эффективностью трансформации, дало возможность выявить десять локусов, получивших наименования *TFA1–TFA10* (transformation amenability). H. Hisano с коллегами (2017) представили способ получения генотипов, на которых в дальнейшем планируется проведение геномного редактирования, при этом в качестве донора генов эффективности трансформации (*TFA1*, *TFA2* и *TFA3*) предложено использовать Golden Promise.

Заключение

Благодаря секвенированию генома ячменя, которое было завершено в 2012 г., произошла интенсификация генетических исследований, направленных на расшифровку механизмов формирования хозяйственно ценных признаков. Информация о последовательности генома оказалась полезной для широкого круга исследований. С помощью методов QTL и GWAS при применении SNP- и GBS-генотипирования выявлен ряд новых геномных районов, сцепленных с хозяйственно ценными признаками. В настоящее время результаты секвенирования в совокупности с технологиями высокопроизводительного генотипирования можно использовать для эффективного направленного отбора нужных генотипов среди селекционных линий, что существенно ускорит создание новых сортов ячменя с заданными характеристиками.

Список литературы / References

Афанасенко О.С. Генетическая защита растений: проблемы и перспективы. *Защита и карантин растений*. 2016;1:13-16.
[Afanasenko O.S. Genetic plant protection: problems and prospects. *Zaschita i Karantin Rasteniy = Plant Protection and Quarantine*. 2016;1:13-16. (in Russian)]

Брагина М.К., Афонников Д.А., Салина Е.А. Прогресс в секвенировании геномов растений – направления исследований. *Вавиловский журнал генетики и селекции*. 2019;23(1):38-48. DOI 10.18699/VJ19.459.
[Bragina M.K., Afonnikov D.A., Salina E.A. Progress in plant genome sequencing: research directions. *Vavilovskii Zhurnal Genetiki i Selektsii = Vavilov Journal of Genetics and Breeding*. 2019;23(1): 38-48. DOI 10.18699/VJ19.459. (in Russian)]

Короткова А.М., Герасимова С.В., Шумный В.К., Хлесткина Е.К. Гены сельскохозяйственных растений, модифицированные с помощью системы CRISPR/Cas. *Вавиловский журнал генетики и селекции*. 2017;21(2):250-258. DOI 10.18699/VJ17.244.

[Korotkova A.M., Gerasimova S.V., Shumny V.K., Khlestkina E.K. Crop genes modified using CRISPR/Cas system. *Russ. J. Genet. Appl. Res*. 2017;7(8):822-832. DOI 10.1134/S2079059717050124.]

Хлесткина Е.К. Молекулярные методы анализа структурно-функциональной организации генов. *Вавиловский журнал генетики и селекции*. 2011;15(4):757-768.
[Khlestkina E.K. Molecular methods of the analysis of the structural and functional organization of genes and genomes in higher plants. *Vavilovskii Zhurnal Genetiki i Selektsii = Vavilov Journal of Genetics and Breeding*. 2011;15(4):757-768. (in Russian)]

Хлесткина Е.К. Молекулярные маркеры в генетических исследованиях и в селекции. *Вавиловский журнал генетики и селекции*. 2013;17(4/2):1044-1054.
[Khlestkina E.K. Molecular markers in genetic studies and breeding. *Vavilovskii Zhurnal Genetiki i Selektsii = Vavilov Journal of Genetics and Breeding*. 2013;17(4/2):1044-1054. (in Russian)]

Хлесткина Е.К., Шумный В.К. Перспективы использования прорывных технологий в селекции: система CRISPR/Cas9 для редактирования генома растений. *Генетика*. 2016;52(7):774-787. DOI 10.7868/s0016675816070055.
[Khlestkina E.K., Shumny V.K. Prospects for application of breakthrough technologies in breeding: The CRISPR/Cas9 system for plant genome editing. *Russ. J. Genet*. 2016;52(7):676-687. DOI 10.1134/S102279541607005X.]

Щапова А.И. О структуре кариотипа и порядке расположения хромосом в интерфазном ядре. *Цитология*. 1971;13(9):1157-1163.
[Schapova A.I. On the karyotype structure and chromosome location order in the interphase nurclear. *Tsitologiya = Cytology.* 1971;13(9): 1157-1163. (in Russian)]

Anamthawat-Jónsson K., Heslop-Harrison J.S. Centromeres, telomeres and chromatin in the interphase nucleus of cereals. *Caryologia*. 1990;43(3-4):205-213. DOI 10.1080/00087114.1990.10796999.

Andrews K.R., Good J.M., Miller M.R., Luikart G., Hohenlohe P.A. Harnessing the power of RADseq for ecological and evolutionary genomics. *Nat. Rev. Genet*. 2016;17(2):81-92. DOI 10.1038/nrg.2015.28.

Appels R., Eversole K., Feuillet C., Keller B., Rogers J., Stein N., Pozniak C.J., ..., Visendi P., Cui L., Du X., Feng K., Nie X., Tong W., Wang L. Shifting the limits in wheat research and breeding using a fully annotated reference genome. *Science.* 2018;361(6403): eaar7191. DOI 10.1126/science.aar7191.

Ariyadasa R., Mascher M., Nussbaumer T., Schulte D., Frenkel Z., Poursarebani N., Zhou R., Steuernagel B., Gundlach H., Taudien S., Felder M., Platzer M., Himmelbach A., Schmutzer T., Hedley P.E., Muehlbauer G.J., Scholz U., Koro A., Mayer K.F.X., Waugh R., Langridge P., Graner A., Stein N. A sequence-ready physical map of barley anchored genetically by two million single-nucleotide polymorphisms. *Plant Physiol.* 2014;164(1):412-423. DOI 10.1104/pp.113.228213.

Bayer M.M., Rapazote-Flores P., Ganal M., Hedley P.E., Macaulay M., Plieske J., Ramsay L., Russell J., Shaw P.D., Thomas W., Waugh R. Development and evaluation of a barley 50k iSelect SNP array. *Front. Plant Sci*. 2017;8:1792. DOI 10.3389/fpls.2017.01792.

Blennow A., Jensen S.L., Shaik S.S., Skryhan K., Carciofi M., Holm P.B., Hebelstrup K.H., Tanackovic V. Future cereal starch bioengineering: cereal ancestors encounter gene technology and designer enzymes. *Cereal Chem*. 2013:90(4):274-287.

Botstein D., White R.L., Skolnick M., Davis R.V. Construction of a genetic linkage map in man using restriction fragment length polymorphisms. *Am. J. Hum. Genet.* 1980;32:314-331.

Chutimanitsakun Y., Nipper R.W., Cuesta-Marcos A., Cistué L., Corey A., Filichkina T., Johnson E.A., Hayes P.M. Construction and application for QTL analysis of a restriction site associated DNA (RAD) linkage map in barley. *BMC Genomics*. 2011;12(1):4. DOI 10.1186/1471-2164-12-4.

Cistué L., Cuesta-Marcos A., Chao S., Echávarri B., Chutimanitsakun Y., Corey A., Filichkina T., Garcia-Mariño N., Romagosa I., Hayes P.M. Comparative mapping of the Oregon Wolfe Barley using doubled haploid lines derived from female and male gametes. *Theor. Appl. Genet*. 2011;122(7):1399-1410.

Close T.J., Bhat P.R., Lonardi S., Wu Y., Rostoks N., Ramsay L., Druka A., Stein N., Svensson J.T., Wanamaker S., Bozdag S., Roose M.L., Moscou M.J., Chao S., Varshney R.K., Szűcs P., Sato K., Hayes P.M., Matthews D.E., Kleinhofs A., Muehlbauer G.J., DeYoung J., Marshall D.F., Madishetty K., Fenton R.D., Condamine P., Graner A., Waugh R. Development and implementation of high-throughput SNP genotyping in barley. *BMC Genomics.* 2009; 10:582. DOI 10.1186/1471-2164-10-582.

Comadran J., Kilian B., Russell J., Ramsay L., Stein N., Ganal M., Shaw P., Bayer M., Thomas W., Marshall D., Hedley P., Tondelli A., Pecchioni N., Francia E., Korzun V., Walther A., Waugh R. Natural variation in a homolog of antirrhinum CENTRORADIALIS contributed to spring growth habit and environmental adaptation in cultivated barley. *Nat. Genet*. 2012;44(12):1388-1391. DOI 10.1038/ng.2447.

Cowan C.R., Carlton P.M., Cande W.Z. The polar arrangement of telomeres in interphase and meiosis. Rabl organization and the bouquet. *Plant Physiol*. 2001;125(2):532-538. DOI 10.1104/pp.125.2.532.

Darrier B., Russell J., Milner S.G., Hedley P.E., Shaw P.D., Macaulay M., Ramsay L.D., Halpin C., Mascher M., Fleury D.L., Langridge P., Stein N., Waugh R. A comparison of mainstream genotyping platforms for the evaluation and use of barley genetic resources. *Front. Plant Sci*. 2019;10:1-14. DOI 10.3389/fpls.2019.00544.

Davey J.W., Hohenlohe P.A., Etter P.D., Boone J.Q., Catchen J.M., Blaxter M.L. Genome-wide genetic marker discovery and genotyping using next-generation sequencing. *Nat. Rev. Genet*. 2011;12(7): 499-510. DOI 10.1038/nrg3012.

Dong F., Jiang J. Non-rabl patterns of centromere and telomere distribution in the interphase nuclei of plant cells. *Chromosome Res*. 1998;6(7):551-558. DOI 10.1023/A:1009280425125.

Elshire R.J., Glaubitz J.C., Sun Q., Poland J.A., Kawamoto K., Buckler E.S., Mitchell S.E. A robust, simple genotyping-by-sequencing (GBS) approach for high diversity species. *PLoS One*. 2011;6(5): e19379. DOI 10.1371/journal.pone.0019379.

Fan J.B., Oliphant A., Shen R., Kermani B.G., Garcia F., Gunderson K.L., Hansen M.J., Steemers F., Butler S.L., Deloukas P., Galver L., Hunt S., Mcbride C., Bibikova M., Rubano T., Chen J., Wickham E., Doucet D., Chang W., Campbell D., Zhang B., Kruglyak S., Bentley D., Haas J., Rigault P., Zhou L., Stuelpnagel J., Chee M.S. Highly parallel SNP genotyping. *Cold Spring Harb. Symp. Quant. Biol*. 2003;68:69-78. DOI 10.1101/sqb.2003.68.69.

Fan X., Zhu J., Dong W., Sun Y., Lv C., Guo B., Xu R. Comparative mapping and candidate gene analysis of *SSIIa* associated with grain amylopectin content in barley (*Hordeum vulgare* L.). *Front. Plant Sci*. 2017;8:1531. DOI 10.3389/fpls.2017.01531.

Gerasimova S.V., Hertig C., Korotkova A.M., Otto I., Hiekel S., Kochetov A.V., Kumlehn J., Khlestkina E.K. Converting hulled into naked barley through targeted knock-out of the *Nud1* gene. *In Vitro Cell. Dev. Biol.-Plant*. 2018a;54(Suppl. 1):S101. DOI 10.1007/s11627-018-9923-0.

Gerasimova S.V., Korotkova A.M., Hertig C., Hiekel S., Hoffie R., Budhagatapalli N., Otto I., Hensel G., Shumny V.K., Kochetov A.V., Kumlehn J., Khlestkina E.K. Targeted genome modification in protoplasts of a highly regenerable Siberian barley cultivar using RNA-guided Cas9 endonuclease. *Vavilovskii Zhurnal Genetiki i Selektsii = Vavilov Journal of Genetics and Breeding*. 2018b;22(8):1033-1039. DOI 10.18699/VJ18.447.

Ghazvini H., Tekauz A. Virulence diversity in the population of *Bipolaris sorokiniana*. *Plant Dis.* 2007;91(7):814-821.

Goddard R., Vos S., Steed A., Muhammed A., Thomas K., Griggs D., Ridout C., Nicholson P. Mapping of agronomic traits, disease resistance and malting quality in a wide cross of two-row barley cultivars. *Plos One*. 2019;14(7):e0219042. DOI 10.1371/journal.pone.0219042.

Hayes P., Szucs P. Disequilibrium and association in barley: thinking outside the glass. *Proc. Natl. Acad. Sci. USA*. 2006;103(49): 18385-18386. DOI 10.1007/s00438-006.

Hisano H., Meints B., Moscou M.J., Cistue L., Echávarri B., Sato K., Hayes P.M. Selection of transformation-efficient barley genotypes based on TFA (transformation amenability) haplotype and higher resolution mapping of the TFA loci. *Plant Cell Rep*. 2017;36(4): 611-620. DOI 10.1007/s00299-017-2107-2.

Hyne V., Kearsey M.J. QTL analysis: further uses of 'marker regression' regression. *Theor. Appl. Genet*. 1995;91(3):471-476. DOI 10.1007/BF00222975.

International Barley Genome Sequencing Consortium; Mayer K.F.X., Waugh R., Brown J.W.S., Schulman A., Langridge P., Platzer M., Fincher G.B., Muehlbauer G.J., Sato K., Close T.J., Wise R.P., Stein N. A physical, genetic and functional sequence assembly of the barley genome. *Nature*. 2012;491(7426):711-716. DOI 10.1038/nature11543.

Jensen J. Estimation of recombination parameters between a quantitative trait locus (QTL) and two marker gene loci. *Theor. Appl. Genet*. 1989;78(5):613-618. DOI 10.1007/BF00262554.

Kearsey M.J., Farquhar A.G.L. QTL analysis in plants; where are we now? *Heredity.* 1998;80(2):137-142. DOI. 10.1038/sj.hdy.6885001.

Konieczny A., Ausubel F.M. A procedure for mapping *Arabidopsis* mutations using co-dominant ecotype-specific PCR-based markers. *Plant J*. 1993;4(2):403-410.

Korotkova A.M., Gerasimova S.V., Khlestkina E.K. Current achievements in modifying crop genes using CRISPR/Cas system. *Vavilovskii Zhurnal Genetiki i Selektsii = Vavilov Journal of Genetics and Breeding*. 2019;23(1):29-37. DOI 10.18699/vj19.458.

Kumar N., Galli M., Ordon J., Stuttmann J., Kogel K.H., Imani J. Further analysis of barley MORC1 using a highly efficient RNA-guided Cas9 gene-editing system. *Plant Biotechnol. J*. 2018;16(11):1892-1903. DOI 10.1111/pbi.12924.

Kumpatla S.P., Buyyarapu R., Abdurakhmonov I.Y., Mammadov J.A. Genomics-assisted plant breeding in the 21st century: technological advances and progress. In: Abdurakhmonov I. (Ed). Plant Breeding. 2012;131-183.

Künzel G., Korzun L., Meister A. Cytologically integrated physical restriction fragment length polymorphism maps for the barley genome based on translocation breakpoints. *Genetics*. 2000;154(1):397-412.

Lawrenson T., Shorinola O., Stacey N., Li C., Østergaard L., Patron N., Uauy C., Harwood W. Induction of targeted, heritable mutations in barley and brassica oleracea using RNA-guided Cas9 nuclease. *Genome Biol*. 2015;16(1):1-13. DOI 10.1186/s13059-015-0826-7.

Leng Y., Wang R., Ali S., Zhao M., Zhong S. Sources and genetics of spot blotch resistance to a new pathotype of *Cochliobolus sativus* in the USDA National small grains collection. *Plant Dis*. 2016; 100(10):1988-1093. DOI 10.1094/PDIS-02-16-0152-RE.

Lorenz A.J., Hamblin M.T., Jannink J.L. Performance of single nucleotide polymorphisms versus haplotypes for genome-wide association analysis in barley. *PLoS One*. 2010;5(11):e14079. DOI. 10.1371/journal.pone.0014079.

Luo M.C., Thomas C., You F.M., Hsiao J., Ouyang S., Buell C.R., Malandro M., McGuire P.E., Anderson O.D., Dvorak J. High-throughput fingerprinting of bacterial artificial chromosomes using the SNaPshot labeling kit and sizing of restriction fragments by capillary electrophoresis. *Genomics*. 2003;82(3):378-389. DOI 10.1016/S0888-7543(03)00128-9.

Madishetty K., Condamine P., Svensson J.T., Rodriguez E., Close T.J. An improved method to identify BAC clones using pooled overgos. *Nucleic Acids Res*. 2007;35(1):1-5. DOI 10.1093/nar/gkl920.

Mascher M., Gundlach H., Himmelbach A., Beier S., Twardziok S.O., Wicker T., Radchuk V., …, Hansson M., Zhang G., Braumann I., Spannagl M., Li C., Waugh R., Stein N. A chromosome conformation capture ordered sequence of the barley genome. *Nature*. 2017; 544(7651):427-433. DOI 10.1038/nature22043.

Mascher M., Muehlbauer G.J., Rokhsar D.S., Chapman J., Schmutz J., Barry K., Muñoz Amatriaín M., Close T.J., Wise R.P., Schulman A.H., Himmelbach A., Mayer K.F.X., Scholz U., Poland J.A., Stein1 N., Waugh R. Anchoring and ordering NGS contig assemblies by population sequencing (POPSEQ). *Plant J*. 2013;76(4): 718-727. DOI 10.1111/tpj.12319.

Olson M., Hood L., Cantor C., Botstein D. A common language for physical mapping of the human genome. *Science*. 1989;245(4925): 1434-1435. DOI 10.1126/science.2781285.

Pauli D., Muehlbauer G.J., Smith K.P., Cooper B., Hole D., Obert D.E., Ullrich S.E., Blake T.K. Association mapping of agronomic QTLs in US spring barley breeding germplasm. *Plant Genome*. 2014;7(3): 1-15. DOI 10.3835/plantgenome2013.11.0037.

Prieto P., Santos A.P., Moore G., Shaw P. Chromosomes associate premeiotically and in xylem vessel cells via their telomeres and centromeres in diploid rice (*Oryza sativa*). *Chromosoma*. 2004;112(6): 300-307. DOI. 10.1007/s00412-004-0274-8.

Rasheed A., Hao Y., Xia X., Khan A., Xu Y., Varshney R.K., He Z. Crop breeding chips and genotyping platforms: progress, challenges, and perspectives. *Mol. Plant*. 2017;10(8):1047-1064. DOI 10.1016/j.molp.2017.06.008.

Rostoks N., Mudie S., Cardle L., Russell J., Ramsay L., Booth A., Svensson J.T., Wanamaker S.I., Walia H., Rodriguez E.M., Hedley P.E., Liu H., Morris J., Close T.J., Marshall D.F., Waugh R. Genome-wide SNP discovery and linkage analysis in barley based on genes responsive to abiotic stress. *Mol. Genet. Genomics*. 2005;274(5):515-527. DOI 10.1007/s00438-005-0046-z.

Schulte D., Close T.J., Graner A., Langridge P., Matsumoto T., Muehlbauer G., Sato K., Schulman A.H., Waugh R., Wise R.P., Stein N. Update on the international barley sequencing consortium – at the threshold of efficient access to the barley genome. *Plant Physiol*. 2009;149(1):142-147. DOI 10.1104/pp.108.128967.

Semagn K., Babu R., Hearne S., Olsen M. Single nucleotide polymorphism genotyping using kompetitive allele specific PCR (KASP): overview of the technology and its application in crop improvement. *Mol. Breed*. 2014;33(1):1-14.

Shavrukov Y.N. CAPS markers in plant biology. *Vavilovskii Zhurnal Genetiki i Selektsii = Vavilov Journal of Genetics and Breeding*. 2015;19(2):205-213. DOI 10.18699/VJ15.026.

Tautz D., Renz M. Simple sequences are ubiquitous repetitive components of eukaryotic genomes. *Nucleic Acids Res*. 1984;12(10):4127-4138. DOI 10.1093/nar/12.10.4127.

Wang D.G., Fan J.B., Siao C.J., Berno A., Young P., Sapolsky R., Ghandour G., Perkins N., Winchester E., Spencer J., Kruglyak L., Stein L., Hsie L., Topaloglou T., Hubbell E., Robinson E., Mittmann M., Morris M.S., Shen N., Kilburn D., Rioux J., Nusbaum C., Rozen S., Hudson T.J., Lipshutz R., Chee M., Lander E.S. Large-scale identification, mapping, and genotyping of single-nucleotide polymorphisms in the human genome. *Science*. 1998;280(5366):1077-1082. DOI 10.1126/science.280.5366.1077.

ORCID ID

E.K. Khlestkina orcid.org/0000-0002-8470-8254

Acknowledgements. This work was supported by the Russian Science Foundation, project 16-14-00086.

Conflict of interest. The authors declare no conflict of interest.

Received September 23, 2019. Revised December 2, 2019. Accepted December 5, 2019.

Вавиловский журнал генетики и селекции. 2020;24(4):356-362
DOI 10.18699/VJ20.628

Полегание пшеницы: генетические и экологические факторы и способы преодоления

Е.В. Агеева[1] ✉, И.Н. Леонова[2], И.Е. Лихенко[1]

[1] Сибирский научно-исследовательский институт растениеводства и селекции – филиал Федерального исследовательского центра Институт цитологии и генетики Сибирского отделения Российской академии наук, Новосибирск, Россия
[2] Федеральный исследовательский центр Институт цитологии и генетики Сибирского отделения Российской академии наук, Новосибирск, Россия
✉ e-mail: elenakolomeec@mail.ru

Аннотация. Полегание является одной из основных проблем снижения урожайности и качества зерна озимой и яровой пшеницы. Устойчивость этой культуры к полеганию в значительной степени зависит от факторов внешней среды, биологических и морфологических особенностей стебля и корневой системы. Селекция сортов на устойчивость к полеганию актуальна во многих странах мира, и в данном направлении получен ряд достижений. Высота растений – важный морфологический признак, связанный с устойчивостью к полеганию. Основным направлением для снижения риска возникновения полегания стало выведение сортов, несущих гены короткостебельности (*Rht*). Гены *Rht-B1b*, *Rht-D1b*, *Rht8*, *Rht11* получили широкое распространение во всем мире среди сортов мягкой пшеницы благодаря значительному влиянию на хозяйственно ценные признаки, включая полегание. Немаловажным оказалось изучение анатомо-морфологических особенностей и химического состава тканей стебля, которые дополняют оценку устойчивости к полеганию и позволяют более полно характеризовать изучаемый сортовой материал. Особенно большую роль в прочности стебля многие исследователи отводят толщине стенок междоузлий и их анатомическому строению. Диаметр соломины, ее толстостенность и вес, большое количество сосудистых пучков и широкое кольцо механических тканей коррелируют с устойчивостью к полеганию. Важными структурными компонентами, обеспечивающими прочность стебля у пшеницы, являются содержание лигнина, кремния и целлюлозы. Большое значение в выявлении генетической основы взаимоотношений между анатомическими и морфофизиологическими признаками стебля и корневой системы и полеганием имеют молекулярно-генетический анализ и картирование генов и локусов количественных признаков. Генетические факторы, отражающие корреляции между полеганием и толщиной стенки стебля, числом проводящих пучков и другими параметрами, были картированы в хромосомах 1A, 1B, 2A, 2D, 3A, 4B, 4D, 5A, 5D, 6D и 7D. Установлено, что локусы с высоким фенотипическим эффектом в отношении толерантности к полеганию колокализуются с локусами, ответственными за высоту растения, диаметр и прочность стебля. Для повышения устойчивости к полеганию необходимы разработка комплекса агротехнических методов, снижающих влияние почвенно-климатических факторов, и создание толерантных к полеганию сортов.
Ключевые слова: пшеница; полегание; стебель; гены *Rht*; лигнин; анатомо-морфологические признаки.

Для цитирования: Агеева Е.В., Леонова И.Н., Лихенко И.Е. Полегание пшеницы: генетические и экологические факторы и способы преодоления. Вавиловский журнал генетики и селекции. 2020;24(4):356-362. DOI 10.18699/VJ20.628

Lodging in wheat: genetic and environmental factors and ways of overcoming

E.V. Ageeva[1] ✉, I.N. Leonova[2], I.E. Likhenko[1]

[1] Siberian Research Institute of Plant Production and Breeding – Branch of the Institute of Cytology and Genetics of Siberian Branch of the Russian Academy of Sciences, Novosibirsk, Russia
[2] Institute of Cytology and Genetics of Siberian Branch of the Russian Academy of Sciences, Novosibirsk, Russia
✉ e-mail: elenakolomeec@mail.ru

Abstract. Lodging is one of the main factors in reducing the yield and grain quality of winter and spring wheat varieties. The resistance of wheat cultivars to lodging largely depends on environmental factors, biological and morphological features of the stem and root systems. Selection of the varieties for resistance to lodging is relevant in many countries of the world and has a number of achievements. Plant height is one of the most important morphological characters associated with lodging resistance. Breeding of the varieties carrying the dwarfing genes (*Rht*) is the main direction to reduce the risk of lodging. The *Rht-B1b*, *Rht-D1b*, *Rht8* and *Rht11* genes are widely used throughout the world due to their significant influence on agronomically valuable traits, including lodging. It turned out to be important to study the anatomical and morphological features and chemical composition of

stem tissues, which complement the assessment of resistance to lodging and allow the varietal material to be more fully characterized. The thickness of stem internodes and their anatomical structure play an important role in the stem strength. The diameter of the stem, its thickness and weight, a large number of vascular bundles and a wide ring of mechanical tissues correlate with resistance to lodging. The content of lignin, silicon and cellulose are important structural components and provide the stem strength of wheat plants. Molecular genetic analysis and mapping of genes and quantitative trait loci are of great importance in identifying the genetic basis of the relationship between the anatomical and morphophysiological characters of the stem and root system and lodging. Genetic factors reflecting correlations between the lodging and the thickness of the stem wall, the number of vascular bundles and other characters were mapped to chromosomes 1A, 1B, 2A, 2D, 3A, 4B, 4D, 5A, 5D, 6D and 7D. It has been found that loci with high phenotypic effects on lodging tolerance are colocalized with loci responsible for plant height, stem diameter and stem strength. To increase resistance to lodging, it is necessary to develop a set of agrotechnical methods that reduce the influence of soil and climatic factors and create wheat varieties tolerant to lodging.

Key words: wheat; lodging; stem; *Rht* genes; lignin; anatomical and morphological characters.

For citation: Ageeva E.V., Leonova I.N., Likhenko I.E. Lodging in wheat: genetic and environmental factors and ways of overcoming. *Vavilovskii Zhurnal Genetiki i Selektsii = Vavilov Journal of Genetics and Breeding*. 2020;24(4):356-362. DOI 10.18699/VJ20.628 (in Russian)

Введение

Полегание – один из главных факторов, влияющих на урожайность пшеницы, качество зерна и содержание в нем питательных веществ. При полегании понижается устойчивость растений к болезням, формируется щуплое зерно, возникают проблемы с уборкой урожая. Полегание пшеницы в предуборочный и уборочный периоды, сопровождающиеся неблагоприятными погодными условиями и частым выпадением дождей, влечет за собой прорастание зерна на корню и значительно снижает хлебопекарные качества. Формирование мелкого зерна с низкой массой 1000 зерен в результате нарушения транспортировки ассимилянтов в колос – частое явление при полегании, наступившем до налива зерна (Berry et al., 2004; Packa et al., 2015; Khobra et al., 2019). Потери зерна на полегающих посевах озимой и яровой пшеницы составляют в среднем от 20 до 50 %. Полегание посевов на стадиях колошения, молочной, восковой и полной спелости зерна приводит к снижению урожайности на 31, 25, 20 и 12 % соответственно (Weibel, Pendleton, 1964; Fischer, Stapper, 1987). Даже кратковременное полегание растений вызывает потери урожая (Иванов, Дохунаев, 1979). Исследования А.Н. Лубнина (2006) показали наличие прямой средней зависимости ($r = 0.346 \pm 0.08$) между устойчивостью к полеганию и урожайностью; при этом в годы со слабым увлажнением эта связь выражена слабее. Чем устойчивее стебель, тем лучше развит колос: он крупнее, лучше озернен и имеет большой вес зерен. В полеглом ценозе у растений активнее развиваются листостеблевые болезни (мучнистая роса, бурая и стеблевая ржавчина, септориоз) и корневые гнили.

Анализ многочисленных работ (Носатовский, 1965; Терентьев, 1974; Иванов, Дохунаев, 1979; Лелли, 1980; Захаров и др., 2014; Packa et al., 2015; Shah et al., 2017; Khobra et al., 2019) позволяет сделать заключение, что полегание – это по существу физиологическая реакция растений на определенные условия внешней среды: недостаток света, структуру почвы, ее избыточную влажность, влажный с высокой температурой микроклимат воздуха, высокое содержание азота и других минеральных составляющих (Mavi et al., 2004; Dahiya et al., 2018). Перечисленные факторы внешней среды считаются основными причинами полегания зерновых культур. Немаловажную роль играют климатические и погодные условия, в том числе скорость ветра, дожди и град. В подтверждение такого вывода говорят факты массового распространения полегания во влажных районах с обильными естественными осадками (Niu et al., 2016).

Устойчивость к полеганию зависит также от комплекса взаимосвязанных признаков, таких как анатомические и морфологические особенности стебля и корневой системы, биохимические и физиологические процессы, протекающие в организме растения. Согласно проведенным исследованиям, основными характеристиками, которые определяют устойчивость пшеницы к полеганию, являются: высота растения, длина и толщина стебля, размеры верхнего и нижнего междоузлий, число продуктивных побегов, диаметр и число проводящих пучков, содержание лигнина и целлюлозы в стебле, содержание растворимых сахаров, вес зерна в колосе (Kelbert et al., 2004; Ионова, 2009; Berry, 2012; Packa et al., 2015; Xiao et al., 2015; Khobra et al., 2019; Shah et al., 2019).

Последние достижения в разработке методов биотехнологии позволили идентифицировать ряд генов и локусов количественных признаков (QTL), контролирующих признаки, связанные с полеганием. С использованием двуродительских картирующих популяций были локализованы генетические факторы, ассоциированные с толерантностью к полеганию. Многие из них картированы в тех же геномных районах, где локализованы гены, отвечающие за высоту растения, диаметр и толщину стебля, урожайность (Verma et al., 2005; Kong et al., 2013; Berry P., Berry S., 2015). Сочетание методов полногеномного поиска ассоциаций и высокопроизводительного фенотипирования с использованием обширных коллекций сортов выявило новые геномные районы, коррелирующие с устойчивостью к полеганию (Kaur et al., 2017; Singh et al., 2019).

Селекция зерновых культур на продуктивность неразрывно связана с селекцией на устойчивость растений к неблагоприятным факторам внешней среды, включая устойчивость к полеганию. В настоящем обзоре рассмотрена роль различных факторов, влияющих на устойчивость пшеницы к полеганию, в том числе приведены результаты исследований по молекулярно-генетическому картированию генетических локусов, ассоциированных с проявлением данного признака.

Типы полегания

Под полеганием принято понимать смещение стебля или всего растения от его вертикального положения. На практике различают прикорневое и стеблевое полегание пшеницы (Носатовский, 1965; Захаров и др., 2014; Khobra et al., 2019). Проявление корневого или стеблевого типа полегания зависит от характеристик конкретного сорта и факторов внешней среды. Прикорневое полегание связано с недостаточной механической прочностью самих корней либо недостаточно прочным сцеплением корневой системы с почвой (Packa et al., 2015; Shah et al., 2019). Архитектура корневой системы играет важную роль в поддержании устойчивости растения к полеганию. Известно, что глубина залегания корней, длина и плотность корневых волосков, угол расположения базальных корней и их изгиб влияют на устойчивость (Pinthus, 1967; Crook, Ennos, 1993). Одной из причин слаборазвитой корневой системы может быть дефицит влаги в почве в первую половину вегетации. Кроме того, прикорневое полегание встречается в районах с большим количеством осадков в фазы кущения и выхода в трубку, а также при орошении. Как правило, у генотипов с таким типом полегания прочный стебель, их анатомические показатели вполне соответствуют показателям соломины хорошо устойчивых к полеганию форм (Иванов, Дохунаев, 1979; Лелли, 1980). В результате переувлажнения верхнего слоя почвы под тяжестью надземной массы растений наблюдается смещение и растяжение корней, а иногда и их разрыв. Стебли растений теряют вертикальное положение и полегают. Более широкий угол распространения корневой системы снижает риск возникновения прикорневого полегания (Носатовский, 1965; Berry, 2012; Packa et al., 2015).

Стеблевое полегание пшеницы происходит под влиянием нагрузки на стебель, которая возрастает с увеличением веса на колос и удлинением соломины. Другими словами, происходит изгиб и даже слом соломины, преимущественно в районе второго и третьего междоузлия снизу (Терентьев, 1974; Zuber et al., 1999; Packa et al., 2015; Khobra et al., 2019). Особенно часто стеблевое полегание встречается у сортов с длинным и тонким стеблем. Наибольший вес колоса отмечается в конце спелости. Несмотря на то что третье нижнее междоузлие обладает меньшей устойчивостью соломины на излом, чем второе, в силу большей нагрузки, приходящейся на последнее, полегание пшеницы чаще всего отмечается именно во втором междоузлии. Увлажнение колоса увеличивает нагрузку на стебель, поэтому дожди в это время наиболее опасны для полегания пшеницы. Условия внешней среды приобретают особое значение во время формирования второго и третьего междоузлия.

Факторы, вызывающие полегание

Факторы, вызывающие полегание, можно подразделить на четыре группы: особенности самих растений (строение и свойства стебля, развитие и строение корней и др.); физические факторы (ветер, дождь, град, температура и световой режим и др.); агротехнические факторы (избыточное увлажнение и питание, в первую очередь азотное, недостаток фосфора и калия, завышенные нормы посева и др.); поражение пшеницы болезнями, которое в немалой степени связано с сортовыми особенностями и агротехникой.

Особое значение имеет выпадение осадков, а точнее не количество выпавших осадков, а интенсивность дождя и само его формирование. Как правило, сильный и порывистый ветер с дождем или после дождя является основной причиной полегания. Немаловажный фактор – загущенность посевов, которая приводит к возникновению взаимозатенения, в результате чего формируются тонкие и длинные стебли со слаборазвитой корневой системой (Иванов, Дохунаев, 1979; Foulkes et al., 2011).

Высокий уровень плодородия и структура почв тоже способствуют полеганию. Доступный для растения азот может поступать в него в результате минерализации растительных остатков или через минеральные удобрения (Berry et al., 2004). Применение минеральных удобрений ведет к мощному вегетативному росту пшеницы, к сильной кустистости, что влечет повышенную плотность агроценоза растений. Повышается конкуренция за пространство, свет и питательные вещества, что в конечном итоге приводит к формированию растений с более тонкими и длинными и более слабыми стеблями с меньшим количеством сухого вещества в нижней части междоузлия. Помимо удлинения стебля, наблюдается формирование тонких корней со слабой силой сцепления с почвой (Berry et al., 2004; Foulkes et al., 2011). Большое количество азота снижает также содержание целлюлозы и лигнина. Удобрения с калием, фосфором и микроэлементами оказывают меньшее воздействие на изменение прочности стебля, чем азотные, хотя эти данные неоднозначны (Mulder, 1954; Zhang et al., 2017; Khobra et al., 2019).

В современном производстве применяют интенсивные технологии возделывания пшеницы: внесение минеральных удобрений с целью получения высоких урожаев и повышения качества зерна. Поскольку применение минеральных удобрений может привести к полеганию, одним из способов решения данной задачи стало использование регуляторов роста (ретардантов), тормозящих процессы роста растения. Оказалось, что своевременное торможение роста вегетативных органов растений может способствовать развитию у них ряда полезных хозяйственных признаков: расширение пластинок листьев, повышение интенсивности их зеленой окраски, рост объема корневой системы, уменьшение продолжительности покоя семян, повышение всхожести и увеличение энергии прорастания. При этом важно, что сам ход физиологических процессов, определяющих продукционную способность обработанных растений, не должен претерпевать существенных изменений. Данные о влиянии ретардантов на физиологические функции растений противоречивы, однако большинство результатов свидетельствует, что регуляторы роста растений не оказывают отрицательного воздействия на фотосинтез, ограничивают чрезмерный расход воды и обеспечивают более благоприятный водный режим (Шаповал и др., 2010; Souza et al., 2010).

Анатомические и морфофизиологические параметры стебля

Длина стебля – один из наиболее важных морфологических признаков, коррелирующий с устойчивостью к по-

леганию. Значительная склонность к полеганию у пшеницы наблюдается при высоте растения свыше 120 см (Дорофеев и др., 1976; Packa et al., 2015). Генотипы, имеющие укороченную соломину, отличаются толерантностью к полеганию и большей урожайностью зерна. Активное выведение короткостебельных сортов началось в 1960–1970-х гг. при использовании в селекции различных аллелей генов *Rht* (Reduced height). Согласно каталогу генных символов, у пшеницы обнаружено более 40 аллелей генов *Rht*, локализованных в хромосомах второй и четвертой гомеологических групп и в хромосомах 5A, 5D, 6A, 7A, 7B (McIntosh et al., 2013, Supplements 2014–2017). Гены *Rht* условно делятся на две группы по их реакции на гиббереллиновую кислоту. Нечувствительные к гиббереллинам гены *Rht1* и *Rht2* картированы в коротких плечах хромосом 4B и 4D. Гены, чувствительные к гиббереллинам, были локализованы в хромосомах 2A, 2DS, 7BS и 5A. Кроме генов с постоянными символами, практически во всех хромосомах пшеницы картировано большое число QTL (Wurschum et al., 2017).

Несмотря на многочисленное число генов и аллелей *Rht*, только четыре из них – *Rht-B1b* (4BS), *Rht-D1b* (4DS), *Rht8* (2DL) и *Rht11* (*Rht-B1e*) – получили практическое применение при создании новых сортов (Knopf et al., 2008; Pearce et al., 2011; Xiao et al., 2015). Присутствие этих генов в сортах приводит к уменьшению числа и размеров междоузлий, сокращению длины колеоптиля, снижению длины стебля на 14–17 % и способствует увеличению урожайности до 20 % (Berry, 2012). Аллель *Rht-B1e* стимулирует существенно большее снижение высоты растений и увеличение урожайности по сравнению с аллелем *Rht-B1b* (Дивашук и др., 2012; Коршунова и др., 2014). На сегодняшний день более 70 % сортов в мире содержат по крайней мере один из этих *Rht* генов (Evans, 1998; Borojevic, Borojevic, 2005; Коршунова и др., 2014; Shah et al., 2019). Остальные локусы *Rht* не используются из-за негативных эффектов на урожайность и другие хозяйственно важные признаки (Daoura et al., 2014; Wang et al., 2014; Li et al., 2015).

В настоящее время известно, что гены *Rht-B1b* и *Rht-D1b* пшеницы кодируют мутантные белки DELLA, которые при образовании комплекса с гиббереллином и рецепторным белком репрессируют гиббереллиновый сигнал, влияя таким образом на рост и развитие растения (Peng et al., 1999; Yamaguchi, 2008; Pearce et al., 2011; Thomas, 2017). Мутации в структуре белков DELLA, снижающие чувствительность к действию гиббереллина, были выявлены у многих видов растений и детально изучены на примере арабидопсиса и риса (Билова и др., 2016; Vera-Sirera et al., 2016). Что касается пшеницы, то на данный момент молекулярные и биохимические функции мутантных белков DELLA недостаточно изучены, что серьезно затрудняет перспективы использования таких мутаций на практике.

Помимо длины, немаловажную роль играют другие параметры стебля. Установлено, что диаметр соломины, ее толстостенность и вес, количество сосудистых пучков и широкое кольцо механических тканей коррелируют с устойчивостью к полеганию (Емельянова, Резниченко, 1970; Иванов, Дохунаев, 1979; Shah et al., 2017). Особенную роль в прочности стебля многие исследователи отводят толщине стенок междоузлий и их анатомическому строению. Увеличение диаметра и толщины стебля приводит к повышению его прочности (Packa et al., 2015; Shah et al., 2017). Толщину стенок соломины обеспечивают клетки основной и механической тканей, а также компоненты проводящей системы. Толщина стебля пшеницы является ценным признаком, маркирующим потенциальную продуктивность растений (Лазаревич, 1999; Packa et al., 2015). Увеличение диаметра стебля способствует снижению риска возникновения полегания. Достигается это за счет увеличения диаметра проводящих пучков паренхимы и толщины склеренхимной ткани, которая, в свою очередь, зависит от числа слоев клеток и их диаметра (Лазаревич, 1999).

Имеется ряд исследований по выявлению генетических локусов, ассоциированных с параметрами стебля. С использованием дигаплоидной (DH) популяции озимой мягкой пшеницы шесть QTL для признаков «прочность стебля», «толщина стенки стебля», «диаметр сердцевины» и «диаметр стебля» идентифицированы в хромосомах 1A, 2D, 3B (Hai et al., 2005). В других работах генетические локусы, отражающие корреляции между полеганием и толщиной стенки стебля, были картированы в хромосомах 2A, 3A, 5A, 1B, 4B, 4D, 6D и 7D (Keller et al., 1999; Xiao et al., 2015). Для числа проводящих пучков были зарегистрированы QTL в хромосомах 1A, 2D, 5D и 7D (Shah et al., 2017). Результаты картирования также свидетельствуют, что локусы с высоким фенотипическим эффектом в отношении толерантности к полеганию колокализуются с QTL, которые ответственны за высоту растения, диаметр и прочность стебля (Berry P., Berry S., 2015; Li et al., 2015).

Для изучения генетической архитектуры такого сложного признака, как полегание, необходимы масштабные фенотипические и генотипические эксперименты с использованием популяций большого размера. По последним данным (Singh et al., 2019), генетическая основа полегания была исследована с помощью нового методического подхода высоковоспроизводительного фенотипирования (HTP, high-throughput phenotyping). Применение методов геномной селекции и геномного прогнозирования позволило идентифицировать ключевой геномный район в хромосоме 2A и минорные локусы в других хромосомах, совпадающие по локализации с QTL, картированными ранее в других исследованиях.

С помощью современной микроскопической техники установлено, что прочность стебля обеспечивается комплексом анатомических признаков: численностью и взаимным расположением проводящих пучков, топографическим положением в стебле механических тканей и их параметрами (Лазаревич, Мыхлык, 2014). Выполненная часть стебля представлена эпидермисом, первичной корой и центральным цилиндром, состоящим из периферического кольца склеренхимы, проводящих пучков и запасающей паренхимы. В сердцевине паренхимы у мягкой пшеницы имеется полость – медуллярная лакуна, которая образуется в результате разрушения сердцевины при удлинении стебля (Носатовский, 1965; Емельянова, Резниченко, 1970).

Проводящие пучки паренхимы и первичной коры вместе составляют проводящую систему растения и одно-

временно входят в состав механической ткани. При изгибе или ломкости стебля в результате полегания происходит повреждение сосудистых проводящих пучков. Несмотря на отсутствие однозначных достоверных корреляций между числом проводящих пучков и устойчивостью к полеганию, при изучении анатомической структуры стебля видов и сортов яровой пшеницы, различающихся по полеганию, отмечена разница в количестве сосудисто-волокнистых пучков в междоузлиях (Ageeva et al., 2019). Увеличенное число сосудистых пучков наблюдалось у сортов, устойчивых к полеганию.

По мнению С.В. Лазаревича (1999), устойчивости к полеганию способствует ритмическое чередование крупных и малых пучков и наличие у крупных пучков склеренхимных обкладок. В случае узкого слоя склеренхимы формируются растения с тонким и ломким стеблем.

Устойчивость к полеганию представляет собой комплекс тесно взаимодействующих между собой признаков, поэтому важен не только широкий слой склеренхимной ткани, но и большое содержание в нем лигнина и целлюлозы (Shah et al., 2017). На сегодняшний день отсутствует достаточная информация о генетическом контроле содержания целлюлозы у пшеницы, за исключением результатов S. Kaur с коллегами (Kaur et al., 2017), которые с помощью полногеномного поиска ассоциаций выявили девять маркеров SNP, с высокой достоверностью связанных с генами, кодирующими β-тубулин, ауксин-индуцируемый белок и трансмембранный белок с неизвестной функцией. Предполагается, что эти гены могут быть вовлечены в биосинтез целлюлозы и влиять на прочность стебля.

Лигнин – важный структурный компонент вторичной клеточной стенки, который связан и с ростом растения, и с прочностью стебля. У пшеницы наблюдается значительная корреляционная связь между устойчивостью к полеганию и содержанием лигнина в стебле. D. Peng с коллегами в своем исследовании установили, что сорта с высоким содержанием лигнина могут быть использованы в качестве источников с целью создания образцов, толерантных к полеганию (Peng et al., 2014). Кроме того, в совокупности увеличение содержание лигнина и гемицеллюлозы увеличивает прочность стебля. Сорта с низким содержанием этих компонентов более склонны к полеганию (Zheng et al., 2017).

Еще одним важным структурным компонентом, обеспечивающим прочность стебля у пшеницы, является кремний (Иванченко, Резанова, 2016; Shah et al., 2017). Биологический активный кремний укрепляет эпидермис, кору и сосудисто-проводящие ткани, тем самым существенно повышая пластичность, упругость, прочность стебля, листьев и защитные функции растений (Иванченко, Резанова, 2016). Это происходит за счет того, что кремний значительно увеличивает содержание целлюлозы и лигнина в клетках склеренхимы. Он накапливается в эпидермальных тканях и коронарных клетках, обеспечивая их механическую прочность и жесткость (Shah et al., 2017; Zhang et al., 2017; Khobra et al., 2019). В тканях зерновых культур двуокись кремния составляет более половины остальных микроэлементов, поглощаемых из почвы. Зерновые поглощают кремния в 10–20 раз больше, чем бобовые. В течение вегетационного периода количество кремния растет, достигая максимума к его завершению (Козлов и др., 2015; Walsh et al., 2018).

Отсутствие необходимого количества других микроэлементов также может оказывать влияние на прочность стебля. Дефицит фосфора вызывает снижение толщины стенки и физической прочности стебля. Этот элемент способствует укреплению корневой системы, играет главную роль в переносе энергии, в дыхании и фотосинтезе. Недостаток калия приводит к уменьшению диаметра стебля, поскольку он участвует в лигнификации клеточной стенки и колленхимы (Емельянова, Резниченко, 1970; Shah et al., 2017).

Заключение

Таким образом, степень устойчивости к полеганию растений зависит от многих внешних и внутренних факторов. Для снижения риска возникновения полегания необходимо учитывать не только анатомо-морфологические и физиологические особенности сорта, такие как длина и толщина стебля, длина междоузлий, содержание лигнина и целлюлозы и др., но и климатические особенности регионов, на территории которых культивируются генотипы. Немаловажно учитывать такие параметры, как время и плотность посева, внесение удобрений и регуляторов роста растений. Связь полегания с высотой стебля и другими анатомо-морфологическими параметрами констатируется во многих научных работах, однако влияние большинства параметров пока до конца не изучено. В свете использования новых биотехнологических методов и результатов секвенирования генома пшеницы и других злаков необходимо продолжать работы по идентификации целевых локусов для установления более точной взаимосвязи между полеганием и другими агрономическими признаками. При осуществлении селекционного процесса, начиная с оценки и подбора родительских пар и заканчивая исследованием новых гибридных форм, следует комплексно подходить к проблеме, решая ее с применением всех возможных подходов в зависимости от особенностей места выращивания и уровня требований к получаемой продукции.

Список литературы / References

Билова Т.Е., Рябова Д.Н., Анисимова И.Н. Молекулярные основы формирования карликовости у культурных растений. Сообщение I. Нарушения роста из-за мутаций генов метаболизма и сигналинга гиббереллинов. *С.-х. биология.* 2016;51(1):3-16. DOI 10.15389/agrobiology.2016.1.3rus.
[Bilova T.E., Ryabova D.N., Anisimova I.N. Molecular basis of the dwarfism character in cultivated plants. I. Growth distortions due to mutations of gibberellin metabolism and signaling. *Selskokhozyaystvennaya Biologiya = Agricultural Biology*. 2016;51(1):3-16. DOI 10.15389/agrobiology.2016.1.3eng.]

Дивашук М.Г., Васильев А.В., Беспалова Л.А., Карлов Г.И. Идентичность генов короткостебельности *Rht-11* и *Rht-B1e*. *Генетика*. 2012;48(7):897-900.
[Divashuk M.G., Vasilyev A.V., Bespalova L.A., Karlov G.I. Identity of the *Rht-11* and *Rht-B1e* reduced plant height genes. *Russ. J. Genet.* 2012;48(7):761-763. DOI 10.1134/S1022795412050055.]

Дорофеев В.Ф., Якубцинер М.М., Руденко М.И., Мигушова Э.Ф., Удачин Р.А., Мережко А.Ф., Семенова Л.В., Новикова М.В., Градчанинова О.Д., Шитова И.П. Пшеницы мира. Л.: Агропромиздат, 1976.

[Dorofeev V.F., Yakubciner M.M., Rudenko M.I., Migushova E.F., Udachin R.A., Merezhko A.F., Semenova L.V., Novikova M.V., Gradchaninova O.D., Shitova I.P. Wheats of the World. Leningrad: Agropromizdat Publ., 1976. (in Russian)]

Емельянова Н.А., Резниченко Н.М. Пшеница и ее улучшение. М.: Колос, 1970.
[Emelyanova N.A., Reznichenko N.M. Wheat and Wheat Improvement. Moscow: Kolos Publ., 1970. (in Russian)]

Захаров В.Г., Сюков В.В., Яковлева О.Д. Сопряженность анатомоморфологических признаков с устойчивостью к полеганию яровой мягкой пшеницы в условиях Среднего Поволжья. *Вавиловский журнал генетики и селекции*. 2014;18(3):506-510.
[Zakharov V.G., Syukov V.V., Yakovleva O.D. Correlation of morphoanatomical traits with lodging resistance in spring wheat in the middle Volga region. *Vavilovskii Zhurnal Genetiki i Selektsii = Vavilov Journal of Genetics and Breeding*. 2014;18(3):506-510. (in Russian)]

Иванов Б.И., Дохунаев В.Н. Биологические особенности яровой пшеницы в Якутии. Новосибирск: Наука, 1979.
[Ivanov B.I., Dokhunaev V.N. Biologic Features of Spring Wheat in Yakutia. Novosibirsk: Nauka Publ., 1979. (in Russian)]

Иванченко Т.В., Резанова Г.И. Перспектива использования кремний-ауксинового биостимулятора на зерновых культурах. *Науч.-агр. журн*. 2016;1(98):29-32.
[Ivanchenko T.V., Rezanova G.I. Prospects of silicon auxin biostimulation of grain crops. *Nauchno-Agronomicheskii Zhurnal = Scientific Agronomy Journal.* 2016;1(98):29-32. (in Russian)]

Ионова Е.В. Устойчивость к полеганию растений озимой твердой пшеницы. *Аграр. вестн. Урала*. 2009;8(62):56-57.
[Ionova E.V. Lodging resistance of winter wheat. *Agrarnii Vestnik Urala = Agrarian Bulletin of the Urals*. 2009;8(62):56-57. (in Russian)]

Козлов А.В., Уромова И.П., Фролов Е.А., Мозолева К.Ю. Физиологическое значение кремния в онтогенезе культурных растений и при их защите от фитопатогенов. *Междунар. студ. науч. вестн*. 2015;1:39.
[Kozlov A.V., Uromova I.P., Frolov E.A., Mozoleva K.Yu. The physiological role of silicon in the development of crops and their protection against plant pathogens. *Mezhdunarodnyy Studencheskiy Nauchnyy Vestnik = International Student Scientific Herald*. 2015; 1:39. (in Russian)]

Коршунова А.Д., Дивашук М.Г., Даебль И.А., Карлов Г.И., Соловьев А.А. Валидация ДНК-маркеров генов короткостебельности у тритикале (*Triticosecale* Wittm.). *Изв. ТСХА*. 2014;3:21-31.
[Korshunova A.D., Divashuk M.G., Daebl I.A., Karlov G.I., Soloviev A.A. Validation of DNA markers for semi-dwarf genes in intriticale (*Triticosecale* Wittm.). *Izvestiya Timiryazevskoy Selskokhozyaystvennoy Akademii = Izvestiya of Timiryazev Agricultural Academy*. 2014;3:21-31. (in Russian)]

Лазаревич С.В. Эволюция анатомического строения стебля пшеницы. Минск: БИТ «Хата», 1999.
[Lazarevich S.V. Evolution of the Anatomical Structure of the Wheat Stem. Minsk: Hata Publ., 1999. (in Russian)]

Лазаревич С.В., Мыхлык А.И. Разнокачественность сортов овса посевного по развитию механических тканей стебля. *Вестн. БГСХА*. 2014;3:73-77.
[Lazarevich S.V., Mykhlyk A.I. Variety of oat cultivars for the development of mechanical tissues of the stem. *Vestnik BGSHA = Bulletin of the Belarussian State Agricultural Academy*. 2014;3:73-77. (in Russian)]

Лелли Я. Селекция пшеницы: теория и практика. М.: Колос, 1980.
[Lelley J. Wheat Breeding: Theory and Practice. Budapest: Akad. Kiado, 1976. (Russ. ed.: Selektsiya Pshenitsy. Teoriya i Praktika. Moscow: Kolos Publ., 1980.]

Лубнин А.Н. Селекция мягкой яровой пшеницы в Сибири. Новосибирск, 2006.
[Lubnin A.N. Spring Wheat Breeding in Siberia. Novosibirsk, 2006. (in Russian)]

Носатовский А.И. Пшеница. Биология. М.: Колос, 1965;281-291.
[Nosatovsky A.I. Wheat. Biology. Moscow: Kolos Publ., 1965;281-291. (in Russian)]

Терентьев В.М. Физиология устойчивости растений к полеганию и методы ее оценки. В: Физиология растений – в помощь селекции. М.: Наука, 1974;108-123.
[Terentyev V.M. Physiology of plant resistance to lodging and methods for its assessment. In: Plant Physiology in Aid of Breeding. Moscow: Nauka Publ., 1974;108-123. (in Russian)]

Шаповал О.А., Вакуленко В.В., Можарова И.П. Ретарданты. *Защита и карантин растений*. 2010;8:4-7.
[Shapoval O.A., VakulenkoV.V., Mozharova I.P. Retardants. *Zashchita i Karantin Rasteniy = Plant Protection and Quarantine*. 2010;8:4-7. (in Russian)]

Ageeva E.V., Leonova I.N., Salina E.A., Likhenko I.E. Anatomo-morphological stem features of spring bread wheat varieties. In: Proc. 5th Int. Conf. PlantGen2019. Novosibirsk, 2019;26. DOI 10.18699/PlantGen2019-008.

Berry P.M. Lodging resistance in cereals. In: Encyclopedia of Sustainability Science and Technology. Springer, NY, 2012. DOI 10.1007/978-1-4419-0851-3_228.

Berry P.M., Berry S.T. Understanding the genetic control of lodging-associated plant characters in winter wheat (*Triticum aestivum* L.). *Euphytica*. 2015;205:671-689. DOI 10.1007/s10681-015-1387-2.

Berry P.M., Sterling M., Spink J.H., Baker C.J., Sylvester-Bradley R., Mooney S.J., Tams A.R., Ennos A.R. Understanding and reducing lodging in cereals. *Adv. Agron*. 2004;84:217-271. DOI 10.1016/S0065-2113(04)84005-7.

Borojevic K., Borojevic K. The transfer and history of "reduced height genes" (*Rht*) in wheat from Japan to Europe. *Heredity*. 2005;96(4): 455-459. DOI 10.1093/jhered/esi060.

Crook M.J., Ennos A.R. The mechanics of root lodging in winter wheat (*Triticum aestivum* L.). *J. Exp. Bot*. 1993;44:1219-1224.

Dahiya S., Kumar S., Harender, Chaudhary C. Lodging: significance and preventive measures for increasing crop production. *Int. J. Chem. Studies*. 2018;6(1):700-705.

Daoura B.G., Chen L., Du Y., Hu Y.-G. Genetic effects of dwarfing gene *Rht-5* on agronomic traits in common wheat (*Triticum aestivum* L.) and QTL analysis on its linked traits. *Field Crops Res*. 2014;156: 22-29. DOI 10.1016/j.fcr.2013.10.007.

Evans L.T. Crop evolution, adaptation and yield. *Photosynthetica*. 1998;34:56-60. DOI 10.1023/A:1006889901899.

Fischer R.A., Stapper M. Lodging effects on high yielding crops of irrigated semi-dwarf wheat. *Field Crops Res*. 1987;17:245-248.

Foulkes M.J., Slafer G.A., Davies W.J., Berry P.M., Sylvester-Bradle R., Martre P., Calderini D.F., Griffiths S., Reynolds M.P. Raising yield potential of wheat. III. Optimizing partitioning to grain while maintaining lodging resistance. *J. Exp. Bot*. 2011;62(2):469-486. DOI 10.1093/jxb/erq300.

Hai L., Guo H., Xiao S., Jiang G., Zhang X., Yan C., Xin Z., Jia J. Quantitative trait loci (QTL) of stem strength and related traits in a doubled-haploid population of wheat (*Triticum aestivum* L.). *Euphytica*. 2005;141:1-9. DOI 10.1007/s10681-005-4713-2.

Kaur S., Zhang X., Mohan A., Dong H., Vikram P., Singh S., Zhang Z., Gill K.S., Dhugga K.S., Singh J. Genome-Wide Association Study reveals novel genes associated with culm cellulose content in bread wheat (*Triticum aestivum* L.). *Front. Plant Sci*. 2017;8:1913. DOI 10.3389/fpls.2017.01913.

Kelbert A.J., Spaner D., Briggs K.G., King J.R. The association of culm anatomy with lodging susceptibility in modern spring wheat genotypes. *Euphytica*. 2004;136:211-221. DOI 10.1023/B:EUPH.0000030670.36730.a4.

Keller M., Karutz C., Schmid J.E., Stamp P., Winzler M., Keller B., Messner M.M. Quantitative trait loci for lodging resistance in a segregating wheat × spelt population. *Theor. Appl. Genet*. 1999;98: 1171-1182.

Khobra R., Sareen S., Meena B.K., Kumar A., Tiwari V.K., Singh G.P. Exploring the traits for lodging tolerance in wheat genotypes. *Phy-*

siol. Mol. Biol. Plants. 2019;25(3):589-600. DOI 10.1007/s12298-018-0629-x.

Knopf C., Becker H., Ebmeyer E., Korzun V. Occurrence of three dwarfing *Rht* genes in German winter wheat varieties. *Cereal Res. Commun.* 2008;36(4):553-560. DOI 10.1556/CRC.36.2008.4.4.

Kong E., Liu D., Guo X., Yang W., Sun J., Li X., Zhan K., Cui D., Lin J., Zhang A. Anatomical and chemical characteristics associated with lodging resistance in wheat. *Crop J.* 2013;1:43-49. DOI 10.1016/j.cj.2013.07.012.

Li C., Bai G., Carver B.F., Chao S., Wang Z. Mapping quantitative trait loci for plant adaptation and morphology traits in wheat using single nucleotide polymorphisms. *Euphytica*. 2015;208:299-312. DOI 10.1007/s10681-015-1594-x.

Mavi G.S., Nanda G.S., Sohu V.S. Screening bread wheat genotypes for lodging resistance. *Crop Improv.* (*India*). 2004;31(1):113-118.

McIntosh R.A., Dubcovsky J., Rogers W.J., Morris C., Appels R., Xia X.C. Catalogue of Gene Symbols for Wheat: 2013, Supplement 2014–2017. Available at: www.shigen.nig.ac.jp/wheat/komugi/genes/

Mulder E.G. Effect of mineral nutrition on lodging of cereals. *Plant Soil*. 1954;5(3):246-306.

Niu L., Feng S., Ding W., Li G. Influence of speed and rainfall on large-scale wheat lodging from 2007 to 2014 in China. *PLoS One.* 2016; 11(7):e0157677. DOI 10.1371/journal.pone.0157677.

Packa D., Wiwart M., Suchowilska E., Dienkowska T. Morpho-anatomical traits of two lowest internodes related to lodging resistance in selected genotypes of *Triticum*. *Int. Agrophys*. 2015;29:475-483. DOI 10.1515/intag-2015-0053.

Pearce S., Saville R., Vaughan S.P., Chandler P.M., Wilhelm E.P., Sparks C.A., Al-Ka N., Korolev A., Boulton M.I., Phillips A.L. Molecular characterization of *Rht-1* dwarfing genes in hexaploid wheat. *Plant Physiol*. 2011;157:1820-1831. DOI 10.1104/pp.111.183657.

Peng D., Chen X., Yin Y., Lu K., Yang W., Tang Y., Wang Z. Lodging resistance of winter wheat (*Triticum aestivum* L.) lignin accumulation and its related enzymes activities due to the application of paclobutrazol or gibberellin acid. *Field Crops Res*. 2014;157:1-7. DOI 10.1016/j.fcr.2013.11.015.

Peng J., Richards D.E., Hartley N.M., Murphy G.P., Devos K.M., Flintham J.E., Beales J., Fish L.J., Worland A.J., Pelica F., Sudhakar D., Christou P., Snape J.W., Gale M.D., Harberd N.P. 'Green revolution' genes encode mutant gibberellin response modulators. *Nature*. 1999;400(6741):256-261.

Pinthus M.J. Spread of the root system as indicator for evaluating lodging resistance of wheat. *Crop Sci.* 1967;7:107-110.

Shah A.N., Tanveer M., Rehman A.U., Anjum S.A., Iqbal J., Ahmad R. Lodging stress in cereal – effects and management: an overview. *Environ. Sci. Pollut. Res.* 2017;24:5222-5237. DOI 10.1007/s11356-016-8237-1.

Shah L., Yahya M., Shah S., Nadeem M., Ali A., Ali A., Wang J., Riaz M.W., Rehman S., Wu W., Khan R.M., Abbas A., Riaz A., Anis G.B., Si H., Jiang H., Ma C. Improving lodging resistance: using wheat and rice as classical examples. *Int. J. Mol. Sci.* 2019;20:4211. DOI 10.3390/ijms20174211.

Singh D., Wang X., Kumar U., Gao L., Noor M., Imtiaz M., Singh R.P., Poland J. High-throughput phenotyping enabled genetic dissection of crop lodging in wheat. *Front. Plant Sci*. 2019;10:394. DOI 10.3389/fpls.2019.00394.

Souza L.T., Espíndula M.C., Rocha V.S., Fernandes D.C., Souza M.A. Growth retardants in wheat and its effect in physiological quality of seeds. *Ciência Rural.* 2010;40(6):1431-1434. DOI 10.1590/S0103-84782010000600031.

Thomas S.G. Novel *Rht-1* dwarfing genes: tools for wheat breeding and dissecting the function of DELLA proteins. *J. Exp. Bot.* 2017;68(3): 354-358. DOI 10.1093/jxb/erw509.

Vera-Sirera F., Gomez M.D., Perez-Amador M.A. DELLA proteins, a group of GRAS transcription regulators that mediate gibberellin signaling. In: Gonzalez D.H. (Ed.). Plant Transcription Factors: Evolutionary, Structural and Functional Aspects. Acad. Press; Elsevier, 2016;313-328. DOI 10.1016/B978-0-12-800854-6.00020-8.

Verma V., Worland A., Savers E., Fish L., Caligari P., Snape J. Identification and characterization of quantitative trait loci related to lodging resistance and associated traits in bread wheat. *Plant Breed.* 2005;124:234-241. DOI 10.1111/j.1439-0523.2005.01070.x.

Walsh O.S., Shafian S., McClintick-Chess J.R., Belmont K.M., Blanscet S.M. Potential of silicon amendment for improved wheat production. *Plants*. 2018;7(2):26. DOI 10.3390/plants7020026.

Wang Y., Chen L., Du Y., Yang Z., Condon A.G., Hu Y.-G. Genetic effect of dwarfing gene *Rht13* compared with *Rht-D1b* on plant height and some agronomic traits in common wheat (*Triticum aestivum* L.). *Field Crops Res.* 2014;162:39-47. DOI 10.1016/j.fcr.2014.03.014.

Weibel R.O., Pendleton J.W. Effect of artificial lodging on winter wheat grain yield and quality. *Agron. J.* 1964;56:487-488.

Wurschum T., Langer S.M., Longin C.F.H., Tucker M.R., Leiser W.L. A modern Green Revolution gene for reduced height in wheat. *Plant J.* 2017;92:892-903. DOI 10.1111/tpj.13726.

Xiao Y., Liu J., Li H., Cao X., Xia X., He Z. Lodging resistance and yield potential of winter wheat: effect of planting density and genotype. *Front. Agr. Sci. Eng.* 2015;2(2):168-178. DOI 10.15302/J-FASE-2015061.

Yamaguchi S. Gibberellin metabolism and its regulation. *Annu. Rev. Plant Biol.* 2008;59:225-251. DOI 10.1146/annurev.arplant.59.032607.092804.

Zhang M., Wang H., Yi Y., Ding J., Zhu M., Li C. Effect of nitrogen levels and nitrogen ratios on lodging resistance and yield potential of winter wheat (*Triticum aestivum* L.). *PLoS One.* 2017;12(11): e0187543. DOI 10.1371/journal.pone.0187543.

Zheng M., Chen J., Shi Y., Li Y., Yin Y., Yang D., Luo Y., Pang D., Xu X., Li W., Ni J., Wang Y., Wang Z., Li Y. Manipulation of lignin metabolism by plant densities and its relationship with lodging resistance in wheat. *Sci. Rep.* 2017;7:41805. DOI 10.1038/srep41805.

Zuber U., Winzeler H., Messmer M.M., Keller M., Keller B., Schmid J.E., Stamp P. Morphological traits associated with lodging resistance of spring wheat. *J. Agron. Crop Sci.* 1999;182:17-24.

ORCID ID

E.V. Ageeva orcid.org/0000-0002-7714-5609
I.N. Leonova orcid.org/0000-0002-6516-0545

Acknowledgements. This work was supported by the Russian Science Foundation, project 16-16-00011P.

Conflict of interest. The authors declare no conflict of interest.

Received January 22, 2020. Revised March 30, 2020. Accepted April 17, 2020.

Вавиловский журнал генетики и селекции. 2020;24(4):363-375
DOI 10.18699/VJ20.629

Устойчивость к возбудителям фитофтороза и глободероза современного сортимента семенного картофеля и его фитосанитарное состояние в различных агроклиматических зонах европейской части России

А.В. Хютти[1, 3] ✉, Д.А. Рыбаков[2], Т.А. Гавриленко[2, 3], О.С. Афанасенко[1, 3]

[1] Всероссийский научно-исследовательский институт защиты растений, г. Пушкин, Санкт-Петербург, Россия
[2] Федеральный исследовательский центр Всероссийский институт генетических ресурсов растений им. Н.И. Вавилова (ВИР), Санкт-Петербург, Россия
[3] Федеральный исследовательский центр Институт цитологии и генетики Сибирского отделения Российской академии наук, Новосибирск, Россия
✉ e-mail: khiutti@mail.ru

Аннотация. Активная экспансия зарубежных сортов картофеля на территорию Российской Федерации привела к смене доминирующих видов патогенов этой культуры и появлению новых патотипов возбудителей вредоносных болезней. Целью работы была оценка устойчивости к возбудителям фитофтороза и глободероза современного сортимента картофеля и определение поражаемости возделываемых сортов картофеля грибными и оомицетными болезнями в различных агроклиматических зонах России. Проведена оценка устойчивости 41 сорта зарубежной селекции, разрешенного к использованию на территории РФ, к патотипу Ro1 *Globodera rostochiensis* и к изоляту VZR17 *Phytophthora infestans*, включающего гены вирулентности 1.2.3.4.5.6.7.8.9.10.11. Устойчивыми к золотистой картофельной нематоде оказались 38 сортов. У 96.6 % изученных нематодоустойчивых сортов выявлен маркер гена *H1* устойчивости к патотипу Ro1 *G. rostochiensis*, восприимчивые сорта этим маркером не обладали. Абсолютной устойчивостью к возбудителю фитофтороза отличались сорта Alouette и Sarpo Mira (балл 9); высоким уровнем устойчивости (баллы 6 и 7) характеризовались сорта Evolution, Red Fantasy и Ricarda. Сорта Baltic Rose, Damaris, Desiree, Gala, Labella, Laperla, Mia, Sanibel, Zekura, Queen Anne, Red Lady и 7 for 7 были отнесены к восприимчивым, хотя в характеристиках оригинаторов указана средняя устойчивость к фитофторозу. Фитопатологическая экспертиза проведена для 92 образцов 39 сортов семенного картофеля из четырех федеральных округов РФ: Приволжского, Северо-Западного, Центрального и Северо-Кавказского. Наибольшее распространение на всех сортах получили ризоктониоз, сухая фузариозная гниль и серебристая парша. Стопроцентное поражение клубней серебристой паршой отмечено в различных регионах на сортах элитных репродукций Red Scarlett, Evolution, Labella, Colombo, Gala, Невский. Широко распространен антракноз картофеля; сильнее всего были поражены клубни элитной и второй репродукции сорта Red Scarlett – от 50.0 до 71.4 % в Центральном федеральном округе.

Ключевые слова: распространенность болезней картофеля; *Phytophthora infestans*; *Globodera rostochiensis*; серебристая парша; антракноз; сорта картофеля; устойчивость; ДНК-маркеры.

Для цитирования: Хютти А.В., Рыбаков Д.А., Гавриленко Т.А., Афанасенко О.С. Устойчивость к возбудителям фитофтороза и глободероза современного сортимента семенного картофеля и его фитосанитарное состояние в различных агроклиматических зонах европейской части России. *Вавиловский журнал генетики и селекции*. 2020;24(4):363-375. DOI 10.18699/VJ20.629

Resistance to causal agents of late blight and golden potato nematode of the modern cultivars of seed potatoes and their phytosanitary status in various agroclimatic zones of the European part of Russia

A.V. Khiutti[1, 3] ✉, D.A. Rybakov[2], T.A. Gavrilenko[2, 3], O.S. Afanasenko[1, 3]

[1] All-Russian Institute of Plant Protection, Pushkin, St. Petersburg, Russia
[2] Federal Research Center the N.I. Vavilov All-Russian Institute of Plant Genetic Resources (VIR), St. Petersburg, Russia
[3] Institute of Cytology and Genetics of Siberian Branch of the Russian Academy of Sciences, Novosibirsk, Russia
✉ e-mail: khiutti@mail.ru

Abstract. The active expansion of foreign potato cultivars on the territory of the Russian Federation has led to a change in the dominant pathogen species and to the emergence of new pathotypes of causal agents of harmful potato diseases. The aim of the study was to evaluate resistance to *Phytophthora infestans* and *Globodera rostochiensis* of modern potato cultivars and determine the distribution of fungal and oomycetic diseases on potato cultivars in various

agroclimatic zones of Russia. The resistance of 41 foreign cultivars was evaluated to pathotype Ro1 *G. rostochiensis* and to isolate VZR17 *P. infestans* with virulence genes 1.2.3.4.5.6.7.8.9.10.11. Resistant to *G. rostochiensis* were 38 cultivars. 57R marker of the *H1* gene conferring resistance to the Ro1 pathotype of *G. rostochiensis* was detected in 96.6 % of the nematode resistant cultivars studied; susceptible varieties did not possess this marker. Absolute resistance to the causative agent of late blight was demonstrated by the cultivars Alouette and Sarpo Mira (score 9); high levels of resistance (score 6 and 7) were determined for the cultivars Evolution, Red Fantasy and Ricarda. The cultivars Baltic Rose, Damaris, Desiree, Gala, Labella, Laperla, Mia, Sanibel, Zekura, Queen Anne, Red Lady and '7 for 7' were classified as susceptible, although the characteristics of originators indicated average resistance to late blight. A phytopathological test was conducted on 92 samples of 39 varieties of seed potatoes from four federal districts of the Russian Federation: Volga, North-West, Central and North Caucasus. *Rhizoctonia solani*, *Fusarium* spp. and *Helminthosporium solani* are most common on all varieties. 100 % defeat of tubers by *H. solani* was recorded in various regions on the cultivars Red Scarlett, Evolution, Labella, Colombo, Gala and Nevsky. Widespread *Colletotrichum coccodes* on tubers of the elite and 2nd reproductions of the potato cultivar Red Scarlett (50.0–71.4 %) was recorded in the Central District.
Key words: distribution of potato diseases; *Phytophthora infestans*; *Globodera rostochiensis*; potato cultivars; resistance to diseases; *Helminthosporium solani*; *Colletotrichum coccodes*; DNA markers.

For citation: Khiutti A.V., Rybakov D.A., Gavrilenko T.A., Afanasenko O.S. Resistance to causal agents of late blight and golden potato nematode of the modern cultivars of seed potatoes and their phytosanitary status in various agroclimatic zones of the European part of Russia. *Vavilovskii Zhurnal Genetiki i Selektsii = Vavilov Journal of Genetics and Breeding*. 2020;24(4):363-375. DOI 10.18699/VJ20.629 (in Russian)

Введение

В 2015 г. в Берлине, на Международном конгрессе по защите растений (IPPC 2015) были представлены данные о том, что на картофеле даже при применении химических средств защиты потери от болезней составляют 25–30 % (Oerke, 2006).

Российская Федерация является лидером по выращиванию зарубежных сортов картофеля: из 455 сортов, включенных в «Государственный реестр селекционных достижений, допущенных к использованию» в 2019 г., 182 (40.0 %) – селекции стран дальнего зарубежья, 34 (7.5 %) – стран СНГ, и только 239 (52.5 %) сортов созданы российскими селекционерами (www.gossortrf.ru). Отметим также, что в большинстве картофелеводческих хозяйств представленность зарубежных сортов достигает 100 %.

Активная экспансия зарубежных сортов и несоблюдение регламента по их агротехнике привели к плачевному результату: на территории РФ распространились новые патотипы, относящиеся как к оомицетам и грибам, так и к вирусам, бактериям и нематодам (Еланский, 2015; Кузнецова и др., 2016). Кроме того, появляются новые патогены, например возбудители черной ножки и мокрой гнили *Pectobacterium carotovorum* subsp. *brasiliense*, *P. carotovorum* subsp. *odoriferum*, *P. parmentieri*, новый для России вирус P (PVP), возбудитель розового фитофтороза *Phytophthora erythroseptica* Pethybr. (Игнатов и др., 2019; Yanagisawa et al., 2019).

Наиболее вредоносными в России являются следующие оомицетные и грибные болезни картофеля: фитофтороз (*Phytophthora infestans* (Mont.) de Bary), потери урожая от которого без применения химических средств защиты варьируют от 80 до 100 %; комплекс паршей картофеля, включающий ризоктониоз (*Rhizoctonia solani* Kühn), серебристую (*Helminthosporium solani* Durieu et Mont.), обыкновенную (*Streptomyces* spp.), бугорчатую (*Polyscytalum pustulans* (Owen & Wakef.) Ellis) и порошистую (*Spongospora subterranea* f. sp. *subterranea* Toml.) паршу, потери от которых достигают 30 %; а также антракноз (*Colletotrichum coccodes* (Wallr.) Hughes) – потери до 20–30 %, сухая фузариозная гниль (грибы рода *Fusarium* spp.) и фомоз (*Phoma* spp.) – потери не менее 20 %, и объект как внутреннего, так и внешнего карантина – золотистая картофельная нематода (*Globodera rostochiensis* (Wollenweber, 1923) Skarbilovich, 1959), вредоносность которой достигает 80–90 % (Winslow, Willis, 1972; Dillard, 1992; Johnson, Miliczky, 1993; Johnson, 1994; Tsror et al., 1999; Collins, 2000; Lees, Hilton, 2003; Judelson, Blanco, 2005; Haldar et al., 2006; Gudmestad et al., 2007; Haverkort et al., 2009; Tsror, 2010; Abbas et al., 2013).

Конкурентоспособность сортов картофеля определяется главным образом устойчивостью к наиболее вредоносным в зоне возделывания болезням. В связи с этим создание сортов картофеля, устойчивых к основным болезням, является приоритетным направлением селекции. Доля устойчивых к болезням сортов картофеля, зарегистрированных в Госреестре селекционных достижений, с каждым годом увеличивается. Наиболее существенные результаты получены при селекции картофеля на устойчивость к карантинным болезням. Все новые сорта, внесенные в Госреестр, отличаются устойчивостью к возбудителю рака картофеля, кроме четырех старых сортов (Волжанин, Ермак улучшенный, Лорх и Приобский), доля которых составляет 0.6 %. К настоящему времени 55.4 % сортов, включенных в Госреестр, устойчивы к золотистой картофельной нематоде (ЗКН) (www.gossortrf.ru). Зарегистрированные в Госреестре в 2019 г. 22 сорта картофеля охарактеризованы оригинаторами и Госсортокомиссией по устойчивости только к четырем возбудителям: раку (все устойчивы), золотистой картофельной нематоде (устойчивы 15 сортов) и морщинистой и полосчатой мозаике, возбудителем которых является PVY (устойчивы 8 сортов). Между тем ни отечественные, ни зарубежные сорта в Госреестре не охарактеризованы на устойчивость к таким вредоносным заболеваниям, как фитофтороз, ризоктониоз, обыкновенная и серебристая парша, антракноз, а также к другим вирусным болезням. Информацию по устойчивости некоторых новых отечественных сортов можно найти в издании «Сорта картофеля российской селекции» (2018).

На сайтах зарубежных селекционных фирм приводятся характеристики устойчивости к наиболее экономически значимым болезням, в частности к цистообразующим нематодам, вирусу картофеля Y (PVY) и к фитофторозу. Однако возможны расхождения в оценках, сделанных за рубежом и в условиях разных агроклиматических зон России. Связано это прежде всего с различным составом популяций патогенов и особенностями экологических условий. В этом плане большое значение имеет информация о генах устойчивости сортов, особенно тех, что обладают устойчивостью к различным патотипам и видам цистообразующих нематод, поскольку фитопатологические тесты длительны, трудоемки и не всегда возможны для карантинных объектов. В зарубежных селекционных центрах давно и успешно используются методы ДНК-маркирования для оценки генетической защищенности сортового генофонда. В последнее время такие данные появляются и для отечественных сортов. Так, сотрудниками ВИР проведен скрининг 225 отечественных сортов картофеля, 114 из которых входят в «Государственный реестр селекционных достижений, допущенных к использованию» (Антонова и др., 2016; Клименко и др., 2017; Гавриленко и др., 2018). Наиболее эффективный маркер 57R гена *H1* выявлен лишь у 28 % изученных сортов (и у 26 %, входящих в Госреестр); эти сорта по данным госсортоиспытаний являются устойчивыми к патотипу Ro1 золотистой картофельной нематоды.

В связи с экономической значимостью особо опасных болезней, характеристика поражаемости современных сортов возбудителями этих болезней имеет важное значение для селекции и семеноводства, а также для выбора сортов для возделывания, особенно семенного картофеля, в эпидемиологически опасных зонах. Целью работы была оценка устойчивости к возбудителям фитофтороза и глободероза и определение поражаемости возделываемых сортов картофеля грибными и оомицетными болезнями в различных агроклиматических зонах России.

Материалы и методы

Растительный материал. Экспериментальной выборкой для изучения устойчивости к патогенам послужили 42 сорта зарубежной и 1 сорт (восприимчивый контроль) отечественной селекции. Для 21 сорта из выборки была проведена фитопатологическая экспертиза образцов семенного картофеля из различных регионов РФ.

Оценка на устойчивость к ЗКН. Оценку на устойчивость сеянцев картофеля к *G. rostochiensis* проводили по методике, рекомендованной Европейской и Средиземноморской организацией по защите растений, с небольшими модификациями (OEPP/EPPO, 2006). Исследуемые сорта высаживали в пластиковые горшки объемом 500 см^3, наполовину наполненные почвой (по одному клубню в каждый горшок). В качестве инфекционного материала для инокуляции сортов использовали популяцию золотистой картофельной нематоды, отобранную в Ленинградской области из известного очага *G. rostochiensis* и типированную до патотипа Ro1 (Limantceva et al., 2014).

В каждый горшок вносили инокулюм ЗКН из расчета 1500 яиц и личинок в 100 см^3 почвы. Яйца и личинки получали методом раздавливания цист ЗКН в капле воды на предметном стекле. После инокуляции клубней дополнительно досыпали почву до верха горшка. Горшки оставляли в контролируемых условиях при температуре 22 °С. В качестве восприимчивого контроля использовали сорт Невский, в качестве устойчивого контроля – сорт Red Scarlett. Сорта высаживали в десятикратной повторности и двукратной аналитической. Учет результатов заражения проводили через три месяца, что является достаточным промежутком времени для развития цист ЗКН. Экстракцию цист из почвы осуществляли методом флотации (Turner, 1998). Экстрагированные цисты переносили на покровные стекла в каплю воды, раздавливали и подсчитывали количество яиц и личинок в них.

Оценку результатов заражения проводили по шкале с подразделением образцов на группы: балл 9 (относительная восприимчивость <1 %) – Very high; балл 8 (1.1–3 %) – High/very high; балл 7 (3.1–5 %) – High; балл 6 (5.1–10 %) – Moderate/high; балл 5 (10.1–15 %) – Moderate; балл 4 (15.1–25 %) – Moderate/low; балл 3 (25.1–50 %) – Low; балл 2 (50.1–100 %) – Low/very low; балл 1 (>100 %) – Very low. К классу устойчивых (R) относили растения, тип реакции которых соответствовал 7–9 баллам, среднеустойчивых (RS) – 4–6 баллам, восприимчивых (S) – 1–3 баллам. Относительную восприимчивость определяли по формуле: количество яиц и личинок исследуемого образца делили на количество яиц и личинок эталонного восприимчивого сорта и умножали на 100 %.

Оценка на устойчивость к фитофторозу. Лабораторный скрининг сортов картофеля на устойчивость к фитофторозу проводили по стандартной методике (Brylińska, Śliwka, 2017). В качестве инфекционного материала использовали изолят VZR17, включающий все гены вирулентности 1.2.3.4.5.6.7.8.9.10.11.

Отделенные листья помещали в поддоны (45 × 35 см) на влажную фильтровальную бумагу, абаксиальной стороной вниз: по 3 листа каждого образца, по 3 листа восприимчивого сорта Bintje и по 3 листа устойчивого контроля сорта Sarpo Mira, в двукратной биологической повторности. Для заражения использовали инокулюм, выдержанный в течение 30 мин при температуре 10–12 °С для стимуляции выхода зооспор. Инфекционная нагрузка составляла 50000 спорангиев/мл. Инокулюм наносили по одной капле по центру каждого листа между центральной и отходящей жилками. Объем капли составлял 30 мкл. Инокулированные листья выдерживали в течение 24 ч в темноте при температуре 16 °С. На протяжении всего эксперимента поддоны были закрыты стеклянными крышками для поддержания постоянной влажности (80–100 %). Через сутки после инокуляции листья переворачивали абаксиальной стороной вверх, после чего кюветы переносили в климатический бокс с температурой 16 °С, интенсивностью освещения 1600 лк и 16-часовым фотопериодом.

Учет результатов заражения проводили на 6-е сутки после инокуляции, по стандартной шкале с подразделением образцов на группы: балл 9 (0 % пораженной площади) – Very high; балл 8 (3 %) – High/very high; балл 7 (3.1–10 %) – High; балл 6 (10.1–25 %) – Moderate/high; балл 5 (25.1–75 %) – Moderate; балл 4 (75.1–90 %) – Moderate/

Table 1. DNA primers of the *H1* gene conferring resistance to *Globodera rostochiensis* (pathotypes Ro1, Ro4) used in molecular screening of potato varieties

Chromosome	Gene	Primer	T°m	Diagnostic amplicon size, bp	References
V	*H1*	57R	60	450	Schultz et al., 2012
		239E4left/AluI	52	120 + 230	Bakker et al., 2004

low; балл 3 (90.1–97 %) – Low; балл 2 (97.1–99 %) – Low/very low; балл 1 (100 %) – Very low. Растения с типом реакции, соответствующим баллам 7–9, относили к классу устойчивых (R), 4–6 – среднеустойчивых (RS), 1–4 – восприимчивых (S).

Молекулярный скрининг. ДНК выделяли из листьев тепличных растений методом модифицированной CTAB-экстракции (Gavrilenko et al., 2013). Скрининг проводили на наличие маркеров гена *H1*, контролирующего устойчивость к патотипам Ro1 и Ro4 *G. rostochiensis* (Dalamu et al., 2012). Для маркеров гена *H1* показана различная эффективность в молекулярном скрининге. Высокий уровень специфичности демонстрировал SCAR-маркер 57R и низкую эффективность – CAPS-маркер этого гена, 239E4left/AluI (Антонова и др., 2016). В то же время в исследованиях зарубежных коллег сообщалось о высокой частоте встречаемости CAPS-маркера 239E4left/AluI гена *H1* у нематодоустойчивых зарубежных сортов. Поэтому в данной работе использовали оба эти маркера. Праймеры для работы подбирали по литературным источникам (табл. 1). Использовали SCAR-маркер 57R, интегрированный в ассоциированную с устойчивостью область '341 Kb' локуса *H1*, и CAPS-маркер 239E4left/AluI, расположенный на расстоянии 2.1 сМ от ассоциированного с устойчивостью локуса (Finkers-Tomczak et al., 2011).

ПЦР проводили в 20 мкл реакционной смеси состава: 40 нг тотальной ДНК, 1× реакционный буфер, 2.5 мМ $MgCl_2$, 0.4 мМ каждого из dNTP, по 0.25 мкМ прямого и обратного праймера и 1 ед. Taq-полимеразы («Диалат», Москва). Условия реакции соответствовали указанным в литературе.

В качестве положительных контролей для маркера 57R использовали сорта Живица, Сударыня и Sante, для которых наличие диагностического фрагмента было установлено нами ранее; контролем для маркера 239E4left/AluI служил сорт Sante (Антонова и др., 2016). Рестрикцию осуществляли ферментом AluI («СибЭнзим»), используя протокол фирмы-изготовителя. Фрагменты ДНК разделяли электрофорезом в 2 % агарозных гелях с окрашиванием бромистым этидием и визуализацией в УФ-свете.

Фитопатологический анализ. Отбор клубневых проб и диагностику осуществляли в соответствии с методиками, приведенными в ГОСТ 33996-2016 «Картофель семенной. Технические условия и методы определения качества» (2017), и международным стандартом по семенному картофелю UNECE S-1 (2018). Для каждого анализируемого образца отбиралось по 10 точечных проб, составлявших в совокупности не менее 250 клубней. Однако для образцов, датированных 2018 г., количество анализируемых клубней варьировало от 20 до 100 шт.

Экспериментальная выборка при фитопатологической экспертизе семенного картофеля состояла из 92 образцов 39 сортов из четырех федеральных округов РФ: 24 образца из Приволжского, 35 – из Северо-Западного, 8 – из Центрального, 9 – из Северо-Кавказского.

Диагностику оомицетных, грибных и бактериальных болезней выполняли, руководствуясь информацией, представленной в специализированных компендиумах (Compendium…, 1981, 2001; Diseases…, 2008), а также с использованием определителей UNECE (2014) и AHDB (2018).

Анализировали каждый клубень изучаемого образца. Клубни с нетипичной симптоматикой или малозаметными патологическими изменениями помещали во влажные камеры. Поверхность клубней предварительно дезинфицировали 70 % этиловым спиртом с последующей промывкой дистиллированной водой. При необходимости клубни разрезали на небольшие ломтики размером не менее 1 см. Инкубационный период составлял от 3 до 14 дней, в зависимости от возбудителя, при постоянной температуре 20 °C и 100 % влажности.

Выделение в чистую культуру возбудителей болезней осуществляли с использованием картофельной (картофель 200 г, агар-агар 20 г, H_2O 1000 мл) и ржаной (рожь 60 г, сахароза 20 г, агар-агар 15 г, H_2O 1000 мл) сред.

Результаты

Устойчивость сортов картофеля к золотистой картофельной нематоде

Согласно полученным данным, из 41 сорта зарубежной селекции только три сорта (или 7.3 % от всех изученных) оказались восприимчивыми к ЗКН: Bintje, Desiree и Sarpo Mira; остальные проявили себя как устойчивые. Промежуточных групп устойчивости не было выявлено (табл. 2).

Среди 29 изученных нематодоустойчивых сортов частота встречаемости генотипов со SCAR-маркером 57R гена *H1*, определяющего устойчивость к патотипу Ro1 *G. rostochiensis*, очень высокая – 96.6 % (28 из 29 устойчивых сортов). Исключением является устойчивый (по данным фитопатологических тестов) сорт Red Fantasy, у которого не выявлены маркеры гена *H1* (рис. 1, см. табл. 2).

Коэффициент корреляции Пирсона между наличием маркера 57R и данными об устойчивости сортов к патотипу Ro1 составил +0.88 (n = 33, вместе с контролем – сорт Невский). Другой маркер гена *H1* – CAPS-маркер 239E4Left/AluI – обнаруживался гораздо реже. Этот маркер наряду с 57R был детектирован только у трех сортов (Armada, Estrella, Gala), все они проявляли устойчивость к ЗКН (см. табл. 2).

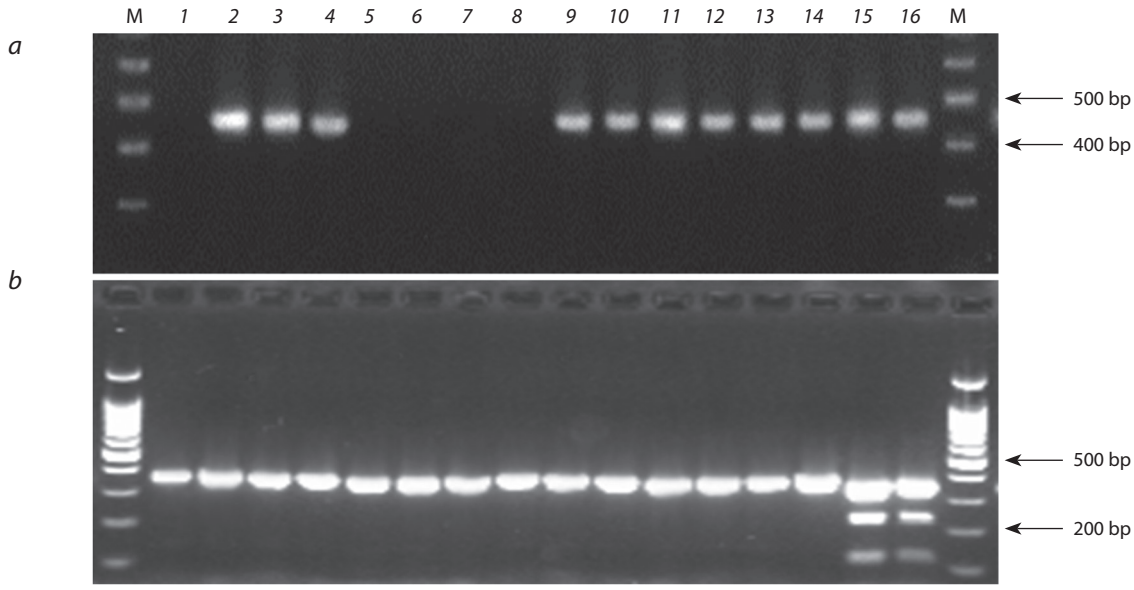

Fig. 1. Molecular screening of potato cultivars using DNA markers 57R (*a*) and 239E4left (*b*) for the *H1* gene.

Varieties: *1*. Nevskiy, *2*. Alouette, *3*. Baltic Rose, *4*. Nandina, *5*. Sarpo Mira, *6*. Bintje, *7*. Desiree, *8*. Red Fantasy, *9*. Christel, *10*. Madeira, *11*. Ramos, *12*. Queen Anne, *13*. Delphine, *14*. Labella, *15*. Armada, *16*. Estrella. M, molecular ladder 100 bp + 1.5 Kb (SibEnzyme, Russia).

Устойчивость сортов картофеля к возбудителю фитофтороза

Только два сорта зарубежной селекции оказались абсолютно устойчивыми к возбудителю фитофтороза картофеля: Alouette и Sarpo Mira (см. табл. 2). Остальные 39 сортов показали разный уровень устойчивости или восприимчивости. Из них можно отметить три сорта: Evolution, Red Fantasy и Ricarda, которые выделялись достаточно высоким уровнем устойчивости (средний балл 7.3, 6.8 и 6.4 соответственно).

Оценка фитосанитарного состояния семенного картофеля различных сортов в регионах РФ

Результаты фитопатологического анализа партий элитного и репродукционного семенного картофеля свидетельствуют, что во всех регионах на семенном картофеле выявлены: *Ph. infestans*, *R. solani*, *H. solani*, *Streptomyces* spp., *P. pustulans*, *C. coccodes*, *Fusarium* spp., *Phoma* spp. (табл. 3). Бугорчатая парша *P. pustulans* отмечена повсеместно, кроме Северо-Кавказского федерального округа. Порошистая парша *S. subterranea* f. sp. *subterranea* отмечена только в одном образце сорта Вектор в Приволжском федеральном округе.

Наибольшее распространение на всех сортах получили ризоктониоз и серебристая парша (рис. 2). Стопроцентное поражение клубней серебристой паршой отмечено в различных регионах на сортах Red Scarlett (СЭ, Э и РС1-2), Evolution (Э, РС1), Labella (Э), Colomba (Э), Gala (Э), Невский (Э). В Северо-Кавказском ФО серебристая парша была отмечена только на 6.0 % образцов сорта Невский (СЭ). Широкое распространение получил антракноз картофеля. Сильнее всего были поражены клубни сорта Red Scarlett (Э и РС2) – от 50 до 71.4 % в Центральном федеральном округе. Максимальное поражение фитофторозом отмечено на сорте Невский (Э) – 63.1 %.

Обсуждение

Одним из приоритетных направлений селекции является создание сортов, сочетающих в себе групповую устойчивость, в первую очередь к таким опасным заболеваниям, как фитофтороз, ризоктониоз, комплекс паршей, вирусные, бактериальные и нематодные болезни. В «Государственном реестре селекционных достижений, допущенных к использованию» на территории Российской Федерации (2019), данные по устойчивости сортов картофеля к комплексу заболеваний отсутствуют. Среди обязательных характеристик приведены показатели устойчивости к раку, золотистой картофельной нематоде и вирусу Y. Для некоторых сортов указана их устойчивость/восприимчивость к фитофторозу. Наши результаты свидетельствуют, что патогенный комплекс на современных сортах картофеля значительно шире и может быть определяющим для конкурентоспособности сорта на отечественном рынке сортов.

Для сортов зарубежной селекции на англоязычных интернет-ресурсах в полной мере отражены все сортовые особенности, включая устойчивость к основным заболеваниям по 9-балльной шкале. Стоит отметить, что для большинства сортов приведена информация по устойчивости к фитофторозу ботвы и клубней и к вирусу картофеля Y (PVY). Наличие остальной информации по устойчивости/восприимчивости к болезням варьирует в зависимости от семеноводческой компании и страны-производителя. Общеизвестно, что оценка сорта на устойчивость к заболеваниям проводится на территории страны-оригинатора к местным популяциям или расам патогенов, которые могут значительно отличаться от представленных в России. Например, при фитопатологическом анализе сорта Sifra, который по данным оригинатора высокоустойчив к фитофторозу по клубням (8 баллов, где 9 – абсолютная устойчивость) (см. табл. 3), количе-

Table 2. Characteristics of resistance of modern potato cultivars to *G. rostochiensis* and *Ph. infestans*

No.	Cultivar	Year of release	Country of origin, originator	Resistance (average score and group of resistance) – data of phytopathological analysis (this paper)				Markers for the *H1* alleles conferring resistance to Ro1 and Ro4 pathotypes of *G. rostochiensis* ("+/–" – presence/absence of marker)		Resistance: data from originators		
				G. rostochiensis, pathotype Ro1		*Ph. infestans*, leaf resistance		57R	239E4left/AluI	*G. rostochiensis*, resistance to pathotypes	*Ph. infestans*	
											Leaves	Tubers
1	Alouette	2018	AGRICO, UK	9.0	R	9.0	R	+	–	R, Ro1–3	R	R
2	Armada	–		9.0	R	5.0	RS	+	+	R, Ro1,4	S	RS
3	Bafana	2013	Netherlands, STET	9.0	R	3.0	S	No data	No data	R, Ro1	S	S
4	Baltic Rose	2019	Germany, Norika	9.0	R	3.0	S	+	–	R, Ro1	RS	S
5	Bintje	–	Netherlands, –	1.0	S	1.0	S	–	–	S, –	S	S
6	Captiva	2018	Germany, Europlant	9.0	R	5.9	RS	No data	No data	R, Ro1–5	–	–
7	Christel	2017	Germany, Norika	9.0	R	2.4	S	+	–	R, Ro1,4	S-RS	S-RS
8	Damaris	2014		9.0	R	1.4	S	+	–	R, Ro1–5	RS	RS
9	Delphine	2011		9.0	R	3.4	S	+	–	R, Ro1,4	S	S
10	Desiree	–	Netherlands, STET/HZPC	1.0	S	1.0	S	–	–	S, –	RS	R
11	Estrella	2011	Germany, Norika	9.0	R	1.8	S	+	+	R, Ro1–5	S	S
12	Evolution	2015	Netherlands, AGRICO	9.0	R	7.3	R	+	–	R, Ro1,4	RS	–
13	Fidelia	2014	Germany, Norika	9.0	R	2.0	S	+	–	R, Ro1,4	S-RS	S
14	Gala	2008		9.0	R	2.3	S	+	+	R, Ro1,4	RS	S
15	Gioconda	2018	Netherlands, HZPC	9.0	R	4.1	RS	No data	No data	R, Ro1	RS	RS
16	Impala	1995	Netherlands, AGRICO	9.0	R	4.1	RS	+	–	R, Ro1,4	RS	S
17	Inara	2013	Netherlands, Norika	9.0	R	1.9	S	+	–	R, Ro1	–	–
18	Juwel	–	Germany, Bavaria Saat	9.0	R	4.3	RS	+	–	R, Ro1,4	RS	–
19	Labadia	2010	Netherlands, STET	9.0	R	2.0	S	+	–	R, Ro1	RS	S

20	Labella	2011	Germany, Solana	9.0	R	1.3	S	+	–	R, Ro1,4	RS	R
21	Laperla	2015		9.0	R	2.1	S	+	–	R, Ro1	RS	R
22	Madeira	2017	Germany, Europlant	9.0	R	1.8	S	+	–	R, Ro1,4	–	–
23	Manifest	2014	Republic of Belarus	9.0	R	1.0	S	+	–	R, –	–	–
24	Mia	2019	Germany, Norika	9.0	R	3.0	S	No data	No data	R, Ro1,4	RS	S
25	Nandina	2015	Germany, Europlant	9.0	R	4.1	RS	+	–	R, Ro1	–	–
26	Paroli	2019	Germany, Norika	9.0	R	4.0	RS	+	–	R, Ro1	RS	S
27	Prada	–	Germany, Solana	9.0	R	3.8	S	+	–	R, Ro1,4	RS	RS
28	Primabelle	–	Netherlands, HZPC	9.0	R	1.1	S	No data	No data	R, Ro1	RS	RS
29	Queen Anne	2015	Germany, Solana	9.0	R	1.6	S	+	–	R, Ro1,4	RS-R	R
30	Ramos	2006	Netherlands, STET	9.0	R	1.0	S	+	–	R, Ro1	S	R
31	Ranomi	2018	Netherlands, AGRICO	9.0	R	4.4	RS	No data	No data	R, Ro1,4	S	S
32	Red Fantasy	2011	Germany, Europlant	9.0	R	6.8	RS-R	–	–	R, Ro1,4	R	–
33	Red Lady	2008	Germany, Solana	9.0	R	2.5	S	+	–	R, Ro1	RS-R	R
34	Red Scarlett	2000	Netherlands, HZPC	9.0	R	2.3	S	+	–	R, Ro1	RS	RS
35	Ricarda	2019	Germany, Europlant	9.0	R	6.4	RS-R	No data	No data	R, Ro1,4	RS-R	R
36	Rosara	1996	Germany, Solana	9.0	R	5.8	RS	+	–	R, Ro1	RS	R
37	Sanibel	2019	Germany, Europlant	9.0	R	3.0	S	No data	No data	R, Ro1	RS-R	R
38	Sarpo Mira	–	Hungary, –	1.0	S	9.0	R	–	–	S	R	R
39	VR 808	2013	Netherlands, STET	9.0	R	3.1	S	No data	No data	R, Ro1	–	R
40	Zekura	1997	Germany, Solana	9.0	R	1.0	S	+	–	R, –	R	R
41	7 for 7	2017		9.0	R	2.3	S	+	–	R, Ro1,4	RS	R
42	Nevskiy (susceptible control)	1982	Russia, VSS company and others	1.0	S	2.1	S	–	–	S	RS	RS

Note: Categories of sustainability are based on the data provided on the Internet portals of originators, the State Register of Breeding Achievements (2019), and catalogs. Designations: R, resistant; RS, moderately resistant; S, susceptible; –, no data.

Table 3. Phytopathological analysis of seed potato from various regions of the Russian Federation

Year	Cultivar	Frequency of pathogen occurrence, %									Mechanical damage
		R. solani	*H. solani*	*Streptomyces* spp.	*C. coccodes*	*Fusarium* spp.	*Phoma* spp.	*Ph. infestans*	*P. pustulans*	*S. subterranea* f. sp. *subterranea*	
						Volga region					
2019	Colomba E	36.0	100.0	6.0	7.0	43.0	5.0	0.0	0.0	0.0	75.0
2019	Evolution E	0.0	100.0	18.0	30.0	8.0	0.0	0.0	0.0	0.0	2.0
2019	Gala E	70.4	96.7	8.1	32.7	57.3	1.6	0.0	0.0	0.0	27.8
		18.0	69.0	0.0	13.0	21.0	0.0	5.0	0.0	0.0	47.0
		0.0	20.0	5.7	5.7	100.0	0.0	0.0	0.0	0.0	8.5
2018	Gala PC1	3.4	58.6	20.7	0.0	10.3	0.0	20.7	0.0	0.0	0.0
2019	Gala PC2	76.0	74.0	16.0	22.0	20.0	2.0	0.0	0.0	0.0	26.0
2019	Gala PC5	0.0	73.3	6.6	30.0	3.3	0.0	0.0	0.0	0.0	3.3
2019	Granada E	0.0	100.0	20.0	15.0	40.0	0.0	0.0	0.0	0.0	25.0
2018	Granada PC1	25.0	55.0	45.0	0.0	15.0	0.0	0.0	0.0	0.0	0.0
2019	Juwel PC1	0.0	83.3	6.6	33.0	13.3	0.0	0.0	3.3	0.0	43.3
2019	Labella E	0.0	100.0	10.0	10.0	30.0	0.0	0.0	0.0	0.0	60.0
2019	Madeira PC1	92.0	100.0	12.0	46.0	30.0	6.0	0.0	0.0	0.0	0.0
2019	Nandina PC1	80.0	90.0	12.0	32.0	46.0	2.0	0.0	0.0	0.0	6.0
2019	Queen Anne PC	24.0	74.0	20.0	12.0	62.0	0.0	0.0	0.0	0.0	42.0
2019	Ramos E	33.0	100.0	8.0	29.0	15.0	2.0	0.0	0.0	0.0	59.0
2019	Rozara PC1	34.0	98.0	10.0	48.0	22.0	0.0	0.0	4.0	0.0	14.0
2018	Sifra E	15.0	55.0	90.0	0.0	10.0	0.0	15.0	0.0	0.0	0.0
2019	Vineta E	0.0	50.0	50.0	40.0	30.0	0.0	0.0	0.0	0.0	20.0
2019	Wega E	0.0	86.1	13.8	16.6	22.2	2.7	0.0	0.0	0.0	50.0
2019	Zekura PC1	94.0	100.0	12.0	50.0	22.0	0.0	0.0	0.0	0.0	6.0
2018	Vector E	30.9	0.0	11.9	28.5	23.8	4.7	2.3	0.0	9.5	0.0
2018	Nevskiy E	57.8	15.7	5.2	0.0	10.5	0.0	63.1	0.0	0.0	0.0
2018	Nevskiy PC1	23.0	57.7	15.4	0.0	3.8	0.0	23.0	0.0	0.0	0.0
						North-West region					
2018	Alouette E	14.0	66.0	3.0	32.0	38.0	0.0	0.0	0.0	0.0	0.0
2019	Arrow SSE	1.5	9.5	4.0	1.5	6.5	0.0	0.0	0.0	0.0	10.0
2019	Asterix SE	0.0	0.0	0.0	0.0	0.0	0.0	0.0	0.0	0.0	0.0
2018	Colomba PC2	23.0	15.3	23.0	0.0	0.0	0.0	0.0	0.0	0.0	0.0
2019	Delphine PC1	0.0	100.0	60.0	50.0	0.0	0.0	0.0	0.0	0.0	0.0
2019	Evolution PC1	0.0	100.0	80.0	0.0	0.0	0.0	0.0	0.0	0.0	0.0
2019	Gala E	7.5	100.0	2.5	5.0	3.5	1.5	0.0	0.0	0.0	16.0
2019	Labadia E	7.0	61.0	59.0	20.0	8.0	0.0	0.0	0.0	0.0	50.0
2018		0.0	30.4	11.6	3.5	6.4	0.0	0.0	5.8	0.0	0.0
2018	Labella E	16.6	88.9	38.8	0.0	16.6	0.0	5.5	0.0	0.0	0.0
2018	Mondeo E	50.0	50.0	66.6	0.0	0.0	0.0	33.3	0.0	0.0	0.0
2018	Ramos E	0.0	71.4	0.0	0.0	0.0	0.0	0.0	0.0	0.0	0.0
2019	Red Scarlett SSE	0.0	19.0	0.0	4.0	2.5	0.0	0.0	0.0	0.0	1.5
2019	Red Scarlett SE	0.0	45.5	0.5	10.0	8.5	1.0	3.5	0.0	0.0	1.0
		0.0	100.0	60.0	0.0	30.0	0.0	0.0	0.0	0.0	50.0

Table 3 (end)

Year	Cultivar	Frequency of pathogen occurrence, %									Mechanical damage
		R. solani	*H. solani*	*Streptomyces* spp.	*C. coccodes*	*Fusarium* spp.	*Phoma* spp.	*Ph. infestans*	*P. pustulans*	*S. subterranea* f. sp. *subterranea*	
2019	Red Scarlett E	0.0	100.0	0.0	58.0	0.0	0.0	0.0	0.0	0.0	0.0
2018		31.5	63.1	0.0	0.0	5.2	0.0	0.0	0.0	0.0	0.0
		50.0	50.0	9.0	0.0	0.0	0.0	0.0	0.0	0.0	0.0
		64.7	58.8	0.0	23.5	47.0	11.7	0.0	0.0	0.0	0.0
2019		2.5	100.0	2.0	4.5	4.0	0.5	0.0	0.0	0.0	10.0
		1.0	48.5	2.5	9.0	4.0	0.0	0.0	0.0	0.0	1.0
2018	Red Scarlett PC1	0.0	100.0	17.8	0.0	0.0	0.0	0.0	0.0	0.0	0.0
2019	Romano E	25.0	31.0	28.0	18.0	4.5	1.5	0.0	0.0	0.0	13.5
2018	Wega E	45.4	27.2	9.1	0.0	4.5	0.0	0.0	0.0	0.0	0.0
2019	Zekura SSE	0.0	29.5	3.0	5.5	3.0	1.0	0.0	0.0	0.0	5.0
2018	Briz E	10.5	5.2	5.2	0.0	10.5	0.0	0.0	0.0	0.0	0.0
2018	Evraziya E	55.0	25.5	5.0	19.0	2.5	0.0	0.0	1	0.0	0.5
2018	Zorachka E	0.0	100.0	20.0	0.0	40.0	0.0	0.0	0.0	0.0	0.0
2018	Lomonosovskiy E	78.0	43.0	16.0	8.0	10.0	0.0	54.0	0.0	0.0	0.0
2019	Nevskiy E	45.0	100.0	75.0	5.0	0.0	0.0	0.0	5.0	0.0	15.0
2018	Skarb E	37.5	0.0	12.5	0.0	25.0	0.0	37.5	0.0	0.0	0.0
2018	Sudarinya E	67.5	57.0	4.0	23.0	3.0	0.0	0.5	0.0	0.0	3.0
2019	Charodey E	45.0	100.0	100.0	50.0	0.0	0.0	0.0	0.0	0.0	5.0
2018		56.0	100.0	76.0	43.0	0.0	0.0	0.0	0.0	0.0	0.0
2019	Charoit SSE	4.0	4.0	58.0	1.0	26.0	0.0	0.0	0.0	0.0	15.0
		Central region									
2019	Evolution E	0.0	16.0	30.0	27.5	45.5	0.0	0.0	0.0	0.0	61.0
2018	Red Fantasy E	3.5	71.4	38.0	0.0	38.0	0.0	28.5	0.0	0.0	0.0
2018	Red Scarlett E	15.7	78.9	0.0	0.0	5.2	5.2	0.0	0.0	0.0	0.0
2018	Red Scarlett PC2	71.4	100.0	0.0	71.4	28.5	0.0	0.0	14.2	0.0	0.0
		42.8	100.0	28.5	71.4	14.2	0.0	14.2	0.0	0.0	0.0
		50.0	83.3	0.0	50.0	0.0	0.0	0.0	0.0	0.0	0.0
		50.0	33.3	0.0	66.6	0.0	0.0	0.0	0.0	0.0	0.0
2018	Rodrigo E	0.0	7.6	23.0	0.0	15.3	0.0	0.0	7.6	0.0	0.0
		North Caucasus region									
2018	Colomba SE	0.0	0.0	5.2	0.0	31.5	0.0	15.7	0.0	0.0	0.0
2018	Desiree E	20.6	31.0	18.9	0.0	32.7	3.4	18.9	0.0	0.0	0.0
2018	Gala SE	2.2	0.0	29.5	0.0	9.0	0.0	13.6	0.0	0.0	0.0
2019	Impala SE	0.0	100.0	0.0	40.0	10.0	0.0	0.0	0.0	0.0	0.0
2018	Labella SSE	3.5	0.0	92.8	0.0	57.1	3.5	25.0	0.0	0.0	0.0
2018	Queen Anne SE	6.3	0.0	48.9	0.0	23.4	2.1	6.3	0.0	0.0	0.0
2018	Ramona E	16.3	22.4	22.4	12.2	18.3	0.0	16.3	0.0	0.0	0.0
2018	Red Scarlett SSE	3.4	0.0	100.0	0.0	31.0	0.0	6.8	0.0	0.0	0.0
2018	Nevskiy SE	9.0	6.0	100.0	0.0	9.0	0.0	12.1	0.0	0.0	0.0

Note: Elite seed potatoes: SSE – super-super elite, SE – super-elite, E – elite. Seed potato: PC1 – the first reproduction, PC2 – the second reproduction, etc.

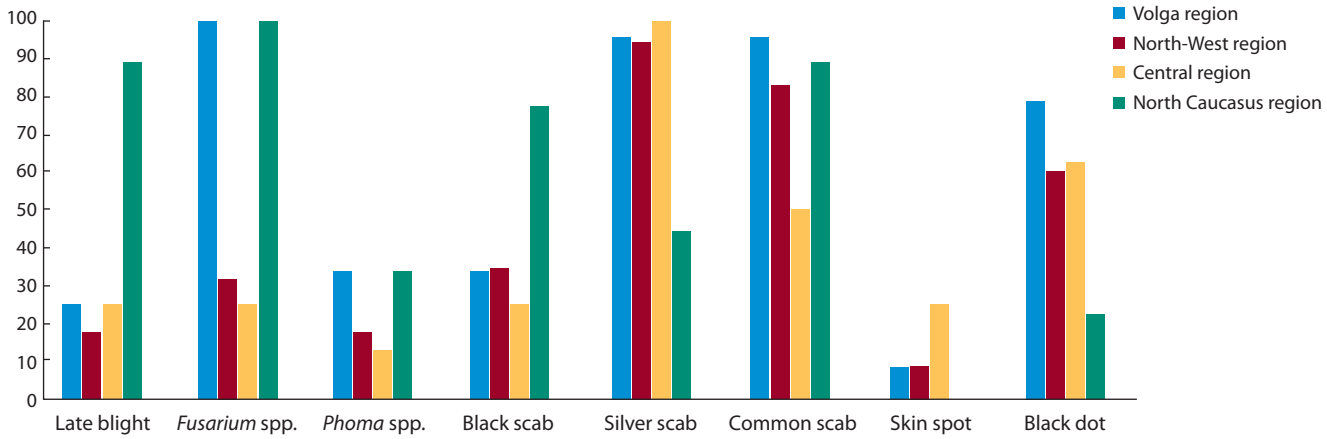

Fig. 2. The prevalence of fungal and oomycete diseases on seed potato in various agroclimatic zones of Russia (average for 92 samples).

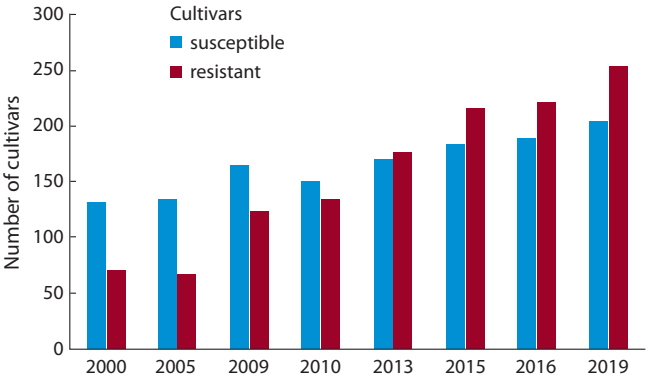

Fig. 3. The numbers of potato cultivars resistant and susceptible to *Globodera rostochiensis* (Ro1 patotype) released from 2000 to 2019.

ство пораженных клубней в Приволжском федеральном округе составило 15 %. У сорта Labella, который тоже высокоустойчив к фитофторозу по клубням, в Северо-Западном федеральном округе выявлено 5.5 % пораженных клубней, а в Северо-Кавказском – 25.0 %.

Такая же ситуация наблюдается и по вирусу картофеля Y. По данным оригинатора, сорт Alouette является иммунным к этому виду вируса, но нами было выявлено три пораженных клубня из четырех (Yanagisawa et al., 2019). Клубни высокоустойчивых к вирусу Y сортов Queen Anne, Rozara и Adretta, районированных в Дальневосточном федеральном округе, были поражены этим вирусом с частотой 1 из 22, 1 из 4 и 3 из 4 соответственно. Сорт Red Lady, по сведениям оригинатора, среднеустойчив к вирусу Y и высокоустойчив к штамму PVY^{NTN}, однако все 29 клубней (100 %) этого сорта были поражены штаммами PVY^{NTN}(A), PVY^{NTN}(B), $PVY^{N}W$(A), $PVY^{N}W$(B) (Yanagisawa et al., 2019).

Полученные данные по устойчивости сортов к ЗКН полностью коррелируют с информацией, приведенной фирмами-производителями и в Государственном реестре селекционных достижений (2019). Все изученные современные зарубежные сорта картофеля, кроме трех (Bintje, Desiree и Sarpo Mira, которые часто используются в качестве контроля восприимчивости), являются полностью иммунными к патотипу Ro1 ЗКН. Остальные зарубежные сорта картофеля, включенные в Госреестр и разрешенные к выращиванию на территории РФ, также отличаются высокой устойчивостью к этому патотипу ЗКН.

По данным Госреестра селекционных достижений, 254 из 455 сортов картофеля устойчивы к ЗКН (рис. 3). Тенденция превалирования устойчивых сортов над восприимчивыми наблюдается начиная с 2013 г. Однако это связано с включением в Госреестр многочисленных иностранных сортов, которые высокоустойчивы не только к Ro1 патотипу ЗКН, но и к другим, включая групповую устойчивость к бледной картофельной нематоде (например, сорта Laperla и Prada, фирма-оригинатор Solana). Свыше половины (124 из 216, или 57.4 %) отечественных сортов селекции РФ и стран СНГ, включенных в Госреестр, к сожалению, по большей части являются восприимчивыми, несмотря на то что признак нематодоустойчивости считается одним из важнейших при создании новых сортов картофеля.

Устойчивость к ЗКН является моногенной и обусловлена наличием генов *H1* или *Gro1–4* устойчивости, локализованных на хромосомах V и VII соответственно. Нематодоустойчивые сорта, созданные селекционерами разных стран, чаще всего несут ген *H1* (Shultz et al., 2012). Подобная закономерность выявлена и для отечественных нематодоустойчивых сортов, 98 % которых обладали маркерами гена *H1* и только 2 % – маркерами гена *Gro1–4* (Клименко и др., 2017). Зарубежные сорта картофеля активно используются отечественными селекционерами в программах по выведению новых сортов; приведенная авторами (Клименко и др., 2017) информация об устойчивости зарубежных сортов, а также о наличии маркера 57R гена *H1* важна при подборе пар для скрещиваний и в программах по пирамидированию генов устойчивости, особенно к карантинным объектам.

Сорта Alouette и Sarpo Mira, по данным оригинаторов, являются иммунными к фитофторозу и в наших экспериментах подтвердили этот статус. Устойчивость сорта Alouette обусловлена наличием генов *Rpi-R3a*, *Rpi-R3b*, *Rpi-vnt1* (Armstrong et al., 2019), а у сорта Sarpo Mira детерминирована генами *R3a*, *R3b*, *R4*, *R8*, *Rpi-Smira1* и

Rpi-Smira2 (Rietman et al., 2012). Сорт Evolution считается среднеустойчивым (RS), однако в проведенном эксперименте был оценен как устойчивый (балл 7.3).

Сорта Baltic Rose, Damaris, Desiree, Gala, Labella, Laperla, Mia, Sanibel, Zekura и 7 for 7 отнесены нами к восприимчивым, хотя в характеристиках оригинаторов указывалась средняя устойчивость к фитофторозу. Восприимчивыми оказались и сорта Queen Anne и Red Lady, которые по данным оригинатора имеют устойчивость выше средней. При проведении фитопатологического анализа семенного картофеля пораженные фитофторозом клубни были обнаружены у сортов Desiree, Labella, Queen Anne и Red Fantasy, которые по данным оригинаторов считаются устойчивыми к клубневой форме фитофтороза.

По групповой устойчивости к обоим возбудителям, золотистой картофельной нематоде и фитофторозу, выделились четыре районированных зарубежных сорта: Alouette, Evolution, Red Fantasy, Ricarda.

Результаты наших исследований свидетельствуют, что распространенность болезней на картофеле варьировала в зависимости от сорта, репродукции семенного материала и зоны выращивания. Зональные различия по распространенности болезней на семенном картофеле отчетливо проявились только по Северо-Кавказскому ФО. В отличие от других регионов РФ, в Северо-Кавказском ФО отсутствовало поражение картофеля антракнозом и только в одном образце сорта Невский (СЭ) обнаружено поражение серебристой паршой.

Повсеместное сильное поражение клубней ризоктониозом выявлено во всех исследованных регионах. Максимальное распространение болезнь получила на сортах Gala (70.4 %), Red Scarlett (64.7 %), Невский (57.8 %), относящихся к категории «элита».

Серебристая парша отмечена в различных регионах на всех изученных сортах картофеля, кроме некоторых из Северо-Кавказского ФО. Вредоносность этого заболевания состоит в поражении глазков, в результате чего клубни теряют всхожесть или дают ослабленные побеги, а также в поражении корневой системы и столонов, вследствие чего образуются невыравненные по размеру клубни, часто уродливые. Пораженные клубни чаще подвергаются развитию вторичной инфекции – фитофтороза и грибов *Fusarium* spp.

Неожиданно сильное распространение получил антракноз картофеля. Сильнее всего были поражены клубни сорта Red Scarlett (Э и РС2) (50.0–71.4 %) в Центральном федеральном округе. Устойчивость к антракнозу никогда не входила в параметры хозяйственно ценных признаков сортов картофеля. Это заболевание отсутствует в актуальном ГОСТ 33996-2016, что отчасти и способствует его распространению. Сильное поражение вегетирующих растений картофеля антракнозом отмечено нами в Северо-Западном и Дальневосточном федеральных округах на сортах Labadia, Labella, Невский и др. Вредоносность болезни состоит в преждевременном отмирании ботвы и гниении клубней во время вегетации и хранения. При диагностике основным признаком является наличие склероциального уплотнения мицелия под кожурой клубня, с выходом на поверхность и образованием щетинок. Широкое распространение антракноза и серебристой парши и очевидная их вредоносность стали новым вызовом для селекции картофеля.

Все проанализированные образцы были поражены комплексом грибов *Fusarium* spp. На сорте Gala их распространенность достигала 100 % в Приволжском ФО. Отчасти это связано с тем, что именно в этом округе зафиксировано наибольшее количество механически поврежденных клубней (от 2 до 75 % в зависимости от образца), что, по нашему мнению, способствовало такому сильному распространению сухой фузариозной гнили.

ГОСТ 33996-2016 устанавливает жесткие нормативные требования, предъявляемые к категориям картофеля по пораженности сухими гнилями, в частности фузариозом: 0.5 % для категорий элитного и 1.0 % для репродукционного семенного картофеля. Ни один проанализированный образец, вне зависимости от репродукции, не соответствовал предъявляемым требованиям, что свидетельствует о неудовлетворительном фитосанитарном состоянии семенного картофеля. Отсутствие поражения фузариозной инфекцией таких сортов, как Mondeo, Asterix, Delphine, Чародей, Зорачка, не может быть доказательством устойчивости к патогену, необходимо их дальнейшее изучение.

Возбудитель фитофтороза картофеля был выявлен во всех федеральных округах, причем наибольшее распространение на районированных сортах получил в Северо-Кавказском ФО (88.8 %). С 2018 г. фитофтороз картофеля отсутствует в регламенте контроля при проведении сертификации семенного материала по новому ГОСТ 33996-2016 (2017), поэтому в настоящее время отсутствуют допустимые критерии по пораженности клубней семенного картофеля. Однако, согласно ЭПВ (Алехин и др., 2016), не допускается присутствия пораженных клубней в семенном материале. Не выявлено корреляционной зависимости по поражению различных категорий сортов картофеля заболеваниями, скорее наоборот: именно элитный семенной картофель был поражен болезнями сильнее, чем репродукционный (см. табл. 3).

Наиболее представленными во всех федеральных округах оказались сорта картофеля, включенные в Госреестр (2019) много лет назад: Невский (год включения 1982), Red Scarlett (2000) и Gala (2008), менее представленными – сорта Evolution (2015), Colomba (2013) и Labella (2010). Все перечисленные сорта районированы в Северо-Западном ФО, остальные сорта присутствовали в трех регионах в разных соотношениях (см. табл. 3).

Заключение

Все зарубежные сорта картофеля, внесенные в Госреестр селекционных достижений, отличаются высокой устойчивостью к распространенному на территории Российской Федерации патотипу Ro1 *G. rostochiensis*. Часть из них генетически защищена и против других патотипов ЗКН. Это косвенно свидетельствует об эффективном использовании молекулярных маркеров генов устойчивости, так как фитопатологические тесты длительные и трудоемкие и могут быть проведены только в контролируемых условиях карантинных лабораторий. У 96.6 % изученных нематодоустойчивых сортов выявлен маркер гена *H1* устойчивости к патотипу Ro1 *G. rostochiensis*, восприимчивые сорта этим маркером не обладали. Подтверждена высо-

кая устойчивость сортов зарубежной селекции Alouette и Sarpo Mira к возбудителю фитофтороза. Обнаружены расхождения в характеристике устойчивости сортов картофеля к фитофторозу, представленной зарубежными оригинаторами и полученной нами при оценке устойчивости и фитопатологической экспертизе семенного картофеля, возделываемого на территории РФ. Сорт Alouette компании Agrico, UK отличается групповой устойчивостью к ЗКН и фитофторозу.

Во всех регионах изучения на семенном картофеле выявлен комплекс оомицетных и грибных болезней, среди которых преобладали ризоктониоз, сухая фузариозная гниль и серебристая парша. Отмечено неожиданно широкое распространение антракноза картофеля. По-видимому, назрела необходимость определить наличие устойчивости к этим болезням как важный хозяйственно ценный признак и направить усилия фитопатологов и селекционеров на создание генетически охарактеризованного исходного материала для селекции на устойчивость. Большая часть районированных сортов не удовлетворяет даже минимальным требованиям, предъявляемым к семенному материалу. Практически весь семенной материал не соответствует требованиям ГОСТ и ЭПВ, что свидетельствует о нарушении технологии возделывания и защиты.

Список литературы / References

Алехин В.Т., Михайликова В.В., Михина Н.Г. Экономические пороги вредоносности вредителей, болезней и сорных растений в посевах сельскохозяйственных культур. М.: Росинформагротех, 2016.
[Alekhin V.T., Mikhaylikova V.V., Mikhina N.G. Economic Harmfulness Thresholds of Pests, Diseases, and Weeds in Crop Fields. Moscow: Rosinformagrotekh Publ., 2016. (in Russian)]

Антонова О.Ю., Швачко Н.А., Новикова Л.Ю., Шувалов О.Ю., Костина Л.И., Клименко Н.С., Шувалова А.Р., Гавриленко Т.А. Генетическое разнообразие сортов картофеля российской селекции и стран ближнего зарубежья по данным полиморфизма SSR-локусов и маркеров *R*-генов устойчивости. *Вавиловский журнал генетики и селекции*. 2016;20(5):596-606. DOI 10.18699/VJ16.181.
[Antonova O.Y., Shvachko N.A., Novikova L.Y., Shuvalov O.Y., Kostina L.I., Klimenko N.S., Shuvalova A.R., Gavrilenko T.A. Genetic diversity of potato varieties bred in Russia and its neighboring countries based on the polymorphism of SSR-loci and markers associated with resistance *R*-genes. *Russ. J. Genet.: Appl. Res.* 2017;7(5):489-500. DOI 10.1134/S2079059717050021.]

Гавриленко Т.А., Клименко Н.С., Антонова О.Ю., Лебедева В.А., Евдокимова З.З., Гаджиев Н.М., Апаликова О.В., Алпатьева Н.В., Костина Л.И., Зотеева Н.М., Мамадбокирова Ф.Т., Егорова К.В. Молекулярный скрининг сортов и гибридов картофеля северо-западной зоны Российской Федерации. *Вавиловский журнал генетики и селекции*. 2018;22(1):35-45. DOI 10.18699/VJ18.329.
[Gavrilenko T.A., Klimenko N.S., Antonova O.Yu., Lebedeva V.A., Evdokimova Z.Z., Gadjiyev N.M., Apalikova O.V., Alpatyeva N.V., Kostina L.I., Zoteyeva N.M., Mamadbokirova F.T., Egorova K.V. Molecular screening of potato varieties bred in the northwestern zone of the Russian Federation. *Vavilovskii Zhurnal Genetiki i Selektsii = Vavilov Journal of Genetics and Breeding*. 2018;22(1):35-45. DOI 10.18699/VJ18.329. (in Russian)]

ГОСТ 33996-2016. Картофель семенной. Технические условия и методы определения качества. Межгосударственный стандарт картофель семенной. 2017.
[State Standard 33996-2016. Seed Potatoes. Specifications and methods of determining the quality. 2017. (in Russian)]

Государственный реестр селекционных достижений, допущенных к использованию. Т. 1. Сорта растений (офиц. изд.). М.: Росинформагротех, 2019.
[The State Register of Selection Achievements Authorized for Use for Production Purposes. Vol. 1. Plant Varieties (official publication). Moscow: Rosinformagrotekh Publ., 2019. (in Russian)]

Еланский С.Н. Особенности развития фитофтороза в России. *Защита картофеля*. 2015;1:8-11.
[Elansky S.N. Features of the development of late blight in Russia. *Zashhita Kartofelya = Potato Protection*. 2015;1:8-11. (in Russian)]

Игнатов А.Н., Панычева Ю.С., Воронина М.В., Васильев Д.М., Джалилов Ф.С.-У. Динамика видового состава патогенов картофеля в европейской части РФ. *Картофель и овощи*. 2019;9:28-32. DOI 10.25630/PAV.2019.57.62.003.
[Ignatov A.N., Panycheva Yu.S., Voronina M.V., Vasiliev D.M., Dzhalilov F.S.-U. Dynamics of species composition of potato pathogens in the European part of the Russian Federation. *Kartofel i Ovoshchi = Potatoes and Vegetables*. 2019;9:28-32. DOI 10.25630/PAV.2019.57.62.003. (in Russian)]

Клименко Н.С., Антонова О.Ю., Костина Л.И., Мамадбокирова Ф.Т., Гавриленко Т.А. Маркер-опосредованная селекция отечественных сортов картофеля с маркерами генов устойчивости к золотистой картофельной нематоде (патотип Ro1). *Труды по прикладной ботанике, генетике и селекции*. 2017;178(4):66-75. DOI 10.30901/2227-8834-2017-4-66-75.
[Klimenko N.S., Antonova O.Y., Kostina L.I., Mamadbokirova F.T., Gavrilenko T.A. Marker-associated selection of Russian potato varieties with using markers of resistance genes to the golden potato cyst nematode (pathotype Ro1). *Trudy po Prikladnoy Botanike, Genetike i Selektsii = Proceedings on Applied Botany, Genetics, and Breeding*. 2017;178(4):66-75. DOI 10.30901/2227-8834-2017-4-66-75. (in Russian)]

Кузнецова М.А., Козловский Б.Е., Бекетова М.П., Соколова Е.А., Малюченко О.П., Алексеев Я.И., Рогозина Е.В., Хавкин Э.Е. Фитопатологическая и молекулярная характеристика изолятов *Phytophthora infestans*, собранных с устойчивых и восприимчивых генотипов картофеля. *Микология и фитопатология*. 2016;50(3):175-184.
[Kuznetsova M.A., Kozlovsky B.E., Beketova M.P., Sokolova E.A., Malyuchenko O.P., Alekseev Y.I., Rogozina E.V., Khavkin E.E. Phytopathological and molecular characterization of *Phytophthora infestans* isolates collected on resistant and susceptible potato genotypes. *Mikologiya i Fitopatologiya = Mycology and Phytopathology*. 2016;50(3):175-184. (in Russian)]

Сорта картофеля российской селекции. Под ред. Е.А. Симакова. М., 2018.
[Simakov E.A. (Ed.). Potato Varieties Bred in Russia. Moscow, 2018. (in Russian)]

Abbas M.F., Naz F., Irshad G. Important fungal diseases of potato and their management – a brief review. *Mycopath*. 2013;11(1):45-50.

AHDB. Agriculture and Horticulture Development Board. 2018. Available at: https://potatoes.ahdb.org.uk/agronomy/plant-health-weed-pest-disease-management

Armstrong M.R., Vossen J., Lim T.Y., Hutten R.C.B., Xu J., Strachan S.M., Harrower B., Champouret N., Gilroy E.M., Hein I. Tracking disease resistance deployment in potato breeding by enrichment sequencing. *Plant Biotechnol. J.* 2019;17:540-549. DOI 10.1111/pbi.12997.

Bakker E., Achenbach U., Bakker J., van Vliet J., Peleman J., Segers B., van der Heijden S., van der Linde P., Graveland R., Hutten R., van Eck H., Coppoolse E., van der Vossen E., Bakker J., Goverse A. A high-resolution map of the *H1* locus harbouring resistance to the potato cyst nematode *Globodera rostochiensis*. *Theor. Appl. Genet.* 2004;109(1):146-152. DOI 10.1007/s00122-004-1606-z.

Brylińska M., Śliwka J. Laboratory assessment of potato resistance to *Phytophthora infestans*. *Plant Breed. Seed Sci.* 2017;76:17-23. DOI 10.1515/plass-2017-00016.

Collins W.W. The global initiative on late blight – alliance for the future. In: Khurana S.M.P., Shekhawat G.S., Singh B.P., Pandey S.K.

(Eds.). Potato Global Research and Development. Indian Potato Association. CPRI, Shimla, India, 2000;1:513-524.

Compendium of Potato Diseases. Hooker W.J. (Ed.). The Disease Compendia Series by the American Phythopathological Society. Publ. by the Am. Phythopathol. Soc., USA, 1981.

Compendium of Potato Diseases, Second Edition. Stevenson W.R., Loria R., Franc G.D., Weingartner D.P. (Eds.). St. Paul, USA: Am. Phytopathol. Soc. Press, 2001.

Dalamu, Bhardwaj V., Umamaheshwari R., Sharma R.P., Kaushik S.K., Joseph T.A., Singh B.P., Gebhardt C. Potato cyst nematode (PCN) resistance: genes, genotypes and markers – an update. *SABRAO J. Breed. Genet.* 2012;44(2):202-228.

Dillard H.R. *Colletotrichum coccodes*: the pathogen and its hosts. In: Bailey J.A., Jeger M.J. (Eds.). Colletotrichum: Biology, Pathology and Control. CAB International, Oxford, 1992;225-236.

Diseases, Pests and Disorders of Potatoes: A Color Handbook. Wale S.J., Platt H.W., Cattlin N.D. Elsevier, 2008.

Finkers-Tomczak A., Bakker E., Boer J., Vossen E., Achenbach U., Golas T., Suryaningrat S., Smant G., Bakker J., Goverse A. Comparative sequence analysis of the potato cyst nematode resistance locus *H1* reveals a major lack of co-linearity between three haplotypes in potato (*Solanum tuberosum* ssp.). *Theor. Appl. Genet.* 2011;122: 595-608. DOI 10.1007/s00122-010-1472-9.

Gavrilenko T., Antonova O., Shuvalova A., Krylova E., Alpatyeva N., Spooner D.M., Novikova L. Genetic diversity and origin of cultivated potatoes based on plastid microsatellite polymorphism. *Genet. Resour. Crop Evol.* 2013;60(7):1997-2015. DOI 10.1007/s10722-013-9968-1.

Gudmestad N.C., Taylor R.J., Pasche J.S. Management of soilborne diseases of potato. *Australas. Plant Pathol.* 2007;36:109-115.

Haldar K., Kamoun S., Hiller N.L., Bhattacharje S., van Ooij C. Common infection strategies of pathogenic eukaryotes. *Nat. Rev. Microbiol.* 2006;4:922-931.

Haverkort A.J., Struik P.C., Visser R.G.F., Jacobsen E. Applied biotechnology to combat late blight in potato caused by *Phytophthora infestans*. *Potato Res.* 2009;52:249-264. DOI 10.1007/s11540-009-9136-3.

Johnson D.A. Effect of foliar infection caused by *Colletotrichum coccodes* on yield of Russet Burbank potato. *Plant Dis.* 1994;78(11): 1075-1078.

Johnson D.A., Miliczky E.R. Effects of wounding and wetting duration on infection of potato foliage by *Colletotrichum coccodes*. *Plant Dis.* 1993;77:13-17.

Judelson H.S., Blanco F.A. The spores of *Phytophthora*: weapons of the plant destroyer. *Nat. Rev. Microbiol.* 2005;3:47-57.

Lees A.K., Hilton A.J. Black dot (*Colletotrichum coccodes*): an increasingly important disease of potato. *Plant Pathol.* 2003;52:3-12.

Limantseva L., Mironenko N., Shuvalov O., Antonova O., Khiutti A., Novikova L., Afanasenko O., Spooner D., Gavrilenko T. Characterization of resistance to *Globodera rostochiensis* pathotype Ro1 in cultivated and wild potato species accessions from the Vavilov Institute of Plant Industry. *Plant Breed.* 2014;133(5):660-665.

OEPP/EPPO. Testing of potato varieties to assess resistance to *Globodera rostochiensis* and *Globodera pallida*. *OEPP/EPPO Bull*. 2006; 36:419-420.

Oerke E.-C. Crop losses to pests. *J. Agric. Sci.* 2006;144:31-43. Available at: https://www.cambridge.org/core/journals/journal-of-agricultural-science/article/crop-losses-to-pests/AD61661AD6D503577B3E73F2787FE7B2

Rietman H., Bijsterbosch G., Cano L.M., Lee H.-R., Vossen J.H., Jacobsen E., Visser R.G.F., Kamoun S., Vleeshouwers V.G.A.A. Qualitative and quantitative late blight resistance in the potato cultivar Sarpo Mira is determined by the perception of five distinct RXLR effectors. *MPMI*. 2012;25(970):910-919. DOI 10.1094/MPMI-01-12-0010-R.

Schultz L., Cogan N.O.I., McLean K., Dale M.F.B., Bryan G.J., Forster J.N.W., Slater A.T. Evaluation and implementation of a potential diagnostic molecular marker for *H1*-conferred potato cyst nematode resistance in potato (*Solanum tuberosum* L.). *Plant Breed.* 2012; 131:315-321. DOI 10.1111/j.1439-0523.2012.01949.x.

Tsror L. Biology, epidemiology and management of *Rhizoctonia solani* on potato. *J. Phytopathol.* 2010;158:649-658. DOI 10.1111/j.1439-0434.2010.01671.x.

Tsror L., Erlich O., Hazanovsky M. Effect of *Colletotrichum coccodes* on potato yield, tuber quality and stem colonization during spring and autumn. *Plant Dis.* 1999;83(6):561-565.

Turner S.J. Sample preparation, soil extraction and laboratory facilities for the detection of potato cyst nematodes. In: Marks R.J., Brodie B.B. (Eds.). Potato Cyst Nematodes: Biology, Distribution and Control. CAB International, Wallingford, 1998;75-90.

UNECE Standard S-1 concerning the marketing and commercial quality control of seed potatoes: UNECE Guide to Seed Potato Diseases, Pests and Defects. United Nations, New York; Geneva, 2014.

UNECE Standard S-1 concerning the marketing and commercial quality control of seed potatoes. United Nations, New York; Geneva, 2018.

Winslow R.D., Willis R.J. Nematode diseases of potatoes. II. Potato cyst nematode, *Heterodera rostochiensis*. In: Webster J. (Ed.). Economic Nematology. N.Y.: Acad. Press, 1972;18-34.

Yanagisawa H., Yosuke M., Khiutti A., Mironenko N., Yasuo O., Afanasenko O. Complete genome sequence of a divergent strain of potato virus P isolated from *Solanum tuberosum* in Russia. *Arch. Virol.* 2019;164:2891-2894. DOI 10.1007/s00705-019-04397-5.

ORCID ID

T.A. Gavrilenko orcid.org/0000-0002-2605-6569

Acknowledgements. This work was supported by the Russian Science Foundation, project 16-16-04073. The authors are grateful to the staff of the Avgust Company, Head of the Department of Product Development D.A. Belov, manager for key clients A.P. Osoblivyy, and the Executive Manager of the Ustyuzhenskiy Kartofel Association A.A. Kuznetsov.

Conflict of interest. The authors declare no conflict of interest.

Received December 6, 2019. Revised December 24, 2019. Accepted December 24, 2019.

Вавиловский журнал генетики и селекции. 2020;24(4):376-382
DOI 10.18699/VJ20.630

An integrated method for taxonomic identification of microorganisms

Yu.E. Uvarova[1, 2] ✉, A.V. Bryanskaya[1, 2], A.S. Rozanov[1, 2], V.N. Shlyakhtun[1, 2], E.A. Demidov[1, 2], K.V. Starostin[1, 2], T.N. Goryachkovskaya[1, 2], S.V. Shekhovtsov[1, 2], N.M. Slynko[1, 2], S.E. Peltek[1, 2]

[1] Institute of Cytology and Genetics of Siberian Branch of the Russian Academy of Sciences, Novosibirsk, Russia
[2] Kurchatov Genomic Center of the Institute of Cytology and Genetics of Siberian Branch of the Russian Academy of Sciences, Novosibirsk, Russia
✉ e-mail: uvarovaye@bionet.nsc.ru

Abstract. For accurate species-level identification of microorganisms, researchers today increasingly use a combination of standard microbiological cultivation and visual observation methods with molecular biological and genetic techniques that help distinguish between species and strains of microorganisms at the level of DNA or RNA molecules. The aim of this work was to identify microorganisms from the ICG SB RAS Collection using an integrated approach that involves a combination of various phenotypic and genotypic characteristics. Key molecular-genetic and phenotypic characteristics were determined for 93 microbial strains from the ICG SB RAS Collection. The strains were characterized by means of morphological, physiological, molecular-genetic, and mass-spectrometric parameters. Specific features of the growth of the strains on different media were determined, and cell morphology was evaluated. The strains were tested for the ability to utilize various substrates. The strains studied were found to significantly differ in their biochemical characteristics. Physiological characteristics of the strains from the collection were identified too, e. g., the relationship with oxygen, type of nutrition, suitable temperature and pH ranges, and NaCl tolerance. In this work, the microorganisms analyzed were combined into separate groups based on the similarities of their phenotypic characteristics. This categorization, after further refinement and expansion of the spectrum of taxa and their metabolic maps, may serve as the basis for the creation of an "artificial" classification that can be used as a key for simplified and quicker identification and recognition of microorganisms within both the ICG SB RAS Collection and other collections.
Key words: identification of microorganisms; biochemical characteristics of bacteria; chemosystematics; mass spectrometric analysis.

For citation: Uvarova Yu.E., Bryanskaya A.V., Rozanov A.S., Shlyakhtun V.N., Demidov E.A., Starostin K.V., Goryachkovskaya T.N., Shekhovtsov S.V., Slynko N.M., Peltek S.E. An integrated method for taxonomic identification of microorganisms. *Vavilovskii Zhurnal Genetiki i Selektsii = Vavilov Journal of Genetics and Breeding*. 2020;24(4): 376-382. DOI 10.18699/VJ20.630

Комплексный метод таксономической идентификации микроорганизмов

Ю.Е. Уварова[1, 2] ✉, А.В. Брянская[1, 2], А.С. Розанов[1, 2], В.Н. Шляхтун[1, 2], Е.А. Демидов[1, 2], К.В. Старостин[1, 2], Т.Н. Горячковская[1, 2], С.В. Шеховцов[1, 2], Н.М. Слынько[1, 2], С.Е. Пельтек[1, 2]

[1] Федеральный исследовательский центр Институт цитологии и генетики Сибирского отделения Российской академии наук, Новосибирск, Россия
[2] Курчатовский геномный центр Федерального исследовательского центра Институт цитологии и генетики Сибирского отделения Российской академии наук, Новосибирск, Россия
✉ e-mail: uvarovaye@bionet.nsc.ru

Аннотация. Для точной видовой идентификации микроорганизмов сегодня все чаще применяют сочетание стандартных микробиологических методов культивирования и визуального наблюдения с методами молекулярной биологии и генетики, помогающими различать виды и штаммы микроорганизмов на уровне молекул ДНК или РНК. Целью данной работы было проведение идентификации микроорганизмов из Коллекции ИЦиГ СО РАН с помощью комплексного подхода, сочетающего использование широкого спектра фенотипических и генотипических признаков. Для 93 штаммов микроорганизмов Коллекции ИЦиГ СО РАН описаны ключевые молекулярно-генетические и фенотипические свойства. Рассмотрены морфологические, физиологические, молекулярно-генетические и масс-спектрометрические характеристики штаммов. Установлены особенности роста штаммов на разных средах, изучена морфология клеток. Штаммы протестированы на способность использовать различные субстраты. Обнаружено, что исследованные штаммы значительно различались по своим био-

химическим признакам. Определены физиологические особенности штаммов коллекции: отношение к кислороду, тип питания, диапазон температур и pH, отношение к NaCl и др. Исследованные микроорганизмы объединены в отдельные группы на основании сходства их фенотипических характеристик, что может при дальнейшей доработке и расширении спектра таксонов и их метаболических карт послужить основой для создания «искусственной» классификации, которая может быть использована в качестве ключа для упрощенной и более быстрой идентификации и распознавания микроорганизмов в рамках как Коллекции ИЦиГ СО РАН, так и других коллекций.
Ключевые слова: идентификация микроорганизмов; биохимические характеристики бактерий; хемосистематика; масс-спектрометрический анализ.

Introduction

Identification of prokaryotes, which are morphologically less diverse than eukaryotes, is based on a wide variety of phenotypic – and in many cases also genotypic – characteristics. During the description and identification of bacteria, researchers study their cultivation properties, morphology, cell organization, physiological and biochemical features, chemical composition of cells, GC content of DNA, nucleotide sequence of the gene coding for 16S ribosomal RNA (rRNA), and other phenotypic and genotypic characteristics.

Phenotypic methods of identification are popular mostly because of their relatively low cost. Phenotypic reactions usually include the responses to various chemical compounds or biochemical markers. Nonetheless, the manifestation of phenotypic traits of a microorganism – e. g., cell size and shape, sporulation, cell composition, antigenicity, biochemical activity, and sensitivity to antimicrobial agents – often depends on the nutrient media and culture conditions being used. Therefore, in recent years, to improve the classic methods of biochemical identification, investigators developed modern methods of biochemical identification (Church, 2016; Reyes, 2018).

Characteristic features of the growth of microorganisms on solid and liquid nutrient media are categorized as cultivation-related or macromorphological properties. Morphological characteristics and bacterial-cell organization include such traits as cell shape and size, cell motility, the presence of flagella, flagellation type, and sporogenesis capacity. In bacterial systematics, the top priority is given to Gram staining and cell wall structure.

Research on physiological and biochemical properties primarily includes determination of the nutrition mode of the bacterium being analyzed (photo-/chemo- and auto-/heterotrophy) and the type of energy metabolism (capacity for fermentation, aerobic or anaerobic respiration, or photosynthesis). It is important to identify such traits as the relationship of this bacterium with molecular oxygen, temperature, pH of the medium, with salinity, illuminance, and other environmental factors. This group of traits also contains the list of substrates utilized as sources of carbon, nitrogen, and sulfur; requirements for vitamins and other growth factors; formation of characteristic products of metabolism; and the expression of certain enzymes. For this purpose, special assays are often performed.

Many assays employed for the detection of the aforementioned traits (they are sometimes called "routine assays") are crucial for clinical diagnoses and are widely used in medical microbiology. These assays require substantial time, a large number of complicated media and reagents, compliance with standardized operating procedures, and meticulous execution. To accelerate and facilitate the identification of some microorganisms, mostly those that are clinically important, researchers have developed various assay kits, such as MIKROLATEST® ID | Erba Lachema s.r.o. and BioLog. For instance, the MIKROLATEST® ID assay is designed for the identification of enterobacteria and represents a plastic chamber with wells containing colored diagnostic media. Whether the result is positive or negative is determined by changes in the color of a medium or by a reaction after the addition of special reagents (e. g., the assay of indole production and the Voges–Proskauer test).

A state-of-the-art phenotypic technology called BioLog yields valuable information about the properties of strains in addition to species level identification. Molecular techniques such as 16S rRNA sequencing and matrix-assisted laser desorption/ionization time of flight (MALDI-TOF) mass spectrometry do not provide information about the properties of a strain. The technology of carbon source utilization in the BioLog assay allows environmental microorganisms and pathogenic microorganisms to be identified by compiling a characteristic profile or "metabolic fingerprint" after certain assay reactions carried out in a microtiter plate. Suspension cultures are tested by means of a panel of preselected assays, then are incubated and analyzed on a signal reader, and the results are queried against databases.

Among the modern methods of biochemical identification is MALDI-TOF mass spectrometry, which is one of the latest methodologies for microbial identification. Even though this assay is "phenotypic," it in a sense eliminates the gap in the reliability of the test results obtained by phenotyping-based biochemical assay systems and genotyping-based identification systems. Additionally, the methodology is very rapid and therefore well exemplifies a "rapid microbiological assay" (Gaudreau et al., 2018).

Determination of the bacterial-cell chemical composition also plays a role in bacterial systematics (chemosystematics). Chemotaxonomic methods may be helpful in particular for classifying the bacterial taxa whose morphological and physiological characteristics vary widely and are insufficient for their satisfactory identification. Additionally, cell wall composition determines serological properties of bacteria. This principle underlies the immunochemical techniques for their identification.

Investigators sometimes also employ the lipid and fatty-acid composition of bacterial cells as chemotaxonomic markers. Active research on fatty acids has become possible with ad-

vancements in gas chromatography. Differences in the lipid profile are used for the identification of bacteria at species and genus levels. This method, however, has some limitations because fatty-acid content of cells may depend on cultivation conditions and culture age.

Analysis of nucleotide sequences of rRNAs has gained much popularity and importance for the identification of bacteria and for the creation of phylogenetic approaches to their classification.

Founded at a federal publicly funded scientific institution, the Federal Research Center ICG SB RAS, a collection of biotechnologically important microorganisms contains more than 1500 strains, cultures of microorganisms, and DNA samples valuable for science and biotechnology and is intended for identification of new microorganisms with promise in terms of biotechnology and bioengineering and for studies on their genetics and metabolism. The collection contains representatives of all major superkingdoms (fungi, bacteria, archaea, and algae) and physiological groups (including anaerobes and extremophiles). Most strains in the collection have been isolated from previously unstudied unique extreme ecosystems: brine lakes, hot springs, soils, offshore areas, and bodies of freshwater.

For accurate species level identification of microorganisms, currently, investigators are increasingly applying a combination of standard microbiological techniques of cultivation and visual observation with molecular biological and genetic methods, which help distinguish the species and strains of microorganisms at the level of DNA or RNA molecules (Kardymon, Kudryavtseva, 2016). For biotechnological purposes, it is important to have information not only about species affiliation of strains but also about their substrate specificity, completeness of metabolic pathways' implementation, activity of metabolic reactions, and the possibility of their modulation. Consequently, an integrated approach to the identification of natural microorganisms will simplify the search for the strains that hold promise for bioengineering tasks.

The purpose of this study was to identify microorganisms from the ICG SB RAS Collection via an integrated approach involving a combination of a wide variety of phenotypic and genotypic characteristics.

Methods

Phenotypic characterization. The shape and size of live and stained cells were determined using light and electron microscopes Axioskop 2 Plus, Axioskop A1, LIBRA 120 (Carl Zeiss) at the Multi-Access Center for Microscopic Analysis of Biological Objects (SB RAS). The samples were prepared by standard methods (Netrusov et al., 2005). Gram staining was conducted by means of the Gram Stain Kit (Sintakon, Russia) according to the manufacturer's instructions.

The optimal temperature and pH for growth, NaCl tolerance, catalase and urease oxidase activities, anaerobic growth, amylolytic and caseinase activities, and other activities as well as the ability to utilize various substrates were determined according to Netrusov et al. (2005) and Logan & De Vos (2009). Most of the assays were carried out using Lachema and BioLog reagents and assay kits.

Sequencing of 16S rRNA genes. Taxonomic affiliation (phylogenetic position) of the strains was determined according to the 16S rRNA gene sequence. To this end, bacterial DNA was isolated by the standard phenol method (Maniatis et al., 1984). Amplification of the 16S rRNA gene was conducted with universal bacterial primers 16S-8-f-B (5′-AGR GTTTGATCCTGGCTCA-3′) and 16S-1350-r-B (5′-GAC GGGCGGTGTGTACAAG-3′). The reaction mixture consisted of 1.5 mM $MgCl_2$, 65 mM Tris-HCl (pH 8.8), 16 mM $(NH_4)_2SO_4$, 0.05 % of Tween 20, 0.2 mM each dNTP, 0.3 mM each primer, and 1 U of recombinant Taq polymerase (SibEnzyme, Novosibirsk, Russia). DNA sequencing was performed by the Genomics Multi-Access Center, SB RAS.

Searches for similar sequences in nucleotide databases were conducted by means of the software of the Blast series (http://blast.ncbi.nlm.nih.gov/Blast.cgi). Sequence alignment was performed in the ClustalW software (http://www.ebi.ac.uk/Tools/msa/clustalw2).

Chemotaxonomic properties. To analyze the fatty-acid composition of cells, the strains were grown at optimal temperature until the exponential growth phase. The biomaterial obtained was processed according to (Jenkins, Tanner, 1977); after alkaline hydrolysis of lipids, acids were extracted with hexane and were methylated with a methanolic HCl solution according to Schäffer et al. (2002). The mixture of methyl esters of fatty acids was analyzed by gas chromatography on an Agilent Technologies 6890N chromatograph coupled with an Agilent Technologies 5973N quadrupole mass spectrometer and a quartz DB-1 column. The carrier gas was He at a constant flow rate of 1 ml/min. Injection temperature was 250 °C, and sample (1 μl) injection was performed via a microsyringe; electron impact ionization was set to 70 eV. Chromatographic-mass-spectrometric analysis of the studied solutions was conducted by means of total ion current in SCAN mode in the mass range 10 to 800 Da, with selective ion monitoring (SIM) of molecular ions of the compound being studied. Identification of methyl esters of fatty acids was performed through comparison with database NIST Mass Spectral Search Program for the NIST/EPA/NIH Mass Spectral Library Version 2.0a, build "Jul 2002."

Mass-spectrometric analysis was conducted on an Ultraflex III MALDI TOF/TOF mass spectrometer (Bruker Daltonics). The spectra were recorded in linear positive mode at a laser frequency of 100 Hz in the mass range 2000–20000 Da. Accelerating electrode voltage was 25 kV, IS2 voltage 23.45 kV, and lens voltage 6 kV, without an extraction delay. For each sample, three spectra were acquired by summing up 500 laser impulses (5 × 100 impulses at different positions of the target cell). External calibration was performed with precise masses of known proteins: *Escherichia coli* RL36: 4365.3 Da, RS22: 5096.8 Da, RL34: 5381.4 Da, RL32: 6315.0 Da, RL29: 7274.5 Da, and RS19: 10300.1 Da. The series of spectra obtained for each strain were employed to generate the characteristic spectra in Biotyper 3.0 software, which constituted a list of mass peaks with averaged m/z values and relative peak intensities.

To identify microorganisms from the ICG SB RAS Collection, the phenotypic and genotypic characteristics deter-

mined were analyzed in Statistica 6.0 software. Dendrograms were constructed by the method of unweighted pairwise arithmetic mean, and two-dimensional graphs by multidimensional scaling. Multivariate analysis was carried out in Past 3, version 3.25 (Hammer et al., 2001). In accordance with the requirements of the software, semiquantitative data on 95 substrates of the BioLog assay system were converted to numerical values: data on the absence/presence were coded as "0" or "1," respectively, and undetermined values as "?".

Results

In this study on microbial identification, 93 strains from the ICG SB RAS Collection were analyzed. Geographic locations of sampling for the isolation of microbial cultures were rather diverse: from vineyards of Crimea to geysers of Kamchatka and the Kuril Islands. Ecological types of habitats varied widely too: from bodies of freshwater to salty soils; temperature conditions were cold or thermal; environmental pH levels were neutral, acidic, or alkaline. The samples were collected both from unaffected natural areas of water and from anthropogenically polluted rock types.

Strains were isolated on various media: e. g., LB, beef extract agar, beef-extract broth, or Pfennig's medium with supplements. The cultivation was conducted at 32 to 55 °C. Each strain was subjected to phylogenetic, phenotypic, and mass-spectrometric characterization.

Morphology and biochemical properties

Most strains produced circular white, cream-colored, or yellow colonies. Colony edges were even or wavy, and the profile was flat or convex. Colony sizes varied from pinpoint size (less than 1 mm) to >5 mm. Cells of the strains were rodlike. Seventeen strains secreted a pigment into the medium. The cell wall was gram-positive. Streak growth varied among the strains: from nondiffuse to highly diffuse and from rosarylike to solid. Seventy-five strains featured sporogenesis.

The temperature ranges for growth tested were within 8–70 °C, and the pH ranges tested were within 2–10. The suitable temperature range for the growth of thermophilic microorganisms was 40–70 °C with an optimum at 60 °C. The suitable range for the growth of mesophilic microorganisms was 25 to 40, 50, and 55 °C, with an optimum mostly at 35 °C. Strong growth of the strains was noted at a NaCl concentration of 1 g/l. Some strains did not grow or grew poorly at 5 g/l NaCl in the medium.

All the strains studied were tested for the ability to utilize various substrates by means of Lachema and BioLog assay systems. The strains were found to be aerobes and/or facultative anaerobes. In terms of nutrition, the strains turned out to be heterotrophs and chemoorganoheterotrophs. An overwhelming majority of the strains grew well on media with casein, starch, or Tween as a sole carbon source. Seventy-three strains showed a well-pronounced caseinase activity, characterized by the presence of clear zones around colonies after treatment with acetic acid (Netrusov et al., 2005). Furthermore, 81 strains had a good amylolytic activity, evidenced by clear zones. In a reaction with iodine, aside from the usual loss of color, in some cases, there was reddening of the medium around colonies, indicating the formation of dextrins.

It was determined that 40 strains possess a β-galactosidase activity. Virtually none of the strains utilized malonate, citrate, ornithine, or sulfur compounds (negative results of an H_2S test). None of the strains except one utilized lysine, and 17 strains had a urease activity. None of the strains manifested a β-glucuronidase activity. The strains either utilized or did not utilize mannitol, trehalose, lactose, cellobiose, arginine, melibiose, sorbitol, salicin, raffinose, inositol, arabitol, adonitol, and dulcite. Twenty strains featured a β-xylosidase activity.

Most of the strains studied did not utilize D-turanose, N-acetyl neuraminic acid, p-hydroxyphenylacetic acid, methyl pyruvate, D-fucose, L-fucose, L-rhamnose, D-aspartic acid, D-serine, glycyl-L-proline glucuronamide, mucic acid, chinic acid, D-saccharic acid, α-hydroxybutyric acid, β-hydroxy-D,L-butyric acid, α-keto-butyric acid, or sodium butyrate.

It was found that an overwhelming majority of the strains belong to the genus *Bacillus*, and the others to the genera *Anoxybacillus*, *Lysinibacillus*, *Geobacillus*, *Paenibacillus*, *Achromobacter*, *Agrobacterium*, and *Stenotrophomonas.*

Characteristic mass spectra of protein profiles were obtained for 83 strains from the collection. The results of phyloproteomic analysis were consistent with taxonomic affiliation of the strains, as determined by the sequencing of 16S rRNA genes. The results of the mass-spectrometric analysis complemented the existing set of characteristic mass spectra and may be useful for further identification of microorganisms in the cases where obtaining a quality DNA sample for sequencing is problematic.

Analysis of the fatty-acid composition of the cell wall revealed the following fatty acids: saturated unbranched: myristic acid (C14:0); branched-chain acids: isomyristic (isoC14:0), isopentadecanoic (isoC15:0), anteiso-pentadecanoic (aC15:0), isopalmitic (isoC16:0), and anteiso-palmitic (aC16:0); and monounsaturated: palmitoleic acid (C16:1). The profile and ratio of fatty acids in the cell wall of bacteria are important traits for the identification of these microorganisms.

Discussion

Fig. 1 depicts a phylogenetic tree built from 16S rRNA sequences; it reflects the clustering of bacterial strains by species affiliation. Fig. 2 presents a statistical analysis of 21 strains for 96 formalized biochemical parameters determined by the BioLog Omnilog assays. This analysis did not reveal clear-cut clustering, especially judging by the strains of *Bacillus subtilis* (see Fig. 2). Ten strains from 21 samples analyzed belong to the species *B. subtilis*. Six of them (strains No. 10, 13, 14, 19, 20, and 21) are components of a relatively loose cluster that is formed by representatives of the *B. subtilis* group and *B. cereus* group. This cluster includes *Lysinibacillus macrolides* (strain No. 6). No other strains of *B. subtilis* (No. 2, 7, 11, and 17) clustered with their own species.

In prokaryotic systematics, for species identification, researchers utilize such parameters as rRNA sequence, cell membrane structure, and certain features of metabolism, e. g., methanogenesis or bacteriorhodopsin-dependent photosynthesis (DasSarma et al., 2019). Our results suggest that the features of metabolism analyzed are not species-determining but may play a major role when the usefulness of one or another strain for biotechnology is determined. This is because

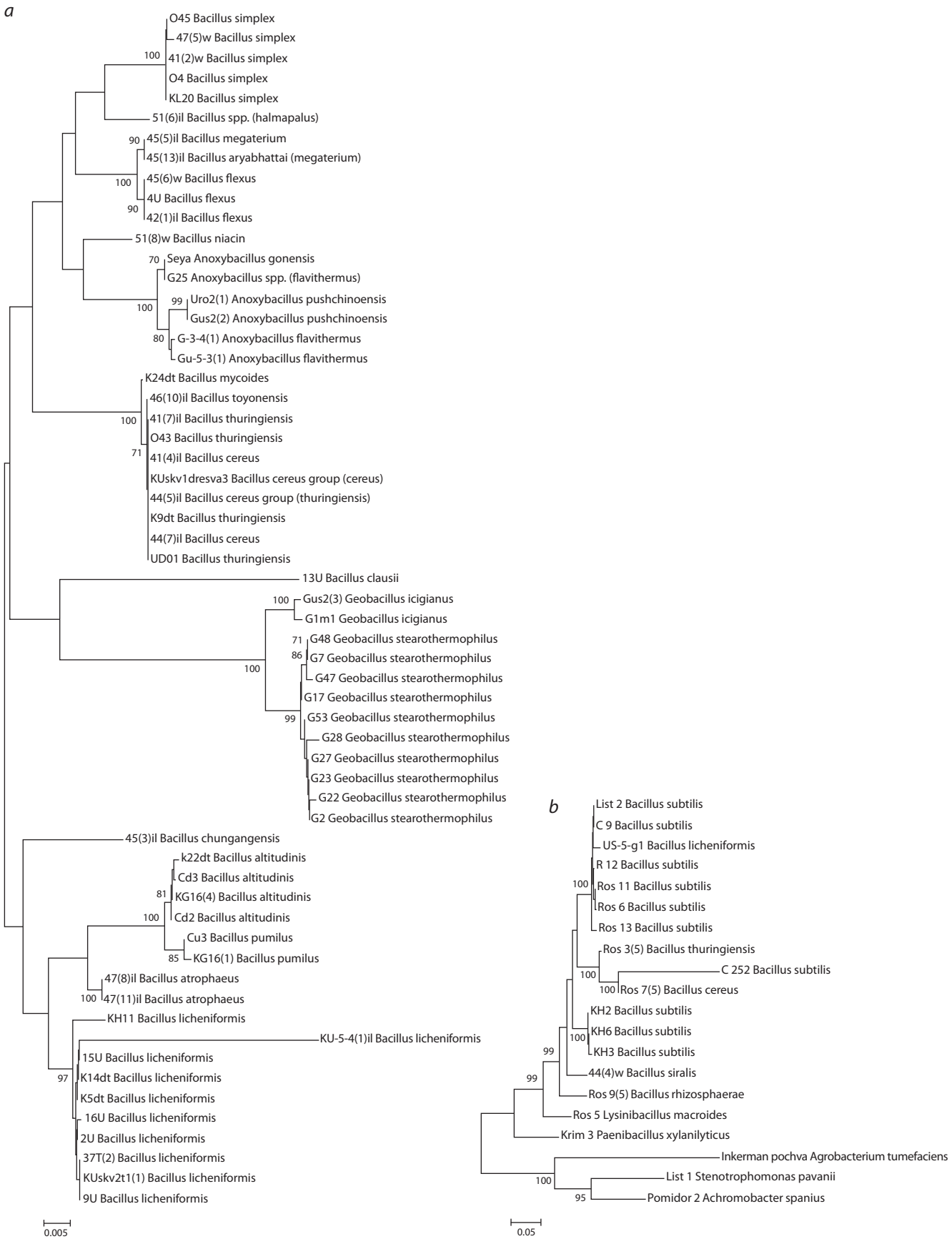

Fig. 1. The phylogenetic tree constructed by the minimum evolution method applied to 16S rRNA sequences of the strains for which biochemical data were obtained by the Lachema assay (*a*) or BioLog assay (*b*).

The numbers near clades denote bootstrap support.

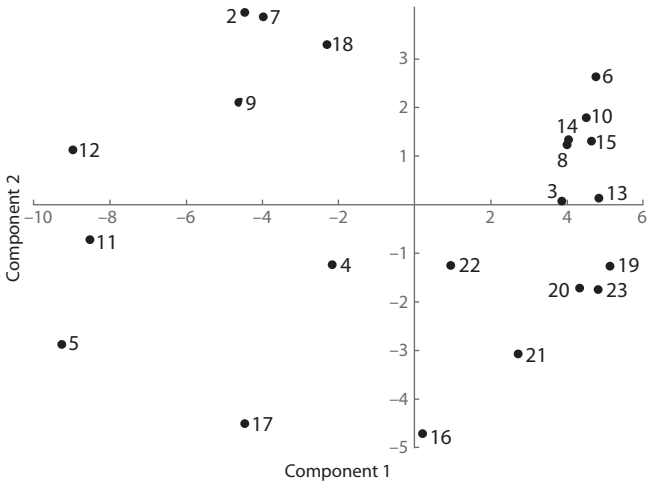

Fig. 2. Results of the statistical analysis of the findings about the taxonomic profile of the microorganisms studied and their specific features of metabolism according to the first pair of principal components. The analysis covers 96 parameters.

the possibility of degradation of various substrates is taken into account.

Fig. 3 shows the results of clustering of 61 strains by 29 parameters of metabolism, as determined by MICROLATEST® Lachema assays. We used such parameters as the ability of bacteria to utilize some sugars (e. g., mannitol, trehalose, lactose, cellobiose, sucrose, raffinose, and glucose), the presence of urease activity, and production of H_2S. The analysis included strains of three *Anoxybacillus* species, 17 *Bacillus* species, and two *Geobacillus* species. Most of the strains formed a relatively tight cluster, regardless of the species of a microorganism, thus indicating a similarity between the substrates used for growth. The ability to grow on various sugars and organic acids (which is what most of the substrates tested were) is typical of the representatives of various taxonomic groups from the bacterial kingdom, irrespective of their origin. The second cluster (a smaller one) is formed by some strains of bacteria belonging to the following species: *B. simplex*, *Anoxybacillus* spp. (*flavithermus*), *G. stearothermophilus*, *B. mycoides*, *A. pushchinoensis*, and *B. licheniformis*. These species were found to be represented by multiple strains, but the other strains of these species ended up in a large cluster according to metabolic characteristics. The unification of these strains into one cluster by metabolic characteristics points to a similarity between the substrates or possibly to the loss of the ability to utilize some of the substrates. In this case, the clustering does not reflect a common evolutionary origin, but rather shows substrate specificity that has developed as a consequence of convergent processes, probably during the adaptation to the substrates. According to the sampling sites, the species that ended up in the small cluster do not have a common origin either.

There was clustering by morphological characteristics too. For instance, the small cluster highlighted in Fig. 4 is formed by the strains of microorganisms that produced relatively large colonies.

Evidently, further refinement and expansion of the spectrum of taxa and of their metabolic maps may lay the foundation for an "artificial" classification that may be helpful as a key for simplified and quicker identification and recognition of microorganisms.

Conclusion

For 93 strains of microorganisms from the ICG SB RAS Collection, we determined key molecular-genetic and phenotypic characteristics. The strains were characterized by morphological, physiological, molecular-genetic, and mass-spectrometric parameters. Specific features of the strains' growth on various media were determined, and cell morphology was assessed. Next, the strains were tested for the ability to utilize various substrates. It was found that the strains studied substantially differ in their biochemical characteristics. Additionally, we evaluated physiological characteristics of the strains from this collection: e. g., the relationship with oxygen, nutrition type, suitable ranges of temperature and pH, and NaCl tolerance.

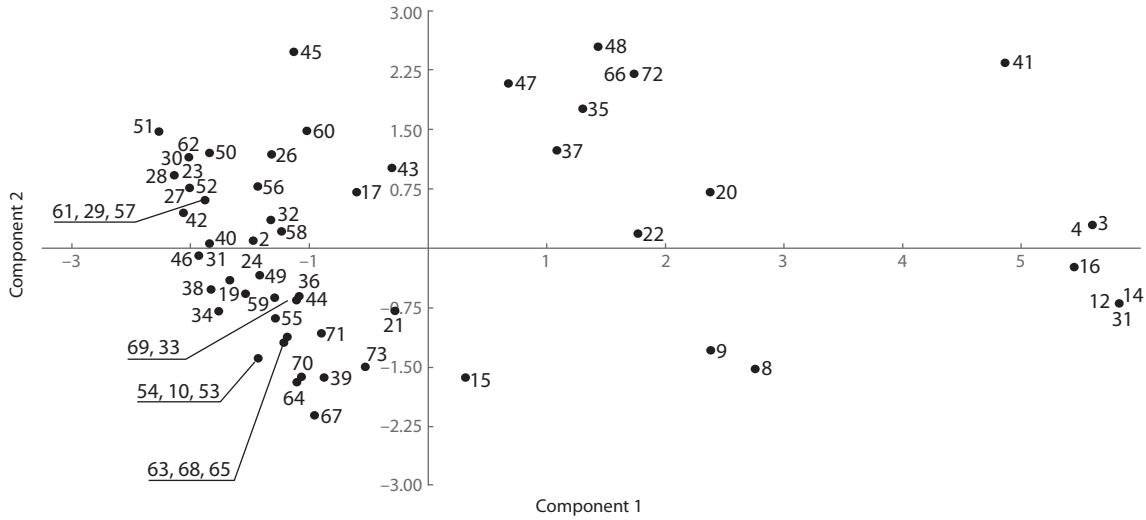

Fig. 3. Results of the statistical analysis of the data on the taxonomic profile of the microorganisms studied and their specific features of metabolism according to the first pair of principal components. The analysis covers 29 parameters.

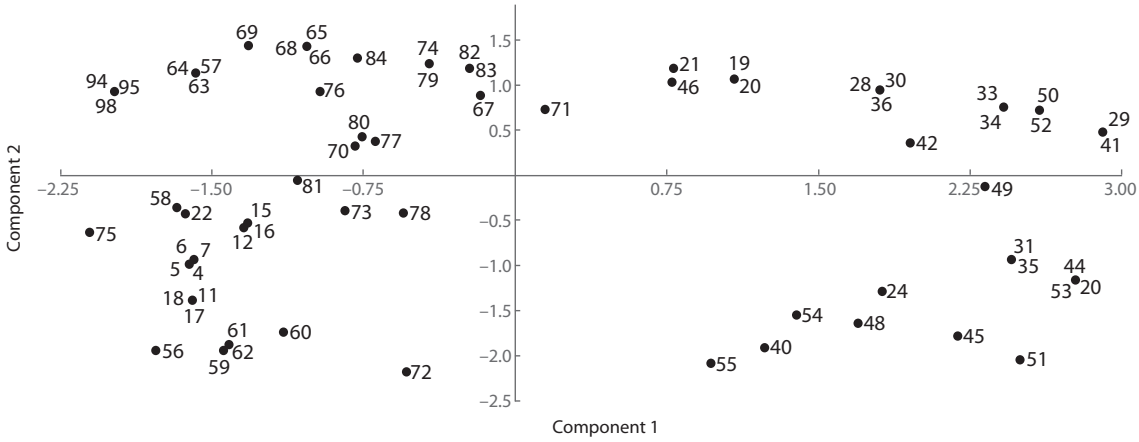

Fig. 4. Results of the statistical analysis of the findings about morphological characteristics according to the first pair of principal components.

Application of the integrated approach to microbial identification is necessary for solving the problems of targeted searches for biotechnologically promising strains. In this study, we combined microbes into separate groups/clusters on the basis of similarities of their phenotypic characteristics. This categorization, after further elaboration and expansion of the spectrum of taxa and of their metabolic maps, may form the basis for the creation of an "artificial" classification that may be helpful as a key for simplified and faster identification and recognition of microbes within both the ICG SB RAS Collection and other collections.

References

Church D.L. Biochemical tests for the identification of aerobic bacteria. In: Leber A. (Ed.). Clinical Microbiology Procedures Handbook. Fourth Edn. AMS Press, Washington, 2016;3.17.1.1-3.17.48.3. DOI 10.1128/9781555818814.ch3.17.

DasSarma P., Capes M.D., DasSarma S. Comparative genomics of *Halobacterium* strains from diverse locations. In: Das S., Dash H.R. (Eds.). Microbial Diversity in the Genomic Era. Acad. Press, 2019; 285-322. DOI 10.1016/B978-0-12-814849-5.00017-4.

Gaudreau A.M., Labrie J., Goetz C., Dufour S., Jacques M. Evaluation of MALDI-TOF mass spectrometry for the identification of bacteria growing as biofilms. *J. Microbiol. Methods*. 2018;145:79-81. DOI 10.1016/j.mimet.2018.01.003.

Hammer O., Harper D.A., Ryan P.D. PAST: paleontological statistics software package for education and data analysis. *Palaeontol. Electronica*. 2001;4(1):9.

Jenkins R.E., Tanner M.J.A. The structure of the major protein of the human erythrocyte membrane. Characterization of the intact protein and major fragments. *Biochem. J*. 1977;161(1):139-147. DOI 10.1042/bj1610139.

Kardymon O.L., Kudryavtseva A.V. Molecular genetic methods for intestinal microbiome investigation. *Rossiiskiy Zhurnal Gastroenterologii, Gepatologii, Koloproktologii = Russian Journal of Gastroenterology, Hepatology, Coloproctology*. 2016;26(4):4-13. DOI 10.22416/1382-4376-2016-26-4-4-13. (in Russian)

Logan N.A., De Vos P. Genus I. *Bacillus*. In: Bergey's Manual of Systematic Bacteriology. Vol. 3. The *Firmicutes*. Springer, 2009;21-128.

Maniatis T., Fritsch E., Sambrook J. Molecular Cloning. Cold Spring Harbor lab., 1982. (Russ. ed. Maniatis T., Frich E., Sembruk D. Metody Geneticheskoy Inzhenerii. Molekulyarnoe Klonirovanie. Moscow: Mir Publ., 1984. (in Russian)

Netrusov A.I., Egorova M.A., Zakharchuk L.M. Workshop on Microbiology. Moscow: Academy Publ., 2005. (in Russian)

Reyes A.T. Morpho-biochemical aided identification of bacterial isolates from Philippine native pig. *Adv. Pharmacol. Clin. Trials*. 2018; 3(5):000148. DOI 10.23880/apct-16000148.

Schäffer C., Wugeditsch T., Kählig H., Scheberl A., Zayni S., Messner P. The surface layer (S-layer) glycoprotein of *Geobacillus stearothermophilus* NRS 2004/3a: analysis of its glycosylation. *J. Biol. Chem*. 2002;277(8):6230-6239. DOI 10.1074/jbc.M108873200.

ORCID ID

S.V. Shekhovtsov orcid.org/0000-0001-5604-5601
S.E. Peltek orcid.org/0000-0002-3524-0456

Acknowledgements. This work was done within the framework of State Assignment Kurchatov Genomic Center of ICG SB RAS (075-15-2019-1662). The English language was corrected and certified by shevchuk-editing.com.

Conflict of interest. The authors declare no conflict of interest.

Received December 28, 2019. Revised March 26, 2020. Accepted April 01, 2020.

Вавиловский журнал генетики и селекции. 2020;24(4):383-390
DOI 10.18699/VJ20.44-o

Genomics and proteomics of the liver fluke *Opisthorchis felineus*

V.A. Mordvinov ✉, N.I. Ershov, O.G. Zaparina, M.Y. Pakharukova ✉

Institute of Cytology and Genetics of Siberian Branch of the Russian Academy of Sciences, Novosibirsk, Russia
✉ e-mail: mordvin@bionet.nsc.ru; pmaria@yandex.ru

Abstract. The causative agent of opisthorchiasis, the liver fluke *Opisthorchis felineus* (Rivolta, 1884) is one of the helminths of humans and animals in Russia. Together with closely related species of trematodes *O. viverrini* (Poirier, 1886) and *Clonorchis sinensis* (Loos, 1907), *O. felineus* is a part of a triad of epidemiologically important trematodes in the family Opisthorchiidae. Adult *O. felineus* worms infest the hepatobiliary system of warm-blooded animals and might provoke the development of severe pathologies, including malignancy of bile duct epithelium. The high medical importance of *O. felineus* attracts the attention of researchers. This review briefly summarizes the data about *O. felineus* genomics and proteomics. The review provides a comparative analysis of the number of genes and sizes of nuclear genomes of a number of flatworms, the distribution of intron lengths, as well as results of synteny between the *O. felineus*, *O. viverrini* and *C. sinensis* genomes. Special attention is paid to a particular form of RNA processing known as trans-splicing, widely presented in the opisthorchiid genomes. We also provide the results of a comparative analysis of the xenobiotic metabolizing system between parasitic and free-living flatworms. Moreover, data on parasitic granulins, which are potential promoters of cholangiocyte neoplasia, are also presented. Data on the *O. felineus* genomics and proteomics provide first insights into the structural and functional organization of the genome of this parasitic flatworm with a complex life cycle as well as provide a significant contribution to our understanding of "host-parasite" interaction and evolution of this group of parasitic flatworms.
Key words: genomics; trematodes; *Opisthorchis felineus*; trans-splicing; microintrones; proteomics; operons; gene expression.

For citation: Mordvinov V.A., Ershov N.I., Zaparina O.G., Pakharukova M.Y. Genomics and proteomics of the liver fluke *Opisthorchis felineus*. *Vavilovskii Zhurnal Genetiki i Selektsii = Vavilov Journal of Genetics and Breeding*. 2020;24(4): 383-390. DOI 10.18699/VJ20.44-o

Геномика и протеомика возбудителя описторхоза *Opisthorchis felineus*

В.А. Мордвинов ✉, Н.И. Ершов, О.Г. Запарина, М.Ю. Пахарукова ✉

Федеральный исследовательский центр Институт цитологии и генетики Сибирского отделения Российской академии наук, Новосибирск, Россия
✉ e-mail: mordvin@bionet.nsc.ru; pmaria@yandex.ru

Аннотация. Возбудитель описторхоза, печеночный сосальщик *Opisthorchis felineus* (Rivolta, 1884) – один из наиболее распространенных видов гельминтов человека и животных на территории России. Вместе с близкородственными видами печеночных трематод *O. viverrini* (Poirier, 1886) и *Clonorchis sinensis* (Loos, 1907), ареалы которых расположены в Юго-Восточной Азии и на Дальнем Востоке, *O. felineus* составляет триаду эпидемиологически значимых трематод семейства Opisthorchiidae. Половозрелые особи (мариты) *O. felineus* паразитируют в гепатобилиарной системе теплокровных и при длительной инвазии провоцируют развитие тяжелых осложнений, включая малигнизацию эпителия желчных протоков. Высокая медицинская значимость *O. felineus* привлекает внимание исследователей, работающих в различных областях биологии и медицины. Так, в последнее время активно проводятся исследования молекулярной биологии этого представителя паразитических плоских червей. В настоящем обзоре кратко суммированы результаты исследований геномики и протеомики *O. felineus*, являющиеся, на наш взгляд, существенным вкладом в решение вопросов структурно-функциональной организации геномов многоклеточных паразитов со сложным жизненным циклом и изучение молекулярных механизмов взаимодействия паразит–хозяин. Приведены сравнительные данные по количеству генов и размерам ядерных геномов ряда плоских червей, распределению длин интронов, а также анализу синтении геномов описторхид *O. felineus*, *O. viverrini* и *C. sinensis*. Отдельное внимание уделено обсуждению особой формы процессинга РНК, известной как транс-сплайсинг, широко представленной в геноме *O. felineus*. В статье приводятся анализ литературных

данных по генам системы метаболизма ксенобиотиков, сравнению представленности генов этой системы между различными видами паразитических и свободноживущих плоских червей и обзор литературы по наличию и уровню экспрессии генов гранулинов – потенциальных промоторов неоплазии холангиоцитов. Данные по геномике и протеомике *O. felineus* пополняют базу знаний, обеспечивающую исследование проблем эволюции трематод, патогенеза печеночных гельминтозов и гельминт-ассоциированного канцерогенеза.
Ключевые слова: геномика; трематоды; *Opisthorchis felineus*; транс-сплайсинг; микроинтроны; протеомика; опероны; экспрессия генов.

Introduction

In 1884, the Italian scientist S. Rivolta described a new species of helminths *Distomum felineum* (synonym *Opisthorchis felineus*, *D. sibiricum* – a liver fluke, a Siberian fluke), extracted from the bile ducts of the cat's liver. In 1891, professor of Tomsk University K.N. Vinogradov discovered this species of liver trematodes in humans (Pozio et al., 2013).

The liver fluke *O. felineus* has a complex life cycle with alternating two intermediate and one definitive hosts. The list of the definitive hosts for this parasite consists of 33 species and subspecies of mammals, primarily from the Order Carnivora (carnivores): domestic cats, dogs, wolves, foxes, bears, badgers. A man is also susceptible to the infection of *O. felineus* (Beer, 2005).

Infection of animals and humans occurs as a result of eating raw or undercooked fish infected with metacercaria of *O. felineus*. After entering the digestive tract of a definitive host, the metacercaria cyst is destroyed and newly excised juvenile worm moves to the bile ducts of the liver. Upon reaching maturation, the parasites produce lots of eggs containing miracidia – the invasive life stage for the first intermediate host, Bithyniidae mollusks. Eggs pass out with the feces of mammals, enter the water reservoirs where they are ingested by the mollusks to enter and develop in. Sporocysts, redia, and cercaria – life stages of fluke with asexual reproduction are successively passed in the Bithyniidae mollusk. Free-swimming cercariae leave the mollusks and are able to infect the second intermediate host, the cyprinid fish. In fish, cercaria is encapsulated and transformed into metacercaria – the only infectious life stage for the infection of fish-eating mammals.

In humans, the infection of *O. felineus*, opisthorchiasis, is a long lasting disease, occurs with the exacerbations and might contribute to the development of primary liver cancer. Opisthorchiasis refers to natural focal diseases. The most indicative endemic area is the West Siberian Lowland – one of the largest lowland plains in the world. There is the world's largest outbreak of opisthorchiasis caused by the *O. felineus* in the Ob-Irtysh basin (Pakharukova, Mordvinov, 2016).

In addition to Western Siberia, the range of *O. felineus* infection also extends to Eastern, Western and Southern Europe. This species of helminths was found in central Russia, Belarus and Ukraine, in the Baltic countries, in Germany (Schuster et al., 1999), Italy (Pozio et al., 2013), on the Balkan and Iberian peninsulas (Petney et al., 2013). According to preliminary estimates, at least 1.6 million people in the world are infected with *O. felineus* (Keiser, Utzinger, 2009). In the Russian Federation, up to 40 thousand cases of opisthorchiasis are detected annually (Rospotrebnadzor…, 2015). Nevertheless, these data most likely do not reflect the actual rate of the infection. The first stages of the disease and the transition to the chronic stage might pass unnoticed, and gradually appearing symptoms do not have specificity. As a result, the true number of patients with opisthorchiasis can significantly exceed the official statistics.

Existing opisthorchiasis therapy does not guarantee complete relief and does not prevent re-infection. In addition, chemotherapy for this disease has side effects and might have negative consequences for patients. In this regard, the issue of the possibility of creating new effective and safe anthelmintic agents for the treatment of opisthorchiasis is very relevant. A thorough study of the molecular biology of *O. felineus* liver fluke provides a key to understand the molecular mechanisms of the host–parasite interaction and to identify potential pharmacological targets for the treatment of opisthorchiasis.

This review is devoted to the research of genomics and proteomics of *O. felineus*, which makes a significant contribution to solving the fundamental problems of molecular parasitology and genetics, as well as the development of new approaches to facilitate diagnosis, prevention and treatment of opisthorchiasis infection.

Genomics of *Opisthorchis felineus*

Nuclear genome

The size of the existing assembly of the nuclear genome of *O. felineus* liver fluke is 684 million base pairs, 30.3 % of the genome is represented by repeating elements, mainly retrotransposons. According to these characteristics, the *O. felineus* genome is very close to the genomes of two other epidemiologically significant species of the Opisthorchiidae family, other liver flukes *O. viverrini* and *Clonorchis sinensis*. The *O. felineus* genome differs significantly from the genomes of the Schistosomatidae and Fasciolidae trematodes (Table 1). There are 11,455 annotated protein-coding genes in *O. felineus* genome (Ershov et al., 2019), as well as 55 genes encoding microRNAs (Ovchinnikov et al., 2015). The total number of *O. felineus* genes is almost a third less than that for *O. viverrini* and *C. sinensis* and almost coincides with the number of *S. mansoni* and *F. hepatica* genes.

Significant structural variability was found when the genomic synteny of opisthorchids *O. felineus*, *O. viverrini*, and *C. sinensis* was analyzed. According to the localization of homologous loci, the degree of similarity between the *O. felineus* and *C. sinensis* genomes is higher than that between *O. viver-*

Table 1. Characteristics of the genomes of five species of trematodes

Species	Size	Number of genes	Repeating elements, %
O. felineus (Ershov et al., 2019)	680.0 Mb	11,455	30.3
C. sinensis (Wang et al., 2011)	516 Mb	16,000	29.6
O. viverrini (Young et al., 2014)	634.5 Mb	16,379	30.9
S. mansoni (Berriman et al., 2009)	364.5 Mb	11,809	40
F. hepatica (Cwiklinski et al., 2015)	1.3 Gb	11,700	54.2

rini with *O. felineus* (Ershov et al., 2019). These data correlate well with the results of karyotype analysis: *O. felineus* and *C. sinensis* have seven pairs of chromosomes, *O. viverrini* has six pairs of chromosomes (Zadesenets et al., 2012).

The data on genome synteny also align well with the results of phylogeny using separate genetic markers and genome-wide data from three species of opisthorchids. The results of these studies indicate that *C. sinensis* belongs to the genus *Opisthorchis* and do not support the isolation of this species into a separate genus *Clonorchis* (Shekhovtsov et al., 2009; Cai et al., 2012; Pomaznoy et al., 2016; Ershov et al., 2019). Thus, according to the findings of molecular biological studies, the taxonomic rank of *C. sinensis* should be reviewed.

When studying the genome and transcriptome of *O. felineus*, it was found, that expression regulation of almost 50 % of genes is carried out with the participation of trans-splicing machinery (Ershov et al., 2019). This particular form of RNA processing is quite common in flatworms, but the widespread involvement of trans-splicing in trematodes is unusual. For instance, trans-splicing in *Schistosoma mansoni* is involved in the regulation of transcription of only 11 % of genes in the genome (Protasio et al., 2012).

Trans-splicing is a leader-dependent type of splicing in *O. felineus* genome. As a result of this process, the 5′-region of the newly synthesized pre-mRNA is replaced by a short sequence of the splice leader encoded by a single gene. In flatworms, this insertion sequence ends in the conservative AUG triplet. It is likely that this triplet can act as a start codon during translation of mature mRNA subjected to trans-splicing. On the other hand, the reason for the expansion of trans-splicing machinery in *O. felineus* may be its role in the removal of long 5′-non-coding regions from pre-mRNA, which is necessary for the efficient translation of mature transcripts.

Another hypothesis is that trans-splicing is necessary for expression regulation of individual genes in operons. The *O. felineus* genome revealed 355 potential operons that unite 736 genes separated by trans-splicing sites (Ershov et al., 2019). Predicted operons contain from two to four genes showing different levels of expression. It is possible that the stability of the levels of expression of operon genes is achieved by the fact that the processing of pre-mRNAs synthesized under control of the same promoter is regulated by trans-splicing.

Most *O. felineus* genes, the expression of which is controlled by this mechanism, encode proteins of basic cellular processes (Ershov et al., 2019). Similar data were obtained in the analysis of the *Caenorhabditis elegans* genome – the most conservative trans-splicing sites were found in the ribosomal genes (Sleumer et al., 2010). An analysis of the genomic data of *O. viverrini* and *C. sinensis* also revealed conservative targets for trans-splicing involved in the post-transcriptional regulation of most of the “housekeeping” genes. Obviously, this mechanism plays an important role in the life of flat and round worms, although at present the functional significance of trans-splicing has not been fully understood.

An analysis of the intron lengths in the *O. felineus* genome revealed (Ershov et al., 2019) that the distribution of the lengths of these elements is characterized by the presence of a large peak at 3000 bp and two additional peaks with maxima at 37 and 90 bp. Ultrashort introns or microintrons less than 75 bp in length make up about 34 % of all annotated introns and are included in the structure of 4997 (44 %) genes. Microintrons are also widely represented in the *O. viverrini* and *C. sinensis* genomes. The presence of two peaks of short introns was previously described in tapeworm genomes, and it was assumed that the bimodal distribution of microintrons is a distinctive feature of this group of helminths (Tsai et al., 2013). However, this feature can be traced, albeit less pronouncedly, in the trematodes of the family Opisthorchiidae.

The distribution of microintrons in the genome of *O. felineus* has some features (Ershov et al., 2019). Firstly, in the presence of several microintrons in a gene, they, as a rule, form clusters. Secondly, microintrons are more often located at the beginning of an exon portion of a gene, i. e. tend to start of gene transcription (Ershov et al., 2019). These facts indicate the separate functional significance of this class of introns in the mechanisms of transcription and processing. Thus, clustering can be associated with recognition of the intron-exon structure by the spliceosome (intron-definition mechanism), and the small size of the microintrons enhances transcriptional efficiency (Urrutia, Hurst, 2003; Belshaw, Bensasson, 2006).

Mitochondrial genome

The size of the mitochondrial genome of *O. felineus* is 13,875 bp, it contains 36 genes: 12 protein-coding genes, two ribosomal RNA genes and 22 transport RNA genes. The mitochondrial genomes of *O. felineus*, *C. sinensis*, *F. hepatica*, and *Paragonimus westermani* are similarly organized, but differ from the schistosomatid genomes (Shekhovtsov et al., 2010).

Proteomics and a system of xenobiotic metabolism of *O. felineus*

The life cycle of the trematode is accompanied by a change in the repertoire of genes expressed at a certain life stage of the parasite. Recently, the results of a comparative study of transcriptomes of metacercariae and adult *O. felineus* worms (Pomaznoy et al., 2016; Ershov et al., 2019) were published. It was shown, that the transcriptomic profiles of the two life stages of the liver fluke are significantly different: the expression of 903 and 648 genes is registered only in adult or metacercaria, respectively (Pomaznoy et al., 2016). In adult worms, the highest expression is demonstrated for genes encoding proteases, myoglobin, egg shell protein, glutathione S-transferase, and also proteins modulating antigen processing by the host immune cells. In metacercaria, genes encoding "housekeeping" proteins, for example, ribosomal proteins, ubiquitin, and heat shock proteins, have the highest level of expression.

When comparing the transcriptomes of adult *O. felineus*, *O. viverrini* and *C. sinensis* worms, it was found, that the expression levels of the vast majority of genes in the three species of opisthorchids differ slightly (Ershov et al., 2019). This indicates a high similarity in the metabolic processes that ensure the life of helminths in the final host. Nevertheless, the expression of several tens of genes in genomes was species specific. It is important that most of these differentially expressed genes encode the proteins of the excretory secretory product (ESP) of opisthorchids. Species-specific expression of ESP proteins may reflect the host-parasite interaction pecularities.

O. felineus ESPs include various proteins: protective proteins from reactive oxygen species, proteolytic enzymes, carbohydrate metabolism enzymes, protective proteins from the host immune system, cytoskeletal proteins, etc. (Lvova et al., 2014). The one of the major component of the *O. felineus* ESP is glutathione S-transferase σ (GST-σ). This enzyme retains its activity in an incubation media and is accumulated in the liver tissues of infected animals and patients suffering from opisthorchiasis (Petrenko et al., 2017; Pakharukova et al., 2019). According to a comparative analysis of transcriptomes of adult *O. felineus*, *O. viverrini*, and *C. sinensis* worms, the presence of GST-σ mRNA in the *O. felineus* transcriptome is many times higher than in the transcriptomes of other opisthorchids. It is likely that this enzyme plays an important role in the host-parasite interaction and can mediate species-specific manifestations of the pathogenesis of opisthorchiasis caused by *O. felineus*. It is important to note that GST-σ might be involved in the metabolism of endogenous substrates and xenobiotics (exogenous substrates), including drugs.

The *O. felineus* system of xenobiotic metabolism

Currently, there are no vaccines or any other means of specific prophylaxis of opisthorchiasis, and the available drugs for chemotherapy of this disease cause complaints (Prichard et al., 2012). In this regard, the study of the xenobiotic metabolism system of liver flukes, the components of which are promising pharmacological targets (Bartley et al., 2012; Prichard et al., 2012), is of particular importance.

With very few exceptions, exogenous substrates that enter living organisms undergo one or more stages of biotransformation, which are carried out by enzymatic biotransformation by means of three phases of metabolism. Phase 1 enzymes, among which the P450 family of proteins (CYPs) are most represented, carry out oxidation, reduction, or hydrolytic reactions of the substrate. An analysis of the available genomic and transcriptomic data of parasitic and free-living flatworms revealed that the composition of CYPs in these groups is markedly different. In free-living species, as in most studied organisms, dozens of weakly homologous to each other diverged CYP genes were found (Table 2). However, parasitic species of the families Opisthorchiidae, Schistosomatidae, Taeniidae, and Fasciolidae own only one cytochrome P450 gene (Pakharukova et al., 2012, 2015). It was shown, that the product of this single gene, CYP in *O. felineus* liver fluke, is involved in the metabolism of exogenous substrates, is important for the survival of adult worms and represents a promising target for anthelmintic therapy (Pakharukova et al., 2015; Mordvinov et al., 2017b).

In addition to CYP gene, other genes encoding phase 1 of xenobiotic biotransformation enzymes were found in the liver fluke genome, in particular, aldo-keto reductase, aldehyde dehydrogenase, and alcohol dehydrogenase genes (Ershov et al., 2019). However, flavin monooxygenase genes, also belonging to phase 1 enzymes, were not found in the *O. felineus* genome. Interestingly, the sequences of these genes were also not found in the genomic data of other parasitic flatworms.

Glutathione peroxidase and glutathione S-transferase are actively involved in the implementation of phase 2 of xenobiotic metabolism. The *O. felineus* genome contains nine glutathione S-transferase genes, which are the most highly expressed among all the genes of the xenobiotic metabolism of this liver trematode. The gene encoding GTS-σ is particularly highly expressed, the level of expression of this gene in adult worms is 2–3 orders of magnitude higher than that of other xenobiotic metabolism genes. As already mentioned above, GST-σ is a part of helminth ESP and enters the tissues of infected mammals (Pakharukova et al., 2019). It is important to mention here that, in addition to the transferase activity, GST-σ has the properties of prostaglandin synthase, is involved in the production of prostaglandins, and might retain this enzymatic activity in the host tissues (Morphew et al., 2007).

Another group of enzymes that are usually involved in the implementation of phase 2 metabolism of xenobiotics in eukaryotes is UDF-glucuronyl transferase (UGT). The functions of these proteins are to increase the hydrophilicity of substrates and their availability for the cell excretion, phase 3. The superfamily of UGTs consists of two families of UGT1 and UGT2, combining more than 20 isoenzymes. In the genomes of parasitic and free-living nematodes, from 30 to 70 genes encoding UGT were found (Matouskova et al., 2016). These enzymes play an important role in the formation of parasite resistance to anthelmintics (Lindblom et al., 2006; Laing et al., 2013; Matouskova et al., 2016). However, neither the genome of *O. felineus*, nor the genomes of other representatives of the Opisthorchiidae family, trematodes of the Schistosomatidae family, contained UGT genes. In addition, genes encoding

Table 2. The number of CYP genes in parasitic and free-living flatworms

Species	Class	Family	Number of CYPs
Opisthorchis felineus	Trematoda	Opisthorchiidae	1
Clonorchis sinensis	Trematoda	Opisthorchiidae	1
Opisthorchis viverrini	Trematoda	Opisthorchiidae	1
Schistosoma mansoni	Trematoda	Schistosomatidae	1
Schistosoma japonicum	Trematoda	Schistosomatidae	1
Fasciola hepatica	Trematoda	Fasciolidae	1
Fasciola gigantyca	Trematoda	Fasciolidae	1
Taenia solium	Cestoda	Taeniidae	1
Schmidtea mediterranea	Rhabditophora	Dugesiidae	35
Macrostomum lignano	Turbellaria	Macrostomidae	39

arylamine N-acetyltransferase, enzymes involved in phase 2 reactions of xenobiotic metabolism in vertebrates were not found in the opisthorchid and schistostomatid genomes (Ershov et al., 2019).

Proteins of phase 3 of xenobiotic metabolism are responsible for excretion from cells into the extracellular space of compounds formed as a result of the action of phase 1 and 2 enzymes. Excretion is carried out by proteins belonging to five families of membrane transporters. ABC transporters are the best studied phase 3 proteins, since these proteins are involved in the drug resistance mechanisms of eukaryotic and prokaryotic cells (Saier et al., 2014; Wong et al., 2014). Twenty-three genes encoding ABC transporters were found in the *O. felineus* genome (Mordvinov et al., 2017a). Interestingly, four of them, *P1–P4*, are similar to the single human P-glycoprotein gene. The product of this gene is also known as multidrug resistance protein 1 (Saier et al., 2014; Wong et al., 2014). It was found that in two *O. felineus* P-glycoprotein genes, the expression level depends on the stage of development of the parasite. So, in adult worms, the expression of the P1 and P4 genes is 20–30 times higher than in metacercariae and recently excised juvenile worms. It is probably, that these proteins are most significant for the metabolism of xenobiotics in adult parasites.

In conclusion, it should be emphasized that the *O. felineus* xenobiotic metabolism system, as, probably, in other parasitic flatworms, has clear structural and functional features. First, it differs significantly from the xenobiotic metabolism system of the mammalian hosts. A detailed study of the xenobiotic metabolism system of the liver flukes will expand our understanding of the development of parasitism mechanisms and the evolution of host–parasite relationship. Knowledge of the structure and functions of this metabolic system can also be applied in the identification of new pharmacological targets for the treatment of opisthorchiasis and other trematodiases.

The products of the xenobiotic metabolism system of *O. felineus* and other trematodes can be metabolites presented in the ESP of parasites. Low molecular weight components of *O. felineus* ESP, parasite-specific cholesterol metabolites were found (Gouveia et al., 2017). These oxysterol-like compounds possess genotoxic properties and might cause damage to the host DNA. The accumulation of such damage leads to malignant transformation of bile duct tissue. It is possible that specific *O. felineus* oxysterols are involved in triggering cholangiocarcinogenesis mechanisms during opisthorchiasis.

The synthesis of parasite-specific oxysterols can be carried out by CYP and other redox enzymes, such as glutathione S-transferase, thioredoxin peroxidase, etc. The search for proteins involved in the enzymatic pathway for the generation of specific genotoxic helminthic oxysterols remains a priority for molecular parasitology.

Granulins as potential promoters of cholangiocyte neoplasia

There is a hypothesis that granulin, a protein that is part of the opisthorchid ESP, participate in carcinogenic processes associated with helminth infection (Smout et al., 2015). Granulins of *O. felineus*, *O. viverrini* and *C. sinensis* liver flukes have conserved structure and are homologous to human granulin. Human and helminthic granulins stimulate the proliferation of epithelial cells, including cholangiocytes (Smout et al., 2015), however, they use various cellular signaling pathways. Human granulin acts as an antagonist of the tumor necrosis factor (TNF) signaling pathway. The helminthic granulin receptor is unknown, but it was found that *O. viverrini* granulin enters into cholangiocytes and activates the MAP kinase and epidermal growth factor receptor signaling pathway. This is a much more powerful way to activate proliferation than that used by human granulin.

O. viverrini granulin effectively promotes the healing of injuries (Smout et al., 2015). In addition, this protein stimulates the growth of blood vessels (Smout et al., 2015) and can probably activate cell migration. It is believed, that granulin facilitates the proliferation of malignant cholangiocytes arising from chronic opisthorchiasis, and contributes to the development of a bile duct cancer.

In the *O. felineus* genome, as in the *O. viverrini* and *C. sinensis* genomes, four genes (GRN-1–GRN-4) encoding single-domain granulins, as well as one multi-domain progranulin (PGRN) gene were found (Ershov et al., 2019). Genes of single-domain granulins are localized in one chromosomal locus and form a conservative syntenic group of genes. The sequences of the GRN-1 and GRN-4 *O. felineus* genes have 95 % homology, which suggests the duplication of a single gene. The fixation of this duplication in the genomes of opisthorchids can probably be associated with a significant functionality of granulin.

The highest level of expression of the *O. felineus* GRN-1 and GRN-4 genes was shown in adult helminths, while in metacercaria the GRN-3 gene is dominantly expressed (Ershov et al., 2019). All experimental work on the determination of the potentially carcinogenic properties of opisthorchid granulins was performed with the *O. viverrini* GRN-1. It can be assumed that the product of the *O. felineus* GRN-4 gene also has mitogenic, angiogenic properties and the ability to increase cell migration. In adults, expression of the GRN-2 and GRN-3 genes is practically absent. It is likely that the products of these genes may be involved in the host–parasite relationship in intermediate hosts of trematodes, mollusks and fish.

Conclusion

The causative agent of opisthorchiasis, the *O. felineus* liver fluke is epidemiologically significant species of Opisthorchiidae trematodes. Its range covers vast areas of Europe and Asia, and outbreaks of opisthorchiasis caused by this helminth can be expected in many countries. One cannot but take into account the growing migration of the population and the tourist flow between different countries. Due to these factors, patients suffering from *O. felineus* infection can be detected far beyond the endemic areas. Thus, opisthorchiasis caused by *O. felineus* infection becomes a global challenge that goes beyond the biomedical problems of individual regions.

The appearance of the genomic and proteomic data of *O. felineus* significantly strengthens the basis of molecular biological studies of epidemiologically important liver flukes. In-depth studies of the genomics and proteomics of *O. felineus* will allow the generation of substantiated hypotheses about the carcinogenesis mechanisms associated with opisthorchiasis, the identification of species-specific pathogenesis of helminthiases, and the targeted search for molecular targets for the treatment of these diseases. The research strategies should consider the urgent need of practical health care for effective means of therapy and prevention of trematodiases.

References

Bartley D.J., Morrison A.A., Dupuy J., Bartley Y., Sutra J.F., Menez C., Alvinerie M., Jackson F., Devin L., Lespine A. Influence of Pluronic 85 and ketoconazole on disposition and efficacy of ivermectin in sheep infected with a multiple resistant *Haemonchus contortus* isolate. *Vet. Parasitol*. 2012;187:464-472. DOI 10.1016/j.vetpar.2012. 02.011.

Beer S.A. The Biology of the Opisthorchiasis Agent. Moscow: KMK Publ., 2005. (in Russian)

Belshaw R., Bensasson D. The rise and falls of introns. *Heredity*. 2006;96:208-213. DOI 10.1038/sj.hdy.6800791.

Berriman M., Haas B.J., LoVerde P.T., Wilson R.A., Dillon G.P., Cerqueira G.C., Mashiyama S.T., Al-Lazikani B., Andrade L.F., Ashton P.D., Aslett M.A., Bartholomeu D.C., Blandin G., Caffrey C.R., Coghlan A., Coulson R., Day T.A., Delcher A., DeMarco R., Djikeng A., Eyre T., Gamble J.A., Ghedin E., Gu Y., Hertz-Fowler C., Hirai H., Hirai Y., Houston R., Ivens A., Johnston D.A., Lacerda D., Macedo C.D., McVeigh P., Ning Z., Oliveira G., Overington J.P., Parkhill J., Pertea M., Pierce R.J., Protasio A.V., Quail M.A., Rajandream M.A., Rogers J., Sajid M., Salzberg S.L., Stanke M., Tivey A.R., White O., Williams D.L., Wortman J., Wu W., Zamanian M., Zerlotini A., Fraser-Liggett C.M., Barrell B.G., El-Sayed N.M. The genome of the blood fluke *Schistosoma mansoni*. *Nature*. 2009;460:352-358. DOI 10.1038/nature08160.

Cai X.Q., Liu G.H., Song H.Q., Wu C.Y., Zou F.C., Yan H.K., Yuan Z.G., Lin R.Q., Zhu X.Q. Sequences and gene organization of the mitochondrial genomes of the liver flukes *Opisthorchis viverrini* and *Clonorchis sinensis* (Trematoda). *Parasitol. Res*. 2012;110:235-243. DOI 10.1007/s00436-011-2477-2.

Cwiklinski K., Dalton J.P., Dufresne P.J., La Course J., Williams D.J., Hodgkinson J., Paterson S. The *Fasciola hepatica* genome: gene duplication and polymorphism reveals adaptation to the host environment and the capacity for rapid evolution. *Genome Biol*. 2015;16:71. DOI 10.1186/s13059-015-0632-2.

Ershov N.I., Mordvinov V.A., Prokhortchouk E.B., Pakharukova M.Y., Gunbin K.V., Ustyantsev K., Genaev M.A., Blinov A.G., Mazur A., Boulygina E., Tsygankova S., Khrameeva E., Chekanov N., Fan G., Xiao A., Zhang H., Xu X., Yang H., Solovyev V., Lee S.M., Liu X., Afonnikov D.A., Skryabin K.G. New insights from *Opisthorchis felineus* genome: update on genomics of the epidemiologically important liver flukes. *BMC Genomics*. 2019;20:399. DOI 10.1186/s12864-019-5752-8.

Gouveia M.J., Pakharukova M.Y., Laha T., Sripa B., Maksimova G.A., Rinaldi G., Brindley P.J., Mordvinov V.A., Amaro T., Santos L.L., Costa J.M.C.D., Vale N. Infection with *Opisthorchis felineus* induces intraepithelial neoplasia of the biliary tract in a rodent model. *Carcinogenesis*. 2017;38:929-937. DOI 10.1093/carcin/bgx042.

Keiser J., Utzinger J. Food-borne trematodiases. *Clin. Microbiol. Rev*. 2009;22(3):466-483. DOI 10.1128/CMR.00012-09.

Laing R., Kikuchi T., Martinelli A., Tsai I.J., Beech R.N., Redman E., Holroyd N., Bartley D.J., Beasley H., Britton C., Curran D., Devaney E., Gilabert A., Hunt M., Jackson F., Johnston S.L., Kryukov I., Li K., Morrison A.A., Reid A.J., Sargison N., Saunders G.I., Wasmuth J.D., Wolstenholme A., Berriman M., Gilleard J.S., Cotton J.A. The genome and transcriptome of *Haemonchus contortus*, a key model parasite for drug and vaccine discovery. *Genome Biol*. 2013;14:R88. DOI 10.1186/gb-2013-14-8-r88.

Lindblom T.H., Dodd A.K. Xenobiotic detoxification in the nematode *Caenorhabditis elegans*. *J. Exp. Zool. A. Comp. Exp. Biol*. 2006;305(9):720-729. DOI 10.1002/jez.a.324.

Lvova M.N., Duzhak T.G., Tsentalovitch Y.P., Katokhin A.V., Mordvinov V.A. Secretome of the adult liver fluke *Opisthorchis felineus*. *Parazitologiya = Parasitology*. 2014;48(3):169-184. (in Russian)

Matouskova P., Vokral I., Lamka J., Skalova L. The role of xenobiotic-metabolizing enzymes in anthelmintic deactivation and resistance in helminths. *Trends Parasitol*. 2016;32:481-491. DOI 10.1016/j.pt. 2016.02.004.

Mordvinov V.A., Ershov N.I., Pirozhkova D.S., Pakharukov Y.V., Pakharukova M.Y. ABC transporters in the liver fluke *Opisthorchis felineus*. *Mol. Biochem. Parasitol*. 2017a;216:60-68. DOI 10.1016/j.molbiopara.2017.07.001.

Mordvinov V.A., Shilov A.G., Pakharukova M.Y. Anthelmintic activity of cytochrome P450 inhibitors miconazole and clotrimazole: in-vitro effect on the liver fluke *Opisthorchis felineus*. *Int. J. Antimicrob. Agents*. 2017b;50:97-100. DOI 10.1016/j.ijantimicag.2017. 01.037.

Morphew R.M., Wright H.A., LaCourse E.J., Woods D.J., Brophy P.M. Comparative proteomics of excretory-secretory proteins released by the liver fluke *Fasciola hepatica* in sheep host bile and during in vitro culture ex host. *Mol. Cell. Proteomics*. 2007;6:963-972. DOI 10.1074/mcp.M600375-MCP200.

Ovchinnikov V.Y., Afonnikov D.A., Vasiliev G.V., Kashina E.V., Sripa B., Mordvinov V.A., Katokhin A.V. Identification of microRNA genes in three opisthorchiids. *PLoS Negl. Trop. Dis*. 2015;9:e0003680. DOI 10.1371/journal.pntd.0003680.

Pakharukova M.Y., Ershov N.I., Vorontsova E.V., Katokhin A.V., Merkulova T.I., Mordvinov V.A. Cytochrome P450 in fluke *Opisthorchis felineus*: Identification and characterization. *Mol. Biochem. Parasitol*. 2012;181:190-194. DOI 10.1016/j.molbiopara.2011.11.005.

Pakharukova M.Y., Kovner A.V., Trigolubov A.N., Fedin E.N., Mikhailova E.S., Autenshlyus A.I., Mordvinov V.A., Shtofin S.G. Mechanisms of trematodiases pathogenicity: the presence of the secretory proteins from the liver fluke *Opisthorchis felineus* in the gallbladder tissues of the patients with chronic opisthorchiasis. *Vavilovskii Zhurnal Genetiki i Selektsii = Vavilov Journal of Genetics and Breeding*. 2017;21:312-316. DOI 10.18699/VJ16.17-o.

Pakharukova M.Y., Mordvinov V.A. The liver fluke *Opisthorchis felineus*: biology, epidemiology and carcinogenic potential. *Trans. R. Soc. Trop. Med. Hyg*. 2016;110(1):28-36. DOI 10.1093/trstmh/trv085.

Pakharukova M.Y., Vavilin V.A., Sripa B., Laha T., Brindley P.J., Mordvinov V.A. Functional analysis of the unique cytochrome P450 of the liver fluke *Opisthorchis felineus*. *PLoS Negl. Trop. Dis*. 2015;9(12):e0004258. DOI 10.1371/journal.pntd.0004258.

Petney T.N., Andrews R.H., Saijuntha W., Wenz-Mücke A., Sithithaworn P. The zoonotic, fish-borne liver flukes *Clonorchis sinensis*, *Opisthorchis felineus* and *Opisthorchis viverrini*. *Int. J. Parasitol*. 2013;43(12-13):1031-1046. DOI 10.1016/j.ijpara.2013.07.007.

Pomaznoy M.Y., Logacheva M.D., Young N.D., Penin A.A., Ershov N.I., Katokhin A.V., Mordvinov V.A. Whole transcriptome profiling of adult and infective stages of the trematode *Opisthorchis felineus*. *Parasitol. Int*. 2016;65(1):12-19. DOI 10.1016/j.parint.2015. 09.002.

Pozio E., Armignacco O., Ferri F., Gomez Morales M.A. *Opisthorchis felineus*, an emerging infection in Italy and its implication for the European Union. *Acta Trop*. 2013;126(1):54-62. DOI 10.1016/j.actatropica.2013.01.005.

Prichard R.K., Basanez M.G., Boatin B.A., McCarthy J.S., Garcia H.H., Yang G.J., Sripa B., Lustigman S. A research agenda for helminth diseases of humans: intervention for control and elimination. *PLoS Negl. Trop. Dis*. 2012;6:e1549. DOI 10.1371/journal.pntd.0001549.

Protasio A.V., Tsai I.J., Babbage A., Nichol S., Hunt M., Aslett M.A., De Silva N., Velarde G.S., Anderson T.J., Clark R.C., Davidson C., Dillon G.P., Holroyd N.E., LoVerde P.T., Lloyd C., McQuillan J., Oliveira G., Otto T.D., Parker-Manuel S.J., Quail M.A., Wilson R.A., Zerlotini A., Dunne D.W., Berriman M. A systematically improved high quality genome and transcriptome of the human blood fluke *Schistosoma mansoni*. *PLoS Negl. Trop. Dis*. 2012;6:e1455. DOI 10.1371/journal.pntd.0001455.

Rospotrebnadzor. On Preventive Measures against Opisthorchiasis. 2015. https://rospotrebnadzor.ru/about/info/news/news_details.php?ELEMENT_ID=3480&sphrase_id=462082. (in Russian)

Saier M.H. Jr., Reddy V.S., Tamang D.G., Västermark A. The transporter classification database. *Nucleic Acids Res*. 2014;42:D251-D258. DOI 10.1093/nar/gkt1097.

Schuster R., Bonin J., Staubach C., Heidrich R. Liver fluke (Opisthorchiidae) findings in red foxes (*Vulpes vulpes*) in the eastern part of the Federal State Brandenburg, Germany – a contribution to the epidemiology of opisthorchiidosis. *Parasitol. Res*. 1999; 85(2):142-146. DOI 10.1007/s004360050523.

Shekhovtsov S.V., Katokhin A.V., Kolchanov N.A., Mordvinov V.A. The complete mitochondrial genomes of the liver flukes *Opisthorchis felineus* and *Clonorchis sinensis* (Trematoda). *Parasitol. Int*. 2010;59:100-103. DOI 10.1016/j.parint.2009.10.012.

Shekhovtsov S.V., Katokhin A.V., Romanov K.V., Besprozvannykh V.V., Fedorov K.P., Yurlova N.I., Serbina E.A., Sithithaworn P., Kolchanov N.A., Mordvinov V.A. A novel nuclear marker, Pm-int9, for phylogenetic studies of *Opisthorchis felineus*, *Opisthorchis viverrini*, and *Clonorchis sinensis* (Opisthorchiidae, Trematoda). *Parasitol. Res*. 2009;106:293-297. DOI 10.1007/s00436-009-1628-1.

Sleumer M.C., Mah A.K., Baillie D.L., Jones S.J. Conserved elements associated with ribosomal genes and their trans-splice acceptor sites in *Caenorhabditis elegans*. *Nucleic Acids Res*. 2010; 38(9):2990-3004. DOI 10.1093/nar/gkq003.

Smout M.J., Sotillo J., Laha T., Papatpremsiri A., Rinaldi G., Pimenta R.N., Chan L.Y., Johnson M.S., Turnbull L., Whitchurch C.B., Giacomin P.R., Moran C.S., Golledge J., Daly N., Sripa B., Mulvenna J.P., Brindley P.J., Loukas A. Carcinogenic parasite secretes growth factor that accelerates wound healing and potentially promotes neoplasia. *PLoS Pathog*. 2015;11:e1005209. DOI 10.1371/journal.ppat.1005209.

Tsai I.J., Zarowiecki M., Holroyd N., Garciarrubio A., Sánchez-Flores A., Brooks K.L., Tracey A., Bobes R.J., Fragoso G., Sciutto E., Aslett M., Beasley H., Bennett H.M., Cai X., Camicia F., Clark R., Cucher M., De Silva N., Day T.A., Deplazes P., Estrada K., Fernández C., Holland P.W.H., Hou J., Hu S., Huckvale T., Hung S.S., Kamenetzky L., Keane J.A., Kiss F., Koziol U., Lambert O., Liu K., Luo X., Luo Y., Macchiaroli N., Nichol S., Paps J., Parkinson J., Pouchkina-Stantcheva N., Riddiford N., Rosenzvit M., Salinas G., Wasmuth J.D., Zamanian M., Zheng Y.; Taenia solium Genome Consortium, Cai J., Soberón X., Olson P.D., Laclette J.P., Brehm K., Berriman M. The genomes of four tapeworm species reveal adaptations to parasitism. *Nature*. 2013;496:57-63. DOI 10.1038/nature 12031.

Urrutia A.O., Hurst L.D. The signature of selection mediated by expression on human genes. *Genome Res*. 2003;13:2260-2264. DOI 10.1101/gr.641103.

Wang X., Chen W., Huang Y., Sun J., Men J., Liu H., Luo F., Guo L., Lv X., Deng C., Zhou C., Fan Y., Li X., Huang L., Hu Y., Liang C., Hu X., Xu J., Yu X. The draft genome of the carci-

nogenic human liver fluke *Clonorchis sinensis. Genome Biol*. 2011;12:R107. DOI 10.1186/gb-2011-12-10-r107.

Wong K., Ma J., Rothnie A., Biggin P.C., Kerr I.D. Towards understanding promiscuity in multidrug efflux pumps. *Trends Biochem. Sci*. 2014;39:8-16. DOI 10.1016/j.tibs.2013.11.002.

Young N.D., Nagarajan N., Lin S.J., Korhonen P.K., Jex A.R., Hall R.S., Safavi-Hemami H., Kaewkong W., Bertrand D., Gao S., Seet Q., Wongkham S., Teh B.T., Wongkham C., Intapan P.M., Maleewong W., Yang X., Hu M., Wang Z., Hofmann A., Sternberg P.W., Tan P., Wang J., Gasser R.B. The *Opisthorchis viverrini* genome provides insights into life in the bile duct. *Nat. Commun*. 2014;5:4378. DOI 10.1038/ncomms 5378.

Zadesenets K.S., Katokhin A.V., Mordvinov V.A., Rubtsov N.B. Comparative cytogenetics of opisthorchid species (Trematoda, Opisthorchiidae). *Parasitol. Int*. 2012;61:87-89. DOI 10.1016/j.parint.2011.07.006.

ORCID ID

V.A. Mordvinov orcid.org/0000-0002-6173-0774
N.I. Ershov orcid.org/0000-0003-3423-3497
M.Y. Pakharukova orcid.org/0000-0003-1054-2068

Acknowledgements. This work was financially supported by the Russian Foundation for Basic Research (No. 18-04-00417A (VAM), No. 19-34-90060-Aspirants (OZ)) and state projects of the Institute of Cytology and Genetics (0324-2019-0041 (MYP), No. 0259-2019-0010 (OZ)).

Conflict of interest. The authors declare no conflict of interest.

Received October 25, 2019. Revised December 20, 2019. Accepted December 20, 2019. Published online April 23, 2020.

Вавиловский журнал генетики и селекции. 2020;24(4):391-398
DOI 10.18699/VJ20.631

The role of polymorphic variants of arginase genes (*ARG1*, *ARG2*) involved in beta-2-agonist metabolism in the development and course of asthma

O.N. Savelieva[1] ✉, A.S. Karunas[1, 2] ✉, Yu.Yu. Fedorova[2], R.R. Murzina[3], A.N. Savelieva[1], R.F. Gatiyatullin[3], E.I. Etkina[3], E.K. Khusnutdinova[2, 4]

[1] Bashkir State University, Ufa, Russia
[2] Institute of Biochemistry and Genetics – Subdivision of the Ufa Federal Research Centre of the Russian Academy of Sciences, Ufa, Russia
[3] Bashkir State Medical University of the Ministry of Healthcare of the Russian Federation, Ufa, Russia
[4] St. Petersburg State University, St. Petersburg, Russia
✉ e-mail: olyasavelie@yandex.ru, carunas@list.ru

Abstract. Asthma is a common severe disease of the respiratory tract, it leads to a significant impairment in the quality of a patient's life unless effectively treated. Uncontrolled asthma symptoms are a cause of disease progression and development, they lead to an increase in the patient's disability. The sensitivity to asthma therapy largely depends on the interaction of genetic and epigenetic factors, which account for about 50–60 % of variability of therapeutic response. Beta-2-agonists are some of the major class of bronchodilators used for asthma management. According to published data, allelic variants of the arginase *ARG1* and *ARG2* genes are associated with a risk of asthma development, spirometry measures and efficacy of bronchodilator therapy. High arginase activity results in a low level of plasma L-arginine and in a decrease in nitric oxide, and, as a result, in an increase in airway inflammation and remodeling. Arginase genetic polymorphisms (rs2781667 of the *ARG1* gene, rs17249437, rs3742879, rs7140310 of the *ARG2* gene) were studied in 236 children with asthma and 194 unrelated healthy individuals of Russian, Tatar and Bashkir ethnicity from the Republic of Bashkortostan. Association analysis of the studied polymorphisms with asthma development and course, the sensitivity to therapy in patients was carried out. It was found that the rs2781667**C* allele of the *ARG1* gene is a marker of an increased risk of asthma in Tatars. In Russians, the association of rs17249437**TT* and rs3742879**GG* genotypes of the *ARG2* gene with a decrease in spirometry measures (FEV1, MEF25) was established. In Russians and Tatars receiving glucocorticoid monotherapy or combination therapy, the association of the rs17249437**T* allele and rs17249437**TT* genotype of the *ARG2* gene with a partially controlled and uncontrolled course of asthma was shown.
Key words: asthma; beta-2-agonists; arginase 1 (*ARG1*); arginase 2 (*ARG2*); association; predisposition genes.

For citation: Savelieva O.N., Karunas A.S., Fedorova Yu.Yu., Murzina R.R., Savelieva A.N., Gatiyatullin R.F., Etkina E.I., Khusnutdinova E.K. The role of polymorphic variants of arginase genes (*ARG1*, *ARG2*) involved in beta-2-agonist metabolism in the development and course of asthma. *Vavilovskii Zhurnal Genetiki i Selektsii = Vavilov Journal of Genetics and Breeding*. 2020;24(4):391-398. DOI 10.18699/VJ20.631

Роль полиморфных вариантов генов аргиназ (*ARG1*, *ARG2*), участвующих в метаболизме бета-2-агонистов, в развитии и течении бронхиальной астмы

О.Н. Савельева[1] ✉, А.С. Карунас[1, 2] ✉, Ю.Ю. Федорова[2], Р.Р. Мурзина[3], А.Н. Савельева[1], Р.Ф. Гатиятуллин[3], Э.И. Эткина[3], Э.К. Хуснутдинова[2, 4]

[1] Башкирский государственный университет, Уфа, Россия
[2] Институт биохимии и генетики – обособленное структурное подразделение Уфимского федерального исследовательского центра Российской академии наук, Уфа, Россия
[3] Башкирский государственный медицинский университет Министерства здравоохранения Российской Федерации, Уфа, Россия
[4] Санкт-Петербургский государственный университет, Санкт-Петербург, Россия
✉ e-mail: olyasavelie@yandex.ru, carunas@list.ru

Аннотация. Бронхиальная астма (БА) – широко распространенное тяжелое заболевание дыхательных путей, которое при недостаточно эффективном лечении приводит к значительному ухудшению качества жизни пациентов. Отсутствие контроля над симптомами БА ведет к быстрому прогрессированию, утяжелению заболевания и инвалидизации пациентов. Чувствительность к лекарственной терапии БА во многом зависит от взаимодействия генетических и эпигенетических факторов, которые на 50–60 % определяют вариабельность терапевтического ответа пациентов. Одной из основных групп препаратов, ис-

пользуемых для лечения БА, являются бета-2-агонисты, оказывающие значительное бронходилатирующее действие. По литературным данным, аллельные варианты генов аргиназ *ARG1* и *ARG2* ассоциированы с риском развития БА, показателями спирографии и эффективностью терапии бронходилататорами. Повышенная экспрессия генов аргиназ ведет к снижению биодоступности L-аргинина и уровня оксида азота в организме и, как следствие, к увеличению степени воспаления и ремоделирования дыхательных путей. Выполнено исследование полиморфных вариантов генов аргиназ (rs2781667 гена *ARG1* и rs17249437, rs3742879, rs7140310 гена *ARG2*) у 236 детей, больных БА, а также у 194 неродственных здоровых индивидов русской, татарской и башкирской этнической принадлежности, проживающих на территории Республики Башкортостан. Проведен поиск ассоциаций изученных полиморфных вариантов с развитием, течением БА и чувствительностью к терапии у пациентов с БА. Установлено, что аллель rs2781667**C* гена *ARG1* является маркером повышенного риска развития БА у татар. В группе русских пациентов с БА генотипы rs17249437**TT* и rs3742879**GG* гена *ARG2* ассоциированы со снижением показателей спирографии (ОФВ1, МОС25). У русских и татар, находящихся на монотерапии ингаляционными глюкокортикостероидами или на комбинированной терапии, показана ассоциация аллеля rs17249437**T* и генотипа rs17249437**TT* гена *ARG2* с частично контролируемым и неконтролируемым течением астмы.
Ключевые слова: бронхиальная астма; бета-2-агонисты; аргиназа 1 (*ARG1*); аргиназа 2 (*ARG2*); ассоциация; гены предрасположенности.

Introduction

Bronchial asthma (BA) is a heterogeneous chronic respiratory disease that caused by an interaction of genetic and environmental risk factors. The prevalence of asthma in the world is 1–18 %, while a significant proportion of patients have insufficient asthma control (GINA, 2018). Beta-2-adrenergic receptor agonists are one of the main groups of drugs used in asthma treatment. Short-acting beta-2-agonists (SABA) are drugs of choice for the treatment of bronchospasm in acute asthma exacerbations. Long-acting beta-2-agonists (LABA) have anti-inflammatory effects due to reduced vascular permeability, reduced secretion of mediators from mast cells and basophils, and reduced bronchial hyperreactivity in prolonged use by patients (National Program…, 2017).

According to the literature, the contribution of genetic factors to individual response of BA patients to therapy is about 50–60 % (Farzan et al., 2017). More than 20 candidate genes associated with beta-2-agonist sensitivity (*ADRB2*, *CRHR2*, *ADCY9*, *ARG1*, *ARG2*, etc.) have been detected (Martinez et al., 1997; Litonjua et al., 2008; Poon et al., 2008; Vonk et al., 2010; Kim et al., 2011; Fedorova et al., 2013; Batozhargalova et al., 2017; Scaparrotta et al., 2019). Genome-wide association studies (GWAS) and the examination of large samples within the framework of international consortia allowed to significantly increase the number of genes and intergenic polymorphisms associated with the effectiveness of bronchodilator therapy (*COL22A1*, *SLC22A15*, *SLC22A23*, *OXR1*, *THRB*, *NTM*, etc.) (www.genome.gwas.org).

For the most studied rs1042713 (c.46A>G, p.Arg16Gly) polymorphism of the beta-2 adrenergic receptor gene *ADRB2*, involved in metabolism of beta-2-agonists, clinical trial of the third stage was performed (Bateman et al., 2011), and the level 2A annotation of that polymorphism was published on the PharmGB website, proving the practical relevance of asthma pharmacogenetic studies (https://www.pharmgkb.org/gene/PA39/clinicalAnnotation/). Furthermore, an important role of other polymorphisms on the efficacy of beta-2-agonist therapy in asthma patients of different ethnicity has been established. The association of genotypes and haplotypes of the adenylyl cyclase type 9 (*ADCY9*) gene with improvement of lung function measurements in response to using beta-2-agonists in asthma patients from Korea was identified, besides genetic variants of the thyroid hormone receptor beta (*THRB*) gene and the corticotropin-releasing hormone receptor 2 (*CRHR2*) gene were associated with a more significant bronchodilator response in patients from Europe (Kim et al., 2011; Duan et al., 2013; Drake et al., 2014). A number of studies have shown that allelic variants of *ARG1* and *ARG2* genes are associated with BA development, spirometry measures and the effectiveness of bronchodilator therapy (Li et al., 2006; Salam et al., 2009; Vonk et al., 2010; Duan et al., 2011). The increased expression of arginase genes leads to reduced bioavailability of L-arginine and nitrogen oxide levels in the body, increased production of polyamines and proline, and as a consequence, to increased inflammation and remodeling of the respiratory tract (Li et al., 2006; Cloots et al., 2018; Meurs et al., 2019; Said et al., 2019).

The aim of our research was to analyze the association of arginase 1 *ARG1* (rs2781667) and arginase 2 *ARG2* (rs17249437, rs3742879, rs7140310) genetic polymorphisms with development and course of asthma in children of different ethnicity.

Materials and methods

DNA samples of 430 unrelated individuals aged 2–17 years from the Republic of Bashkortostan were used in the present study (Table 1). The group of patients consisted of 236 children with bronchial asthma (70 girls, 166 boys) of different ethnicities (Russians – 84, Tatars – 108, Bashkirs – 44). All examined individuals were patients at the children's clinic at Bashkir State Medical University of the Ministry of Health of Russia (Ufa, Russia) and the Allergology Department of the Republican Children's Clinical Hospital (Ufa, Russia). The criteria for inclusion of children in the main observation group included the established diagnosis of "bronchial asthma" in accordance with GINA (Global Initiative for Asthma) criteria and the criteria of Russian program documents on BA diagnosis, treatment, and prevention (National Program…, 2012).

All asthma patients were treated for at least three months with inhaled glucocorticosteroids (ICS) monotherapy or the combination of inhaled glucocorticosteroids and long-acting

Table 1. Characteristics of asthma patients and control group

Parameters	Samples		
	Russians	Tatars	Bashkirs
BA patients			
Sample size	84	108	44
Age, years (M ± SE)	10.45 ± 0.39	10.72 ± 0.31	10.34 ± 0.54
Age of asthma onset, years (M ± SE)	3.85 ± 0.34	3.48 ± 0.29	3.73 ± 0.47
Total serum IgE levels, IU/mL (M ± SE)	432.15 ± 46.15	431.67 ± 38.86	425.30 ± 58.0
FEV1, % of normal (M ± SE)	62.51 ± 3.59	73.27 ± 4.64	81.22 ± 8.30
Control group			
Sample size	75	83	36
Age, years (M ± SE)	11.49 ± 0.43	13.54 ± 0.42	14.19 ± 0.58

Note: M – mean; SE – standard error of mean.

beta-agonist (ICS–LABA) in a once-daily dose of 100 to 1000 micrograms of fluticasone propionate, depending on the disease severity. The group of asthma patients on ICS monotherapy was included 187 individuals, patient group receiving ICS–LABA combination therapy was composed of 49 individuals. Patient group with controlled asthma on the background therapy by ICS and ICS–LABA was included 172 individuals, group with partially controlled asthma – 50 individuals, group with uncontrolled asthma – 14 individuals.

The evaluation of respiratory function was performed using a computer spirometer (Erich Jaeger, Germany) with flow–volume curve analysis. The following parameters were assessed (in percent of the expected value present in the computer database of the spirometer): vital capacity (VC), forced vital capacity (FVC), forced expiratory volume in 1 sec (FEV1), forced expiratory flow between 25 and 75 % of forced vital capacity (MEF75, MEF50, MEF25, respectively). The normal range and reduction in parameters of spirogram (in percent of the standard value) for children under 18 years were assessed according to Klement and Zilber (1993). Patients with clinical asthma symptoms who were unable to perform spirometry were subjected to multiple measurements of peak expiratory flow rate (PEFR).

Assessment of current level of asthma control on the background of at least 3 months of therapy was carried out on the basis of clinical signs for the last 4 weeks (frequency of daytime symptoms and frequency of night waking up per week, the need for drugs to control attacks in a week, activity restriction due to asthma) by using a validated questionnaire "Asthma Control Test". A group of apparently healthy children without bronchopulmonary, allergic, and autoimmune diseases and any familial history of allergic diseases consisting of 194 individuals (119 girls, 75 boys) of the corresponding ethnicity (75 Russians, 83 Tatars, 36 Bashkirs) served as a control. Children in the control group had low levels of immunoglobulin E (IgE) and no deviations from normal respiratory function according to spirometry or picfluometry data. An informed consent to participate in the study was obtained from all the children over 15 years and parents of children under 15 years participating in the study. The study protocol was approved by the local Bioethical Committees at the Bashkir State Medical University (Protocol no. 28 dated October 29, 2012) and the Institute of Biochemistry and Genetics of the Ufa Federal Research Centre of the Russian Academy of Sciences (Protocol no. 4 dated November 15, 2012).

Genomic DNA was isolated from peripheral blood lymphocytes by phenol-chloroform extraction (Mathew, 1984). Analysis of the rs2781667 (c.57+665C > T) polymorphism of the arginase 1 *ARG1* gene and rs17249437 (c.185-8016T > C), rs3742879 (c.859+101A > G), rs7140310 (c.363-1623T > G) polymorphisms of the arginase 2 *ARG2* gene was carried out using DNA amplification by the polymerase chain reaction (PCR) with fluorescent detection (FLASH/RTAS) (TestGen, Moscow) according to the manufacturer's protocol using the CFX96 real-time PCR detection system (Bio-Rad, USA).

Selection of single-nucleotide polymorphisms (SNP) in studied genes was based on literature data, information from databases about variation allele frequencies (over 5 %), their possible regulatory influence on gene expression and functional significance (Li et al., 2006; Salam et al., 2009; Vonk et al., 2010; Duan et al., 2011).

The χ^2 criterion was used to verify the correspondence of the observed distribution of genotype frequencies to the expected one according to the Hardy–Weinberg equilibrium. A pairwise comparison of allele and genotype frequencies between the patients and controls was based on the χ^2 criterion for 2×2 contingency tables with Yates correction. In the case of significant differences in the studied samples, the odds ratio (OR) and the boundaries of 95 % confidence interval (95 % CI) were estimated. Statistical analysis of quantitative data was performed using parametric and nonparametric tests depending on the scales and the distribution of variables via SPSS v.23 (SPSS Inc.). The distribution of quantitative data was assessed according to the Kolmogorov–Smirnov criterion. The equality of general variances was assessed using Levene's test. Nonparametric tests (Mann–Whitney *t* criterion and Kruskal–Wallis H criterion) were used in similar comparisons in the case of abnormal distribution or failed equality of variances. The linkage disequilibrium between polymorphisms

was estimated by applying the D′ coefficient, proposed by Lewontin, and Pearson correlation coefficient r^2. The EM-algorithm realized in program Haploview version 4.2 was used for definition of haplotype frequencies and for testing of differences in haplotype frequencies distributions (https://www.broadinstitute.org/haploview/haploview).

Results

Allele and genotype frequencies of four polymorphisms of arginase *ARG1* (rs2781667) and *ARG2* (rs17249437, rs3742879, rs7140310) genes were analyzed in asthma patients and healthy individuals from the Republic of Bashkortostan (Table 2). The distribution of genotype frequencies in all polymorphisms

Table 2. Distribution of allele and genotype frequencies of ARG1 rs2781667, ARG2 rs17249437, rs3742879, rs7140310 gene polymorphisms in asthma patients and control group

Groups		*N*	Genotypes			Alleles	
			n (%)	*n* (%)	*n* (%)	*n* (%)	*n* (%)
rs2781667			*CC*	*CT*	*TT*	*C*	*T*
Patients	Russians	84	40 (47.62)	36 (42.86)	8 (9.52)	116 (69.05)	52 (30.95)
	Tatars	107	54 (50.47)	44 (41.12)	9 (8.41) $p = 0.03$ OR = 0.38 (0.16–0.91)	152 (71.03) $p = 0.04$ OR = 1.57 (1.02–2.41)	62 (28.97) $p = 0.04$ OR = 0.64 (0.41–0.98)
	Bashkirs	44	22 (50.0)	18 (40.91)	4 (9.09)	62 (70.45)	26 (29.55)
Controls	Russians	75	37 (49.93)	33 (44.0)	5 (6.67)	107 (71.33)	43 (28.67)
	Tatars	82	34 (41.46)	32 (39.02)	16 (19.51)	100 (60.98)	64 (39.02)
	Bashkirs	35	17 (48.57)	17 (48.57)	1 (2.86)	51 (72.86)	19 (27.14)
rs17249437			*TT*	*TC*	*CC*	*T*	*C*
Patients	Russians	84	48 (57.14)	29 (34.52)	7 (8.33)	125 (74.4)	43 (25.6)
	Tatars	107	43 (40.19)	53 (49.53)	11 (10.28)	139 (64.95)	75 (35.05)
	Bashkirs	44	17 (38.64)	21 (47.73)	6 (13.64)	55 (62.5)	33 (37.5)
Controls	Russians	74	31 (41.89)	36 (48.65)	7 (9.46)	98 (66.22)	50 (33.78)
	Tatars	82	33 (40.24)	35 (42.68)	14 (17.07)	101 (61.59)	63 (38.41)
	Bashkirs	36	13 (36.11)	18 (50.0)	5 (13.89)	44 (61.11)	28 (38.89)
rs3742879			*AA*	*AG*	*GG*	*A*	*G*
Patients	Russians	84	37 (44.05)	31 (36.9)	16 (19.05)	105 (62.5)	63 (37.5)
	Tatars	106	57 (53.77)	41 (38.68)	8 (7.55)	155 (73.11)	57 (26.89)
	Bashkirs	44	23 (52.27)	19 (43.18)	2 (4.55)	65 (73.86)	23 (26.14)
Controls	Russians	75	36 (48.0)	32 (42.67)	7 (9.33)	104 (69.33)	46 (30.67)
	Tatars	82	42 (51.22)	37 (45.12)	3 (3.66)	121 (73.78)	43 (26.22)
	Bashkirs	36	17 (47.22)	17 (47.22)	2 (5.56)	51 (70.83)	21 (29.17)
rs7140310			*AA*	*AC*	*CC*	*A*	*C*
Patients	Russians	82	63 (76.83)	19 (23.17)	–	145 (88.41)	19 (11.59)
	Tatars	107	72 (67.29)	34 (31.87)	1 (0.93)	178 (83.18)	36 (16.82)
	Bashkirs	44	21 (47.73)	22 (50.0)	1 (2.27)	64 (72.73)	24 (27.27)
Controls	Russians	75	53 (70.67)	22 (29.33)	–	128 (85.33)	22 (14.67)
	Tatars	83	56 (67.47)	22 (26.51)	5 (6.02)	134 (80.72)	32 (19.68)
	Bashkirs	36	24 (66.67)	11 (30.56)	1 (2.78)	59 (81.94)	13 (18.06)

Note: *N* is the number of individuals; *n* is the sample size; alleles and genotype frequencies are shown in brackets; *p* is the P-value and is shown in the case of statistical significance ($p \leq 0.05$); OR is the odds ratio and 95 % confidence interval (in brackets).

corresponded to the Hardy–Weinberg equilibrium ($p > 0.05$). The association analysis of the studied polymorphisms with asthma development, with clinical and functional parameters of BA (degree of asthma control, age of asthma onset, level of total IgE, spirometry parameters) was carried out.

The arginase 1 (*ARG1*) gene is located on the chromosome 6 (6q23.2) and contains 8 exons (Vonk et al., 2010). The rs2781667**T* allele frequency in control groups were as follows: 28.67 % in Russians, 39.02 % in Tatars, 27.14 % in Bashkirs. An association of the rs2781667**C* allele with asthma in Tatars ($p = 0.04$; OR = 1.57; CI 95% 1.02–2.41) was established. The rs2781667**TT* genotype and the rs2781667**T* allele are markers of reduced risk for asthma development in Tatars ($p = 0.03$; OR = 0.38; CI 95% 0.16–0.91 and $p = 0.04$; OR = 0.64; CI 95% 0.41–0.98, respectively).

The contribution of allelic variants of studied candidate genes to the variability of quantitative traits (IgE level, age of disease onset) was determined by Kruskal–Wallis test (in case of three groups) or Mann–Whitney test (in case of two groups). The analysis of variations in IgE levels among asthma patients of Russian ethnicity with different genotypes of the rs2781667 polymorphism of the *ARG1* gene demonstrated higher IgE values in patients bearing the rs2781667**CC* genotype compared to patients with rs2781667**CT* and rs2781667**TT* genotypes. As a result of pairwise comparison of groups, a statistically significant increase of IgE level was observed in patients bearing the rs2781667**CC* genotype compared with individuals with the rs2781667**CT* genotype ($p = 0.003$).

Genotypes	IgE (M ± SE, IU/mL)
rs2781667**CC*	520.70 ± 72.47
rs2781667**CT*	331.7 ± 66.28
rs2781667**TT*	471.5 ± 108.3
Kruskal–Wallis test	H = 8.49, $p = 0.01$
U Mann–Whitney test	
rs2781667**CC*/rs2781667**CT*	U = 354.0, $p = 0.003$
rs2781667**CC*/rs2781667**TT*	U = 136.0, $p = 0.91$
rs2781667**CT*/rs2781667**TT*	U = 93.0, $p = 0.18$

The *ARG2* gene is located at the chromosome region 14q24.1 and contains 8 exons (Vonk et al., 2010). An analysis of allele and genotype frequency distributions of the *ARG2* polymorphism rs17249437 showed that the rs17249437**C* allele was less prevalent in control groups of Russians, Tatars and Bashkirs (33.78, 38.41 and 38.89 % respectively) (see Table 2). No statistically significant associations of the *ARG2* polymorphism rs17249437 with asthma were found ($p > 0.05$). Differences in genotype distribution of rs17249437 polymorphic variant while dividing patients with account for deviations from normal spirometry values in comparison to the controls were revealed. The frequency of the homozygous rs17249437**TT* genotype (67.74 and 67.74 %) in Russian asthma patients with significant decreases FEV1 and MEF25 was significantly higher than in the control group of individuals (41.89 %; $p = 0.02$; OR = 2.91; CI 95% 1.2–7.05 and $p = 0.02$; OR = 2.91; CI 95% 1.2–7.05, respectively). The frequency of the heterozygous rs17249437**TC* genotype in Russians with significantly reduced FEV1 and MEF25 was lower (19.35 and 22.58 %) than in the controls (48.65 %; $p = 0.005$; OR = 0.25; CI 95% 0.09–0.69 and $p = 0.01$; OR = 0.31; CI 95% 0.12–0.8, respectively).

The increased frequency of the rs17249437**T* allele (87.93 %) and the rs17249437**TT* genotype (82.76 %) was detected in Russian patients with partially controlled and uncontrolled asthma, who required treatment with beta-2-agonists more often than three times a week, compared to patients with controlled asthma: 67.27 % for the rs17249437**T* allele ($p = 0.004$; OR = 3.54; CI 95% 1.46–8.59) and 43.64 % for the rs17249437**TT* genotype ($p = 0.0006$; OR = 6.20; CI 95% 2.06–18.64). A similar association has been found in asthma patients of Tatar ethnicity. The rs17249437**T* allele (77.59 %) and the rs17249437**TT* genotype (58.62 %) were detected more frequently in patients with partially controlled and uncontrolled asthma, in comparison with children with controlled asthma: 60.26 % for rs17249437**T* allele ($p = 0.02$; OR = 2.28; CI 95% 1.14–4.58) and 33.33 % for rs17249437**TT* genotype ($p = 0.02$; OR = 2.83; CI 95% 1.18–6.80).

The study results of the *ARG2* polymorphism rs3742879 in children with asthma and individuals of the control group from the Republic of Bashkortostan are presented in Table 2. The rs3742879**G* allele is less common in all ethnic groups, it was revealed with a *frequency* of 30.67 % in Russians, 26.22 % in Tatars and 29.17 % in Bashkirs control groups. The association analysis of the *ARG2* polymorphism rs3742879 with asthma in individuals of different ethnic origin did not reveal statistically significant differences between groups of patients and controls ($p > 0.05$). A comparative analysis of allele and genotype frequencies of the rs3742879 polymorphism in asthma patients with different spirometry measures revealed that the rs3742879**GG* genotype was significantly more frequently (25.81 %) in Russians with significant decrease of FEV1 compared to the control group (9.33 %, $p = 0.03$; OR = 3.38; CI 95% 1.1–10.35).

The study of the *ARG2* polymorphism rs7140310 did not identify statistically significant differences in the allele and genotype frequency distributions between asthma patients and controls of different ethnicity ($p > 0.05$). The minor allele frequencies (MAF) in control groups were as follows: 14.67 % in Russians, 19.28 % in Tatars, 18.06 % in Bashkirs.

The analysis of rs17249437, rs3742879, rs7140310 polymorphisms of the *ARG2* gene in samples of different ethnicity showed significant linkage disequilibrium between rs17249437 and rs3742879 polymorphisms (in Russians $D' = 0.76$, in Tatars $D' = 0.85$, in Bashkirs $D' = 0.9$) in all studied groups. Haplotype analysis of *ARG2* gene polymorphisms did not find statistically significant differences in haplotype frequencies between asthma patients and the control group ($p > 0.05$).

Discussion

Insufficient control of inflammation in respiratory tract at asthma leads to the disease progression, contributes to increasing the number of severe forms, deaths, and disabilities of patients. Currently, highly effective drugs have been developed and available, many significant mechanisms of asthma pathogenesis have been discovered, but the problem of insufficient asthma control remains one of the most important public health problems. Many studies provide evidence of interethnic differences in genetic markers for the asthma development and

for drug susceptibility in different individuals (Martinez et al., 1997; Litonjua et al., 2008; Poon et al., 2008; Vonk et al., 2010; Kim et al., 2011; Batozhargalova et al., 2017; Scaparrotta et al., 2019). An association of the rs1042713**A* allele of the *ADRB2* gene with moderate reduction of FEV1 in asthma patients from the Republic of Bashkortostan was found in our earlier study (Fedorova et al., 2013). In this paper, we analyzed associations of arginase *ARG1* (rs2781667) and *ARG2* (rs17249437, rs3742879, rs7140310) gene polymorphisms with asthma development and course and with sensitivity to therapy in patients.

Arginase is an enzyme that catalyzes the hydrolysis of L-arginine to produce ornithine and urea (Dimitriades et al., 2014). Two isoforms of arginase (types I and II) are encoded by *ARG1* and *ARG2* genes (Vonk et al., 2010). Allergic inflammation causes a decrease in the total amount of NO and an increase in the production of pro-contact and pro-inflammatory peroxynitrite ($ONOO^-$), in particular iNOS, which leads to obstruction, inflammation and increase in airway hyperreactivity. Moreover, allergic asthma under the influence of Th2-cytokines (IL-4, IL-13) and TGF-β increases the arginase expression, which raises the L-ornithine, polyamines and L-proline production, which participates in airway remodeling, by inducing cell proliferation, and enhanced collagen production and fibrosis (see the Figure) (Meurs et al., 2019).

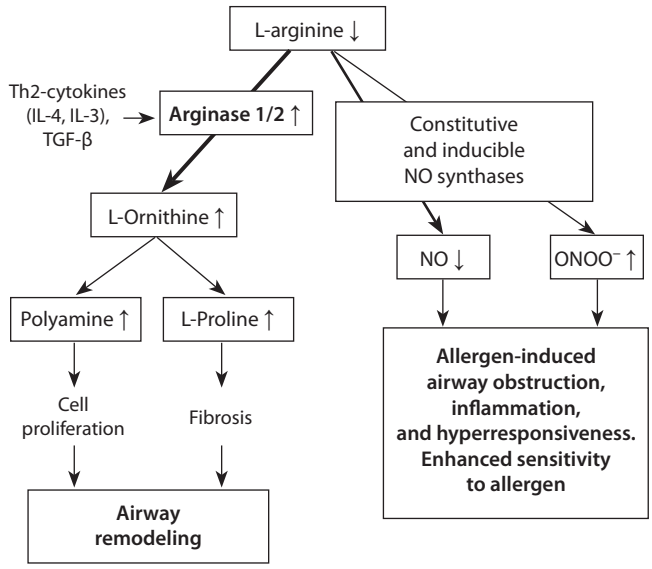

Pathways of arginine metabolism and their relationship to allergen-induced airway obstruction, airway inflammation, airway hyperresponsiveness, airway remodeling, and enhanced allergen sensitivity (Meurs et al., 2019).

This research revealed that the rs2781667**C* allele of the *ARG1* gene is associated with asthma in Tatars. Comparative analysis of qualitative traits detected higher IgE values in Russian patients with the rs2781667**CC* genotype compared to children bearing the rs2781667**CT* genotype. According to literature, the association of *ARG1* gene polymorphisms with the effectiveness of asthma therapy was first established by Litonjua A. et al. in asthma children of European origin treated with beta-2-agonists. The authors found a significant association of the rs2781659**G* allele of the *ARG1* gene with a more pronounced bronchodilatation response, and the *ARG1* gene was proposed as a possible risk marker to determine the effectiveness of asthma therapy (Litonjua et al., 2008). Vonk et al. (2010) found a significant decrease of bronchodilatation response to beta-2-agonists in asthma patients from Netherlands with the rs2781667**TT* genotype of the *ARG1* gene. At the same time, inhaled glucocorticosteroids slowed down the annual FEV1 decline, which was significantly less effective in homozygote carriers of the *C* allele at rs2781667 polymorphism in the *ARG1* gene (Vonk et al., 2010). An association of the rs2781666**T* allele and *CT* haplotype (rs60389358, rs2781666) of the *ARG1* gene with asthma and a considerably higher level of serum arginase was established in asthma patients from India (Donthi et al., 2018). On the contrary, some studies did not detect a significant association of *ARG1* gene polymorphisms with the efficacy of asthma therapies (Almomani et al., 2019; Scaparrotta et al., 2019). Together, this results and literature data confirm that *ARG1* gene allelic variants can contribute to asthma pathogenesis and the effectiveness of disease therapy.

In the present study associations of rs17249437**TT* and rs3742879**GG* genotypes of the *ARG2* gene with reduced spirometry values (FEV1, MEF25), of the rs17249437**T* allele and the rs17249437**TT* genotype of the *ARG2* gene with partially controlled and uncontrolled asthma were found in patients of Russian and Tatar ethnicity. Contrary, Vonk et al. revealed associations of the rs17249437**T* allele, rs3742879**G* allele and rs7140310**TT* genotype with higher FEV1 in adult asthma patients from Netherlands. It was found association of the rs3742879**AA* genotype with increased bronchial hyperresponsiveness (Vonk et al., 2010). In addition, our findings are partially inconsistent with studies Batozhargalova et al., that did not find an association of a combination of NOS2A*(CCTTTT)nS/L and rs3742879**AA* genotypes of the *ARG2* gene with asthma in girls from Russia (Batozhargalova et al., 2017). Salam et al. in the study of *ARG2* gene polymorphisms found an association of the rs3742879**G* allele in the haplotype structure (TAGTCATGC, rs12885261, rs7144243, rs3759757, rs4902501, rs7156352, rs4902503, rs7140310, rs742869, rs3742879, rs10483801) with asthma in patients of European origin (Salam et al., 2009). Allelic variants of the *ARG2* gene specifically in the haplotype structure might represent an important risk factor of asthma development and progression. In our study of *ARG2* gene polymorphisms in samples of different ethnicity, we found a significant linkage disequilibrium between rs17249437 and rs3742879 polymorphisms in all studied groups. Haplotype analysis did not reveal any significant associations of studied *ARG2* gene polymorphisms, which is probably due to the small number of compared groups.

Conclusion

Thus, an association study of polymorphic variants of *ARG1* and *ARG2* genes involved in beta-2-agonists metabolism was carried out in asthma patients and corresponding control groups from the Republic of Bashkortostan. It was found that the rs2781667**C* allele of the *ARG1* gene is a marker of increased risk of asthma development in Tatars. Higher

values of total IgE were revealed in Russian patients with the rs2781667**CC* genotype. It was found that rs17249437**TT* and rs3742879**GG* genotypes of the *ARG2* gene were associated with a decline in lung function (FEV1, MEF25) in Russian patients. In asthma patients of Russian and Tatar ethnicity association of the rs17249437**T* allele and the rs17249437**TT* genotype with partially controlled and uncontrolled asthma was established. The results obtained in the present study made it possible to thoroughly understand the molecular basis of BA pathogenesis and to identify genetic markers of efficacy of bronchodilator therapy in BA patients.

References

Almomani B.A., Al-Eitan L.N., Al-Sawalha N.A., Samrah S.M., Al-Quasmi M.N. Association of genetic variants with level of asthma control in the Arab population. *J. Asthma Allergy*. 2019; 12:35-42. DOI 10.2147/JAA.S186252.

Bateman E.D., Kornmann O., Schmidt P., Pivovarova A., Engel M., Fabbri L.M. Tiotropium is noninferior to salmeterol in maintaining improved lung function in B16-Arg/Arg patients with asthma. *J. Allergy Clin. Immunol.* 2011;128(2):315-322. DOI 10.1016/j.jaci. 2011.06.004.

Batozhargalova B.T., Mizernitski Y.L., Diakova S.E., Petrova N.V., Zinchenko R.A. Role of polymorphic variants of NO synthase and arginase genes in child bronchial asthma. *Meditsinskaya Genetika = Medical Genetics*. 2017;16(2):40-48. (in Russian)

Cloots R.H.E., Poynter M.E., Terwindt E., Lamers W.H., Köhler S.E. Hypoargininemia exacerbates airway hyperresponsiveness in a mouse model of asthma. *Respir. Res.* 2018;19:98. DOI 10.1186/s12931-018-0809-9.

Dimitriades V., Rodriguez P.C., Zabaleta J., Ochoa A.C. Arginase I levels are decreased in the plasma of pediatric patients with atopic dermatitis. *Ann. Allergy Asthma Immunol*. 2014;113(3): 271-275. DOI 10.1016/j.anai.2014.06.010.

Donthi S., Neela V.S.K., Gaddam S., Mohammed H.H., Ansari S.S., Valluri V.L., Sivasai K.S.R. Association of increased risk of asthma with elevated arginase & interleukin-13 levels in serum & rs2781666 G/T genotype of arginase I. *Indian J. Med. Res.* 2018;148(2):159-168. DOI 10.4103/ijmr.IJMR_379_16.

Drake K.A., Torgerson D.G., Gignoux C.R., Galanter J.M., Roth L.A., Huntsman S., Eng C., Oh S.S., Yee S.W., Lin L., Bustamante C.D., Moreno-Estrada A., Sandoval K., Davis A., Borrell L.N., Farber H.J., Kumar R., Avila P.C., Brigino-Buenaventura E., Chapela R., Ford J.G., Lenoir M.A., Lurmann F., Meade K., Serebrisky D., Thyne S., Rodríguez-Cintrón W., Sen S., Rodríguez-Santana J.R., Hernandez R.D., Giacomini K.M., Burchard E.G. A genome-wide association study of bronchodilator response in Latinos implicates rare variants. *J. Allergy Clin. Immunol*. 2014;133(2):370-378. DOI 10.1016/j. jaci.2013.06.043.

Duan Q.L., Du R., Lasky-Su J., Klanderman B.J., Partch A.B., Peters S.P., Irvin C.G., Hanrahan J.P., Lima J.J., Blake K.V., Liggett S.B., Litonjua A.A., Tantisira K.G. A polymorphism in the thyroid hormone receptor gene is associated with bronchodilator response in asthmatics. *Pharmacogenomics J.* 2013; 13(2):130-136. DOI 10.1038/tpj.2011.56.

Duan Q.L., Gaume B.R., Hawkins G.A., Himes B.E., Bleecker E.R., Klanderman B., Irvin C.G., Peters S.P., Meyers D.A., Hanrahan J.P., Lima J.J., Litonjua A.A., Tantisira K.G., Liggett S.B. Regulatory haplotypes in *ARG1* are associated with altered bronchodilator response. *Am. J. Respir. Crit. Care Med.* 2011; 183(4):449-454. DOI 10.1164/rccm.201005-0758OC.

Farzan N., Vijverberg S.J., Arets H.G., Raaijmakers J.A., Maitland-van der Zee A.H. Pharmacogenomics of inhaled corticosteroids and leukotriene modifiers: a systematic review. *Clin. Exp. Allergy*. 2017;47(2):271-293. DOI 10.1111/cea.12844.

Fedorova Yu.Yu., Karunas A.S., Murzina R.R., Mukhtarova L.A., Ramazanova N.N., Gimalova G.F., Gatiyatullin R.F., Zagidullin Sh.Z., Etkina E.I., Khusnutdinova E.K. Association study of the β2-adrenergic receptor gene polymorphisms with bronchial asthma in Russians. *Prakticheskaya Meditsina = Practical Medicine*. 2013;5(74):116-120. (in Russian)

Global Initiative for Asthma. Global strategy for asthma management and prevention. Updated 2018. Vancouver, USA GINA, 2018.

Kim S.H., Ye Y.M., Lee H.Y., Sin H.J., Park H.S. Combined pharmacogenetic effect of *ADCY9* and *ADRB2* gene polymorphisms on the bronchodilator response to inhaled combination therapy. *J. Clin. Pharm. Ther.* 2011;36(3):399-405. DOI 10.1111/j.1365-2710.2010. 01196.x.

Klement R.F., Zilber H.A. Functional Diagnostic Tests in Pulmonology: Guidelines. St. Petersburg, 1993. (in Russian)

Li H., Romieu I., Sienra-Monge J., Ramirez-Aguilar M., Estela del Rio-Navarro B., Kistner E.O., Gjessing H.K., Lara-Sanchez I. del C., Chiu G.Y., London S.J. Genetic polymorphisms in arginase I and II and childhood asthma and atopy. *J. Allergy Clin. Immunol*. 2006;117(1):119-126. DOI 10.1016/j.jaci.2005.09.026.

Litonjua A.A., Lasky-Su J., Schneiter K., Tantisira K.G., Lazarus R. *ARG1* is a novel bronchodilator response gene: screening and replication in four asthma cohorts. *Am. J. Respir. Crit. Care Med*. 2008;178(7):688-694. DOI 10.1164/rccm.200709-1363OC.

Martinez F.D., Graves P.E., Baldini M., Solomon S., Erickson R. Association between genetic polymorphisms of the beta-2 adrenoceptor and response to albuterol in children with and without a history of wheezing. *J. Clin. Invest.* 1997;100(12):3184-3188. DOI 10.1172/JCI119874.

Mathew C.G.P. The isolation of high molecular weight eucariotic DNA. In: Walker J.M. (Ed.). Methods in Molecular Biology. Vol. 2. Nucleic Acids. Humana Press, Clifton, New Jersey, 1984;31-34.

Meurs H., Zaagsma J., Maarsingh H., Duin M. Recent patents in allergy/immunology: use of arginase inhibitors in the treatment of asthma and allergic rhinitis. *Allergy*. 2019;74(6):1206-1208. DOI 10.1111/all.13770.

National Program "Bronchial Asthma in Children. Treatment Strategy and Prevention". 4th edn. Moscow: Original-Maket Publ., 2012. (in Russian)

National Program "Bronchial Asthma in Children. Treatment Strategy and Prevention". 5th edn. Moscow: Original-Maket Publ., 2017. (in Russian)

Poon A.H., Tantisira K.G., Litonjua A.A., Lazarus R., Xu J., Lasky-Su J., Lima J.J., Irvin C.G., Hanrahan J.P., Lange C., Weiss S.T. Association of corticotropin-releasing hormone receptor-2 genetic variants with acute bronchodilator response in asthma. *Pharmacogenet. Genomics*. 2008;18(5):373-382. DOI 10.1097/ FPC.0b013e 3282fa760a.

Said A.M.A., Naqshbandi A.A.A., Amin Y.K., Ali R.J. Association of the arginase I with bronchial asthma. *J. Univ. Babylon Pure Appl. Sci*. 2019;27(2):238-243. DOI 10.29196/jubpas. v27i2.2092.

Salam M.T., Islam T., Gauderman W.J., Gilliland F.D. Roles of arginase variants, atopy, and ozone in childhood asthma. *J. Allergy Clin. Immunol*. 2009;123:596-602. DOI 10.1016/j.jaci.2008.12.020.

Scaparrotta A., Franzago M., Loredana Marcovecchio M., Pillo S.D., Chiarelli F., Mohn A., Stuppia L. Role of *THRB*, *ARG1*, and *ADRB2* genetic variants on bronchodilators response in asthmatic children. *J. Aerosol. Med. Pulm. Drug Deliv*. 2019;32:1-10. DOI 10.1089/jamp.2018.1493.

Vonk J.M., Postma D.S., Maarsingh H., Bruinenberg M., Koppelman G.H., Meurs H. Arginase 1 and arginase 2 variations associate with asthma, asthma severity and β2 agonist and steroid response. *Pharmacogenet. Genomics*. 2010;20(3):179-186. DOI 10.1097/FPC.0b013e328336c7fd.

ORCID ID

O.N. Savelieva orcid.org/0000-0002-9690-1481
A.S. Karunas orcid.org/0000-0002-2570-0789
Yu.Yu. Fedorova orcid.org/0000-0002-9344-828X
E.I. Etkina orcid.org/0000-0003-1371-7927
E.K. Khusnutdinova orcid.org/0000-0003-2987-3334

Acknowledgements. The study was carried out with the financial support of the Russian Foundation for Basic Research (grant No. 17-04-02195 and No. 19-315-90055), state assignment of the Ministry of Education and Science of the Russian Federation (No. AAA-A16-116020350032-1). DNA samples were used from the "Collection of human biomaterials IBG UFRC RAS", supported by the Program of bioresource collections of the FASO of Russia (agreement No. 007-030164/2).

Conflict of interest. The authors declare no conflict of interest.

Received November 06, 2019. Revised March 18, 2020. Accepted April 29, 2020.

Вавиловский журнал генетики и селекции. 2020;24(4):399-406
DOI 10.18699/VJ20.632

Single nucleotide polymorphism and expression of genes for immune competent cell proliferation and differentiation in radiation-exposed individuals

E.A. Blinova[1, 2] ✉, V.S. Nikiforov[1], M.A. Yanishevskaya[1, 2], A.A. Akleyev[1, 3]

[1] Urals Research Center for Radiation Medicine, Chelyabinsk, Russia
[2] Chelyabinsk State University, Chelyabinsk, Russia
[3] South-Urals State Medical University of the Ministry of Healthcare of Russian Federation, Chelyabinsk, Russia
✉ e-mail: blinova@urcrm.ru

Abstract. It is known that ionizing radiation influences the expression of the genes that play a key role in the mechanisms of maintaining the stability of cellular homeostasis. As a rule, changes in the transcriptome of an exposed cell occur within the first 24 hours following radiation exposure. And it predetermines early response in the case of genome damage. Later on modulations in gene transcription activity are also possible and could result in a carcinogenic effect. However, in order to find the role of exogenous factors (ionizing radiation), it is also necessary to take into account the contribution of endogenous factors that are able to modify gene transcription activity. This is especially important for long after the onset of radiation exposure. Single nucleotide polymorphisms located in regulatory regions of the genes may belong to this group of factors. The objective of the current study was to analyze the influence of ionizing radiation on the transcription activity of the *STAT3*, *GATA3*, *NFkB1*, *PADI4* genes, which regulate proliferation and differentiation of immune competent human cells; and to assess the potential influence of single nucleotide polymorphisms located in regulatory regions of the genes on the amount of mRNA. The study involved people who had been chronically exposed due to releases of radioactive waste into the Techa River. It was observed that 60 years after the onset of radiation exposure changes in the transcription activity of the *NFkB1* and *PADI4* genes were registered in people with cumulative doses to RBM within the range 78–3510 mGy. In people who had been chronically exposed, the effect of allelic variations in rs1053023, rs4143094, rs28362491, rs874881 on the level of mRNAs of the *STAT3*, *GATA3*, *PADI4*, *NFkB1* genes has not been established.
Key words: exposed persons; mRNA; single-nucleotide polymorphism; real-time PCR; modification of gene expression.

For citation: Blinova E.A., Nikiforov V.S., Yanishevskaya M.A., Akleyev A.A. Single nucleotide polymorphism and expression of genes for immune competent cell proliferation and differentiation in radiation-exposed individuals. *Vavilovskii Zhurnal Genetiki i Selektsii = Vavilov Journal of Genetics and Breeding*. 2020;24(4):399-406. DOI 10.18699/VJ20.632

Полиморфизм и экспрессия генов пролиферации и дифференцировки иммунокомпетентных клеток у лиц, подвергшихся радиационному воздействию

Е.А. Блинова[1, 2] ✉, В.С. Никифоров[1], М.А. Янишевская[1, 2], А.А. Аклеев[1, 3]

[1] Уральский научно-практический центр радиационной медицины Федерального медико-биологического агентства России, Челябинск, Россия
[2] Челябинский государственный университет, Челябинск, Россия
[3] Южно-Уральский государственный медицинский университет Министерства здравоохранения Российской Федерации, Челябинск, Россия
✉ e-mail: blinova@urcrm.ru

Аннотация. Известно, что ионизирующее излучение влияет на экспрессию генов, выполняющих ключевую роль в механизмах поддержания стабильности клеточного гомеостаза. Как правило, изменение в транскриптоме облученной клетки происходит в первые часы и сутки после радиационного воздействия, что обусловливает ее ранний ответ при повреждении генома. В отдаленном периоде также возможны модуляции в транскрипционной активности генов, приводящие к развитию канцерогенных эффектов облучения. Однако для установления роли экзогенных факторов (ионизирующего излучения) в модификации экспрессии генов клеточного гомеостаза необходимо учитывать и роль эндогенных факторов, способных модифицировать транскрипционную активность генов, что особенно актуально в отдаленном периоде после начала радиационного воздействия. К таким факторам могут относиться полиморфные варианты генов, расположенные в регуляторных областях. Цель настоящего исследования – анализ влияния ионизирующего излучения в отдаленном периоде на содержание мРНК генов *STAT3*, *GATA3*, *NFkB1*, *PADI4*, регулирующих процессы пролиферации и дифференцировки иммунокомпетентных клеток человека, а также оценка связи аллельных вариаций rs1053023,

rs4143094, rs28362491, rs874881 на количество мРНК генов *STAT3*, *GATA3*, *PADI4*, *NFkB1*. Исследование проведено у лиц, подвергшихся аварийному хроническому радиационному воздействию в результате сбросов радиоактивных отходов в реку Течу. Установлено, что спустя 60 лет после начала радиационного воздействия у лиц, имеющих кумулятивные дозы облучения ККМ в диапазоне от 78 до 3510 мГр, регистрируются изменения в транскрипционной активности генов *NFkB1* и *PADI4*. Не выявлено влияния аллельных вариаций rs1053023, rs4143094, rs28362491, rs874881 на количество мРНК генов *STAT3*, *GATA3*, *PADI4*, *NFkB1* у облученных лиц.
Ключевые слова: облученные лица; мРНК; однонуклеотидный полиморфизм; ПЦР в реальном времени; модификация экспрессии генов.

Introduction

Ionizing radiation induces changes in transcription activity of the genes that have a pivotal role in mechanisms of maintaining the stability of cellular homeostasis. However, the profile of gene expression differs considerably under exposure at low to high doses (Ding et al., 2005). It has been shown that exposure at low to medium doses leads to increase not only in the expression of genes involved in the response to DNA damage, but also genes of apoptosis activation (Azimian et al., 2015), cytoskeleton elements and transport of secretory vesicles (Woloschak et al., 1990), cell proliferation and differentiation (Amundson et al., 2003), as well as genes of lymphocyte activation, cytokine and chemokine expression (Wyrobek et al., 2011). It is well-known that changes in the transcriptome of an exposed cell occur within the first hours and days following the radiation exposure. It predetermines the early response in case of genome damage.

Aberrant expression of a number of genes is registered in the long-term period as well. The studies of (Fachin et al., 2009; Ilienko, Bazyka, 2016) show changes in the transcription activity of the genes, the products of which regulate intracellular transport, DNA reparation, immune response of cells 10–20 years after the onset of radiation exposure. Earlier on we have also discovered that people who have been chronically exposed at medium to high doses (0.1–4.5 Gy) as compared to unexposed individuals demonstrate a decrease in the amount of mRNA of the anti-apoptotic *BCL2* gene more than 60 years after the radiation exposure (Nikiforov et al., 2019).

At the molecular level changes in the expression of genes that code various enzymes and regulatory proteins may lead to changes in the number of reactive oxygen intermediate, disbalance of the pro- and anti-inflammatory cytokines and chemokines (Barnes, Karin, 1997). However, it should be taken into account that besides the exogenous environmental factors, including ionizing radiation, the level of gene transcription activity could be influenced by endogenous (genetic) factors. In this respect, to define the role of ionizing radiation in the changes of gene transcription activity in the long-term period it is necessary to take account of genetic component.

In recent decades single nucleotide polymorphism (SNP) has been extensively studied as a marker associated with various diseases (Visscher et al., 2012; Tan, 2017). The mechanism allowing the polymorphism to influence the phenotype is determined first and foremost by the functional role of the DNA sequence where it is located. SNP can influence both the structure and activity of the gene product as well as its amount.

Of all the SNP located in the coding sequences of a gene (exons), about 58 % are non-synonymous and could affect enzymatic activity of a protein, its stability, ligand binding to a certain protein. They may lead to changes in the protein folding process and thus result in alterations of the formation of its quaternary structure (Bhattacharya et al., 2017). Other SNP are synonymous and could modify the protein expression level by influencing the secondary structure of a mature mRNA (Robert, Pelletier, 2018), promote changes of the mRNA-mediated regulation of gene expression (Brest et al., 2011). Besides changing the expression level, synonymous SNP could influence mRNA stability and splicing (Wang et al., 2015).

The influence on the phenotype of SNP located in introns is largely predetermined by modifications in various regulatory elements (Shastry, 2009). Several possible mechanisms of the influence on the phenotype of SNP located in introns are known. Among these are changes in the cis-regulatory elements – enhancers and silencers modules leading to changes in trans-factors binding to these elements and to the corresponding variation of the expression level (Campbell et al., 2016), as well as other possible mechanisms of the influence of intron SNP on the level of gene expression, for example due to formation of additional chromatin loops (Wright et al., 2010).

The objective of the present study has been the analysis of the effect of ionizing radiation in the long-term period on the mRNA level of *STAT3*, *GATA3*, *NFkB1*, *PADI4* genes that regulate the process of proliferation and differentiation of immune competent human cells, as well as the assessment of the association of alleles variation rs1053023, rs4143094, rs28362491, rs874881 with the amount of mRNA of *STAT3*, *GATA3*, *PADI4*, *NFkB1* genes.

Materials and methods

The study involved persons who had been chronically exposed due to releases of liquid radioactive waste of Mayak Production Association into the Techa River in 1949–1956. Residents of communities along the Techa River had combined external and internal exposure. Bottom sediments and floodplain soils contaminated with radionuclides were the sources of external γ-exposure. Internal exposure was due to radionuclide intake with river water and locally produced foodstuffs. The main dose-forming radionuclide was ^{90}Sr. A β-emitter, it accumulated in bone tissue and for a long time affected the red bone marrow (RBM) (Akleyev A.V. (Ed.) The Consequences of Radioactive Pollution of the Techa River, 2016). Earlier on, increased risks of leukemia (Schüz et al., 2016) and malignant tumor (Krestinina et al., 2017) development have been proved in the cohort of exposed residents of the Techa River communities.

The study engaged 309 people with dose to RBM reconstructed with the Techa River Dosimetry System 2016 (TRDS

Table 1. Characteristics of the studied individuals

Parameter		Comparison group *n* = 146	Exposed *in utero* *n* = 48	Exposed postnatally *n* = 115
Ethnic group, % (*n*)	Slavs	66.4 (97)	50 (24)	52.2 (60)
	Tartars and Bashkirs	33.6 (49)	50 (24)	47.8 (55)
Sex, % (*n*)	Males	30.8 (45)	39.6 (19)	37.4 (43)
	Females	69.2 (101)	60.4 (29)	62.6 (72)
Mean age, years, M ± SE		62.4 ± 0.5 (57–81)[1]	65.1 ± 0.3 (60–68)	73.2 ± 0.8 (65–86)
Cumulative exposure dose to RBM, mGy, M ± SE		16 ± 1 (0–68)[2]	506 ± 58 (78–1721)	799 ± 63 (80–3510)
Cumulative dose of *in utero* exposure to RBM, mGy, M ± SE		0	85 ± 12 (0–358)	0

Note. RBM – red bone marrow; M – mean; SE – standard error; *n* – number of people; [1] – age range; [2] – range of individual dose values.

2016) (Degteva et al., 2019). The main group of exposed people included 163 persons with individual accumulated doses to RBM within the dose range 78–3510 mGy. For 48 persons in this group chronic exposure began during the period of their *in utero* development. Mean *in utero* dose to RBM for these people was 85 ± 12 mGy, mean postnatal dose to RBM was 506 ± 58 mGy. Another study group consisted of 115 people born before the beginning of radioactive contamination of the Techa River. Mean postnatal dose to RBM in this group was 799 ± 63 mGy. Comparison group included 146 people living in similar socio-economic conditions but with exposure dose rate to RBM not exceeding 1 mGy/year and dose accumulated over a lifetime < 70 mGy in accordance with paragraph 3.1.4 of Radiation standards 99/2009 (Sanitary Regulations and Standards SanPiN 2.6.1.2523-09). The studied group consisted of people of both sexes belonging to two ethnic groups: (1) Tartars and Bashkirs, (2) Slavs (Table 1).

Transcription activity of genes in exposed individuals could be influenced by various factors. In this respect the following persons were excluded from the study: those who had autoimmune diseases, cancer, chronic inflammatory diseases in the exacerbation phase, those who were taking cytostatic drugs and antibiotics, those who underwent diagnostic exposure during last 6 months prior to the blood sampling, as well as those who had contact with genotoxic (chemical) agents as part of their professional activity. By the time of blood sampling all the studied individuals had undergone scheduled examination in the Urals Research Center for Radiation Medicine Clinical department within the framework of the program of healthcare provision to the exposed population (over the period 2016–2019). According to international norms in force all the examined subjects gave written informed consent to participate in the study. Research has been approved by the Institutional Review Board of the Urals Research Center for Radiation Medicine of FMBA of Russia.

Transcription activity of *STAT3*, *GATA3*, *NFkB1* and *PADI4* genes was studied with real-time PCR. In 2016–2019 venous blood samples from patients were collected directly into Tempus Blood RNA Collection Tubes (Applied Biosystem, USA). Native RNA was isolated immediately after stabilization or after the specimens had been stored at –80 °C.

RNA extraction has been performed with GeneJET Whole Blood RNA Purification Kit (Thermo Scientific™, USA) according to the protocol provided by the manufacturer. Information on concentration and purity of extracted RNA samples was obtained with spectrophotometer NanoDrop 2000C (Thermo Scientific, USA). A 260/280 ratio for the purified RNA extracted from all the blood samples was 2.1 ± 0.02.

Reverse transcription (RT) to synthesize complementary DNA (cDNA) was performed using High-Capacity cDNA Reverse Transcription Kit (Applied Biosystem, USA) that contains recombinant reverse transcriptase M-MLV (Moloney Murine Leukemia Virus), random hexa-nano-nucleotide primers, dNTP mixture and OT buffer. According to the manufacturer's protocol, to synthesize cDNA we used 10 µl of total RNA.

The analysis of mRNA amount was performed using quantitative polymerase chain reaction (real-time PCR) with commercial kits TaqMan (Applied Biosystem, USA). Characteristics of primers and probes used to assess mRNA expression is given in Table 2.

To obtain statistically significant results each reaction was performed three times with negative control using StepOnePlus™ Real-Time PCR (Applied Biosystem, USA). Temperature requirements: 1 cycle of preliminary denaturation at 95 °C/10 min, then 50 cycles at 95 °C/15 s, 60 °C/1 min. The data were analyzed using the method of ΔΔCt with normalization to "housekeeping" *B2M* gene expression in every sample.

To be included into the study, SNP were selected based on the analysis of internet databases of genome-wide studies (www.hapmap.ncbi.nlm.nih.gov) and database of SNP (www.snpedia.com). The selection criteria were SNP location and the potential of SNP to influence gene transcription activity. Characteristics of the polymorphic regions is provided in Table 3.

To perform genotyping we used DNA extracted from blood samples stored at –80 °C. DNA extraction from whole blood was done using the ExtraPhen kit (ATG-Biotech, Russia). Quantitative and qualitative assessment of the DNA samples after extraction was carried out with the help of spectrophotometer NanoDrop 2000C (Termo Scientific, USA).

Table 2. Characteristics of primers and probes to determine the content of mRNA

Gene	Primers and probes (length, bps)	Tm	GC,%	Amplicon size, bps	References to targets (transcripts) in NCBI
STAT3	F: Exon-exon junctions – ex13-ex14 (20)	51.71	55.00	70	NM_003150.3
	R: Exon-exon junctions – ex14-ex15 (20)	51.96	55.00		
	Probe: Exon – ex14 (20)	52.81	56.01		
GATA3	F: Exon-exon junctions – ex3-ex4 (18)	47.4	61.1	86	NM_001002295.1
	R: Exon-exon junctions – ex4-ex5 (18)	47.4	61.1		
	Probe: Exon – ex4 (20)	50.5	60.00		
PADI4	F: Exon-exon junctions – ex5-ex6 (20)	52.90	55.00	107	NM_012387.2
	R: Exon-exon junctions – ex6-ex7 (20)	51.7	55.00		
	Probe: Exon – ex6 (20)	52.35	55.00		
NFkB1	F: Exon-exon junctions – ex22-ex23 (21)	51.60	42.90	66	NM_001165412.1
	R: Exon-exon junctions – ex23-ex24 (21)	51.50	42.90		
	Probe: Exon – ex22 (23)	52.00	44.10		
B2M	F: Exon-exon junctions – ex1-ex2 (22)	53.7	59.00	64	NM_004048.2
	R: Exon-exon junctions – ex2-ex3 (23)	53.4	45.5		
	Probe: Exon – ex2 (23)	53.9	46.00		

Note. F – forward primer; R – revers primer; Tm – melting temperature; GC,% – GC content.

Table 3. Characteristics of the polymorphic regions of *STAT3*, *GATA3*, *NFkB1*, *PADI4* genes

Gene	Polymorphism	Alleles	Location[1]	Position[1]
STAT3	rs1053023	T/C	3'UTR	chr17:42313598
GATA3	rs4143094	A/C	Intron	chr10:8047173
NFkB1	rs28362491	Del/ATTG	Intron	chr4:102500998-102501005
PADI4	rs874881	G/C	5'UTR	chr1:17334004

Note. [1] – According to whole genome database 1000Genom, version GRCh38.p12 (www.ncbi.nlm.nih.gov).

Specimen genotyping and detection of results were performed using the real-time PCR on Applied Biosystems StepOnePlus (USA) with the reagent kit that contained primers and probes for genotyping (TestGene, Russia)

Characteristics of primers and probes for genotyping is given in Table 4.

Amplification was carried out as directed by the manufacturer's user's manual guide for a particular kit. Deionized water was used as negative control.

Statistical processing of data was performed using Statistica 10.0 and WinPepi for Windows version 11.65 software packages. Kolmogorov–Smirnov's test was used to check the normality of distribution of the mRNA amount. The obtained distribution of values differed from normal one, that is why Mann–Whitney test was applied. Genotype frequencies between ethnic groups were compared using Pearson's χ^2 test. Gene expression was assessed with $p = 0.05$. The significance level $p = 0.01$ was used in assessment of the association between SNP and gene expression.

Results

Quantitative analysis of mRNA in all the exposed individuals testified to a decrease in the *NFkB1* mRNA and increase in *PADI4* mRNA relative to the comparison group. Similar patterns were registered in the group of people exposed both *in utero* and postnatally as well as in the group of people exposed only postnatally (Table 5).

No statistically significant differences were revealed in comparative analysis of median values of mRNA of the studied genes in representatives of different ethnic groups (Tartars/Bashkirs and Slavs) in the group of exposed individuals and in the comparison group (Table 6).

Table 7 presents the distribution of frequencies of polymorphic loci of the studied genes in exposed people.

Table 4. Primer and probe sequences to perform genotyping

Gene, polymorphism	Primers and probes (length, bps)
STAT3 rs1053023	F: 5′-GGTCTTAACTCTGATTGTAG-3′ (20)
	R: 5′-CAGCTTATAAACCACCTTATAG-3′ (22)
	Probe: 5′-FAM-tcttTaaTggGccac-BHQ-1-3′ (15)
	Probe: 5′-VIC-tcttTaaCggGccac-BHQ-2-3′ (15)
GATA3 rs4143094	F: 5′-GCAGAAGATAAACGAGGTG-3′ (19)
	F: 5′-GACGCAAACTGCTTTAAC-3′ (18)
	Probe: 5′-FAM-caaccCaaAagAaaaccc-BHQ-1-3′ (18)
	Probe: 5′-VIC-caaccCaaCagAaaaccc-BHQ-2-3′ (18)
NFkB1 rs28362491	F: 5′-TGGACCGCATGACTCTATC-3′ (19)
	R: 5′-GCTCTGGCTTCCTAGCAG-3′ (18)
	Probe: 5′-FAM-ccccgacCattgGgc-BHQ-1-3′ (15)
	Probe: 5′-VIC-cccgacCattgattgGgc-BHQ-2-3′ (18)
PADI4 rs874881	F: 5′-GGTGTTTGTTGAATGACTAA-3′ (20)
	R: 5′-CACTGACTAAGGATGGAATA-3′ (20)
	Probe: 5′-FAM-tcaccgGggTggg-BHQ-1-3′ (13)
	Probe: 5′-VIC-tcaccgCggTggg-BHQ-2-3′ (13)

Note. F – forward primer; R – revers primer.

In ethnic groups of Slavs and Tartars/Bashkirs the genotype distribution for all the polymorphic regions corresponded to the expected distribution in accordance with the Hardy–Weinberg law, except for the polymorphic region rs4143094 of *GATA3* gene in the group of Tartars/Bashkirs. Moreover, distribution of alleles and genotypes did not differ between the groups of Slavs and Tartars/Bashkirs.

No association of allele variations rs1053023, rs4143094, rs28362491, rs874881 and mRNA amount of *STAT3*, *GATA3*, *PADI4*, *NFkB1* genes was established in the group of Slavs, group of Tartars and Bashkirs and in the pooled population (Table 8).

Discussion

We have stated that 60 years after the onset of radiation exposure people with cumulative doses to RBM in the range 78–3510 mGy showed changes in the transcription activity of *NFkB1* and *PADI4* genes as compared to the comparison group (with doses to RBM < 70mGy). Changes in the transcription activity of genes of immune surveillance have been earlier registered in other groups of exposed individuals. For example, excessive expression of immune surveillance and apoptosis genes was observed in persons with cumulative doses of 0.1–113.35 mGy due to trans-uranium radionuclides five years after the onset of exposure (Bazyka et al., 2018). Findings of the study of the gene expression in the Chernobyl Nuclear Plant clean-up workers also demonstrate modulation of activity of more than 100 genes, including genes of cytokines and immune response, in persons with exposure doses > 400 mGy 11–12 years after the onset of radiation exposure (Albanese et al., 2007).

Transcription factors are often used as candidate markers of various pathological states of immune system as their work provides plasticity of immune-competent cell population that is observed in autoimmune diseases or malignant neoplasms. For example, in different types of cancer one may observe decrease in the functional abilities of $CD8^+$-cells, and T-cells of effector memory (T_{EM}-cells) start to predominate phenotypically. But at the same time increase in the number of T-cells of central memory (T_{CM}) and short-lived effector cells (T_{EMRA}) increases the activity of anti-tumor immunity (DuPage, Bluestone, 2016).

Earlier on, we have shown the correlation relationship between expression of *NFkB1* and *PADI4* genes and parameters of system immunity in exposed individuals in the group of exposed residents of the Techa riverside communities. In particular, mRNA amount correlated with the absolute number of B-lymphocytes and levels of serum IgG and IgM, and amount of *PADI4* mRNA correlated with the intensity of intracellular oxygen-dependent metabolism of neutrophils (Akleyev et al., 2019). Apparently, changes in the transcription activity of *NFkB1* and *PADI4* genes could contribute to the changes in the work of immune system.

Table 5. Amount of mRNA (r. u.) of the studied genes in the peripheral blood cells of chronically exposed individuals

Gene	Comparison group	All exposed people	Individuals exposed only postnatally	Individuals exposed both *in utero* and postnatally
			Median 25–75 %	
STAT3	0.95* (0.57–1.43)**	0.90 (0.62–1.46)	0.92 (0.61–1.46)	0.88 (0.71–1.46)
GATA3	0.86 (0.58–1.38)	0.85 (0.61–1.41)	0.89 (0.62–1.49)	0.82 (0.61–1.15)
NFkB1	1.05 (0.57–1.66)	0.69 (0.46–1.31) $p = 0.0005$	0.71 (0.45–1.36) $p = 0.004$	0.69 (0.50–1.07) $p = 0.003$
PADI4	0.71 (0.43–1.12)	0.83 (0.54–1.89) $p = 0.003$	0.78 (0.54–1.81) $p = 0.02$	1.05 (0.58–2.08) $p = 0.006$

Note. Hereinafter: * – median; ** – 25 % and 75 % quartiles; *p* – significance level of differences in parameters between the group of exposed individuals and comparison group.

Table 6. Amount of mRNA (r. u.) of the studied genes depending on the ethnicity of the studied individuals

Gene	Comparison group		Exposed individuals	
	Slavs	Tartars/Bashkirs	Slavs	Tartars/Bashkirs
PADI4	0.71 (0.42–1.11)	0.71 (0.49–1.13)	0.83 (0.46–1.72)	0.88 (0.59–2.25)
NFkB1	0.99 (0.57–1.50)	1.17 (0.61–1.85)	0.69 (0.49 –1.20)	0.70 (0.44 –1.38)
STAT3	0.97 (0.56–1.40)	0.93 (0.63–1.47)	0.84 (0.59–1.34)	0.98 (0.70–1.55)
GATA3	0.89 (0.61–1.37)	0.85 (0.51–1.57)	0.82 (0.57–1.21)	0.88 (0.65–1.47)

Table 7. Distribution of genotypes by the studied polymorphic loci in the group of exposed individuals

Gene polymorphism	Parameter	Ethnic group		*p*-value
		Slavs	Tartars/ Bashkirs	
STAT3 rs1053023	The allele frequency, % (*N*)			
	Allele T	81 (151)	87 (120)	$p = 0.165$
	Allele C	19 (35)	13 (18)	
	The genotype frequency, % (*N*)			
	T/T	69 (64)	77 (53)	$p = 0.426$
	T/C	25 (23)	20 (14)	
	C/C	6 (6)	3 (2)	
	pE_{H-W}	0.08	0.31	
GATA3 rs4143094	The allele frequency, % (*N*)			
	Allele C	73 (130)	80 (107)	$p = 0.164$
	Allele A	27 (48)	20 (27)	
	The genotype frequency, % (*N*)			
	C/C	53 (47)	69 (46)	$p = 0.059$
	C/A	40 (36)	22 (15)	
	A/A	7 (6)	9 (6)	
	pE_{H-W}	1.00	0.02	
NFkB1 rs28362491	The allele frequency, % (*N*)			
	Allele Del	52 (92)	48 (62)	$p = 0.489$
	Allele ATTG	48 (86)	52 (68)	
	The genotype frequency, % (*N*)			
	Del/Del	25 (22)	20 (13)	$p = 0.756$
	Del/ATTG	54 (48)	55 (36)	
	ATTG/ATTG	21 (19)	25 (16)	
	pE_{H-W}	0.53	0.46	
PADI4 rs874881	The allele frequency, % (*N*)			
	Allele G	47 (84)	41 (43)	$p = 0.052$
	Allele C	53 (94)	59 (77)	
	The genotype frequency, % (*N*)			
	G/G	21 (19)	15 (10)	$p = 0.519$
	G/C	52 (46)	51 (33)	
	C/C	27 (24)	34 (22)	
	pE_{H-W}	0.83	0.80	

Note. *p*-value – significance of difference of allele and genotype frequency between Slavs and Tartars/Bashkirs; pE_{H-W} – Hardy–Weinberg equilibrium.

Besides the influence of external factors, genetic component also plays certain role in transcription activity of genes. Specifically, SNP that are located in non-coding regions (enhancers, donors of splicing and acceptor sites of introns). Such SNP could influence the level of gene expression via changes in binding sites, formation of new sites, or changes in the degree of affinity of various transcription factors to certain sites of DNA binding. However, no association of allele variations rs1053023, rs4143094, rs28362491, rs874881 with the amount of mRNA of *STAT3*, *GATA3*, *PADI4*, *NFkB1* genes in exposed individuals have been established in the current study.

Conclusion

Thus, people who have been affected by accidental chronic exposure demonstrate decrease in the level of *NFkB1* mRNA and increase in the level of *PADI4* mRNA relative to the comparison group members. No influence of allele variations rs1053023, rs4143094, rs28362491, rs874881 on the level of mRNA of *STAT3*, *GATA3*, *PADI4*, *NFkB1* genes have been registered in exposed individuals.

In view of small number of people examined by the studied polymorphic regions the findings of the research are preliminary and require further checking with greater sampling size.

Table 8. Assessment of SNP influence on gene transcription activity in exposed people

Gene, polymorphism	Model	Genotype	Pooled population		Slavs		Tartars/Bashkirs	
			Number of mRNA, median 25–75 %	*p*	Number of mRNA, median 25–75 %	*p*	Number of mRNA, median 25–75 %	*p*
STAT3 rs1053023	Codominant	T/T (109/58/51) T/C (36/23/13) C/C (7/5/2)	0.95 (0.60–1.46) 1.08 (0.67–1.43) 0.84 (0.60–1.34)	0.46	1.02 (0.59–1.36) 0.96 (0.64–1.40) 1.04 (0.77–1.34)	0.87	0.93 (0.60–1.53) 1.25 (0.97–1.46) –	–
	Dominant	T/T (109/58/51) T/C-C/C (43/28/15)	0.95 (0.60–1.46) 1.04 (0.66–1.40)	0.79	1.02 (0.59–1.38) 0.96 (0.64–1.40)	0.85	0.93 (0.60–1.52) 1.17 (0.71–1.46)	0.28
	Recessive	T/T-T/C (145/81/64) C/C (7/5/2)	0.96 (0.62–1.46) 0.84 (0.60–1.34)	0.56	1.02 (0.62–1.39) 1.04 (0.77–1.34)	0.83	0.96 (0.69–1.49) –	–
GATA3 rs4143094	Codominant	C/C (109/58/51) A/C (49/35/14) A/A (13/6/7)	0.85 (0.65–1.16) 0.74 (0.59–1.38) 1.20 (0.44–1.49)	0.24	0.82 (0.64–1.09) 0.80 (0.61–1.54) 0.79 (0.36–2.03)	0.97	0.91 (0.66–1.60) 0.68 (0.46–0.74) 1.21 (0.67–1.49)	0.77
	Dominant	C/C (109/58/51) C/A-A/A (43/28/15)	0.85 (0.65–1.16) 0.76 (0.53–1.47)	0.59	0.82 (0.64–1.09) 0.80 (0.59–1.54)	0.44	0.91 (0.66–1.60) 0.69 (0.49–1.15)	0.10
	Recessive	C/C-C/A (134/77/58) A/A (13/6/7)	0.81 (0.64–1.21) 1.20 (0.44–1.49)	0.51	0.80 (0.65–1.09) 0.79 (0.36–2.03)	0.89	0.76 (0.65–1.21) 1.21 (0.67–1.49)	0.29
NFkB1 rs28362491	Codominant	Del/Del (31/19/12) Del/ATTG (79/45/34) ATTG/ATTG (34/18/16)	1.09 (0.50–1.92) 0.85 (0.51–1.39) 1.05 (0.53–1.36)	0.50	1.14 (0.66–1.92) 0.82 (0.53–1.44) 0.68 (0.43–1.28)	0.19	0.82 (0.43–1.89) 1.01 (0.51–1.27) 1.24 (0.89–1.67)	0.22
	Dominant	Del/Del (31/19/12) Del/ATTG-ATTG/ATTG (113/63/50)	1.09 (0.5–1.92) 0.99 (0.53–1.39)	0.78	1.14 (0.66–1.92) 0.77 (0.46–1.39)	0.25	0.82 (0.43–1.89) 1.09 (0.56–1.54)	0.71
	Recessive	Del/Del-Del/ATTG (110/64/46) ATTG/ATTG (34/18/16)	0.96 (0.51–1.54) 1.05 (0.53–1.36)	0.44	0.87 (0.53–1.57) 0.68 (0.43–1.28)	0.17	0.98 (0.5–1.3) 1.24 (0.89–1.67)	0.11
PADI4 rs874881	Codominant	G/G (29/19/10) G/C (79/46/33) C/C(46/24/22)	0.75 (0.44–1.07) 0.82 (0.45–1.37) 0.60 (0.39–0.93)	0.09	0.75 (0.44–0.99) 0.80 (0.46–1.37) 0.66 (0.39–0.90)	0.36	0.75 (0.33–1.42) 0.91 (0.45–1.44) 0.57 (0.39–0.93)	0.30
	Dominant	G/G (29/19/10) G/C-C/C (125/70/55)	0.75 (0.43–1.07) 0.67 (0.44–1.21)	0.85	0.75 (0.44–0.99) 0.69 (0.41–1.21)	0.99	0.75 (0.33–1.42) 0.64 (0.44–1.19)	0.55
	Recessive	G/G-G/C (108/65/43) C/C (46/24/22)	0.78 (0.45–1.32) 0.60 (0.39–0.93)	0.04	0.78 (0.46–1.16) 0.66 (0.39–0.90)	0.14	0.91 (0.44–1.44) 0.57 (0.39–0.93)	0.12

References

Akleyev A.A., Nikiforov V.S., Blinova E.A., Dolgushin I.I. Delayed expression of immune response genes in persons chronically exposed to radiation. *Rossiyskiy Immunologicheskiy Zhurnal = Russian Journal of Immunology*. 2019;13(22):1042-1044. (in Russian)

Akleyev A.V. (Ed.) The Consequences of Radioactive Pollution of the Techa River. Chelyabinsk: The Book Publ., 2016. (in Russian)

Albanese J., Martens K., Karanitsa L.V., Schreyer S.K., Dainiak N. Multivariate analysis of low-dose radiation-associated changes in cytokine gene expression profiles using microarray technology. *Exp. Hematol.* 2007;35(4):47-54. DOI 10.1016/j.exphem.2007.01.012.

Amundson S.A., Lee R., Koch-Paiz C.A. Differential responses of stress genes to low dose-rate gamma irradiation. *Mol. Cancer Res.* 2003;1(6):445-452.

Azimian H., Bahreyni-Toossi M., Rezaei A., Rafatpanah H., Hamzehloei T., Fardid R. Up-regulation of Bcl-2 expression in cultured human lymphocytes after exposure to low doses of gamma radiation. *J. Med. Phys.* 2015;40(1):38-44. DOI 10.4103/0971-6203.152249.

Barnes P.J., Karin M. Nuclear factor-kappaB: a pivotal transcription factor in chronic inflammatory diseases. *N. Engl. J. Med.* 1997; 336(15):1066-1071. DOI 10.1056/NEJM199704103361506.

Bazyka D., Ilienko I., Sushko V., Loganovsky K., Lyashenko L., Golyarnik N., Lyaskivska O., Nechaev S., Shvayko L., Bazyka K., Pilinska M., Bezdrobna L. Biological markers of external and internal exposure in shelter construction workers: a 13-year experience. *Radiat. Prot. Dosim.* 2018;182(1):146-153. DOI 10.1093/rpd/ncy128.

Bhattacharya R., Rose P.W., Burley S.K., Prlić A. Impact of genetic variation on three dimensional structure and function of proteins. *PloS One.* 2017;12(3):e0171355. DOI 10.1371/journal.pone.0171355.

Brest P., Lapaquette P., Souidi M., Lebrigand K., Cesaro A., Vouret-Craviari V., Mari B., Barbry P., Mosnier J.F., Hebuterne X., Harel-Bellan A., Mograbi B., Darfeuille-Michaud A., Hofman P. A synonymous variant in IRGM alters a binding site for miR-196 and causes deregulation of IRGM-dependent xenophagy in Crohn's disease. *Nat. Genet.* 2011;43(3):242-245. DOI 10.1038/ng.762.

Campbell T.M., Castro M.A.A., de Santiago I., Fletcher M.N.C., Halim S., Prathalingam R., Ponder B.A.J., Meyer K.B. FGFR2 risk SNPs confer breast cancer risk by augmenting estrogen responsiveness. *Carcinogenesis.* 2016;37(8):741-750. DOI 10.1093/carcin/bgw065.

Degteva M.O., Napier B.A., Tolstykh E.I., Shishkina E.A., Shagina N.B., Volchkova A.Y., Bougrov N.G., Smith M.A., Anspaugh L.R. Enhancements in the Techa River Dosimetry System: TRDS-2016D code for reconstruction of deterministic estimates of dose from environmental exposures. *Health Phys.* 2019;117(4):378-387. DOI 10.1097/HP.0000000000001067.

Ding L.H., Shingyoji M., Chen F., Hwang J.J., Burma S., Lee C., Cheng J.F., Chen D.J. Gene expression profiles of normal human fibroblasts after exposure to ionizing radiation: A comparative study of low and high doses. *Radiat. Res*. 2005;164(1):17-26. DOI 10.1667/rr3354.

DuPage M., Bluestone J.A. Harnessing the plasticity of CD4(+) T cell to treat immune-mediated disease. *Nat. Rev. Immunol*. 2016;16(3):149-163. DOI 10.1038/nri.2015.18.

Fachin A.L., Mello S.S., Sandrin-Garcia P., Junta C.M., Ghilardi-Netto T., Donadi E.A., Passos G.A., Sakamoto-Hojo E.T. Gene expression profiles in radiation workers occupationally exposed to ionizing radiation. *J. Radiat. Res*. 2009;50(1):61-71. DOI 10.1269/jrr.08034.

HapMap Genotype Data Portal. – URL: www.hapmap.ncbi.nlm.nih.gov

Ilienko I.N., Bazyka D.A. Overexpression of TP53, TP53I3 and BIRC5, alterations of gene regulation of apoptosis and aging of human immune cells in a remote period after radiation exposure. *Probl. Radiac. Med. Radiobiol.* 2016;21:238-246.

Krestinina L.Yu., Silkin S.S., Mikryukova L.D., Epifanova S.B., Akleyev A.V. Risk of death from solid cancer among residents of the Techa Riverside and the East Urals radioactive trace areas exposed to radiation: comparative analysis. *Radiatciya i Risk = Radiation and Risk* (*Bulletin of the National Radiation and Epidemiological Registry*). 2017;26(1):100-114. DOI 10.21870/0131-3878-2017-26-1-100-114. (in Russian)

National Center for Biotechnology Information (NCBI). – URL: www.ncbi.nlm.nih.gov (in Russian)

Nikiforov V.S., Blinova E.A., Akleyev A.V. Influence of a combination of radiation and non-radiation factors on gene transcriptional activity profile in chronically exposed persons. *Voprosy Radiatsionnoy Bezopasnosti = Radiation Safety Issues*. 2019;2(94):64-70. (in Russian)

Robert F., Pelletier J. Exploring the impact of single-nucleotide polymorphisms on translation. *Front. Genet.* 2018;9:507. DOI 10.3389/fgene.2018.00507.

Sanitary Regulations and Standards SanPiN 2.6.1.2523-09. Radiation Safety Standard-99/2009 (NRB-99/2009). p. 3.1.4. (in Russian)

Schüz J., Deltour I., Krestinina L.Y., Tsareva Y.V., Tolstykh E.I., Sokolnikov M.E., Akleyev A.V. *In utero* exposure to radiation and haematological malignancies: pooled analysis of Southern Urals cohorts. *Br. J. Cancer.* 2017;116(1):126-133. DOI 10.1038/bjc.2016.373.

Shastry B.S. SNPs: impact on gene function and phenotype. *Methods Mol. Biol.* (Clifton, N.J.). 2009;578:3-22. DOI 10.1007/978-1-60327-411-1_1.

Single-Nucleotide Polymorphism Database (SNP) – URL: www.snpedia.com

Tan H. The association between gene SNPs and cancer predisposition: Correlation or causality? *EBioMedicine.* 2017;16:8-9. DOI 10.1016/j.ebiom.2017.01.047.

Visscher P.M., Brown M.A., McCarthy M.I., Yang J. Five years of GWAS discovery. *Am. J. Hum. Genet.* 2012;90(1):7-24. DOI 10.1016/j.ajhg.2011.11.029.

Wang Y., Qiu C., Cui Q. A large-scale analysis of the relationship of synonymous SNPs changing microRNA regulation with functionality and disease. *Int. J. Mol. Sci.* 2015;16(10):23545-23555. DOI 10.3390/ijms161023545.

Woloschak G.E., Shearin-Jones P., Chang-Liu C.M. Effects of ionizing radiation on expression of genes encoding cytoskeletal elements: Kinetics and dose effects. *Mol. Carcinog.* 1990;3(6):374-378. DOI 10.1002/mc.2940030609.

Wright J.B., Brown S.J., Cole M.D. Upregulation of c-MYC in cis through a large chromatin loop linked to a cancer risk-associated single-nucleotide polymorphism in colorectal cancer cells. *Mol. Cell. Biol*. 2010;30(6):1411-1420. DOI 10.1128/MCB.01384-09.

Wyrobek A.J., Manohar C.F., Krishnan V.V., Nelson D.O., Furtado M.R., Bhattacharya M.S., Marchetti F., Coleman M.A. Low dose radiation response curves, networks and pathways in human lymphoblastoid cells exposed from 1 to 10 cGy of acute gamma radiation. *Mutat. Res.* 2011;722(2):119-130. DOI 10.1016/j.mrgentox.2011.03.002.

ORCID ID

E.A. Blinova orcid.org/0000-0002-2567-7945
V.S. Nikiforov orcid.org/0000-0002-6685-1823
M.A. Yanishevskaya orcid.org/0000-0002-2649-5123

Acknowledgements. The manuscript has been prepared within the framework of the Federal targeted program "Optimization of high-tech methods aimed at detection of health consequences of radiation exposure of the Mayak Production Association personnel and population of the Urals region", Contract No. 27.501.19.2 dated 08.07.2019.

Conflict of interest. The authors declare no conflict of interest.

Recieved March 17, 2020. Revised May 17, 2020. Accepted May 19, 2020.

Вавиловский журнал генетики и селекции. 2020;24(4):407-419
DOI 10.18699/VJ20.633

Causes of global extinctions in the history of life: facts and hypotheses

T.M. Khlebodarova ✉, V.A. Likhoshvai

Institute of Cytology and Genetics of Siberian Branch of the Russian Academy of Sciences, Novosibirsk, Russia
✉ e-mail: tamara@bionet.nsc.ru

Abstract. Paleontologists define global extinctions on Earth as a loss of about three-quarters of plant and animal species over a relatively short period of time. At least five global extinctions are documented in the Phanerozoic fossil record (~500-million-year period): ~65, 200, 260, 380, and 440 million years ago. In addition, there is evidence of global extinctions in earlier periods of life on Earth – during the Late Cambrian (~500 million years ago) and Ediacaran periods (more than 540 million years ago). There is still no common opinion on the causes of their occurrence. The current study is a systematized review of the data on recorded extinctions of complex life forms on Earth from the moment of their occurrence during the Ediacaran period to the modern period. The review discusses possible causes for mass extinctions in the light of the influence of abiogenic factors, planetary or astronomical, and the consequences of their actions. We evaluate the pros and cons of the hypothesis on the presence of periodicity in the extinction of Phanerozoic marine biota. Strong evidence that allows us to hypothesize that additional mechanisms associated with various internal biotic factors are responsible for the emergence of extinctions in the evolution of complex life forms is discussed. Developing the idea of the internal causes of periodicity and discontinuity in evolution, we propose our own original hypothesis, according to which the bistability phenomenon underlies the complex dynamics of the biota development, which is manifested in the form of global extinctions. The bistability phenomenon arises only in ecosystems with predominant sexual reproduction. Our hypothesis suggests that even in the absence of global abiotic catastrophes, extinctions of biota would occur anyway. However, our hypothesis does not exclude the possibility that in different periods of the Earth's history the biota was subjected to powerful external influences that had a significant impact on its further development, which is reflected in the Earth's fossil record.
Key words: Earth's fossil record; evolution of global ecosystems; mass extinctions; dynamic systems; complex dynamics; periodicity; modeling.

For citation: Khlebodarova T.M., Likhoshvai V.A. Causes of global extinctions in the history of life: facts and hypotheses. *Vavilovskii Zhurnal Genetiki i Selektsii = Vavilov Journal of Genetics and Breeding*. 2020;24(4):407-419. DOI 10.18699/VJ20.633

Причины глобальных вымираний в истории жизни: факты и гипотезы

Т.М. Хлебодарова ✉, В.А. Лихошвай

Федеральный исследовательский центр Институт цитологии и генетики Сибирского отделения Российской академии наук, Новосибирск, Россия
✉ e-mail: tamara@bionet.nsc.ru

Аннотация. Палеонтологи характеризуют глобальные вымирания на Земле как потерю ~3/4 существующего биоразнообразия на большей части земного шара за относительно короткий геологический промежуток времени. В палеонтологической летописи Земли, описывающей период фанерозоя (~500 млн лет), документировано как минимум пять таких глобальных вымираний: ~65, 200, 260, 380 и 440 млн лет назад. Существуют данные о возможности глобальных вымираний в более отдаленные периоды жизни на Земле – в позднем кембрии (~500 млн лет назад) и эдиакарии (более 540 млн лет назад). Общего мнения о причинах их возникновения до сих пор не сформировано. В настоящем обзоре систематизированы документированные факты глобальных вымираний сложных форм жизни на Земле с момента их возникновения в эдиакарии и до современного периода. Рассматриваются возможные причины их возникновения с точки зрения воздействия абиогенных факторов, планетарных или астрономических, и последствий их действия. Анализируются данные «за» и «против» гипотезы периодичности массовых вымираний биоразнообразия морской биоты в фанерозойский период. Обсуждаются факты, позволяющие высказывать гипотезы о наличии дополнительных механизмов возникновения кризисов в эволюции сложных форм жизни на Земле, связанных с различными внутренними биотическими факторами. Развивая тему внутренних причин периодичности и прерывистости эволюционного процесса, мы высказываем собственную, оригинальную гипотезу, согласно которой глобальные вымирания являются отражением сложной дина-

мики изменения уровня биоразнообразия на Земле и следствием феномена бистабильности. Этот феномен возникает только в экосистеме, бóльшая часть организмов которой размножается половым путем. Данная гипотеза говорит о том, что, если бы даже не было никаких глобальных катастроф абиотического характера, кризисы в развитии биоты возникали бы все равно. Однако гипотеза не исключает, что в определенные моменты времени биота Земли подвергалась мощным внешним воздействиям, оказавшим существенное влияние на ее дальнейшее развитие, что нашло отражение в конкретных палеонтологических данных.
Ключевые слова: палеонтологическая летопись Земли; эволюция глобальных экосистем; массовые вымирания; динамические системы; сложная динамика; периодичность; моделирование.

Introduction

Global extinctions on Earth are defined by paleontologists as a loss of about three-quarters of the existing biodiversity in a relatively short interval of geologic time. At least five global extinctions are documented in the Phanerozoic fossil record (~500 million years). These are the Cretaceous-Paleogene extinction event (~65 million years ago), the Triassic-Jurassic extinction event (~200 million years ago), extinction near the Permian-Triassic boundary (~260 million years ago), the late Devonian extinction (~380 million years ago), and extinction near the Ordovician-Silurian boundary (~440 million years ago). These five extinction events were first described as "Big Five" extinctions based on the analysis of more than 36 thousand kinds of marine invertebrate fossils, which were catalogued in the D.M. Raup and J.J. Sepkoski's database (Raup, Sepkoski, 1982). Some researchers argue that a sixth mass extinction is currently underway on our planet. This opinion is based on the estimates of species extinction rates in the current period, which were found to be comparable to those during global extinctions estimated on the basis of paleontological data (Barnosky et al., 2011; Ceballos et al., 2015).

In the last decade, intensive analysis of fossil material has revealed new examples of mass extinctions of complex life forms on Earth. There is evidence that during the early periods of life on Earth – in the Late Cambrian (~500 million years ago) and during the Ediacaran period (> 540 million years ago) (Gill et al., 2011; Darroch et al., 2015), extinctions were global. Extinction during the Ediacaran period is considered to be the first mass extinction of complex life forms on Earth (Darroch et al., 2015). Let us consider the facts and hypotheses concerning the causes of global extinctions.

Mass extinctions as a result of global disasters of an abiotic nature

A number of abiogenic factors has been described that could potentially cause most of the big extinctions detected in the Earth's fossil record. This does not apply to the biodiversity loss during the late Ediacaran period (Xiao, Laflamme, 2009; Buatois et al., 2014; Darroch et al., 2015), the late Cambrian period (Gill et al., 2011), and the modern period (Barnosky et al., 2011; Ceballos et al., 2015).

The most well-known abiogenic factors that have been associated with the environmental disasters are: the struck of a massive asteroid ~65 million years ago (Alvarez et al., 1980, 1981; Schulte et al., 2010; Kaiho, Oshima, 2017), volcanic activity and global warming ~200 million years ago (Marzoli et al., 1999; Whiteside et al., 2010; Blackburn et al., 2013; Thibodeau et al., 2016; Miller et al., 2017; Percival et al., 2017; Heimdal et al., 2018), trappean eruptions ~260 million years ago (Huey, Ward, 2005; Wignall et al., 2009; Rampino et al., 2017), as well as the major Gondwanan glaciation and climate cooling ~440 million years ago (Sutcliffe et al., 2000; Sheehan, 2001; Finnegan et al., 2011, 2012; Sheets et al., 2016). These phenomena and their consequences associated with climate change allow us to explain, at least to a certain extent, the extinction near the Cretaceous-Paleogene boundary (Alvarez et al., 1980, 1981; Schulte et al., 2010; Kaiho et al., 2016), the Triassic-Jurassic extinction event (Marzoli et al., 1999; Whiteside et al., 2010; Blackburn et al., 2013; Percival et al., 2017), the Late Permian extinction (Wignall et al., 2009), and the extinction near the Ordovician-Silurian boundary (Sutcliffe et al., 2000; Sheehan, 2001; Finnegan et al., 2011, 2012; Sheets et al., 2016).

However, it should be noted that the described external influences during these periods are quite diverse and there is still no single opinion on the causes of known extinctions, especially regarding the Late Devonian extinction ~380 million years ago.

Therefore, analysis of another dataset demonstrates the link between the extinction near the Cretaceous-Paleogene boundary ~65 million years ago and the sea-level changes caused by movements of the tectonic plates (Peters, 2008) or volcanic activity (Archibald et al., 2010; Courtillot, Fluteau, 2010; Keller et al., 2010; Schoene et al., 2015, 2019).

Some researchers explain the Triassic-Jurassic extinction event ~200 million years ago by significant climate warming as a result of abnormally high concentrations of atmospheric carbon dioxide of magmatic origin (McElwain et al., 1999; Beerling, 2002; Schaller et al., 2011), which could be accompanied by storms, lightning strikes and, as a result, fires. The latter could directly cause the global extinction of the terrestrial biota (Petersen, Lindström, 2012). Some authors deny the link between the global biodiversity loss and changes in atmospheric carbon dioxide concentration during that period (Tanner et al., 2001). Other scientists attribute mass extinction to the emission of large volumes of volcanic sulphurous gas (Bacon et al., 2013) or to frequent warming and cooling of the climate caused by volcanic emissions of large volumes of sulphurous gas followed by carbon dioxide emission (Guex et al., 2016). Recent studies confirm the great impact of volcanic activity on the climate change at the end of the Triassic period and provide evidence that toxic effect of volcanic emissions can be associated with mercury – the most genotoxic element on Earth (Percival et al., 2017; Lindström et al., 2019).

Biodiversity loss during the Late Permian ~260 million years ago, when more than 90 % of marine invertebrates

became extinct, has been explained by various reasons: low oxygen concentration in the surface layer of the ocean (Knoll et al., 1996; Wignall et al., 2009; Shen et al., 2011; Zhang et al., 2018a), including in combination with warm climate which is harmful to shallow-water organisms (Song et al., 2013); ocean acidification associated with carbon dioxide release into the atmosphere and the accompanying rapid global warming and acid rain (Clarkson et al., 2015; Sun et al., 2018); climate cooling, combined with aridity, hypoxia, and acid rain (Zhu et al., 2019). Mathematical modeling of the Late Permian climate supports the hypothesis that reduced biodiversity during that period could be due to hypoxia and ocean warming (Penn et al., 2018). Recently, additional data in favor of the volcanic hypothesis of the biotic crisis in the Late Permian period have been obtained (Burgess et al., 2017; Shen et al., 2019).

Biodiversity loss near the Ordovician-Silurian boundary ~440 million years ago, when ~85 % of marine organisms became extinct, has been traditionally associated with the global cooling of the tropical ocean (Sutcliffe et al., 2000; Sheehan, 2001; Finnegan et al., 2011, 2012), which was accompanied by a drop of the sea level and the loss of shallow habitats (Finnegan et al., 2012).

According to some researchers, such cooling was triggered by a significant increase in cosmic dust in the inner space of the solar system due to the decay of the L-chondrite parent body in the asteroid belt ~466 million years ago (Schmitz et al., 2019), while others deny the connection between the asteroid destruction and the level of biodiversity (Lindskog et al., 2017).

Some researcher believe that scenario of the Ordovician-Silurian extinction was more complicated, included three ice ages and the cause of the initial extinction was not the sea cooling, but the ice melt from glaciers due to the presence of a large ice cover and a relatively warm ocean during that period causing sea level to rise (Ghienne et al., 2014). The cause of the second extinction has been considered to be the decreased oxygen concentration in water that occurred when the sea level was high before the glaciation peak in the Late Ordovician period (Bartlett et al., 2018). Nowadays, volcanic activity is considered to be the cause of the second extinction (Gong et al., 2017; Rasmussen et al., 2019; Smolarek-Lach et al., 2019).

There are many different hypotheses about the cause of the Late Devonian extinction ~380 million years ago (Sallan, Coates, 2010), which mainly affected the marine biota, especially in shallow water (Ma et al., 2016). Some researchers associate it with climate cooling (Huang et al., 2018; Wang et al., 2018), which was provoked by the burial of a large amount of organic carbon with a subsequent decrease in atmospheric carbon dioxide concentration (Huang et al., 2018), and was accompanied by the sea-level decrease (Wang et al., 2018). Others attribute the Devonian extinction to global warming caused by a massive release of methane gas into the atmosphere, which could be caused by volcanic activity (Gharaie et al., 2004, 2007). And others link it to the frequent climate change from warming to cooling (Chen et al., 2005), which was accompanied by sea level fluctuations (Joachimski, Buggisch, 1993) and was provoked by various processes, including the burial of a large amount of organic carbon and the dissociation of gas hydrates (Chen et al., 2002). Devonian extinction has also been associated with the spread of fires, the cause of which is considered to be the high concentration of atmospheric oxygen together with dry climate (Kaiho et al., 2013), trap eruptions (Ricci et al., 2013), asteroid fall (Claeys et al., 1992), etc. It is overall recognized that causes of Devonian extinction are still not clear (Percival et al., 2018).

It is also worth noting the potential uniqueness of biotic crises during the late Devonian period and near the end of the Triassic period, which were associated not with an increased extinction rate, but with a decrease in the rate of speciation (Bambach et al., 2004; Lamsdell, Selden, 2017).

As for the remaining documented extinctions: during late Cambrian period ~499 million years ago (Gill et al., 2011), near the end of the Ediacaran period > 540 million years ago (Xiao, Laflamme, 2009; Buatois et al., 2014; Darroch et al., 2015; Zhang et al., 2018b), as well as the loss of biodiversity observed in the modern period (Barnosky et al., 2011; Ceballos et al., 2015), they have not been associated with global catastrophes of an abiotic nature.

Recently, the lack of oxygen in water is more and more often considered one of the main causes of global extinctions of biota, including during the Ediacaran period (Zhang et al., 2018b), during the Late Cambrian period (Gill et al., 2011), near the Ordovician-Silurian boundary (Bartlett et al., 2018), during the late Devonian period (Bond, Wignall, 2008; Liu et al., 2016), at the end of the Permian period (Brennecka et al., 2011; Shen et al., 2011; Lau et al., 2016; Zhang et al., 2018a), and during the early Jurassic period (Them et al., 2018). However, if during the late Permian period the lack of dissolved oxygen is believed to be a consequence of a global warming (Zhang et al., 2018a), and during the late Ordovician period – a consequence of a climate cooling (Bartlett et al., 2018), what could cause it during other periods of mass extinctions is not yet clear. Moreover, there is evidence (Darroch et al., 2015) that contradicts the assertion (Zhang et al., 2018b) of oxygen deficiency in the late Ediacaran ocean.

Periodicity in the history of global extinctions

It is important to note that episodes of mass extinctions on the Earth are strongly believed to be cyclical, which was first noted when creating the first comprehensive database on the fossil record of marine families during the Phanerozoic period (Raup, Sepkoski, 1984, 1986; Sepkoski, 1989). Over a time span of 250 million years, eight largest extinction-intensity peaks with a periodic fluctuation in marine biodiversity of ~26–27 million years have been detected. Since then, data from the Sepkoski's dataset (Sepkoski, 2002) have been intensively analyzed using various methods; some authors report the presence of a slightly pronounced periodicity of extinctions of ~27 million years (Lieberman, Melott, 2007), whereas data obtained by other researchers indicate a strict periodicity of ~62–63 million years (Rohde, Muller, 2005; Lieberman, Melott, 2007), which appeared over an interval of 500 million years (Rohde, Muller, 2005) (Fig. 1).

Similar studies were conducted using alternative databases: Paleobiology Database (PBDB) of marine invertebrate fossils (Alroy, 2008; Melott, 2008; Lieberman, Melott, 2012; Roberts, Mannion, 2019) and Fossil Record 2 databases for marine and

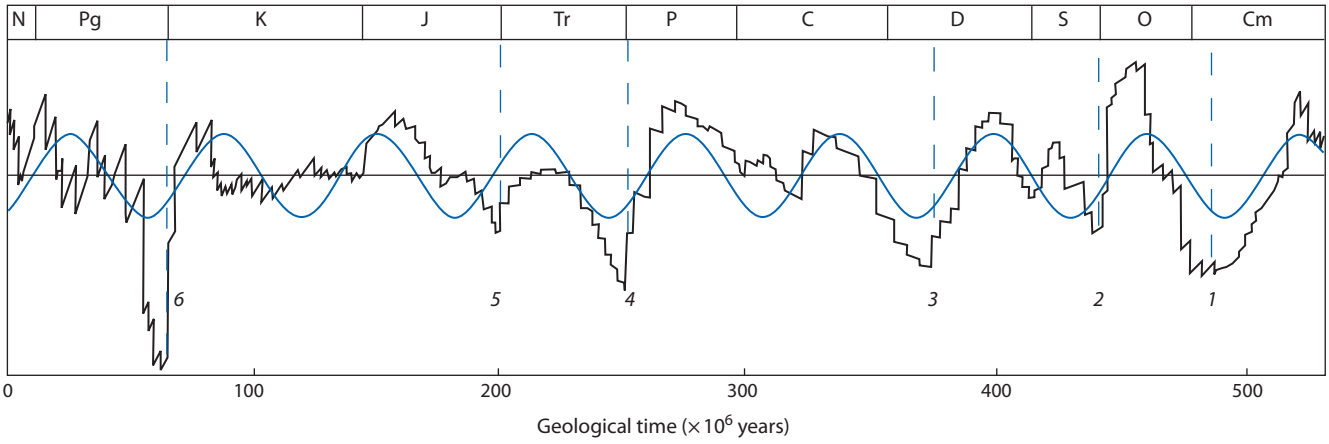

Fig. 1. Diversity dynamics of the Phanerozoic marine biota.

The main geological periods are indicated above, according to (Raup, Sepkoski, 1982), the vertical dashed line shows the times of six global extinctions of biota on Earth: *1* – during the Late Cambrian; *2* – near the Ordovician-Silurian boundary; *3* – during the late Devonian period; *4* – near the Permian-Triassic boundary; *5* – near the Triassic-Jurassic boundary; *6* – near the Cretaceous-Paleogene boundary. Blue curve is a sine wave, black curve is adapted from (Rohde, Muller, 2005; Fig. 1, *c*).

terrestrial fossils (Benton, 1995). Data were obtained both in favor of the presence of periodicity (Melott, 2008; Lieberman, Melott, 2012; Roberts, Mannion, 2019) and against strict cyclicality (Benton, 1995; Alroy, 2008).

In the study (Benton, 1995) seven peaks of mass extinctions of marine families were identified within the past 250 million years with a time interval between them varying from 20 to 60 million years. As for the PBDB material, the results of the study (Alroy, 2008) did not reveal any evidence in favor of periodic extinctions. However, other results confirmed the existence of a fairly strict periodicity of ~62–63 million years in the occurrence of major extinction events in the Phanerozoic (Melott, 2008; Lieberman, Melott, 2012), which was also shown in the analysis of the Sepkoski's dataset (Rohde, Muller, 2005; Lieberman, Melott, 2007, 2012). Recent studies of the Paleobiology Database (Roberts, Mannion, 2019) confirm the extinction periodicity of ~27 million years, but limit them to the last 200 million years. The certainty and significance of the cyclical nature of extinctions with periods of ~27 and ~62 million years in the last 465 million years has been demonstrated in other studies (Melott, Bambach, 2014, 2017).

It is necessary to add that one more cycle of marine biodiversity change with a period of 140 ± 15 million years was found in the analyses based on the Sepkoski's dataset (Rohde, Muller, 2005), but cyclicality of global extinctions in Phanerozoic with ~62–63 million years period was more strict.

Hense, based on various databases, researchers have reported at least three cycles of mass extinctions with periods of 26–30, 62–63, and ~140 million years during the Phanerozoic eon (Raup, Sepkoski, 1984, 1986; Sepkoski, 1989; Rohde, Muller, 2005; Lieberman, Melott, 2007, 2012; Melott, 2008; Melott, Bambach, 2014, 2017; Roberts, Mannion, 2019). A cycle with a period of ~27 million years was most clearly manifested during the last 200 million years (Roberts, Mannion, 2019).

In this regard, the question arises – is there a connection between the observed periodicity in the diversity of terrestrial biota and those processes that are considered above to be causes of global extinctions? In other words, is there a periodic abiotic process that could underlie the observed periodicity in the diversity of marine or terrestrial biota or even Earth's entire biota?

Here it is important to emphasize once again that extinctions described above are global, that is, they affect almost the entire Earth's biota, which means that if observed periodicity was associated with abiotic factors, it could reflect only those processes that affect the entire planet and are cyclical. From this point of view, two types of processes that have similar characteristics can be distinguished. The first are "inside planetary" processes, that is, they are associated with dynamic processes involved in plate tectonic motion that lead to continental drift, volcanic activity, changes in sea level, etc. The second are associated with extra-planetary influences and are a reflection of processes associated with the dynamics of the planet itself being a space object interacting with other objects of the universe.

Let us consider the existing hypotheses on the relationship between the periodicity of global extinctions and global catastrophes, which could be caused by such cyclical processes.

Frequency of extinctions as a reflection of planetary processes and the evolution of the Sun

Nowadays, there is a number of hypotheses regarding possible connection between the periodicity of extinctions on Earth and astronomical processes. For example, a model of large-scale fluctuations in the magnetic field of the Sun shows an impressive periodicity of 66 million years (Baker, Flood, 2015), which is very close to the periodicity of mass extinctions of ~62–63 million years identified by analyzing at least two databases of marine invertebrate fossils (Rohde, Muller, 2005; Lieberman, Melott, 2007, 2012). Other hypotheses have been proposed linking frequency of extinctions with fluctuations of extragalactic cosmic-ray intensity as a result of vertical oscillations of the solar system about the galactic plane

(Medvedev, Melott, 2007); with the periodicity of the solar system passage through the plane of the Milky Way galaxy (Rampino et al., 1997, 2015; Lieberman, Melott, 2012); and with the periodicity of the passage of comets near Earth and the fall of asteroids, which can form different periodicities depending on the size of celestial body (Rampino, Stothers, 1984; Rampino et al., 1997).

However, in recent years, new findings indicate that periodicities associated with solar system oscillations about the galactic plane are statistically unreliable (Erlykin et al., 2017, 2018) and could not cause the periodicity of extinctions on Earth. And, although some researchers disagree, it is generally recognized that there is no direct evidence of astronomical reasons for the periodicity of biota extinctions on the planet Earth (Melott, Bambach, 2017).

As for the planetary processes, there is also a wide variety of opinions. Some researchers explain changes in the fossilized organisms by periodic changes in sea level (Peters, 2008; Tennant et al., 2016) or connect them with the dynamics of tectonic movement of continental plates and their fragmentation (Valentine, Moores, 1970; Zaffos et al., 2017). One of the assumptions regarding the fact that tectonic processes on Earth could cause periodicity of mass extinctions has been based on the data on the 60-million-year periodicity of seawater Sr^{87}/Sr^{86} ratio in marine sediments (Melott et al., 2012).

Other researchers detect a definite correlation between the biodiversity dynamics and the temperature regime on Earth (Mayhew et al., 2012) and consider periodic global climate changes to be the cause of extinctions. It can be noted here that glacial-interglacial cycles on Earth had a periodicity of ~135 million years (Veizer et al., 2000), which is statistically indistinguishable from the periodicity of 140 ± 15 million years, which was revealed based on the Sepkoski's dataset (Rohde, Muller, 2005).

Of interest is the volcano crater dating over the past 260 million years, which demonstrates the cyclicity close to 26–27 million years (Rampino, Caldeira, 2015) characteristic of this particular period of time (Raup, Sepkoski, 1984, 1986; Sepkoski, 1989; Roberts, Mannion, 2019). However, in general, volcanic activity during the last 300 million years is characterized by weakly manifested cycles with a period of 15, 30, and 60 million years (Prokoph et al., 2004).

As for the rather strict ~62–63 million-years mass-extinction cycle identified by different researchers using different databases of marine invertebrate fossils (Rohde, Muller, 2005; Lieberman, Melott, 2007, 2012; Melott, 2008; Melott, Bambach, 2014, 2017), the existing data on 60-million-year periodicity associated with the dynamic processes involved in plate tectonic motion (Melott et al., 2012) and modeling data on the large-scale fluctuations of the solar magnetic field, both show periodicity of 66 million years (Baker, Flood, 2015), but do not allow strong connection with the periodicity of global extinctions on Earth.

Several times in the history of biological life on Earth have we detected serious external influences such as fall of asteroids and meteorites without subsequent extinction (Archibald et al., 2010), as well as extinctions without abiotic catastrophes, which leads us to an assumption that internal causes of a biotic nature could underlie mass extinctions of biota, which at different periods could coincide with global catastrophes or be provoked by them. We believe that these internal causes may be a reflection of a complex dynamic behavior of a living system, such as terrestrial or marine biota, or even the biota of the entire Earth.

Mass extinctions and their periodicity as a reflection of internal properties of a global ecosystem

The idea that fossil biodiversity on Earth is a reflection of the internal laws of functioning of a global ecosystem, which is the Earth's biota, has arisen more than once. Mass extinctions, which have been observed in the Earth's fossil record over the past 500 million years and lead to intermittent and irregular evolutionary pace, represent just one aspect of the complex dynamic behavior of a global ecosystem. To explain the phenomenon of punctuated evolution, S.J. Gould and N. Eldredge have formulated the "theory of punctuated equilibrium" back in 1972 (Gould, Eldredge, 1977, 1993; Eldredge, Gould, 1997).

This theory is not strict. It is based on "empirical generalizations" of a number of facts that have long been noticed by paleontologists, which indicate that long periods of evolutionary stability, when species remain almost unchanged, alternate with short intervals of rapid qualitative change, which are characterized by "sudden" extinction of old species and subsequently replacement by new types. The authors of this theory and other researchers have found quite striking examples in the Earth's fossil record confirming such pattern (Ovcharenko, 1969; Bambach, 1977; Gould, Eldredge, 1977, 1993; Williamson, 1981; Sepkoski, 1988; Jackson, Cheetham, 1999). Although the interpretation of some studies has been questioned (Van Bocxlaer et al., 2008), in general, presence of such pattern in the evolutionary process is not denied (Hunt, 2007; Mattila, Bokma, 2008; Rasskin-Gutman, Esteve-Altava, 2008).

Previously, the idea of internal biotic causes that determine the evolutionary dynamics was formulated as "self-organizing criticality" (Bak, Paczuski, 1995; Sneppen et al., 1995; Solé, Manrubia, 1996), which reflects interactions between different ecosystems and was used to explain mass extinctions and the hypothesis of punctuated evolution. It was assumed that these interactions, together with spontaneous mutations and genetic variations that are always present in populations, could lead to large evolutionary rearrangements called the "co-evolutionary avalanches". Recently, the concept of "self-organizing criticality" has again attracted the attention of researchers (Nykter et al., 2008; Solé et al., 2010; Hesse, Gross, 2014; Valverde et al., 2015). However, already in the 1990s (Newman, 1997a, b) and later (Alroy, 2008), arguments against this concept have been expressed, which were based on the demonstration of the possibility of mass extinctions using simple models of species adaptation to existing conditions and nutrition resources without involvement of co-evolution and critical processes, both with and without influence of the abiotic factors (Roberts, Newman, 1996; Newman, 1997a, b).

There exist other ideas on the internal biotic causes of the biodiversity on Earth that relate the Phanerozoic biodiversity to the intensity of predation in marine communities (Huntley,

Kowalewski, 2007) and suggest a certain role for predators in the formation of marine biota diversity, although no correlation between predators and preys were found in other studies (Madin et al., 2006). Other researchers, seeing a definite relationship between biodiversity and the age of the oceanic crust, connect the history of the seafloor with the biodiversity level via the availability of food resources (Cermeño et al., 2017).

In the existing models of the diversity dynamics of the Phanerozoic marine biota that has clear signs of punctuated evolution in its development, the periodicity of extinctions was not examined and was introduced into the models as a given (Markov, 2001a, b; Markov, Korotaev, 2007). However, discussing the modeling results, the authors noted that the causes of "staging" should be sought in the structure of developing communities (Markov, 2001a). A.V. Markov and A.V. Korotaev (2007) paid special attention to those life forms that have an increased adaptive capacity associated with sexual reproduction. In this regard, we should pay attention to the studies of A.M. Bush et al. (2016) who believe that diversification of marine predators starting from the Cretaceous-Cenozoic period (~200 million years ago) can be explained by the peculiarities of sexual reproduction during the directed transfer of sperm. However, given that internal fertilization has probably developed as early as in the late Neoproterozoic Era (> 500 million years), such delayed diversification requires an explanation (Novack-Gottshall, 2016).

A number of theoretical studies has connected discontinuity and staging in the Earth's fossil record with the negative and positive feedback regulatory loops that *a priori* exist in nature, and the combination of which leads to system instability (Robertson, 1991; Seaborg, 1999). This property of feedback regulatory loops has long been noted and was demonstrated in models of biological systems at various levels of their organization (Mackey, Glass, 1977; Decroly, Goldbeter, 1982; Martinez de la Fuente, 1996; Goldbeter et al., 2001; Harish, Hansel, 2015; Likhoshvai et al., 2015, 2016; Kogai et al., 2017; Khlebodarova et al., 2017, 2018). However, it turned out that this is not the only mechanism that can cause instability in a nonlinear dynamic system.

Periodicity and discontinuity in the history of life viewed through the prism of a mathematical model

No one doubts today that models of mathematical physics are a powerful tool for understanding the deepest laws of the Universe. Methods of mathematical modeling do not yet play such a role in the science of living systems. However, living systems are part of dynamic systems. They are open and non-linear at all levels of their organization, so the method of mathematical modeling is potentially able to help identify the laws of their functioning. And, the more global the system is, the more fundamental and, at the same time, simple in essence, but not in content, should be the laws that determine system's functioning.

To develop the idea of the internal causes of the discontinuity in evolution, we studied the evolution of large ecosystems using methods of mathematical modeling. We define large ecosystem as a group of organisms (population) of one species, which we designated as "transit" species. In our models, such population mimics the biota of an ecosystem large enough to be correlated with terrestrial or marine biota. These are traditional logistic models of a frame type, in which the efficiency of reproduction and mortality of organisms depends on population density. According to A.V. Markov, hypothesis that the dynamics of the Phanerozoic marine biota calculated by traditional methods (without amendments) adequately reflects real changes in biodiversity has not been unproved and remains the most convenient and reliable basis for meaningful biological interpretations (Markov, Korotaev, 2007, p. 4).

Evolution is described in models as process of ecosystem self-development (population of a "transit" type), during which there is a local increase in the adaptability of its individuals to the conditions of existence due to mutational variability and natural selection.

Analysis of the dynamics of functioning of such models have showed that living systems with different reproduction methods implement different evolutionary laws of self-development: "asexual" ecosystems showed stasis, whereas "sexual" ecosystems evolved cyclically (Likhoshvai, Khlebodarova, 2016; Likhoshvai et al., 2017). That is, it turned out that if natural selection in a population is directed towards increasing the adaptability of its individuals to the conditions of existence, then, at a certain stage of its evolution (the occurrence of sexual reproduction), such selection can act as destabilizing factor.

Moreover, it turned out that these same factors can explain the peculiarities of punctuated evolution observed in the fossil record, such as mass extinctions and phases of rapid diversity increase, as well as phases of stasis diversity, the causes of which are still not understood (Voje, 2016; Voje et al., 2018). Figure 2 shows evolutionary phases of the density parameter of a "transit" population using one full cycle of the parameter value fluctuation. In the model, phases of decrease and increase in the parameter value repeat an unlimited number of times with approximately the same time interval. The exact duration of each phase cannot be predicted, since the oscillatory dynamics observed in the model is chaotic.

One full evolutionary cycle of a "transit" population is completed over time interval $t \in [32{,}000, 44{,}000]$ conv. units, which in the model is ~12,000 conv. units of time (Fig. 2). The concept of fractal evolution (Dieckmann, Law, 1996), which is based on the similarity of laws that regulate the dynamics of population density, variety of species, genera and higher levels of organization of living systems at different time scales, allows to transfer these data when changing the time scale according with a level of organization of living systems with more than a single population. It is easy to verify that if one conv. unit of time equals 50 years, then duration of one evolutionary cycle is close to the species lifespan estimate, and if it equals 500 years, we receive an estimate of the genus lifetime, the durations of which are ~0.5 and ~5.9 million years, respectively, according to (Gingerich, 1976; Severtsov, 1990, 2014). These rough estimates do not prove anything, but suggest that time scales characteristic of dynamic processes at the level of large ecosystems are one order of magnitude larger, that is, such time scales range up to tens of millions of years and cyclic changes in the diversity of Phanerozoic marine biota with a period of 62–63 million years may repre-

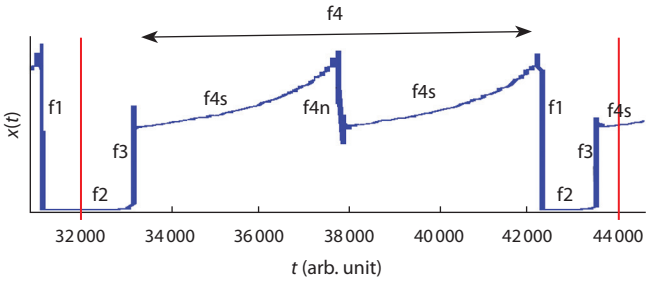

Fig. 2. Phases of the *x*(*t*) parameter evolution (biota density) demonstrated on the example of one complete oscillation of the *x*(*t*) value.

Boundaries of the analyzed period are marked with red vertical lines. Phase f1 corresponds to extinction; phase f2 corresponds to the stage of biota development after global extinction; phase f3 corresponds to the stage of explosive growth of biota biodiversity; phase f4 corresponds to the stage of biota development when a high diversity of life forms and a relatively low growth rate are observed. Within the f4 phase, the stasis stage f4s and the local extinction stage f4n are observed.

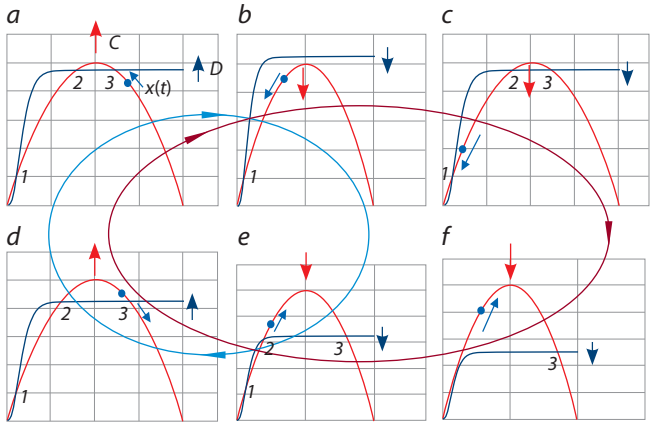

Fig. 3. Charts of the reproduction *C* (red curve) and mortality *D* (blue curve) functions at different time moments of system evolution.

1 – stable stationary state x_{min}; *2* – unstable stationary state x_{mdl}; *3* – stable stationary state x_{max}; blue dot – current *x*(*t*) value; colored arrows indicate the direction of evolution (change) of the parameters; blue oval corresponds to the contour of local extinctions and red oval – to global ones.

sent their reflection (Rohde, Muller, 2005; Lieberman, Melott, 2007, 2012; Melott, 2008; Melott, Bambach, 2014, 2017).

Thus, the modeling results have shown that if the efficiency of reproduction and mortality in a population depends on its density and the most adapted individuals, the genetic diversity of which is a result of genome replication errors during self-reproduction, are being selected, then these conditions are *sufficient* for the formation of cyclical intermittent dynamics of biodiversity in a living system with sexual type of reproduction.

The question arises – what is the origin of cyclicality and intermittency observed in the evolution of life on Earth?

Global extinctions in the evolutionary history of life on Earth as a reflection of the bistability phenomenon: the hypothesis of two "trees of life"

The idea that the phenomenon of punctuated evolution can be based on the bistability in biological systems has been expressed by V.A. Likhoshvai long ago in the work dedicated to the modeling of the evolution of a simple self-developing living system. It was expressed as an idea of a latent phenotype in a self-developing living system, which represents an internal resource of its evolutionary development (Likhoshvai, Matushkin, 2000, 2004). Subsequently, when applied to global ecosystems, this idea was transformed into the hypothesis of the two "trees of life".

Here it should be noted that Ch. Darwin defined the diversity of living things on Earth as the "tree of life". Such comparison very accurately reflects the deepest essence of life, which constantly gives rise to new thin branches of species during its continuous evolutionary development that can eventually form into new genera, types, classes, etc., but can also dry out and disappear (Darwin, 1991).

The most common characteristics of the "tree of life" are biota density and species diversity. These characteristics are reflected in our model as the population density of a "transit" species, which at each moment in time depends on the ratio between the rates of self-reproduction and mortality of its individuals. Analysis of the behaviour of functions that describe changes in these parameters at different time moments depending on the density of a "transit" population have shown that evolving ecosystems with asexual type of reproduction have only one stable state, while for ecosystems with sexual type of reproduction the bistability is possible, that is, two stable stationary states, each of which can be interpreted as the "tree of life", one of which is being manifested and the other is not. Moreover, if evolution is directed towards improving the adaptability of individuals of a "transit" species to habitat conditions, which should be accompanied by niche expansion and increased utilization of resources, then at some point in time the stability of the manifested state becomes lost and the system jumps into a new steady state that existed before, but was unmanifested. The result of such transition can be interpreted as sudden "disappearance" of old species followed by explosive appearance of new types, that is, the change of one "tree of life" to another. From a mathematical point of view, such event is not unusual in dynamic nonlinear systems. Figure 3 demonstrates the mechanism of local and global extinctions depending on the rates of change of functions describing self-reproduction *C* (red curve) and mortality *D* (blue curve) of individuals of a "transit" population at different moments of its evolution.

The intersection of functions *C* and *D* corresponds to the stationary states of the system, which can be stable (x_{min} and x_{max}) or unstable (x_{mdl}). If current value of density and biodiversity of biota *x*(*t*) is located near the stable stationary state, it falls into the region of its attraction and will tend to either x_{max} (see Fig. 3, *a*, *d*, *e*) or x_{min} (see Fig. 3, *c*). The fact that at the same time moment there is one more stable stationary state does not affect the state of the system, since *x*(*t*) value falls outside the region of its attraction and the system cannot get into it without external influence. Therefore, we can assume that at the time moment described in Fig. 3, *c*, stationary state x_{min} is manifested and stationary state x_{max} is not. In Fig. 3, *a*, *d*, *e*, on the contrary, stationary state x_{max} is manifested, whereas stationary state x_{min} is not.

Since the system evolves over time towards biota size and diversity increase, value of the $x(t)$ parameter increases, while the attraction region of the manifested stationary state decreases and approaches the stationary state x_{mdl}, so that at some point they merge and disappear. At this time moment we observe only one stationary state in the system – either x_{min} (see Fig. 3, *b*) or x_{max} (see Fig. 3, *f*), which passes from the unmanifested state to the manifested one. Since at this time moment the $x(t)$ value is significantly different from the value of the manifested stationary state (see Fig. 3, *b*,*f*), an explosive change in the $x(t)$ value is observed. We believe that a rapid change in system parameters during the transition from one state to another can be a reflection of the uneven evolutionary rates observed in phylogenetic studies (Nichol et al., 1993; Pagel et al., 2006; Wolf et al., 2006; Palmer et al., 2012).

It also follows from these data that local extinctions (blue outline) are associated with fluctuations in the current density and diversity of biota $x(t)$ in the attraction region of the stable stationary state x_{max} (see Fig. 3, *a*, *d*), while global extinctions are associated with the loss of stationary state stability and the $x(t)$ transition to the attraction region of the stationary state x_{min}, which at this time moment becomes single, similar to that shown in Fig. 3, *b*. It is this transition that we interpret as the change of one "tree of life" to another.

Thus, we came to the conclusion that adaptation of organisms to the habitat conditions as a result of gradual accumulation of mutations (the evolution) may by itself be one of the causes of instability in a living system, which manifested itself as periodically occurring mass extinctions of biota. However, this instability manifested itself only at a certain stage of the evolution of living systems and was associated with the development of sexual dimorphism. This does not contradict with the fact that during certain periods of life on Earth mass extinctions could coincide with planetary environmental disasters or be provoked by them.

Conclusions

Analysis of the causes of global extinctions in the Earth's history have shown that, although abiogenic factors are recognized as prevailing and their various combinations can explain most mass extinctions described in the Earth's fossil record, they do not explain such aspects of the evolutionary process as periodic discontinuity and uneven evolution of living organisms. However, these are evolutionary characteristics that are manifested at all known levels of organization of living systems – from molecular level to biosphere as a whole. It has now been proven that "spasmodicity" of evolution at the paleontological level is reflected on the molecular level (Nichol et al., 1993; Pagel et al., 2006; Wolf et al., 2006; Palmer et al., 2012).

We believe that in addition to external factors, there are other, internal, reasons for the occurrence of global extinctions of terrestrial biota. According to our hypothesis, these internal factors are associated with the phenomenon of bistability, which occurs only in ecosystems with prevalent sexual reproduction. The fossil record of life on Earth over the past 500 million years reflects the life history of just such organisms. Our hypothesis suggests that even with no global catastrophes of an abiotic nature, extinctions in the evolution of living organisms would happen anyway. The possibility of this is evidenced by the existence of extinctions that are not yet associated with global catastrophes of an abiotic nature, as well as the evidence of serious external influences that were not accompanied by extinctions (Archibald et al., 2010).

We believe that the bistability phenomenon should be manifested in the evolution of a living system at all levels of its organization. And at least at the cellular level, we have demonstrated the contribution of bistability phenomenon to the evolution of cellular complexity (Likhoshvai, Khlebodarova, 2017; Khlebodarova, Likhoshvai, 2018, 2019). There is no doubt that at the level of the entire Earth's biota the bistability phenomenon should interfere with the abiogenic factors observed in the fossil record of life on Earth. This is evidenced by the extinction cycle with a period of ~140 million years, although it was dimly manifested (Rohde, Muller, 2005), which can be associated with the frequency of glaciations preceding extinctions (Veizer et al., 2000); as well as by the extinction cycle with a period close to 26–27 million years, which was manifested during the last 250 million years (Raup, Sepkoski, 1984, 1986; Sepkoski, 1989; Roberts, Mannion, 2019) and coincided with the dating of volcano craters (Rampino, Caldeira, 2015).

As for the rather strict cyclicity of marine extinctions manifested over the last 500 million years, the period of which was ~63 million years (Rohde, Muller, 2005; Lieberman, Melott, 2007, 2012; Melott, 2008; Melott, Bambach, 2014, 2017), both the empirical data on the ~60 million-years periodicity of the Sr^{87}/Sr^{86} ratio change in marine sediments (Melott et al., 2012), which indicates the possibility of cyclicity associated with motion of tectonic plates on Earth, as well as modeling data on the fluctuations of the Sun's large-scale magnetic field with the periodicity of 66 million years (Baker, Flood, 2015), did not conclusively link them to the periodicity of global extinctions.

At this stage, the modeling results do not explain the existence of such periodicity of extinctions. For this, the model is too simple. The dynamics of changes in the biota density observed in the model makes it possible to rather roughly reproduce, with a change in the time scale, the oscillation period characteristic of the specific level of organization of living systems. However, these estimates suggest that the time scales characteristic of dynamic processes at the level of large ecosystems or even the entire Earth, are tens of millions of years. At the moment, this question remains open.

References

Alroy J. Colloquium paper: dynamics of origination and extinction in the marine fossil record. *Proc. Natl. Acad. Sci. USA*. 2008; 105(Suppl. 1):11536-11542. DOI 10.1073/pnas.0802597105.

Alvarez L.W., Alvarez W., Asaro F., Michel H.V. Extraterrestrial cause for the Cretaceous-Tertiary extinction. *Science.* 1980;208(4448): 1095-1108.

Alvarez L.W., Alvarez W., Asaro F., Michel H.V. Asteroid extinction hypothesis. *Science*. 1981;211(4483):654-656.

Archibald J.D., Clemens W.A., Padian K., Archibald J.D., Clemens W.A., Padian K., Rowe T., Macleod N., Barrett P.M., Gale A., Holroyd P., Sues H.D., Arens N.C., Horner J.R., Wilson G.P., Goodwin M.B., Brochu C.A., Lofgren D.L., Hurlbert S.H., Hartman J.H., Eberth D.A., Wignall P.B., Currie P.J., Weil A., Prasad G.V., Din-

gus L., Courtillot V., Milner A., Milner A., Bajpai S., Ward D.J., Sahni A. Cretaceous extinctions: multiple causes. *Science.* 2010; 328(5981):973.

Bacon K.L., Belcher C.M., Haworth M., McElwain J.C. Increased atmospheric SO_2 detected from changes in leaf physiognomy across the Triassic-Jurassic boundary interval of East Greenland. *PLoS One*. 2013;8(4):e60614. DOI 10.1371/journal.pone.0060614.

Bak P., Paczuski M. Complexity, contingency, and criticality. *Proc. Natl. Acad. Sci. USA.* 1995;92(15):6689-6696.

Baker R.G., Flood P.G. The Sun-Earth connect 3: lessons from the periodicities of deep time influencing sea-level change and marine extinctions in the geological record. *SpringerPlus.* 2015;4:285. DOI 10.1186/s40064-015-0942-6.

Bambach R.K. Species richness in marine benthic habitats through the Phanerozoic. *Paleobiology.* 1977;3(2):152-167.

Bambach R.K., Knoll A.J., Wang S.C. Origination, extinction, and mass depletions of marine diversity. *Paleobiology.* 2004;30:522-542. DOI 10.1666/0094-8373(2004)030<0522:OEAMDO>2.0.CO;2.

Barnosky A.D., Matzke N., Tomiya S., Wogan G.O., Swartz B., Quental T.B., Marshall C., McGuire J.L., Lindsey E.L., Maguire K.C., Mersey B., Ferrer E.A. Has the Earth's sixth mass extinction already arrived? *Nature*. 2011;471(7336):51-57. DOI 10.1038/nature 09678.

Bartlett R., Elrick M., Wheeley J.R., Polyak V., Desrochers A., Asmerom Y. Abrupt global-ocean anoxia during the Late Ordovician-early Silurian detected using uranium isotopes of marine carbonates. *Proc. Natl. Acad. Sci. USA.* 2018;115(23):5896-5901. DOI 10.1073/pnas.1802438115.

Beerling D. CO_2 and the end-Triassic mass extinction. *Nature*. 2002; 415(6870):386-387.

Benton M.J. Diversification and extinction in the history of life. *Science*. 1995;268(5207):52-58.

Blackburn T.J., Olsen P.E., Bowring S.A., McLean N.M., Kent D.V., Puffer J., McHone G., Rasbury E.T., Et-Touhami M. Zircon U-Pb geochronology links the end-Triassic extinction with the Central Atlantic Magmatic Province. *Science*. 2013;340(6135):941-945. DOI 10.1126/science.1234204.

Bond D.P.G., Wignall P.B. The role of sea-level change and marine anoxia in the Frasnian-Famennian (Late Devonian) mass extinction. *Palaeogeogr. Palaeoclimatol. Palaeoecol*. 2008;263(3-4):107-118.

Brennecka G.A., Herrmann A.D., Algeo T.J., Anbar A.D. Rapid expansion of oceanic anoxia immediately before the end-Permian mass extinction. *Proc. Natl. Acad. Sci. USA*. 2011;108(43):17631-17634. DOI 10.1073/pnas.1106039108.

Buatois L.A., Narbonne G.M., Mángano M.G., Carmona N.B., Myrow P. Ediacaran matground ecology persisted into the earliest Cambrian. *Nat. Commun.* 2014;5:3544. DOI 10.1038/ncomms4544.

Burgess S.D., Muirhead J.D., Bowring S.A. Initial pulse of Siberian Traps sills as the trigger of the end-Permian mass extinction. *Nat. Commun*. 2017;8:164. DOI 10.1038/s41467-017-00083-9.

Bush A.M., Hunt G., Bambach R.K. Sex and the shifting biodiversity dynamics of marine animals in deep time. *Proc. Natl. Acad. Sci. USA*. 2016;113(49):14073-14078.

Ceballos G., Ehrlich P.R., Barnosky A.D., García A., Pringle R.M., Palmer T.M. Accelerated modern human-induced species losses: Entering the sixth mass extinction. *Sci. Adv*. 2015;1(5):e1400253. DOI 10.1126/sciadv.1400253.

Cermeño P., Benton M.J., Paz Ó., Vérard C. Trophic and tectonic limits to the global increase of marine invertebrate diversity. *Sci. Rep*. 2017;7:15969. DOI 10.1038/s41598-017-16257-w.

Chen D.Z., Qing H.R., Li R.W. The Late Devonian Frasnian-Famennian (F/F) biotic crisis: Insights from delta C-13(carb), delta C-13(org) and Sr-87/Sr-86 isotopic systematics. *Earth Planet. Sci. Lett*. 2005; 235(1-2):151-166.

Chen D.Z., Tucker M.E., Shen Y.N., Yans J., Preat A. Carbon isotope excursions and sea-level change: implications for the Frasnian-Famennian biotic crisis. *J. Geol. Soc*. 2002;59(6):623-626. DOI 10.1144/0016-764902-027.

Claeys P., Casier J.G., Margolis S.V. Microtektites and mass extinctions: evidence for a late devonian asteroid impact. *Science.* 1992; 257(5073):1102-1104.

Clarkson M.O., Kasemann S.A., Wood R.A., Lenton T.M., Daines S.J., Richoz S., Ohnemueller F., Meixner A., Poulton S.W., Tipper E.T. Ocean acidification and the Permo-Triassic mass extinction. *Science.* 2015;348(6231):229-232. DOI 10.1126/science.aaa0193.

Courtillot V., Fluteau F. Cretaceous extinctions: the volcanic hypothesis. *Science*. 2010;328(5981):973-974.

Darroch S.A., Sperling E.A., Boag T.H., Racicot R.A., Mason S.J., Morgan A.S., Tweedt S., Myrow P., Johnston D.T., Erwin D.H., Laflamme M. Biotic replacement and mass extinction of the Ediacara biota. *Proc. Biol. Sci*. 2015;282(1814):pii20151003. DOI 10.1098/rspb.2015.1003.

Darwin C. The Origin of Species by Means of Natural Selection, or the Preservation of Favoured Races in the Struggle for Life. London, 1872. (Russ. ed.: Darvin Ch. Proiskhozhdenie Vidov Putem Estestvennogo Otbora, ili Sokhranenie Blagopriyatnykh Ras v Bor'be za Zhizn'. Saint-Petersburg: Nauka Publ., 1991).

Decroly O., Goldbeter A. Birhythmicity, chaos, and other patterns of temporal self-organization in a multiply regulated biochemical system. *Proc. Natl. Acad. Sci. USA*. 1982;79(22):6917-6921.

Dieckmann U., Law R. The dynamical theory of coevolution: a derivation from stochastic ecological processes. *J. Math. Biol*. 1996; 34(5-6):579-612.

Eldredge N., Gould S.J. On punctuated equilibria. *Science*. 1997; 276(5311):338-341.

Erlykin A.D., Harper D.A.T., Sloan T., Wolfendale A.W. Mass extinctions over the last 500 myr: an astronomical cause? *Palaeontology*. 2017;60(2):159-167. DOI 10.1111/pala.12283.

Erlykin A.D., Harper D.A.T., Sloan T., Wolfendale A.W. Periodicity in extinction rates. *Palaeontology*. 2018;61:149-158. DOI 10.1111/pala.12334.

Finnegan S., Bergmann K., Eiler J.M., Jones D.S., Fike D.A., Eisenman I., Hughes N.C., Tripati A.K., Fischer W.W. The magnitude and duration of Late Ordovician-Early Silurian glaciation. *Science*. 2011;331(6019):903-906.

Finnegan S., Heim N.A., Peters S.E., Fischer W.W. Climate change and the selective signature of the Late Ordovician mass extinction. *Proc. Natl. Acad. Sci. USA*. 2012;109(18):6829-6834.

Gharaie M.H.M., Matsumoto R., Kakuwa Y., Milroy P.G. Late Devonian facies variety in Iran: volcanism as a possible trigger of the environmental perturbation near the Frasnian-Famennian boundary. *Geol. Quart*. 2004;48(4):323-332.

Gharaie M.H.M., Matsumoto R., Racki G., Kakuwa Y. Chemostratigraphy of Frasnian-Famennian transition: Possibility of methane hydrate dissociation leading to mass extinction. Large ecosystem perturbations: causes and consequences. *Geological Society of America Special Paper*. 2007;424:109-125. DOI 10.1130/2007.2424(07).

Ghienne J.F., Desrochers A., Vandenbroucke T.R., Achab A., Asselin E., Dabard M.P., Farley C., Loi A., Paris F., Wickson S., Veizer J. A Cenozoic-style scenario for the end-Ordovician glaciation. *Nat. Commun.* 2014;5:4485. DOI 10.1038/ncomms5485.

Gill B.C., Lyons T.W., Young S.A., Kump L.R., Knoll A.H., Saltzman M.R. Geochemical evidence for widespread euxinia in the later Cambrian ocean. *Nature.* 2011;469(7328):80-83. DOI 10.1038/nature09700.

Gingerich P.D. Paleontology and phylogeny: patterns of evolution of the species level in early tertiary mammals. *Am. J. Sci*. 1976;276:1-28.

Goldbeter A., Gonze D., Houart G., Leloup J.C., Halloy J., Dupont G. From simple to complex oscillatory behavior in metabolic and genetic control networks. *Chaos.* 2001;11(1):247-260.

Gong Q., Wang X., Zhao L., Grasby S.E., Chen Z.Q., Zhang L., Li Y., Cao L., Li Z. Mercury spikes suggest volcanic driver of the Ordo-

vician-Silurian mass extinction. *Sci. Rep.* 2017;13(7(1)):5304. DOI 10.1038/s41598-017-05524-5.

Gould S.J., Eldredge N. Punctuated equilibria: the tempo and mode of evolution reconsidered. *Paleobiology*. 1977;3:115-151.

Gould S.J., Eldredge N. Punctuated equilibrium comes of age. *Nature*. 1993;366(6452):223-227.

Guex J., Pilet S., Müntener O., Bartolini A., Spangenberg J., Schoene B., Sell B., Schaltegger U. Thermal erosion of cratonic lithosphere as a potential trigger for mass-extinction. *Sci. Rep*. 2016;6:23168. DOI 10.1038/srep23168.

Harish O., Hansel D. Asynchronous rate chaos in spiking neuronal circuits. *PLoS Comput. Biol.* 2015;11(7):e1004266. DOI 10.1371/journal.pcbi.1004266.

Heimdal T.H., Svensen H.H., Ramezani J., Iyer K., Pereira E., Rodrigues R., Jones M.T., Callegaro S. Large-scale sill emplacement in Brazil as a trigger for the end-Triassic crisis. *Sci. Rep*. 2018;8(1):141. DOI 10.1038/s41598-017-18629-8.

Hesse J., Gross T. Self-organized criticality as a fundamental property of neural systems. *Front. Syst. Neurosci.* 2014;8:166. DOI 10.3389/fnsys.2014.00166.

Huang C., Joachimski M.M., Gong Y.M. Did climate changes trigger the Late Devonian Kellwasser Crisis? Evidence from a high-resolution conodont delta O-18(PO4) record from South China. *Earth Planet. Sci. Lett*. 2018;495:174-184. DOI 10.1016/j.epsl.2018.05.016.

Huey R.B., Ward P.D. Hypoxia, global warming, and terrestrial late Permian extinctions. *Science*. 2005;308(5720):398-401.

Hunt G. The relative importance of directional change, random walks, and stasis in the evolution of fossil lineages. *Proc. Natl. Acad. Sci. USA*. 2007;104(47):18404-18408.

Huntley J.W., Kowalewski M. Strong coupling of predation intensity and diversity in the Phanerozoic fossil record. *Proc. Natl. Acad. Sci. USA*. 2007;104(38):15006-15010.

Jackson J.B., Cheetham A.H. Tempo and mode of speciation in the sea. *Trends Ecol. Evol*. 1999;14(2):72-77.

Joachimski M.M., Buggisch W. Anoxic events in the late Frasnian – causes of the Frasnian-Famennian faunal crisis. *Geology.* 1993; 21(8):675-678.

Kaiho K., Oshima N. Site of asteroid impact changed the history of life on Earth: the low probability of mass extinction. *Sci. Rep.* 2017; 7(1):14855. DOI 10.1038/s41598-017-14199-x.

Kaiho K., Oshima N., Adachi K., Adachi Y., Mizukami T., Fujibayashi M., Saito R. Global climate change driven by soot at the K-Pg boundary as the cause of the mass extinction. *Sci. Rep.* 2016;6: 28427. DOI 10.1038/srep28427.

Kaiho K., Yatsu S., Oba M., Gorjan P., Gorjan P., Casier J.G., Ikeda M. A forest fire and soil erosion event during the Late Devonian mass extinction. *Palaeogeogr. Palaeoclimatol. Palaeoecol.* 2013;392: 272-280. DOI 10.1016/j.palaeo.2013.09.008.

Keller G., Adatte T., Pardo A., Bajpai S., Khosla A., Samant B. Cretaceous extinctions: evidence overlooked. *Science.* 2010;328(5981): 974-975. DOI 10.1126/science.328.5981.974-a.

Khlebodarova T.M., Kogai V.V., Fadeev S.I., Likhoshvai V.A. Chaos and hyperchaos in simple gene network with negative feedback and time delays. *J. Bioinform. Comput. Biol*. 2017;15(2):1650042. DOI 10.1142/S0219720016500426.

Khlebodarova T.M., Kogai V.V., Trifonova E.A., Likhoshvai V.A. Dynamic landscape of the local translation at activated synapses. *Mol. Psychiatry*. 2018;23(1):107-114. DOI 10.1038/mp.2017.245.

Khlebodarova T.M., Likhoshvai V.A. Persister cells – a plausible outcome of neutral coevolutionary drift. *Sci. Rep*. 2018;8(1):14309. DOI 10.1038/s41598-018-32637-2.

Khlebodarova T.M., Likhoshvai V.A. Molecular mechanisms of non-inherited antibiotic tolerance in bacteria and archaea. *Mol. Biol*. (*Moscow*). 2019;53(4):475-483. DOI 10.1134/S0026893319040058.

Knoll A.H., Bambach R.K., Canfield D.E., Grotzinger J.P. Comparative Earth history and Late Permian mass extinction. *Science*. 1996; 273:452-457.

Kogai V.V., Likhoshvai V.A., Fadeev S.I., Khlebodarova T.M. Multiple scenarios of transition to chaos in the alternative splicing model. *Int. J. Bifurcat. Chaos*. 2017;27(2):1730006. DOI 10.1142/S0218127417300063.

Lamsdell J.C., Selden P.A. From success to persistence: Identifying an evolutionary regime shift in the diverse Paleozoic aquatic arthropod group Eurypterida, driven by the Devonian biotic crisis. *Evolution.* 2017;71(1):95-110. DOI 10.1111/evo.13106.

Lau K.V., Maher K., Altiner D., Kelley B.M., Kump L.R., Lehrmann D.J., Silva-Tamayo J.C., Weaver K.L., Yu M., Payne J.L. Marine anoxia and delayed Earth system recovery after the end-Permian extinction. *Proc. Natl. Acad. Sci. USA*. 2016;113(9):2360-2365. DOI 10.1073/pnas.1515080113.

Lieberman B.S., Melott A.L. Considering the case for biodiversity cycles: re-examining the evidence for periodicity in the fossil record. *PLoS One.* 2007;2(8):e759.

Lieberman B.S., Melott A.L. Whilst this planet has gone cycling on: what role for periodic astronomical phenomena in large-scale patterns in the history of life? In: Talent J.A. (Ed.). Earth and Life, International Year of Planet Earth. Springer Science and Business Media B.V., 2012;37-50.

Likhoshvai V.A., Fadeev S.I., Khlebodarova T.M. Stasis and periodicity in the evolution of a global ecosystem: the minimum logistic model. *Matematicheskaya Biologiya i Bioinformatika = Mathematical Biology and Bioinformatics*. 2017;12(1):120-136. DOI 10.17537/2017.12.120. (in Russian)

Likhoshvai V.A., Khlebodarova T.M. The minimum logistic model of global ecosystem evolution. Proc. of the VI Int. Conf. "Mathematical Biology and Bioinformatics", Puschino, 16-21 October. 2016; 6:116-117. (in Russian)

Likhoshvai V.A., Khlebodarova T.M. Phenotypic variability of bacterial cell cycle: mathematical model. *Mathematical Biology and Bioinformatics*. 2017;12(Suppl.):t23-t44. DOI 10.17537/2017.12.t23.

Likhoshvai V.A., Kogai V.V., Fadeev S.I., Khlebodarova T.M. Alternative splicing can lead to chaos. *J. Bioinform. Comput. Biol*. 2015; 13(1):1540003. DOI 10.1142/S021972001540003X.

Likhoshvai V.A., Kogai V.V., Fadeev S.I., Khlebodarova T.M. Chaos and hyperchaos in a model of ribosome autocatalytic synthesis. *Sci. Rep*. 2016;6:38870. DOI 10.1038/srep38870.

Likhoshvai V.A., Matushkin Yu.G. Latent phenotype as adaptation reserve: a simplest model of cell evolution. Proc. of the II Int. Conf. "Bioinformatics of Genome Regulation and Structure". Novosibirsk. 2000;1:195-198.

Likhoshvai V.A., Matushkin Yu.G. Sporadic emergence of latent phenotype during evolution. In: Kolchanov N., Hofestaedt R. (Eds.). Bioinformatics of Genome Regulation and Structure. Boston; Dordrecht; London: Kluwer Academic Publishers, 2004;231-243.

Lindskog A., Costa M.M., Rasmussen C.M., Connelly J.N., Eriksson M.E. Refined Ordovician timescale reveals no link between asteroid breakup and biodiversification. *Nat. Commun.* 2017;8:14066. DOI 10.1038/ncomms14066.

Lindström S., Sanei H., van de Schootbrugge B., Pedersen G.K., Lesher C.E., Tegner C., Heunisch C., Dybkjær K., Outridge P.M. Volcanic mercury and mutagenesis in land plants during the end-Triassic mass extinction. *Sci. Adv.* 2019;5(10):eaaw4018. DOI 10.1126/sciadv.aaw4018.

Liu J.S., Qie W.K., Algeo T.J., Yao L., Huang J.H., Luo G.M. Changes in marine nitrogen fixation and denitrification rates during the end-Devonian mass extinction. *Palaeogeogr. Palaeoclimatol. Palaeoecol*. 2016;448:195-206. DOI 10.1016/j.palaeo. 2015.10.022.

Ma X.P., Gong Y.M., Chen D.Z., Racki G., Chen X.Q., Liao W.H. The Late Devonian Frasnian-Famennian event in South China – patterns and causes of extinctions, sea level changes, and isotope variations. *Palaeogeogr. Palaeoclimatol. Palaeoecol.* 2016;448:224-244. DOI 10.1016/j.palaeo.2015.10.047.

Mackey M.C., Glass L. Oscillation and chaos in physiological control systems. *Science.* 1977;197:287-289.

Madin J.S., Alroy J., Aberhan M., Fürsich F.T., Kiessling W., Kosnik M.A., Wagner P.J. Statistical independence of escalatory ecological trends in Phanerozoic marine invertebrates. *Science*. 2006; 312(5775):897-900.

Markov A.V. A new approach to modeling the diversity dynamics of Phanerozoic marine biota. *Zhurnal Obshchei Biologii = Journal of General Biology.* 2001a;62(6):460-471. (in Russian)

Markov A.V. Dynamics of the marine faunal diversity in the Phanerozoic: a new approach. *Paleontol. J.* 2001b;35(1):1-9.

Markov A.V., Korotaev A.V. The dynamics of Phanerozoic marine animal diversity fits the hyperbolic growth model. *Zhurnal Obshchei Biologii = Journal of General Biology*. 2007;68(1):3-18. (in Russian)

Martinez de la Fuente I., Martinez L., Veguillas J., Aguirregabiria J.M. Quasiperiodicity route to chaos in a biochemical system. *Biophys. J.* 1996;71(5):2375-2379.

Marzoli A., Renne P.R., Piccirillo E.M., Ernesto M., Bellieni G., De Min A. Extensive 200-million-year-old continental flood basalts of the central atlantic magmatic province. *Science*. 1999;284(5414): 616-618.

Mattila T.M., Bokma F. Extant mammal body masses suggest punctuated equilibrium. *Proc. Biol. Sci*. 2008;275(1648):2195-2199. DOI 10.1098/rspb.2008.0354.

Mayhew P.J., Bell M.A., Benton T.G., McGowan A.J. Biodiversity tracks temperature over time. *Proc. Natl. Acad. Sci. USA*. 2012; 109(38):15141-15145.

McElwain J.C., Beerling D.J., Woodward F.I. Fossil plants and global warming at the Triassic-Jurassic boundary. *Science.* 1999;285:1386-1390.

Medvedev M.V., Melott A.L. Do extragalactic cosmic rays induce cycles in fossil diversity? *Astrophys. J.* 2007;664(2):879-889. DOI 10.1086/518757.

Melott A.L. Long-term cycles in the history of life: periodic biodiversity in the paleobiology database. *PLoS One*. 2008;3(12):e4044. DOI 10.1371/journal.pone.0004044.

Melott A.L., Bambach R.K. Analysis of periodicity of extinction using the 2012 geological time scale. *Paleobiology.* 2014;40:177-196. DOI 10.1666/13047.

Melott A.L., Bambach R.K. Periodicity in the extinction rate and possible astronomical causes – comment on mass extinctions over the last 500 myr: an astronomical cause? (Erlykin et al.). *Palaeontology*. 2017;60:911-920. DOI 10.1111/pala.12322.

Melott A.L., Bambach R.K., Petersen K.D., McArthur J.M. An similar to 60-million-year periodicity is common to marine $^{87}Sr/^{86}Sr$, fossil biodiversity, and large-scale sedimentation: what does the periodicity reflect? *J. Geol.* 2012;120(2):217-226. DOI 10.1086/663877.

Miller C.S., Peterse F., da Silva A.C., Baranyi V., Reichart G.J., Kürschner W.M. Astronomical age constraints and extinction mechanisms of the Late Triassic Carnian crisis. *Sci. Rep*. 2017;7(1):2557. DOI 10.1038/s41598-017-02817-7.

Newman M.E. A model of mass extinction. *J. Theor. Biol*. 1997a; 189(3):235-252.

Newman M.E. Evidence for self-organized criticality in evolution. *Physica D.* 1997b;107:293-296.

Nichol S.T., Rowe J.E., Fitch W.M. Punctuated equilibrium and positive Darwinian evolution in vesicular stomatitis virus. *Proc. Natl. Acad. Sci. USA*. 1993;90:10424-10428.

Novack-Gottshall P.M. Love, not war, drove the Mesozoic marine revolution. *Proc. Natl. Acad. Sci. USA*. 2016;113(51):14471-14473. DOI 10.1073/pnas.1617404113.

Nykter M., Price N.D., Aldana M., Ramsey S.A., Kauffman S.A., Hood L.E., Yli-Harja O., Shmulevich I. Gene expression dynamics in the macrophage exhibit criticality. *Proc. Natl. Acad. Sci. USA*. 2008;105(6):1897-1900. DOI 10.1073/pnas.0711525105.

Ovcharenko V.N. Transitional forms and speciation of brachiopods. *Paleontologicheskii Zhurnal = Paleontological Journal*. 1969;3: 57-63. (in Russian)

Pagel M., Venditti C., Meade A. Large punctuational contribution of speciation to evolutionary divergence at the molecular level. *Science*. 2006;314:119-121. DOI 10.1126/science.1129647.

Palmer S.A., Clapham A.J., Rose P., Freitas F.O., Owen B.D., Beresford-Jones D., Moore J.D., Kitchen J.L., Allaby R.G. Archaeogenomic evidence of punctuated genome evolution in Gossypium. *Mol. Biol. Evol*. 2012;29:2031-2038. DOI 10.1093/molbev/mss070.

Penn J.L., Deutsch C., Payne J.L., Sperling E.A. Temperature-dependent hypoxia explains biogeography and severity of end-Permian marine mass extinction. *Science*. 2018;362(6419):eaat1327. DOI 10.1126/science.aat1327.

Percival L.M.E., Davies J.H.F.L., Schaltegger U., De Vleeschouwer D., Da Silva A.C., Föllmi K.B. Precisely dating the Frasnian-Famennian boundary: implications for the cause of the Late Devonian mass extinction. *Sci. Rep*. 2018;8(1):9578. DOI 10.1038/s41598-018-27847-7.

Percival L.M.E., Ruhl M., Hesselbo S.P., Jenkyns H.C., Mather T.A., Whiteside J.H. Mercury evidence for pulsed volcanism during the end-Triassic mass extinction. *Proc. Natl. Acad. Sci. USA*. 2017; 114(30):7929-7934. DOI 10.1073/pnas.1705378114.

Peters S.E. Environmental determinants of extinction selectivity in the fossil record. *Nature*. 2008;454(7204):626-629. DOI 10.1038/nature07032.

Petersen H.I., Lindström S. Synchronous wildfire activity rise and mire deforestation at the Triassic-Jurassic boundary. *PLoS One*. 2012; 7(10):e47236. DOI 10.1371/journal.pone.0047236.

Prokoph A., Ernst R.E., Buchan K.L. Time-series analysis of large igneous provinces: 3500 Ma to present. *J. Geol*. 2004;112(1):1-22. DOI 10.1086/379689.

Rampino M.R. Disc dark matter in the Galaxy and potential cycles of extraterrestrial impacts, mass extinctions and geological events. *MNRAS.* 2015;448(2):1816-1820. DOI 10.1093/mnras/stu2708.

Rampino M.R., Caldeira K. Periodic impact cratering and extinction events over the last 260 million years. *MNRAS.* 2015;454(4):3480-3484. DOI 10.1093/mnras/stv2088.

Rampino M.R., Haggerty B.M., Pagano T.C. A unified theory of impact crises and mass extinctions: quantitative tests. *Ann. N.Y. Acad. Sci.* 1997;822:403-431.

Rampino M.R., Rodriguez S., Baransky E., Cai Y. Global nickel anomaly links Siberian Traps eruptions and the latest Permian mass extinction. *Sci. Rep.* 2017;7(1):12416. DOI 10.1038/s41598-017-12759-9.

Rampino M.R., Stothers R.B. Geological rhythms and cometary impacts. *Science.* 1984;226:1427-1431.

Rasmussen C.M.Ø., Kröger B., Nielsen M.L., Colmenar J. Cascading trend of Early Paleozoic marine radiations paused by Late Ordovician extinctions. *Proc. Natl. Acad. Sci. USA.* 2019;116(15):7207-7213. DOI 10.1073/pnas.1821123116.

Rasskin-Gutman D., Esteve-Altava B. The multiple directions of evolutionary change. *Bioessays*. 2008;30(6):521-525. DOI 10.1002/bies.20766.

Raup D.M., Sepkoski J.J. Jr. Mass extinctions in the marine fossil record. *Science.* 1982;215(4539):1501-1503.

Raup D.M., Sepkoski J.J. Periodicity of extinctions in the geologic past. *Proc. Natl. Acad. Sci. USA.* 1984;81(3):801-805.

Raup D.M., Sepkoski J.J. Jr. Periodic extinction of families and genera. *Science.* 1986;231:833-836.

Ricci J., Quidelleur X., Pavlov V., Orlov S., Shatsillo A., Courtillot V. New $^{40}Ar/^{39}Ar$ and K-Ar ages of the Viluy traps (Eastern Siberia): Further evidence for a relationship with the Frasnian-Famennian mass extinction. *Palaeogeogr. Palaeoclimatol. Palaeoecol.* 2013; 386:531-540. DOI 10.1016/j.palaeo.2013.06.020.

Roberts B.W., Newman M.E. A model for evolution and extinction. *J. Theor. Biol*. 1996;180(1):39-54.

Roberts G.G., Mannion P.D. Timing and periodicity of Phanerozoic marine biodiversity and environmental change. *Sci. Rep*. 2019;9(1): 6116. DOI 10.1038/s41598-019-42538-7.

Robertson D.S. Feedback theory and Darwinian evolution. *J. Theor. Biol*. 1991;152(4):469-484.

Rohde R.A., Muller R.A. Cycles in fossil diversity. *Nature*. 2005; 434(7030):208-210.

Sallan L.C., Coates M.I. End-Devonian extinction and a bottleneck in the early evolution of modern jawed vertebrates. *Proc. Natl. Acad. Sci. USA.* 2010;107(22):10131-10135. DOI 10.1073/pnas.0914000107.

Schaller M.F., Wright J.D., Kent D.V. Atmospheric PCO_2 perturbations associated with the Central Atlantic Magmatic Province. *Science*. 2011;331(6023):1404-1409. DOI 10.1126/science.1199011.

Schmitz B., Farley K.A., Goderis S., Heck P.R., Bergström S.M., Boschi S., Claeys P., Debaille V., Dronov A., van Ginneken M., Harper D.A.T., Iqbal F., Friberg J., Liao S., Martin E., Meier M.M.M., Peucker-Ehrenbrink B., Soens B., Wieler R., Terfelt F. An extraterrestrial trigger for the mid-Ordovician ice age: Dust from the breakup of the L-chondrite parent body. *Sci. Adv.* 2019;5(9):eaax4184. DOI 10.1126/sciadv.aax4184.

Schoene B., Eddy M.P., Samperton K.M., Keller C.B., Keller G., Adatte T., Khadri S.F.R. U-Pb constraints on pulsed eruption of the Deccan Traps across the end-Cretaceous mass extinction. *Science.* 2019;363(6429):862-866. DOI 10.1126/science.aau2422.

Schoene B., Samperton K.M., Eddy M.P., Keller G., Adatte T., Bowring S.A., Khadri S.F., Gertsch B. U-Pb geochronology of the Deccan Traps and relation to the end-Cretaceous mass extinction. *Science*. 2015;347(6218):182-184. DOI 10.1126/science.aaa0118.

Schulte P., Alegret L., Arenillas I., Arz J.A., Barton P.J., Bown P.R., Bralower T.J., Christeson G.L., Claeys P., Cockell C.S., Collins G.S., Deutsch A., Goldin T.J., Goto K., Grajales-Nishimura J.M., Grieve R.A., Gulick S.P., Johnson K.R., Kiessling W., Koeberl C., Kring D.A., MacLeod K.G., Matsui T., Melosh J., Montanari A., Morgan J.V., Neal C.R., Nichols D.J., Norris R.D., Pierazzo E., Ravizza G., Rebolledo-Vieyra M., Reimold W.U., Robin E., Salge T., Speijer R.P., Sweet A.R., Urrutia-Fucugauchi J., Vajda V., Whalen M.T., Willumsen P.S. The Chicxulub asteroid impact and mass extinction at the Cretaceous-Paleogene boundary. *Science.* 2010;327(5970):1214-1218. DOI 10.1126/science.1177265.

Seaborg D.M. Evolutionary feedback: a new mechanism for stasis and punctuated evolutionary change based on integration of the organism. *J. Theor. Biol*. 1999;198(1):1-26.

Sepkoski J.J. Jr. Extinctions of life. *Los Alamos Sci*. 1988;16:36-49.

Sepkoski J.J. Jr. Periodicity in extinction and the problem of catastrophism in the history of life. *J. Geol. Soc. London*. 1989;146:7-19.

Sepkoski J.J. Jr. A compendium of fossil marine animal genera. *Bull. Am. Paleontol*. 2002;363:1-560.

Severtsov A.S. Interspecific variety as a cause of evolutionary stability. *Zhurnal Obshchei Biologii = Journal of General Biology.* 1990; 51(5):579-589. (in Russian)

Sheehan P.M. The Late Ordovician mass extinction. *Annu. Rev. Earth Planet. Sci.* 2001;29:331-364.

Sheets H.D., Mitchell C.E., Melchin M.J., Loxton J., Štorch P., Carlucci K.L., Hawkins A.D. Graptolite community responses to global climate change and the Late Ordovician mass extinction. *Proc. Natl. Acad. Sci. USA.* 2016;113(30):8380-8385. DOI 10.1073/pnas.1602102113.

Shen J., Chen J., Algeo T.J., Yuan S., Feng Q., Yu J., Zhou L., O'Connell B., Planavsky N.J. Evidence for a prolonged Permian-Triassic extinction interval from global marine mercury records. *Nat. Commun*. 2019;10(1):1563. DOI 10.1038/s41467-019-09620-0.

Shen Y., Farquhar J., Zhang H., Masterson A., Zhang T., Wing B.A. Multiple S-isotopic evidence for episodic shoaling of anoxic water during Late Permian mass extinction. *Nat. Commun*. 2011;2:210. DOI 10.1038/ncomms1217.

Smolarek-Lach J., Marynowski L., Trela W., Wignall P.B. Mercury spikes indicate a volcanic trigger for the Late Ordovician mass extinction event: an example from a deep shelf of the Peri-Baltic region. *Sci. Rep.* 2019;9(1):3139. DOI 10.1038/s41598-019-39333-9.

Sneppen K., Bak P., Flyvbjerg H., Jensen M.H. Evolution as a self-organized critical phenomenon. *Proc. Natl. Acad. Sci. USA.* 1995; 92:5209-5213.

Solé R.V., Manrubia S.C. Extinction and self-organized criticality in a model of large-scale evolution. *Phys. Rev. E.* 1996;54(1):R42-R45.

Solé R.V., Saldaña J., Montoya J.M., Erwin D.H. Simple model of recovery dynamics after mass extinction. *J. Theor. Biol*. 2010;267(2): 193-200. DOI 10.1016/j.jtbi.2010.08.015.

Song H., Wignall P.B., Chu D., Tong J., Sun Y., Song H., He W., Tian L. Anoxia/high temperature double whammy during the Permian-Triassic marine crisis and its aftermath. *Sci. Rep*. 2014;4:4132. DOI 10.1038/srep04132.

Sun H., Xiao Y., Gao Y., Zhang G., Casey J.F., Shen Y. Rapid enhancement of chemical weathering recorded by extremely light seawater lithium isotopes at the Permian-Triassic boundary. *Proc. Natl. Acad. Sci. USA*. 2018;115(15):3782-3787. DOI 10.1073/pnas.1711862115.

Sutcliffe O.E., Dowdeswell J.A., Whittington R.J., Theron J.N., Craig J. Calibrating the Late Ordovician glaciation and mass extinction by the eccentricity cycles of Earth's orbit. *Geology*. 2000;28(11): 967-970. DOI 10.1130/0091-7613(2000)028<0967:CTLOGA>2.3.CO;2.

Tanner L.H., Hubert J.F., Coffey B.P., McInerney D.P. Stability of atmospheric CO_2 levels across the Triassic/Jurassic boundary. *Nature.* 2001;411(6838):675-677.

Tennant J.P., Mannion P.D., Upchurch P. Sea level regulated tetrapod diversity dynamics through the Jurassic/Cretaceous interval. *Nat. Commun.* 2016;7:12737. DOI 10.1038/ncomms12737.

Them T.R. 2nd, Gill B.C., Caruthers A.H., Gerhardt A.M., Gröcke D.R., Lyons T.W., Marroquín S.M., Nielsen S.G., Trabucho Alexandre J.P., Owens J.D. Thallium isotopes reveal protracted anoxia during the Toarcian (Early Jurassic) associated with volcanism, carbon burial, and mass extinction. *Proc. Natl. Acad. Sci. USA.* 2018;115(26): 6596-6601. DOI 10.1073/pnas.1803478115.

Thibodeau A.M., Ritterbush K., Yager J.A., West A.J., Ibarra Y., Bottjer D.J., Berelson W.M., Bergquist B.A., Corsetti F.A. Mercury anomalies and the timing of biotic recovery following the end-Triassic mass extinction. *Nat. Commun.* 2016;7:11147. DOI 10.1038/ncomms11147.

Valentine J.W., Moores E.M. Plate-tectonic regulation of faunal diversity and sea level: a model. *Nature*. 1970;228:657-659.

Valverde S., Ohse S., Turalska M., West B.J., Garcia-Ojalvo J. Structural determinants of criticality in biological networks. *Front. Physiol.* 2015;6:127. DOI 10.3389/fphys.2015.00127.

Van Bocxlaer B., Damme D.V., Feibel C.S. Gradual versus punctuated equilibrium evolution in the Turkana Basin molluscs: evolutionary events or biological invasions? *Evolution*. 2008;62(3):511-520. DOI 10.1111/j.1558-5646.2007.00296.x.

Veizer J., Godderis Y., Francois L. Evidence for decoupling of atmospheric CO_2 and global climate during the Phanerozoic eon. *Nature*. 2000;408:698-701. DOI 10.1038/35047044.

Voje K.L. Tempo does not correlate with mode in the fossil record. *Evolution.* 2016;70(12):2678-2689. DOI 10.1111/evo.13090.

Voje K.L., Starrfelt J., Liow L.H. Model adequacy and microevolutionary explanations for stasis in the fossil record. *Am. Nat*. 2018; 191(4):509-523. DOI 10.1086/696265.

Wang X., Liu S.A., Wang Z.R., Chen D.Z., Zhang L.Y. Zinc and strontium isotope evidence for climate cooling and constraints on the Frasnian-Famennian (similar to 372 Ma) mass extinction. *Palaeogeogr. Palaeoclimatol. Palaeoecol*. 2018;498:68-82. DOI 10.1016/j.palaeo.2018.03.002.

Whiteside J.H., Olsen P.E., Eglinton T., Brookfield M.E., Sambrotto R.N. Compound-specific carbon isotopes from Earth's largest flood basalt eruptions directly linked to the end-Triassic mass extinction. *Proc. Natl. Acad. Sci. USA.* 2010;107(15):6721-6725. DOI 10.1073/pnas.1001706107.

Wignall P.B., Sun Y., Bond D.P., Izon G., Newton R.J., Védrine S., Widdowson M., Ali J.R., Lai X., Jiang H., Cope H., Bottrell S.H.

Volcanism, mass extinction, and carbon isotope fluctuations in the Middle Permian of China. *Science.* 2009;324(5931):1179-1182. DOI 10.1126/science.1171956.

Williamson P.O. Palaeontological documentation of speciation in Cenozoic molluscs from Turkana basin. *Nature*. 1981;293:437-443.

Wolf Y.I., Viboud C., Holme E.C., Koonin E.V., Lipman D.J. Long intervals of stasis punctuated by bursts of positive selection in the seasonal evolution of influenza A virus. *Biol. Direct*. 2006;1:34. DOI 10.1186/1745-6150-1-34.

Xiao S., Laflamme M. On the eve of animal radiation: phylogeny, ecology and evolution of the Ediacara biota. *Trends Ecol. Evol*. 2009; 24(1):31-40.

Zaffos A., Finnegan S., Peters S.E. Plate tectonic regulation of global marine animal diversity. *Proc. Natl. Acad. Sci. USA*. 2017;114(22): 5653-5658. DOI 10.1073/pnas.1702297114.

Zhang F., Romaniello S.J., Algeo T.J., Lau K.V., Clapham M.E., Richoz S., Herrmann A.D., Smith H., Horacek M., Anbar A.D. Multiple episodes of extensive marine anoxia linked to global warming and continental weathering following the latest Permian mass extinction. *Sci. Adv.* 2018a;4(4):e1602921. DOI 10.1126/sciadv. 1602921.

Zhang F., Xiao S., Kendall B., Romaniello S.J., Cui H., Meyer M., Gilleaudeau G.J., Kaufman A.J., Anbar A.D. Extensive marine anoxia during the terminal Ediacaran Period. *Sci. Adv*. 2018b;4(6):eaan8983. DOI 10.1126/sciadv.aan8983.

Zhu Z., Liu Y., Kuang H., Benton M.J., Newell A.J., Xu H., An W., Ji S., Xu S., Peng N., Zhai Q. Altered fluvial patterns in North China indicate rapid climate change linked to the Permian-Triassic mass extinction. *Sci. Rep*. 2019;9(1):16818. DOI 10.1038/s41598-019-53321-z.

Acknowledgements. The study was carried out with the financial support of the Russian Foundation for Basic Research in the framework of the scientific project 19-14-50159. The authors are grateful to V.V. Suslov for critical comments and useful discussions during manuscript preparation and T. Kalymbetova for the translation of the article from Russian into English.

Conflict of interest. The authors declare no conflict of interest.

Received December 3, 2019. Revised February 3, 2020. Accepted March 24, 2020.

Вавиловский журнал генетики и селекции. 2020;24(4):420-426
DOI 10.18699/VJ20.634

Diagnosis of the mechanisms of different types of discordances between phylogenies inferred from nuclear and mitochondrial markers

A.A. Poroshina ✉, D.Y. Sherbakov, T.E. Peretolchina

Limnological Institute of Siberian Branch of the Russian Academy of Sciences, Irkutsk, Russia
✉ e-mail: a.poroshina@lin.irk.ru

Abstract. In ancient freshwater lakes, an abnormally large species diversity is observed. The mechanisms that generated extremely high biodiversity in the ancient lakes have not been sufficiently studied and remain only partially known. Sequences of environmental changes in highly complex ecosystems such as Lake Baikal, may induce sophisticated combinations of microevolutionary processes. These processes are likely to result in unusual "patterns" of genetic variability of species. The most unusual patterns include the ones when speciation is followed by incomplete lineage sorting as well as mitochondrial or nuclear introgression. All these phenomena are diagnosed by comparing the topologies of phylogenetic trees inferred from molecular markers of evolution located in mitochondria and nuclei. Mitochondrial and nuclear introgression is a particularly interesting and complex case, which is the process of incorporating the gene alleles of one species into the gene pool of a sister species due to interspecific hybridization (introgressive hybridization). In many cases, existing methods for molecular phylogenetic analysis do not automatically allow the observed patterns of polymorphism to be explained and, therefore, cannot provide hypotheses that would explain the mechanisms which resulted to these patterns. Here we use adaptive dynamics models to study neutral molecular evolution under various scenarios of interaction between sister species and the environment. We propose and justify a set of criteria for detecting how two evolutionary trees may differ, with a special focus on comparing a tree inferred from nuclear DNA to one from mitochondrial DNA. The criteria react to branching pattern and branch lengths, including relative distances from ancestral lineages. Simulations show that the criteria allow fast and automated detection of various types of introgression, secondary breaches of reproductive barriers, and incomplete lineage sorting.

Key words: mitochondrial introgression; incomplete lineage sorting; ancient lakes; sympatric speciation; parapatric speciation; disagreements between phylogenies; Lake Baikal.

For citation: Poroshina A.A., Sherbakov D.Y., Peretolchina T.E. Diagnosis of the mechanisms of different types of discordances between phylogenies inferred from nuclear and mitochondrial markers. *Vavilovskii Zhurnal Genetiki i Selektsii = Vavilov Journal of Genetics and Breeding*. 2020;24(4):420-426. DOI 10.18699/VJ20.634

Метод выявления и определения типов несоответствий между филогенетическими деревьями, построенными по ядерным и митохондриальным маркерам

А.А. Порошина ✉, Д.Ю. Щербаков, Т.Е. Перетолчина

Лимнологический институт Сибирского отделения Российской академии наук, Иркутск, Россия
✉ e-mail: a.poroshina@lin.irk.ru

Аннотация. В древних пресноводных озерах наблюдается аномально большой видовой состав организмов. Механизмы, которые обусловили формирование биоразнообразия в древних озерах, еще недостаточно изучены. Микроэволюционные процессы, приводящие в конечном итоге к видообразованию, включают в себя в качестве элементарных процессов изменения численности особей, миграцию и репродуктивную изоляцию. В природных условиях, особенно в такой сложной экосистеме, как экосистема Байкала, комбинации микроэволюционных процессов могут носить самый причудливый характер и порождать необычные «узоры» генетической изменчивости видов. К наиболее необычным следам сложных видообразовательных процессов относятся унаследованный полиморфизм, а также митохондриальная и ядерная интрогрессии. Эти явления диагностируются на основании сравнения топологий филогенетических деревьев, построенных по ядерным и митохондриальным молекулярным маркерам эволюции. Особенно интересный и сложный случай – митохондриальная и ядерная интрогрессия, представляющая собой процесс включения аллелей генов одного вида в генофонд сестринского вида при межвидовой гибридизации (интрогрессивная гибридизация). Часто существующие методы анализа генетического полиморфизма не позволяют автоматически находить объяснение наблюдаемых картин полиморфизма и, следовательно, предлагать гипотезы, которые бы раскрыли меха-

низмы, породившие эти картины. В настоящей работе мы используем модели адаптивной динамики для изучения нейтральной молекулярной эволюции при различных сценариях взаимодействия между сестринскими видами и окружающей средой. Мы предлагаем набор критериев для определения того, как могут различаться два эволюционных дерева, построенных с использованием последовательностей ядерной и митохондриальной ДНК. Моделирование показывает, что критерии позволяют быстро и автоматически выявлять различные типы интрогрессии, вторичные нарушения репродуктивных барьеров и неполное расхождение видов.
Ключевые слова: митохондриальная интрогрессия; неполная сортировка родословной; древние озера; симпатрическое видообразование; парапатрическое видообразование; разногласия между филогениями; озеро Байкал.

Introduction

Significant advances in gathering the data on genetic polymorphisms of all kinds of organisms have shed light on important features of the evolutionary process. For example, recent technique, allow one to study previously cryptic features of the mechanisms, generating and maintaining the diversity of life. Among the most challenging foci of modern evolutionary studies are the hyper-diverse and geographically constrained ancient freshwater lakes (Lake Baikal in East Siberia, Lake Tanganyika in East Africa etc). These lakes are inhabited by rapidly evolving species assemblages generated by adaptive radiation, mostly in sympatry, and ultimately responding to the fast and powerful environmental challenges generated by global changes (Brooks, 1950; Sherbakov, 1999; Salzburger et al., 2014). Studies of speciation processes in ancient lakes revealed numerous cases of presumably complicated evolutionary histories and therefore many unexpected patterns of genetic diversity. The most striking are the cases of dramatic discordance between the patterns resulting the studies of mitochondrial and nuclear DNA described in (Nevado et al., 2009; Sturmbauer et al., 2010; Kéver et al., 2018).

Although these phenomena are well and long known to exist in many species, their explanations involve the assumption of large-scale range shifts (Toews, Brelsford, 2012; Schön, Martens, 2012) and thus are hardly applicable to the situations of sympatric or parapatric speciation responsible for the most of the species diversification in relatively small and closed ecosystems. A systematic study of disagreements between mitochondrial and nuclear phylogenies requires a formal procedure automating search for such cases, such as testing significance of the disagreement and modelling of evolutionary scenarios likely to cause generation of the discrepancies between nuclear and cytoplasmic phylogenies. Here we describe fast simultaneous analysis of two tree topologies allowing one to detect a discordance, test its significance and diagnose its type. We test this approach on a set of trees resulting simulations of evolutionary events and on the real-world data set on endemic to Lake Baikal gastropods of genus *Baicalia*.

Materials and methods

Individual based modeling. Individual-based models (Grimm, Railsback, 2005) simulating evolution of two sister species of diploid organisms possessing both mitochondrial and nuclear DNA markers were designed as described in (Semovski et al., 2004). Differential responses of the sister species to the same environmental challenges were modelled by pre-setting independent curves of environmental niche capacity for the two sympatrically occurring species. Model also allows independent variation of gene flows between the species thus mimicking asymmetric or symmetric breach of the reproductive barrier during defined periods of time. Each simulation was succeeded by collection of certain amount (usually 100 of each to make it comparable to an experimental study) of marker sequences from the same "individuals", saved in separate files and maximum likelihood trees were inferred with PhyML version 3.3.20180129 (Guindon et al., 2010), using the model of molecular evolution set to JC because of the simulation settings. Tree comparisons were performed with custom Python scripts using ete2 library (Huerta-Cepas et al., 2010).

Types of discordances between mitochondrial and nuclear markers. Discordance between nuclear and mitochondrial trees should be declared when their branching patterns differ significantly so that one of them looks distorted strongly if compared to the other. We test following kinds of phylogeny discordances of two sister groups of organisms may occur:

- **splitting into two species**;
- **introgression** is when on the one tree all groups form separate clades, while on the other tree one group appears inside the cluster formed by the other group. In other words, the common for one group allele becomes fully substituted with the allele originated from the other group;
- **inherited polymorphism (incomplete lineage sorting)** is when due to resent breach of reproductive barrier both groups acquire alleles from the other ones. Discriminating between different types of branching order discordances.

In order to detect the cases of introgressions while comparing data sets, we had developed the test, which was used then to optimize the processing of fairly large amounts of data. The test employs three values estimated from the phylogenies (Fig. 1). The first value is the corrected mutational distance between the common ancestors of the two species (nodes L_A and L_B) and the most basal node *CA* (common ancestor of the two species). In the case of inherited polymorphism all three points in fact are the same point and thus all three distances are equal to zero. Therefore if all three distances insignificantly differ from zero one may assume incomplete sorting of ancestral lineages. Obviously all three distances would have significant lengths if unaccomplished divergence of the two species took place. We can also find the distance between *CA* and *L* (d) for two species and find their difference (D). With inherited polymorphism and separation into two types, the distances d_a and d_b will be approximately equal.

The second value useful for detecting of introgression is the sum of all distances from all representatives of the same species to the most recent common ancestral node of the tree (E_Σ if the number of specimens of the two species analyzed is very far from equal, the average distance $\hat{E}$ by a species must be used). In spite of any accomplishments this value should be approximately equal if molecular clock hypothesis holds.

The latter condition may be tested separately. The significantly different from zero value of the difference between $\hat{E}_A$ and $\hat{E}_b$ determined for one molecular marker, i. e. mitochondrial gene while remaining approximately equal for other marker(s) points at full introgression (see Fig. 1).

The possibility of a dramatic violations of molecular clock hypothesis as well as numerous other reasons make it necessary to support the hypothesis on the introgression independently. Here we propose to use for that purpose the test for monophyly of the clades in question. We employed the simplest form of the test as it is implemented in ete2 and ete3 libraries for Python (http://etetoolkit.org/). Based on the topology of the tree it calculates the coefficient of monophyly, *P*. It becomes 0 in case of a monophyletic clade and 1 in case of polyphyly.

The values and designations involved in the analysis are: P – inherited polymorphism; I – introgression; 2s – two species; *P* – coefficient of polyphyleticity (0: monophyletic, 1: polyphyletic); *CA* – closest common ancestor; L – furthest descendant of the common ancestor indexed by the species; *d* – distance (along the tree) from *CA* to L indexed by the species.

It is important to note that the protocol (pipeline) described here makes it easy to test directly the statistical significance of the diagnosis. This may be done by applying it to the bootstrap replicates of the original data set followed by odds ratio test to estimate the support to the conclusion.

In the case of the full introgression all sequences of one type appear as the ingroup(s) to the recipient type. The other marker yields monophyletic clusters consisting of a single type of sequences. The four cases above may be diagnosed by measuring the distances between the common ancestors of sequences as they appear on the tree and comparing them to distances from the common ancestors to the common root in combination with the monophyleticity test for the both sister groups. Indeed, the inner branch between the common ancestors of two groups passes the node defined by the outgroup in all cases except for complete introgression. In the latter case the common ancestor of the recipient group is connected to the outgroup via the common ancestor of the donor group. In this case the donor group is always polyphyletic, while the recipient may be both monophyletic or polyphyletic if the introgression occurred more then, once or multiple donor's lineages were involved. Mutual introgression from the recent bi-directional hybridization generates the latter pattern in both directions. In this case each type of sequences appears in the other cluster as an ingroup.

Introgression differs from incomplete lineage sorting because in former case common ancestors of the invader (donated) lineages would be significantly younger then the common ancestor of the recipient. In contrast, incomplete sorting of ancestral lineages results in the absence of separate clusters for the two groups in case of one of the markers. The simplest cause of the latter may be the insufficient rate of molecular evolution of the marker affected.

In all cases the internal branching order must be robustly supported, and the branches crucial for the diagnosis must have significant lengths. Therefore testing the diagnosis significance simply turns into testing the significance of the sum of branch lengths between common ancestors of the groups (species)

	Tree	D	*P*
IP	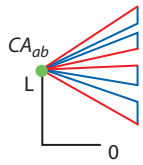	$d_a = d_b$	1
I	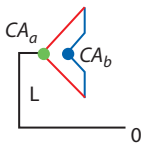	$d_a \neq d_b$	1
2s	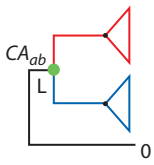	$d_a = d_b$	0

Fig. 1. Schematic representation of the distortions to the tree topology resulting the inherited polymorphism (incomplete lineage sorting) and full introgression as compared to the unspoiled separation of two sister species.

	Mitochondrial introgression	Nuclear introgression	Inherited polymorphism
a	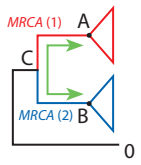	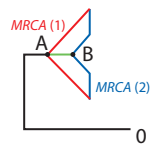	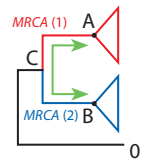
b	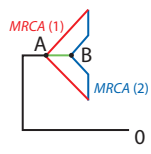	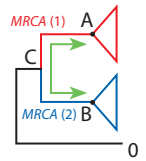	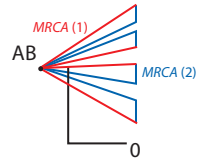

Fig. 2. The respective position of the most recent common ancestors (*MRCA*) in trees inferred from nuclear and mitochondrial introgressions.

Upperraw (*a*): trees inferred from nuclear markers, lower raw (*b*): trees inferred from mitochondrial markers.

and the most ancestral node of the tree. There are several methods of estimating the confidence limits of the branch length (Felsenstein, Felenstein, 2004; Anisimova, Gascuel, 2006).

Additional feature helping to diagnose the distortions of tree topology is the monophyleticity of the groups. In the case of the lack of any discordance, the mutual correspondence must hold between the groups and clades on the tree.

If the tree is rooted by outgroup (Fig. 2, scheme of a fully resolved phylogeny of two groups showing designations used in this paper) CA_A and CA_B labelled with colored dots designate the common ancestors of the respective groups, O is their common ancestor as it is defined by the outgroup) linked to the common ancestor of species A and B with their common ancestors designated as it is shown on the same figure, the relative position of the three nodes will distinguish

Table 1. Diagnostic of the tree distortions (nuclear or mitochondrial)

Pattern	Group A is monophyletic	Group B is monophyletic	CA_A	CA_B	$CA_{A\in B}$	$CA_{B\in A}$
Division into 2 species	+	+	> L	> L	0	0
Introgression	–	+	≥ L	≥ L	> 0	0
Inherited polymorphism	–	–	= L	= L	0	0

between full introgressions if taken together with the results of testing the groups for monophyleticity. All possible outcomes are summarized in Table 1 (L is the distance between the common ancestor of a groups to the common ancestor of the two groups).

***Baicalia* sequences.** Sampling locations of *Baicalia* specimens are specified in (Peretolchina et al., 2007). Genomic DNA was extracted from muscle tissue using a modified method described earlier (Sokolov, 2000). Gene fragments of mitochondrial cytochrome *c* oxidase subunit 1 (COI) were amplified using primers L1490 (5′-GGTCAACAAATCATAAAGATATTGG-3′) and H2198 (5′-TAAACTTCAGGGTGACCAAAAAATCA-3′) (Folmer et al., 1994); fragments of the internal transcribed spacer (ITS1) were amplified using primers Kp-2F (5′-AAAAAGCTTCCGTAGGTGAACCTGCG-3′) and 5.8SR (5′-AGCTTGGTGCGTTCTTCATCGA-3′) (Nazar, Roy, 1978). An average of 1–3 μL of DNA extracted was amplified in a 25 μL reaction using BioMaster HS-Taq PCR Kit (Biolabmix, Russia) under the conditions recommended by the manufacturer. The conditions for amplification, electrophoresis and amplicon purification are those in T.E. Peretolchina et al. (2007). GenBank accession numbers of ITS1 sequences: FJ598711, FJ598712, FJ598715–FJ598723, FJ598727–FJ598732, FJ598735–FJ598741, FJ598743–FJ598745, FJ598748–FJ598760, FJ598762–FJ598771, FJ598832–FJ598848; of COI sequences: Z92995 (Zubakov et al., 1997), HQ113269–HQ113278, DQ436384–DQ436443, GU22640–GU22649, KT885116, FJ749133.

Software availability. All custom software used in this work is available from https://github.com/dysh/MRDR.

Results and discussion

We have used several example phylogenies resulted from computer experiments where various scenarios were used to generate different patterns of disagreements between maternally inherited mitochondrial and nuclear DNA of diploid organisms. The simulations involved differential responses of sister species to the changes of environmental capacity accompanied by periods of reproductive isolation breaches. Each simulation produced two sets of "DNA sequences" (Semovski et al., 2004) used for tree inferences subsequently compared to each other using the procedure described here. All kinds of disagreements between the trees were obtained in course of these simulations and successfully classified using the distances between ancestral roots and tests for motophyleticity (Table 2). An example of full mitochondrial introgression is shown on Fig. 3 (circles designate common ancestors. The trees are rooted with the starting sequence used in the simulation).

Experimental data example: genus *Baicalia*. Gastropod genus *Baicalia* belonging to the subfamily Baicaliinae endemic to Lake Baikal consists of five species diverged from the common ancestor relatively recently in confines of the lake (Sherbakov, 1999). Species of this genus differ morphologically and ecologically. The most remarkable ecological difference between them is their substrate–dependent mating behavior. Both nuclear and mitochondrial markers have been used in phylogenetic inferences involving the species of *Baicalia* (Zubakov et al., 1997; Peretolchina et al., 2007; Sitnikova et al., 2016). Dramatic discrepancies between phylogenies inferred from several nuclear markers and mitochondrial markers are reported to be typical for the whole group and for *Baicalia* in particular (Peretolchina et al., 2007; Sitnikova et al., 2016). Here we have reproduced phylogenetic inferences using the data set consisting of two markers of different inheritance mode belonging to three *Baicalia* species: *B. carinata*, *B. dybowskiana* and *B. turriformis* from (Peretolchina et al., 2007). Two separate phylogenies have been obtained for the nuclear gene ITS1 and mitochondrial COI. Maximum likelihood trees obtained differed from each other (Fig. 4).

The two species, *B. dybowskiana* and *B. turriformis*, appear as monophyletic separate clades in a phylogeny inferred from

Table 2. Metrics of the ML trees inferred from simulated data

Treefiles	Group A is monophyletic	Group B is monophyletic	CA_A	CA_B	$CA_{A\in B}$	$CA_{B\in A}$	Type
tree2S mit root.tre	+	+	0.038290	0.040520	0	0	Division into 2 species
tree2S n root.tre	+	+	0.082230	0.19520	0	0	
treeINT mit root.tre	–	+	0.026070	0	0	> 0	Introgression
treeINT n root.tre	–	+	0.050680	0.087960	> 0	> 0	
treeIP mit root.tre	–	–	0	0	0	0	Inherited polymorphism
treeIP n root.tre	–	–	0	0	0	0	

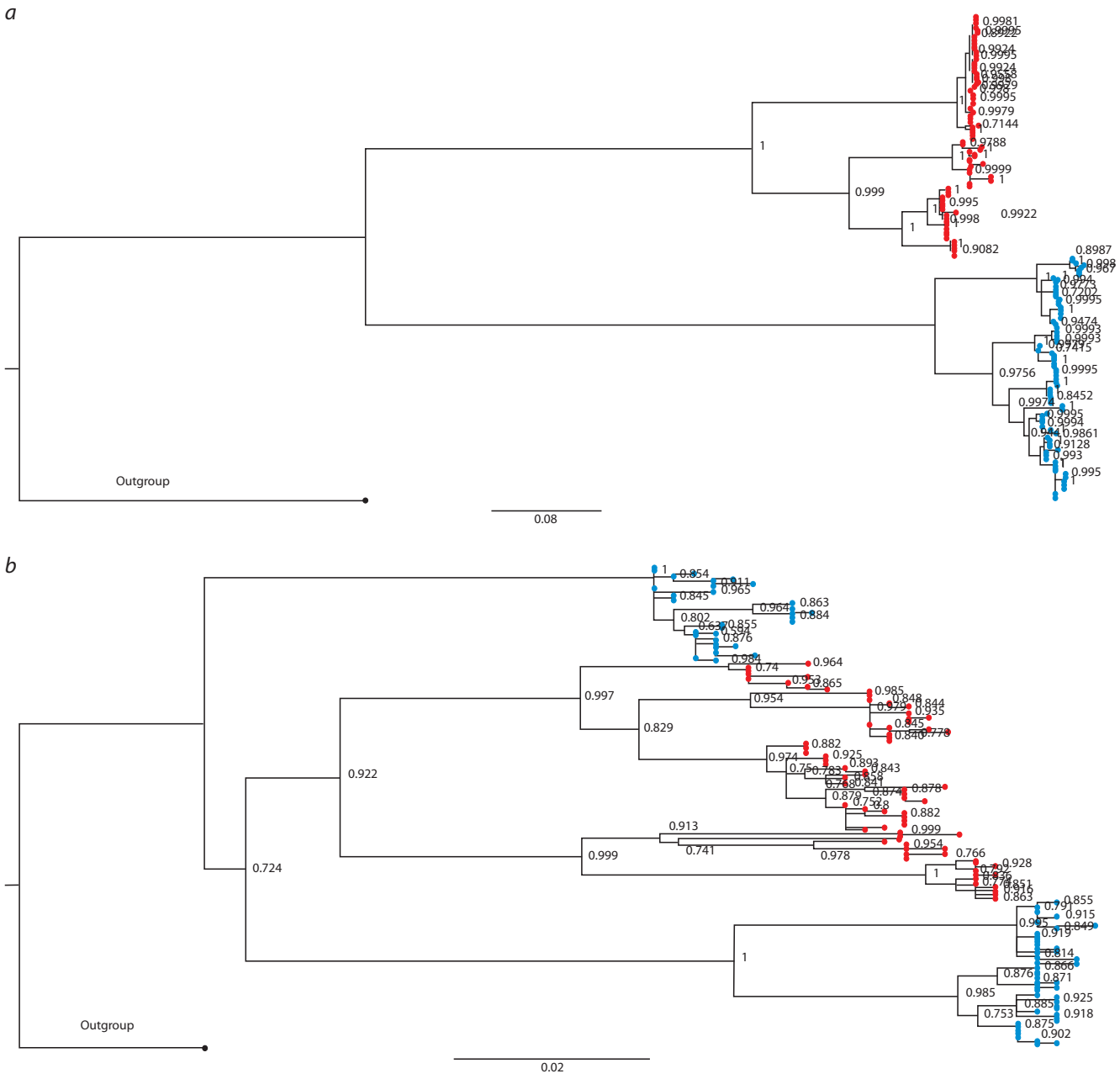

Fig. 3. Phylogenetic trees inferred from simulated data sets.

a – the tree inferred from "sequences" evolving as neutral nuclear marker; *b* – the tree based on "sequences" evolved according to the rules specific for mitochondrial DNA. The aLRT supports are given in the nods of trees.

nuclear sequences. According to the tree inferred from the sequences of mitochondrial origin both *B. dybowskiana* and *B. turriformis* become in-groups to *B. carinata*. However, their clusters are separated from each other. This example illustrates that discrepancies between phylogenies may be relative and complicated if traced in more than two groups: while there are clear indications of full mitochondrial introgressions from *B. carinata* to *B. turriformis* and to *B. dybowskiana*, if the representatives of latter two species are subjected to phylogenetic inference in the absence of *B. carinata* there is no discrepancy between the trees inferred from different markers. Interestingly, the two introgressions were not simultaneous and occurred with a large time gap.

Conclusion

We present here a simple and fast procedure allowing one to distinguish automatically between contrasting patterns of disagreement between trees inferred for the same groups of organisms using different sets of data. In this communication we concentrate on the comparison between trees inferred from DNA sequences of mitochondrial and nuclear origin. First, we define different kinds of disagreements between the tree topologies (introgression, ancestral polymorphism) and propose the set of criteria, which may be estimated from a phylogeny. The approach is based on the estimating distances between common ancestors of groups defined externally, for example, by species identity of their members. Two trees are

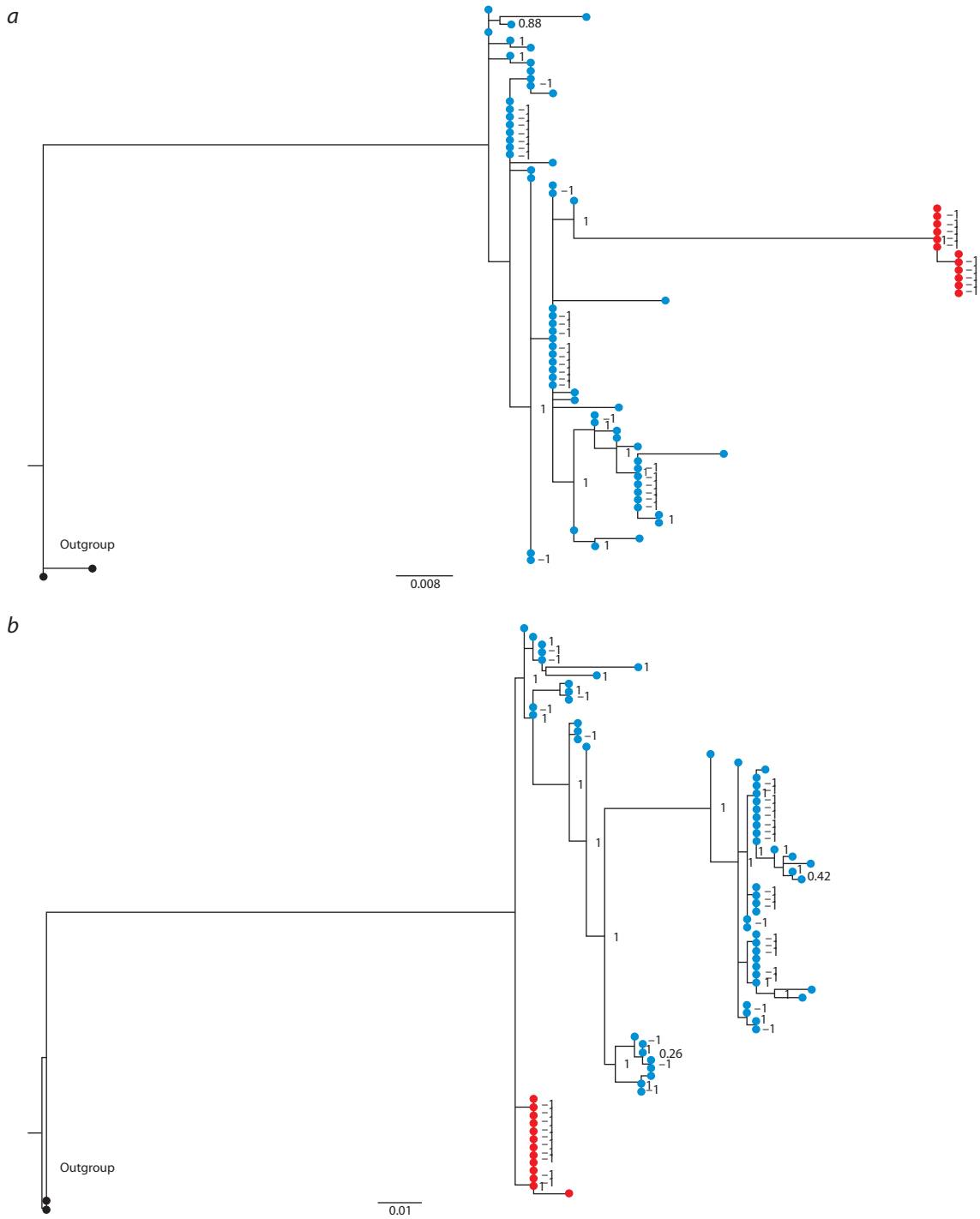

Fig. 4. Phylogenetic trees inferred from DNA sequences of a mitochondrial marker COI (*a*) and nuclear marker ITS1 (*b*) for three sister species of gastropods belonging to genus *Baicalia* (*B. carinata* (blue), and *B. dybowskiana* (red)).

The trees are rooted by outgroups consisting of all paralogous sequences belonging to other Baicaliinae. The aLRT supports are given in the nods of trees.

used as the input, the groups are tested if they are monophyletic and then set of distances between clusters is measured. At this point it is possible to test for the statistical significance of the distortions and their diagnoses using any appropriate approach such as various kinds of bootstrapping.

This procedure is required for any modeling efforts aiming at the elucidation of ecological circumstances favoring different types of disagreements between trees inferred for the same organisms. It is interesting to note, that the same procedure is potentially applicable to the cases when several sets of loci of the same mode of inheritance give rise to dramatically different trees due to selection or adaptation-guided acquisition from sister taxa. The discordance detection procedure proposed here is fast and sufficient to browse transcriptomes in search of sequence cliques evolving accordingly to each other but differently from other large sets of sequences.

References

Anisimova M., Gascuel O. Approximate likelihood-ratio test for branches: a fast, accurate, and powerful alternative. *Syst. Biol*. 2006; 55(4):539-552. DOI 10.1080/10635150600755453.

Brooks J.L. Speciation in ancient lakes (concluded). *Quart. Rev. Biol*. 1950;25(2):131-176. DOI 10.1086/397539.

Felsenstein J., Felenstein J. Inferring Phylogenies. Vol. 2. Sinauer Associates. Sunderland, 2004.

Folmer O., Black M., Hoeh W., Lutz R., Vrijenhoek R. DNA primers for amplification of mitochondrial cytochrome *c* oxidase subunit I from diverse metazoan invertebrates. *Mol. Mar. Biol. Biotechnol*. 1994;3:294-299.

Grimm V., Railsback S.F. Individual-Based Modeling and Ecology. Princeton: Princeton University Press, 2005.

Guindon S., Dufayard J.F., Lefort V., Anisimova M., Hordijk W., Gascuel O. New algorithms and methods to estimate maximum-likelihood phylogenies: assessing the performance of PhyML 3.0. *Syst. Biol*. 2010;59(3):307-321. DOI 10.1093/sysbio/syq010.

Huerta-Cepas J., Dopazo J., Gabaldón T. ETE: a python environment for tree exploration. *BMC Bioinformatics*. 2010;11(1);24. DOI 10.1186/1471-2105-11-24.

Kéver L., Parmentier E., Derycke S., Verheyen E., Snoeks J., Steenberge M., Poncin P. Limited possibilities for prezygotic barriers in the reproductive behaviour of sympatric Ophthalmotilapia species (Teleostei, Cichlidae). *Zoology*. 2018;126:71-81. DOI 10.1016/j.zool.2017.12.001.

Nazar R.N., Roy K.L. Nucleotide sequence of rainbow trout (*Salmo gairdneri*) ribosomal 5.8 S ribonucleic acid. *J. Biol. Chem*. 1978; 253(2):395-399.

Nevado B., Koblmüller S., Sturmbauer C., Snoeks J., Usano-Alemany J., Verheyen E. Complete mitochondrial DNA replacement in a Lake Tanganyika cichlid fish. *Mol. Ecol*. 2009;18(20):4240-4255. DOI 10.1111/j.1365-294X.2009.04348.x.

Peretolchina T.E., Bukin Y.S., Sitnikova T.Y., Sherbakov D.Y. Genetic differentiation of the endemic Baikalian mollusk *Baicalia carinata* (Mollusca: Caenogastropoda). *Russ. J. Genet*. 2007;43(12):1400-1407. DOI 10.1134/S1022795407120095.

Salzburger W., Van Bocxlaer B., Cohen A.S. Ecology and evolution of the African Great Lakes and their faunas. *Annu. Rev. Ecol. Evol. Syst.* 2014;45:519-545. DOI 10.1146/annurev-ecolsys-120213-091804.

Schön I., Martens K. Molecular analyses of ostracod flocks from Lake Baikal and Lake Tanganyika. *Hydrobiologia*. 2012;682(1):91-110. DOI 10.1007/s10750-011-0935-6.

Semovski S.V., Verheyen E., Sherbakov D.Y. Simulating the evolution of neutrally evolving sequences in a population under environmental changes. *Ecol. Modelling*. 2004;176(1-2):99-107. DOI 10.1016/j.ecolmodel.2003.07.013.

Sherbakov D.Y. Molecular phylogenetic studies on the origin of biodiversity in Lake Baikal. *Trends Ecol. Evol*. 1999;14(3):92-95. DOI 10.1016/S0169-5347(98)01543-2.

Sitnikova T., Kovalenkova M., Peretolchina T., Sherbakov D. A new, genetically divergent species of *Pseudobaikalia* Lindholm, 1909 (Caenogastropoda, Baicaliidae). *ZooKeys*. 2016;593:1. DOI 10.3897/zookeys.593.8511.

Sokolov E.P. An improved method for DNA isolation from mucopolysaccharide-rich molluscan tissues. *J. Moll. Stud*. 2000;66(4):573-575. DOI 10.1093/mollus/66.4.573.

Sturmbauer C., Salzburger W., Duftner N., Schelly R., Koblmüller S. Evolutionary history of the Lake Tanganyika cichlid tribe Lamprologini (Teleostei: Perciformes) derived from mitochondrial and nuclear DNA data. *Mol. Phylogenet. Evol*. 2010;57(1):266-284. DOI 10.1016/j.ympev.2010.06.018.

Toews D.P.L., Brelsford A. The biogeography of mitochondrial and nuclear discordance in animals. *Mol. Ecol*. 2012;21(16):3907-3930. DOI 10.1111/j.1365-294X.2012.05664.x.

Zubakov D.I., Shcherbakov D.I., Sitnikova T.I. Analysis of phylogeny of endemic mollusca of family Baicaliidae, Clessin 1878 (Gastropoda, Pectinibranchia) from Baical lake using fragments of nucleotide sequences of the mitochondrial gene *CO1*. *Mol. Biol.* (*Moscow*). 1997;31(6):1092-1097.

ORCID ID

A.A. Poroshina orcid.org/0000-0002-3234-8955
D.Y. Sherbakov orcid.org/0000-0002-1410-392X
T.E. Peretolchina orcid.org/0000-0002-2950-9762

Author contributions. DS wrote the manuscript and wrote the custom computer code, AP wrote computer code and performed the simulations, TP performed the experimental work and preliminary processing of data.

Acknowledgements. The study was funded by the topic of budget financing of Limnological Institute SB RAS 0345-2016-0004 (AAAA-A16-116122110060-9).

Conflict of interest. The authors declare that the research was conducted in the absence of any commercial or financial relationships that could be construed as a potential conflict of interest.

Received October 13, 2019. Revised April 10, 2020. Accepted April 11, 2020.

Вавиловский журнал генетики и селекции. 2020;24(4):427-434
DOI 10.18699/VJ20.635

Effect of gonadectomy and estradiol on the expression of insulin signaling cascade genes in female and male mice

T.V. Iakovleva[1] ✉, N.E. Kostina[1], E.N. Makarova[1], N.M. Bazhan[1, 2]

[1] Institute of Cytology and Genetics of Siberian Branch of the Russian Academy of Sciences, Novosibirsk, Russia
[2] Novosibirsk State University, Novosibirsk, Russia
✉ e-mail: jakov@bionet.nsc.ru

Abstract. A positive effect of estradiol on insulin sensitivity has been shown for females and males. Insulin sensitivity is higher in females than in males, and males show a greater tendency to develop metabolic disorders. It is believed that these sex differences are due to a protective effect of estradiol in females, but not in males. Estradiol is a steroid hormone, and its effect is due to the modulation of target gene expression, but the effect of estradiol on the expression of genes encoding insulin signal transduction and glucose transport has not been sufficiently studied. The aim of the study was to compare the molecular mechanisms of the estradiol influence on insulin sensitivity in mice of both sexes. The effect of gonadectomy and estradiol (1 μg/animal, three days) on the expression of insulin signaling cascade genes in muscle, adipose tissue, and liver, as well as on the expression of *Fgf21*, estradiol receptors (*Esr1/2*), and transcription factor *Stat3* in the liver in female and male mice was investigated. Estradiol levels were lower and glucose blood levels and insulin resistance were higher in Sham operated (Sham) males compared to Sham females. *Irs2*, *Pik3cd*, and *Esr1/2* mRNA levels were lower in the liver of Sham males than in Sham females. In females, gonadectomy reduced the level of estradiol in the blood, increased insulin resistance and blood glucose levels compared to Sham females. Administration of estradiol to gonadectomized females decreased blood insulin levels and insulin resistance. In males, gonadectomy, on the contrary, increased the blood estradiol level, decreased blood insulin level and insulin resistance. Estradiol did not affect the parameters studied in males. The development of insulin resistance in gonadectomized females was associated with a decreased expression of the *Irs2* gene in the liver. Increased insulin sensitivity in gonadectomized males was associated with increased levels of *Irs2* and *Pik3cd* mRNA in the liver. It can be assumed that increasing the level of estradiol in the blood activates the expression of the *Irs2* gene in the liver regardless of animal sex. Also, estradiol seems to regulate the transport of glucose in adipose tissue regardless of animal sex: in females and males, an increase in the blood estradiol level was associated with a decrease in the expression of the *Slc2a4* gene in adipose tissue. Thus, the effects of estradiol on the expression of insulin cascade genes do not seem to depend on animal sex, but have tissue specificity. Since the molecular mechanism of estradiol influence on the expression of insulin cascade genes in females and males is the same, the cause of sexual differences in insulin sensitivity and the rate of development of metabolic disorders may be a decrease in the level of estradiol in the blood, as well as a decrease in the expression of estradiol receptors in the liver in males compared to females.
Key words: gonadectomy; estradiol; testosterone; insulin sensitivity; gene expression; C57BL/6J mice.

For citation: Iakovleva T.V., Kostina N.E., Makarova E.N., Bazhan N.M. Effect of gonadectomy and estradiol on the expression of insulin signaling cascade genes in female and male mice. *Vavilovskii Zhurnal Genetiki i Selektsii = Vavilov Journal of Genetics and Breeding*. 2020;24(4):427-434. DOI 10.18699/VJ20.635

Влияние гонадэктомии и эстрадиола на экспрессию генов сигнального каскада инсулина у самок и самцов мышей

Т.В. Яковлева[1] ✉, Н.Е. Костина[1], Е.Н. Макарова[1], Н.М. Бажан[1, 2]

[1] Федеральный исследовательский центр Институт цитологии и генетики Сибирского отделения Российской академии наук, Новосибирск, Россия
[2] Новосибирский национальный исследовательский государственный университет, Новосибирск, Россия
✉ e-mail: jakov@bionet.nsc.ru

Аннотация. В настоящее время показано положительное влияние эстрадиола на чувствительность к инсулину на уровне целого организма у самок и самцов мышей. При этом чувствительность к инсулину в целом у самок выше, чем у самцов, и самцы демонстрируют большую склонность к развитию метаболических нарушений. Предполагают, что данные половые различия объясняются протективным действием эстрадиола у самок, но не у самцов. Эстрадиол является стероидным гормоном, и его действие обусловлено модуляцией экспрессии генов-мишеней, однако влияние эстрадиола на экспрессию генов, кодирующих трансдукцию сигнала инсулина и транспорт глюкозы в клетку, изучено недостаточно. Целью работы было сравнительное исследование молекулярных механизмов влияния эстрадиола на чувствительность к инсулину у мышей обоих полов. Исследовано

влияние гонадэктомии и эстрадиола (1 мкг/животное, три дня) на экспрессию генов сигнального каскада инсулина в мышцах, жировой ткани и печени, а также на экспрессию *Fgf21*, рецепторов эстрадиола (*Esr1/2*) и транскрипционного фактора *Stat3* в печени у самок и самцов мышей. Ложно оперированные (ЛО) самцы отличались от ЛО самок сниженным уровнем эстрадиола, повышенным уровнем глюкозы и большей резистентностью к инсулину. В печени у ЛО самцов уровни мРНК *Irs2*, *Pik3cd* и *Esr1/2* были ниже, чем у ЛО самок. У самок гонадэктомия снижала уровень эстрадиола в крови, повышала резистентность к инсулину и уровень глюкозы в крови по сравнению с ЛО самками. Введение эстрадиола гонадэктомированным самкам снижало уровень инсулина в крови и резистентность к инсулину. У самцов гонадэктомия, наоборот, повышала уровень эстрадиола в крови, снижала резистентность к инсулину и уровень инсулина в крови. Введение эстрадиола гонадэктомированным самцам не оказывало влияния на исследованные показатели. Развитие инсулинорезистентности у гонадэктомированных самок было ассоциировано со снижением экспрессии гена *Irs2* в печени, а повышение чувствительности к инсулину у гонадэктомированных самцов – с увеличением уровней мРНК *Irs2* и *Pik3cd* в печени. Можно предположить, что повышение уровня эстрадиола в крови активирует экспрессию гена *Irs2* в печени независимо от пола животного. Также независимо от пола животного эстрадиол, по-видимому, регулирует транспорт глюкозы в жировой ткани: у самок и самцов повышение уровня эстрадиола в крови было ассоциировано со снижением экспрессии гена *Slc2a4* в жировой ткани. Таким образом, эффекты эстрадиола на экспрессию генов инсулинового каскада, по-видимому, не зависят от пола животного, но имеют тканевую специфичность. Поскольку молекулярный механизм влияния эстрадиола на экспрессию генов инсулинового каскада у самок и самцов не различается, причиной половых различий в чувствительности к инсулину и скорости развития метаболических нарушений может быть сниженный, по сравнению с самками, уровень эстрадиола в крови и сниженная экспрессия рецепторов эстрадиола в печени.
Ключевые слова: гонадэктомия; эстрадиол; тестостерон; чувствительность к инсулину; экспрессия генов; мыши линии C57BL/6J.

Introduction

Current data suggest that there is a close relationship between estrogens and insulin sensitivity: estradiol increases the uptake of glucose in muscle, suppresses hepatic glucose production, lowers blood glucose levels and increases glucose tolerance in ovariectomized females of mice and rats, in intact female mice with severe genetic or diet-induced obesity, in male mice and in men (Faustini-Fustini et al., 1999; Bryzgalova et al., 2008; Saengsirisuwan et al., 2009; Zhu et al., 2014).

Molecular mechanisms of the estradiol effect on insulin sensitivity are being actively studied. It has already been shown that they are due to its effect on the phosphorylation of insulin receptor substrates (IRS1 and 2), as well as its effect on the glucose transporter 4 (GLUT4) level and GLUT4 translocation into the cell membrane (González et al., 2001; Saengsirisuwan et al., 2009; Gorres et al., 2011; Muthusamy et al., 2011; Narasimhan et al., 2013).

The effects of estradiol as a steroid hormone are related to its effect on gene expression. Currently, the effect of estradiol on the expression of the glucose transporter 4 gene (*Slc2a4*) in females and males and on the expression of the insulin receptor gene (*Insr*) in males has been studied. Ovariectomy has been shown to increase *Slc2a4* expression in adipose tissue in female mice and estradiol administration to reduce it (Iakovleva et al., 2014). Gonadectomy reduces the expression of *Insr* in the liver, muscle and adipose tissue, and reduces the expression of *Slc2a4* in muscle and adipose tissue, but exogenous estradiol does not affect the expressions in male rats (Muthusamy et al., 2009, 2011). The results of *in vitro* experiments performed on cell cultures (CHO, HepG2) suggest that estradiol does not participate in the regulation of *Insr* expression and activates the gene expression of the insulin receptor substrate 1 and 2 (*Irs1/2*) in the liver (Xie et al., 2003; Panno et al., 2006; Parthasarathy et al., 2009).

The estradiol effect on the expression of insulin cascade genes may be mediated by other factors. For example, the effect of estradiol on insulin sensitivity in mice with genetic obesity (ob/ob mice) is due to activation of liver expression of the transcription factor STAT3 (Gao et al., 2006). Fibroblast growth factor 21 (FGF21) increases liver insulin sensitivity (Gong et al., 2016) and may also mediate the effect of estradiol on metabolism, because activation of the estradiol receptor alpha increases the liver expression of *Fgf21* in female mice (Allard et al., 2019).

Estrogens are known to be synthesized in the ovaries, testicles and adrenal glands, as well as in peripheral tissues from androgen precursors under the influence of an aromatase enzyme complex, so the blood estradiol level of male mice is comparable to that of females. However, males show a greater tendency to develop metabolic disorders and reduced insulin sensitivity when consuming high-fat food. In mice, high-fat diet reduces hepatic insulin sensitivity and induces fasting hyperglycemia in males, unlike females (Akoum et al., 2011). It is assumed that gender-related differences in insulin sensitivity and in the development rate of metabolic disorders are due to the fact that in females, unlike males, estradiol has a protective effect and increases insulin sensitivity. However, the molecular mechanisms of the estradiol effect on insulin sensitivity in males remain poorly understood.

The aim of the work was to perform a comparative study of the molecular mechanisms of the estradiol influence on insulin sensitivity in mice of both sexes. The effects of gonadectomy and exogenous estradiol on the expression of insulin signaling cascade genes in muscle, adipose tissue, and liver, as well as on the liver expression of *Fgf21*, estradiol receptors of type alpha and beta (*Esr1/2*), and transcription factor Stat3 in female and male mice were studied.

Materials and methods

Animals. C57BL/6J mice were kept in the vivarium of the Institute of Cytology and Genetics. The mice were housed under a 12:12-h light-dark regime at an ambient tempera-

ture of 22 °C. The mice were provided *ad libitum* access to commercial mouse chow (Assortiment Agro, Turakovo Village, Moscow oblast, Russia) and water. All experiments were performed according to the European Convention for the Protection of Vertebrate Animals used for Experimental and other Scientific Purposes (Council of Europe No. 123, Strasbourg 1985) and Russian national instructions for the care and use of laboratory animals. The protocols were approved by the Independent Ethics Committee of the Institute of Cytology and Genetics, Siberian Branch of the Russian Academy of Sciences.

Experiment. At the age of 10 weeks, females and males were gonadectomized and housed individually. Three weeks after the operation, three experimental groups were formed for each sex: sham surgery animals that received oral administration of oil (SHAM) and served as controls, gonadectomized animals that received an oil administration (GE) or 17β-estradiol administration (E2). Animals received an oral administration of β-estradiol (Sigma-Aldrich) at a dose of 1 μg/animal or a solvent (vegetable oil, 100 μl) for three days at 09:00. A day after the last administration, the animals were decapitated after a night of fasting (18:00–09:00). Blood and tissue samples (liver, muscle, visceral fat) were collected. Blood was collected in tubes with 5 μl of EDTA and centrifuged (4000 g, 20 minutes), and blood plasma was stored at –70 °C. Tissue samples were stored in liquid nitrogen until RNA and protein were isolated. After determining the fasting plasma levels of glucose and insulin, the physiological index of insulin resistance (HOMA-IR) was calculated using the formula [plasma glucose level (mmol/l) × plasma insulin level (ng/ml)]/22.5.

The reaction of reverse transcription and real-time PCR. The total RNA was isolated using the ExtraRNA reagent (Eurogen Lab, Moscow, Russia) in accordance with the manufacturer's instructions. First-strand cDNA was synthesized with Moloney murine leukemia virus (MMLV) reverse transcriptase buffer (SibEnzyme, Novosibirsk, Russia) and oligo (dT) (Evrogen, Moscow, Russia) as a primer. Applied Biosystems TaqMan gene expression assays (Table 1) with β-actin as endogenous control and 2.5× reaction mixture for qPCR in the presence of Rox reference dye (Syntol, Moscow, Russia). Real-time PCR was performed using Applied Biosystems ViiA™ 7 Real-Time PCR System, using the standard protocol according to the manufacturer's instructions (Applied Biosystems). Relative quantitation was performed by the comparative CT method, where CT is the threshold cycle.

Western blot analysis of protein levels. Samples of liver, muscle and adipose tissue were homogenized. Protein extraction was performed in a lysing buffer (Tris-Triton buffer). The protein concentration in the samples was evaluated using the Bradford method using NanoDrop2000 (ThermoScientific). Protein separation by molecular weight was performed using gel electrophoresis in 10 % polyacrylamide gel in Tris-glycine buffer (25 mm Tris, 250 mm Glycine, 0.1 % SDS). Electric transfer of proteins to a 0.45 micron nitrocellulose membrane was performed using the Trans-Blot system (Bio-Rad, USA). The membranes were blocked with 5 % milk (milk powder, PanReac AppliChem). Primary polyclonal rabbit antibodies were used (Santa Cruz Biotechnology, USA, breeding 1:2000): insulin Rα antibody (sc-710) and GLUT4 antibody (sc-7938). After washing with a phosphate-salt buffer (0.1 % Tween-20), the membranes were incubated for 1 hour at room temperature with secondary goat antibodies conjugated with horseradish peroxidase (1:5000 dilution) (sc-2004, At/goat anti-rabbit IgG-HRP, HRP-conjugated, Santa Cruz Biotechnology, USA). Detection of the structural protein beta-actin (1:5000 dilution) (sc-130656, Santa Cruz Biotechnology, USA) was performed on the same membrane. At the end of immunoblotting, the membrane was washed and incubated for 1 minute in a substrate mixture (10 ml 100 mm Tris-Hcl pH 8.5; 50 μl 250 mM luminol; 22 μl 90 mM coumaric acid; 3 μl 33 % H_2O_2), after which chemiluminescence was visualized on the ChemiDocTM XRS device (Bio-Rad, USA). The results were analyzed using the Image Studio Lite Ver 5.2 program. The signal of the test protein in the sample was related to the beta actin signal in the same sample. The level of protein

Table 1. Taqman gene expression assays (Applied Biosystems) for mice used in the work

Name	Symbol	Catalogue No.
Insulin receptor	*Insr*	Mm01211875_m1
Insulin receptor substrate type 1	*Irs1*	Mm01278327_m1
Insulin receptor substrate type 2	*Irs2*	Mm03038438_m1
Catalytic subunit delta of phosphatidylinositol-3-kinase	*Pik3cd*	Mm00435674_m1
Glucose transporter 4	*Slc2a4*	Mm01245502_m1
Beta-actin	*Actb*	Mm006007938_s1
Estradiol receptor alpha	*Esr1*	Mm00433149_m1
Estradiol receptor beta	*Esr2*	Mm00599821_m1
Signal of transduction and activation of transcription 3	*Stat3*	Mm01219775_m1
Fibroblast growth factor 21	*Fgf21*	Mm00840165_g1

expression in a sample is the ratio of the normalized signal in this sample to the normalized signal in the reference sample.

Determination of blood biochemical parameters. Blood glucose concentration was determined using the OneTouch Select glucometer (Lifescan, Johnson and Johnson, USA). Concentrations of estradiol, testosterone, and insulin in blood plasma were determined by the ELISA method using commercial kits (Mouse Estradiol (E2) ELISA Kit (MyBioSource, USA), Testosterone rat/mouse ELISA (Demeditec Diagnostics GmbH, Germany) and Rat/Mouse Insulin ELISA Kit (Millipore, USA)) according to manufacturers' instructions.

Statistical analysis. The results are presented as means ± SE from the indicated number of mice. The effect of gonadectomy and exogenous estradiol on the studied parameters in females and males was determined using a single-factor MANOVA variance analysis (gradations of the factor "experimental group": SHAM, GE, E2) with multiple comparisons using the post hoc Newman–Keuls test. MANOVA with gradations of the factor "experimental group" SHAM and GE was used to analyze the effect of gonadectomy on the plasma estradiol level, since blood samples were taken a day after the last injection of the hormone, and the level of estradiol in the blood of animals E2 could not reflect the actual level of the hormone in the blood after injection. To compare the parameters of SHAM females and SHAM males, a *t*-test was used. Significance was determined as $p < 0.05$.

Results

Blood levels of sex hormones, glucose, and insulin

Sex effects (SHAM mice). In females, the estradiol level was significantly higher, and the testosterone level was significantly lower than in males (Table 2). Females had a higher sensitivity to insulin than males: the insulin level of females and males did not differ significantly, while the glucose level and the index of insulin resistance (HOMA-IR) in females was significantly lower than in males (Table 3).

Effect of gonadectomy and exogenous estradiol. In females, gonadectomy reduced the plasma estradiol level (MANOVA, $p < 0.05$). A significant influence of the "experimental group" on the insulin sensitivity in females was shown: the index of insulin resistance, glucose and insulin levels in GE

Table 2. Body weight and plasma levels of sex hormones in female and male C57BL mice

Sex	Experimental group (number of animals in the group)	Body weight, g	Estradiol, plasma, pg/ml	Testosterone, plasma, ng/ml
Females	SHAM (9)	20.3 ± 0.5	151 ± 15	0.24 ± 0.03
	GE (12)	23.3 ± 1.2	122 ± 6	0.11 ± 0.06
	E2 (10)	21.8 ± 0.5	127 ± 4	0.15 ± 0.04
MANOVA			$p < 0.05$	
Males	SHAM (8)	$25.4 \pm 0.4^{\$\$\$}$	$94 \pm 12^{\$\$}$	$2.80 \pm 0.9^{\$\$}$
	GE (10)	24.6 ± 0.4	133 ± 10	$0.16 \pm 0.05^{*}$
	E2 (11)	25.1 ± 0.5	128 ± 12	$0.12 \pm 0.03^{*}$
MANOVA			$p < 0.05$	$p < 0.01$

$^{\$\$}$ $p < 0.01$, $^{\$\$\$}$ $p < 0.001$ compared to SHAM females, *t*-test; * $p < 0.05$ compared to SHAM animals of the same sex, post hoc Newman–Keuls test.

Table 3. Plasma insulin levels, blood glucose levels, and HOMA-IR in C57BL females and males

Sex	Experimental group (number of animals in the group)	Glucose, blood, mmol/l	Insulin, plasma, ng/ml	HOMA-IR
Females	SHAM (9)	6.1 ± 0.3	0.70 ± 0.14	0.18 ± 0.03
	GE (12)	$7.9 \pm 0.4^{**}$	1.12 ± 0.24	$0.41 \pm 0.10^{*}$
	E2 (10)	6.9 ± 0.5	$0.43 \pm 0.07^{\#}$	$0.13 \pm 0.02^{\#}$
MANOVA		$p < 0.05$	$p < 0.05$	$p < 0.05$
Males	SHAM (8)	$7.7 \pm 0.4^{\$\$}$	1.28 ± 0.31	$0.47 \pm 0.13^{\$}$
	GE (10)	6.8 ± 0.4	0.51 ± 0.11	0.14 ± 0.02
	E2 (11)	7.0 ± 0.4	1.25 ± 0.41	0.40 ± 0.14

$^{\$}$ $p < 0.05$, $^{\$\$}$ $p < 0.01$ compared to SHAM females, *t*-test; * $p < 0.05$, ** $p < 0.01$ compared to SHAM animals of the same sex; $^{\#}$ $p < 0.05$ compared to GE animals of the same sex, post hoc Newman–Keuls test.

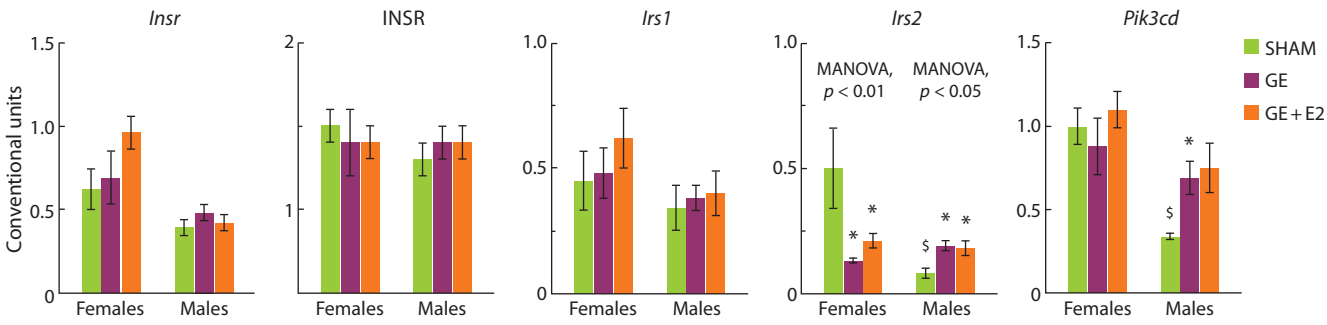

Fig. 1. Effect of gonadectomy and exogenous estradiol (1 μg/animal, 3 days) on mRNA levels of *Insr*, *Irs1*, *Irs2*, *Pik3cd* and the level of INSR protein in the liver in SHAM, GE and GE + E2 female and male mice.

Here and in the Fig. 2–4: $ $p < 0.05$ compared to females; * $p < 0.05$ compared to SHAM animals of the same sex; # compared to GE animals of the same sex. MANOVA, $p < 0.05$ or $p < 0.01$ – the influence of the "experimental group" factor is statistically significant.

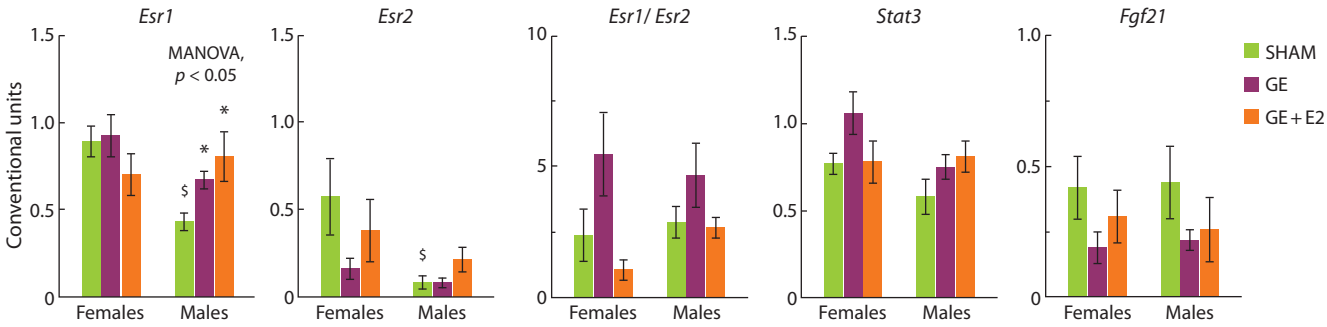

Fig. 2. Effect of gonadectomy and exogenous estradiol (1 μg/animal, 3 days) on the mRNA levels of estradiol receptors (*Esr1* and *Esr2*), *Fgf21* and *Stat3* in the liver in SHAM, GE and GE + E2 female and male mice.

females were higher than in SHAM females, and exogenous estradiol normalized these indicators.

In males, gonadectomy reduced the plasma testosterone level (MANOVA, $p < 0.01$). On the contrary, the plasma estradiol level in GE males was higher than that of SHAM males (MANOVA, $p < 0.05$). Gonadectomy and estradiol did not affect blood glucose and insulin levels and the index of insulin resistance in males.

Expression of insulin cascade components in the liver

Sex effects (SHAM mice). The expression of *Irs2*, *Pik3cd*, *Esr1*, and *Esr2* in females differed from that in males: the mRNA level of these genes was significantly higher in females than in males. The expression of *Insr*, *Irs1*, *Fgf21*, and *Stat3* and the level of the INSR protein were not significantly different in females and males (Fig. 1 and 2).

Effect of gonadectomy and exogenous estradiol. In females, gonadectomy decreased, while exogenous estradiol increased, although not normalized, the *Irs2* mRNA level in the liver (MANOVA, $p < 0.01$).

In males, exogenous estradiol did not affect the expression of the studied genes, while gonadectomy increased hepatic expression of *Irs2* and *Esr1* (MANOVA, $p < 0.05$ in both cases): the mRNA levels of these genes in GE and E2 males were higher than in SHAM males. The level of *Pik3cd* mRNA in the liver of GE and E2 males was also higher than in SHAM males, but the differences did not reach the level of significance (MANOVA, $p = 0.07$). The level of *Esr1* mRNA in males was positively correlated ($p < 0.05$) with the level of *Irs2* mRNA ($r = 0.74$).

Gonadectomy and estradiol did not significantly affect the *Esr1*/*Esr2* ratio in the liver in females and males.

Expression of components of the insulin cascade in muscle and adipose tissues

Sex effects (SHAM mice). The expression of insulin cascade genes and proteins in muscle and adipose tissue did not differ in SHAM females and SHAM males (Fig. 3 and 4).

Effect of gonadectomy and exogenous estradiol. In females, gonadectomy and estradiol did not affect the expression of the studied parameters of the insulin cascade in muscle tissue. In GE males, the *Insr* mRNA level in muscle was higher than in SHAM males, and the INSR protein level was lower in GE and E2 males, compared to SHAM males. In females, gonadectomy increased and exogenous estradiol normalized *Slc2a4* expression in adipose tissue (MANOVA, $p < 0.05$). In GE and E2 males, *Slc2a4* expression in adipose tissue was lower than in SHAM males.

Discussion

One approach to study the effect of estradiol on the expression of genes involved in insulin signal transduction is comparison of females and males. Insulin sensitivity at the whole body level (blood glucose level, insulin resistance index), as well

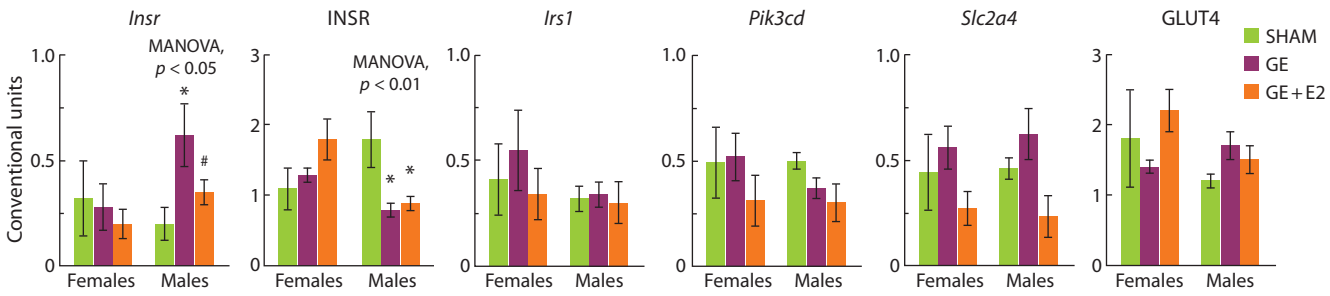

Fig. 3. Effect of gonadectomy and exogenous estradiol (1 μg/animal, 3 days) on the mRNA levels of *Insr*, *Irs1*, *Pik3cd*, *Slc2a4* and the level of INSR and GLUT4 proteins in skeletal muscles in SHAM, GE and GE + E2 female and male mice.

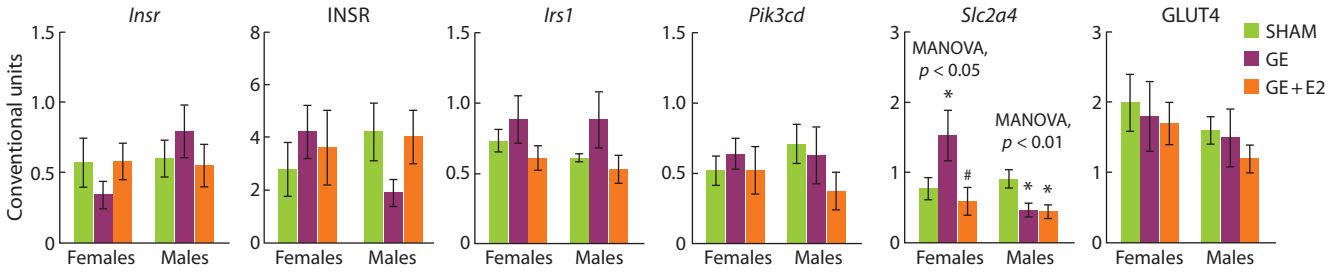

Fig. 4. Effect of gonadectomy and exogenous estradiol (1 μg/animal, 3 days) on the mRNA levels of *Insr*, *Irs1*, *Pik3cd*, *Slc2a4* and the level of INSR and GLUT4 proteins in visceral adipose tissue in SHAM, GE and GE + E2 female and male mice.

as hepatic expression of insulin signal transduction genes (*Irs2* and *Pik3cd*) in SHAM females was higher than that in SHAM males, which coincides with data obtained on intact animals (Parks et al., 2015; Torre et al., 2017; Yakovleva et al., 2017). It was shown for the first time that SHAM females differed from SHAM males not only in increased blood estradiol levels, but also in increased expression of both types of estradiol receptors in the liver, which can be one of the causes of sex differences in effects of estradiol on insulin sensitivity in the liver.

To study the effects of estradiol on the expression of insulin cascade genes, in addition to comparing parameters in females and males, we used a model of gonadectomy with subsequent administration of estradiol. We assumed that gonadectomy would lead to a decrease in the blood estradiol level in females as a result of elimination of the main source of hormone production, and in males – as a result of a decrease in the level of testosterone, as a precursor of estradiol synthesis. However, in males, the level of the hormone in the blood after gonadectomy increased. This result may be due to the activation of hormone production by the adrenal glands. As a result, gonadectomy eliminated differences in the level of sex steroids between females and males: the blood estradiol and testosterone levels did not differ in the gonadectomized females and males. However, in females, gonadectomy induced the development of insulin resistance, and exogenous estradiol normalized insulin sensitivity, while in males, gonadectomy and estradiol did not have a significant effect on the studied parameters of insulin sensitivity (blood glucose and insulin levels, HOMA-IR). The results of the effect of ovariectomy and exogenous estradiol on blood glucose and insulin levels and the index of insulin resistance in females correspond to existing data (Rogers et al., 2009; Oh et al., 2011). Effects of gonadectomy on HOMA-IR in males, as shown by Parks and co-authors (Parks et al., 2015), depends on the animal's genotype, and in C57BL/6J males, it decreases 10 weeks after gonadectomy. In this study, the HOMA-IR index in GE males did not differ significantly, but was 3.4 times lower than in SHAM males. The absence of a significant effect of gonadectomy on insulin sensitivity in males may be due to the shorter duration of the experiment.

In GE females, decreased insulin sensitivity was associated with decreased hepatic expression of *Irs2* and *Esr2* and increased expression of *Slc2a4* in adipose tissue. Exogenous estradiol, in contrast, reduced *Slc2a4* expression in adipose tissue and increased *Irs2* expression in the liver. The effect of gonadectomy on hepatic *Irs2* expression is well consistent with the observed sexual differences: *Irs2* expression in females was higher than in males. The effects of estradiol on the hepatic expression of *Irs1* and *Irs2* in female mice are known to mediate estradiol type alpha (ERα) receptors (Panno et al., 2006). Estradiol beta-type receptors (ERβ) are thought to inhibit the estradiol effects mediated by ERα (Lindberg et al., 2003). According to the obtained data, ovariectomy did not affect ERα expression and reduced ERβ expression in the liver in females, which implies an increase in the estradiol effects mediated by ERα, and may have a compensatory-adaptive effects to maintain insulin sensitivity in conditions of reduced blood estradiol levels.

In males, gonadectomy did not affect blood insulin and glucose levels, but caused increased levels of *Irs2*, *Pik3cd*, and *Esr1* mRNA in the liver. Since males have a tendency to

increase the level of estradiol in the blood after gonadectomy, and there is a correlation between the level of *Irs2* expression and *Esr1* expression in the liver, it can be assumed that the hepatic *Irs2* expression in males, as in females, is regulated by estradiol. Accordingly, activation of the gene expression of the estradiol receptor alpha may be part of the molecular mechanism of the estradiol effect on insulin sensitivity in GE males. Thus, increasing the blood estradiol level in females and males can activate the *Irs2* gene expression in the liver regardless of gender and contribute to improving insulin sensitivity in general.

Transcription factor STAT3 was shown to mediate the estradiol effects on the expression of hepatic lipogenic genes (Gao et al., 2006) and FGF21 may mediate the estradiol effect on the expression of gluconeogenic genes, since it increases the gene expression of *Irs2* and the glucose-6-phosphatase (Fisher et al., 2011). However, the role of STAT3 and FGF21 in mediating the estradiol effects on the expression of insulin signal transduction genes requires additional research, since in the study no differences were found in the *Stat3* and *Fgf21* mRNA levels in the liver in animals of different sexes and experimental groups.

Activation of liver *Pik3cd* expression in GE males appears to be due to a decrease testosterone levels. In females, the *Pik3cd* mRNA level was higher than in males, but these differences were not related to estradiol levels, since ovariectomy and subsequent estradiol administration did not affect the level of *Pik3cd* mRNA in females.

It is believed that the effect of estradiol on insulin sensitivity in adipose and muscle tissues is due to its stimulation of glucose uptake by cells as a result of increasing the level of GLUT4 and activating its translocation into the cell membrane. In female mice, ovariectomy was shown to have no effect after 2 weeks, and caused a decrease in the level of *Slc2a4* mRNA in muscle and adipose tissue after 10 weeks (Kim et al., 2010). In female rats, 12 weeks after ovariectomy, the level of GLUT4 protein in the muscles is reduced, while the estradiol injections prevents this decrease (Saengsirisuwan et al., 2009). In this study, 3 weeks after ovariectomy, the level of *Slc2a4* mRNA in adipose tissue in females increased and exogenous estradiol normalized it, while there was no significant effect on the level of *Slc2a4* mRNA in muscle tissue and the level of GLUT4 protein in adipose tissue and muscle. We have previously shown that ovariectomy for 5 weeks also increases the level of *Slc2a4* mRNA in adipose tissue, and estradiol for 3 weeks reduces it, while in muscle tissue the level of *Slc2a4* mRNA decreases after ovariectomy, but exogenous estradiol does not affect it (Iakovleva et al., 2014). Apparently, the effect of ovariectomy and exogenous estradiol on *Slc2a4* expression in adipose and muscle tissues depends significantly on the duration of the experiment.

The effect of gonadectomy and estradiol on the expression of insulin receptor and glucose transporter 4 in adipose and muscle tissues was studied in male rats. Gonadectomy has been shown to decrease levels of mRNA and protein of INSR and protein level of GLUT4 in adipose and muscle tissues, and exogenous estradiol normalizes levels of these proteins (Muthusamy et al., 2009, 2011). The results of our experiment, obtained on mice, are poorly consistent with these data. This may be due to interspecies differences in the influence of gonadectomy on the blood estradiol levels and sex steroid ratio in males. In our experiment, an increase in estradiol levels after gonadectomy in males was associated with an increase in *Insr* mRNA, but a decrease in INSR protein in muscle, and a decrease in *Slc2a4* mRNA in adipose tissue. It should be noted that an increase in the blood estradiol levels (as a result hormone administration in females and after gonadectomy in males) was associated with a decrease in the *Slc2a4* expression in adipose tissue regardless of sex.

Conclusion

All of the above suggests that the effect of estradiol on the expression of genes and proteins of the insulin cascade is tissue-specific and does not depend on the sex: estradiol can increase the expression of *Irs2* in the liver, and can suppress the expression of *Slc2a4* in adipose tissue. Activation of *Irs2* expression in the liver when the blood estradiol level increases causes an improvement in glucose metabolism, so the effects of estradiol in the liver cause an increase in insulin sensitivity at the whole body. The significance of the estradiol effect on *Slc2a4* expression in adipose tissue in females and males is not clear and requires further research. Despite the universal mechanism of action, the protective effect of estradiol in males is less pronounced than in females, apparently as a result of reduced hormone levels in blood and reduced expression of estradiol receptors in the liver.

References

Akoum S.E., Lamontagne V., Cloutier I., Tanguay J.F. Nature of fatty acids in high fat diets differentially delineates obesity-linked metabolic syndrome components in male and female C57BL/6J mice. *Diabetol. Metab. Syndr*. 2011;3:34.

Allard C., Bonnet F., Xu B., Coons L., Albarado D., Hill C., Fagherazzi G., Korach K.S., Levin E.R., Lefante J., Morrison C., Mauvais-Jarvis F. Activation of hepatic estrogen receptor-α increases energy expenditure by stimulating the production of fibroblast growth factor 21 in female mice. *Mol. Metab*. 2019;22:62-70. DOI 10.1016/j.molmet.2019.02.002.

Bryzgalova G., Lundholm L., Portwood N., Gustafsson J.A., Khan A., Efendic S., Dahlman-Wright K. Mechanisms of antidiabetogenic and body weight-lowering effects of estrogen in high-fat diet-fed mice. *Am. J. Physiol. Endocrinol. Metab*. 2008;295(4):E904-E912.

Faustini-Fustini M., Rochira V., Carani C. Oestrogen deficiency in men: where are we today? *Eur. J. Endocrinol*. 1999;140(2):111-129.

Fisher F.M., Estall J.L., Adams A.C., Antonellis P.J., Bina H.A., Flier J.S., Kharitonenkov A., Spiegelman B.M., Maratos-Flier E. Integrated regulation of hepatic metabolism by fibroblast growth factor 21 (FGF21) *in vivo*. *Endocrinology*. 2011;152(8):2996-3004. DOI 10.1210/en.2011-0281.

Gao H., Bryzgalova G., Hedman E., Khan A., Efendic S., Gustafsson J.A., Dahlman-Wright K. Long-term administration of estradiol decreases expression of hepatic lipogenic genes and improves insulin sensitivity in ob/ob mice: a possible mechanism is through direct regulation of signal transducer and activator of transcription 3. *Mol. Endocrinol*. 2006;20(6):1287-1299.

Gong Q., Hu Z., Zhang F., Cui A., Chen X., Jiang H., Gao J., Chen X., Han Y., Liang Q., Ye D., Shi L., Chin Y.E., Wang Y., Xiao H., Guo F., Liu Y., Zang M., Xu A., Li Y. Fibroblast growth factor 21 improves hepatic insulin sensitivity by inhibiting mammalian target of ra-

pamycin complex 1 in mice. *Hepatology*. 2016;64(2):425-438. DOI 10.1002/hep.28523.

González C., Alonso A., Grueso N.A., Díaz F., Esteban M.M., Fernández S., Patterson A.M. Effect of treatment with different doses of 17-β-estradiol on insulin receptor substrate-1. *JOP. J. Pancreas*. 2001;2(4):140-149.

Gorres B.K., Bomhoff G.L., Morris J.K., Geiger P.C. *In vivo* stimulation of oestrogen receptor α increases insulin-stimulated skeletal muscle glucose uptake. *J. Physiol*. 2011;589(8):2041-2054. DOI 10.1113/jphysiol.2010.199018.

Iakovleva T.V., Makarova E.N., Bazhan N.M. Effect of ovariectomy on GLUT4 mRNA levels in adipose and muscle tissues in females of mice C57BL/6J – *Agouti yellow. Rossiyskiy Fiziologicheskiy Zhurnal im. I.M. Sechenova = Russian Journal of Physiology*. 2014; 100(5):602-612. (in Russian)

Kim J.Y., Jo K.J., Kim O.S., Kim B.J., Kang D.W., Lee K.H., Baik H.W., Han M.S., Lee S.K. Parenteral 17beta-estradiol decreases fasting blood glucose levels in non-obese mice with short-term ovariectomy. *Life Sci*. 2010;87(11-12):358-366. DOI 10.1016/j.lfs.2010.07.009.

Lindberg M.K., Movérare S., Skrtic S., Gao H., Dahlman-Wright K., Gustafsson J.A., Ohlsson C. Estrogen receptor (ER)-β reduces ERα-regulated gene transcription, supporting a "Ying Yang" relationship between ERα and ERβ in mice. *Mol. Endocrinol*. 2003;17(2):203-208. DOI 10.1210/me.2002-0206.

Muthusamy T., Murugesan P., Balasubramanian K. Sex steroids deficiency impairs glucose transporter 4 expression and its translocation through defective Akt phosphorylation in target tissues of adult male rat. *Metabolism*. 2009;58(11):1581-1592.

Muthusamy T., Murugesan P., Balasubramanian K. Sex steroids influence glucose oxidation through modulation of insulin receptor expression and IRS-1 serine phosphorylation in target tissues of adult male rat. *Mol. Cell. Biochem*. 2011;352(1-2):35-45.

Narasimhan A., Sampath S., Jayaraman S., Karundevi B. Estradiol favors glucose oxidation in gastrocnemius muscle through modulation of insulin signaling molecules in adult female rats. *Endocr. Res*. 2013;38(4):251-262. DOI 10.3409/07435800.2013.775148.

Oh Y.S., Lee T.S., Cheon G.J., Jang I.S., Jun H.S., Park S.C. Modulation of insulin sensitivity and caveolin-1 expression by orchidectomy in a nonobese type 2 diabetes animal model. *Mol. Med*. 2011;17(1-2): 4-11. DOI 10.2119/molmed.2009.00105.

Panno M.L., Mauro L., Marsico S., Bellizzi D., Rizza P., Morelli C., Salerno M., Giordano F., Andò S. Evidence that the mouse insulin receptor substrate-1 belongs to the gene family on which the promoter is activated by estrogen receptor α through its interaction with Sp1. *J. Mol. Endocrinol*. 2006;36(1):91-105. DOI 10.1677/jme.1.01848.

Parks B.W., Sallam T., Mehrabian M., Psychogios N., Hui S.T., Norheim F., Castellani L.W., Rau C.D., Pan C., Phun J., Zhou Z., Yang W.P., Neuhaus I., Gargalovic P.S., Kirchgessner T.G., Graham M., Lee R., Tontonoz P., Gerszten R.E., Hevener A.L., Lusis A.J. Genetic architecture of insulin resistance in the mouse. *Cell Metab*. 2015;21(2):334-347.

Parthasarathy C., Renuka V.N., Balasubramanian K. Sex steroids enhance insulin receptors and glucose oxidation in Chang liver cells. *Clin. Chim. Acta*. 2009;399(1-2):49-53.

Rogers N.H., Perfield J.W. 2nd, Strissel K.J., Obin M.S., Greenberg A.S. Reduced energy expenditure and increased inflammation are early events in the development of ovariectomy-induced obesity. *Endocrinology*. 2009;150(5):2161-2168. DOI 10.1210/en.2008-1405.

Saengsirisuwan V., Pongseeda S., Prasannarong M., Vichaiwong K., Toskulkao C. Modulation of insulin resistance in ovariectomized rats by endurance exercise training and estrogen replacement. *Metabolism*. 2009;58(1):38-47. DOI 10.1016/j.metabol.2008.08.004.

Torre S.D., Lolli F., Ciana P., Maggi A. Sexual dimorphism and estrogen action in mouse liver. In: Mauvais-Jarvis F. (Ed.). Sex and Gender Factors Affecting Metabolic Homeostasis, Diabetes and Obesity (Advances in Experimental Medicine and Biology. Vol. 1043). Springer Int. Publ., 2017;141-151. DOI 10.1007/978-3-319-70178-3_8.

Xie P., Liu M.L., Gu Y.P., Lu J., Xu X., Zeng W.M., Song H.P. Oestrogen improves glucose metabolism and insulin signal transduction in HepG2 cells. *Clin. Exp. Pharmacol. Physiol*. 2003;30(9):643-648. DOI 10.1046/j.1440-1681.2003.03899.x.

Yakovleva T.V., Kazantseva A.Yu., Makarova E.N., Bazhan N.M. Sex differences of molecular mechanisms of insulin sensitivity in young and adult C57BL/6J mice. *Vavilovskii Zhurnal Genetiki i Selektsii = Vavilov Journal of Genetics and Breeding*. 2017;21(7):833-840. DOI 10.18699/VJ17.303. (in Russian)

Zhu L., Martinez M.N., Emfinger C.H., Palmisano B.T., Stafford J.M. Estrogen signaling prevents diet-induced hepatic insulin resistance in male mice with obesity. *Am. J. Physiol. Endocrinol. Metab*. 2014; 306(10):E1188-E1197. DOI 10.1152/ajpendo.00579.2013.

ORCID ID

T.V. Iakovleva orcid.org/0000-0001-7628-5856
N.E. Kostina orcid.org/0000-0001-6137-0492
E.N. Makarova orcid.org/0000-0002-6417-9893
N.M. Bazhan orcid.org/0000-0002-7246-4758

Acknowledgements. The study was supported by the Russian Science Foundation, project 17-15-01036. Use of the equipment of the Center for Genetic Resources of Laboratory Animals at ICG SB RAS was supported by the Ministry of Education and Science of Russia (unique project identifier RFMEFI62117X0015).

Conflict of interest. The authors declare no conflict of interest.

Received November 27, 2019. Revised February 17, 2020. Accepted February 27, 2020.

Вавиловский журнал генетики и селекции. 2020;24(4):435-440
DOI 10.18699/VJ20.43-o

Apoptosis in the liver of male *db/db* mice during the development of obesity and type 2 diabetes

S.V. Michurina[1], I.Yu. Ishchenko[1] ✉, S.A. Arkhipov[1], M.A. Cherepanova[1], D.V. Vasendin[3], E.L. Zavjalov[2]

[1] Research Institute of Clinical and Experimental Lymphology – Branch of the Institute of Cytology and Genetics of Siberian Branch of the Russian Academy of Sciences, Novosibirsk, Russia
[2] Institute of Cytology and Genetics of Siberian Branch of the Russian Academy of Sciences, Novosibirsk, Russia
[3] Siberian State University of Geosystems and Technologies, Novosibirsk, Russia
✉ e-mail: irenisch@mail.ru

Abstract. Obesity and diabetes mellitus are known to lead to the development of metabolic syndrome and non-alcoholic fatty liver disease (NAFLD). The mechanisms of programmed cell death are actively involved in maintaining cellular homeostasis along development of NAFLD. Proteins of the BCL-2 family are key regulators of physiological and pathological apoptosis. Homozygous males of BKS.Cg-*Dock7*^{m}*Lepr*^{db}/+/+/J mice (*db/db* mice) are characterized by progressive obesity and the development of type 2 diabetes mellitus (DM2) with severe hyperglycemia at 4–8 weeks and organ lesions at 8–10 weeks of age. The aim of this research was to study the expression of molecular cell regulators of apoptosis in liver cells of *db/db* mice males at different stages of obesity and diabetes development (at the age of 10 and 18 weeks). Immunohistochemical analysis (using the indirect avidin-biotin peroxidase method) and morphometric evaluation of the expression of the antiapoptotic protein Bcl-2 and the proapoptotic protein Bad in liver cells of studied animals at different stages of obesity and DM2 were carried out. An excess of the value of the Bcl-2 protein staining area over the Bad protein staining area was revealed in the liver of 10-week-old animals. The Bcl-2/Bad expression area ratio in 10-week-old animals was twice as high as in 18-week-old animals, which indicates the presence of conditions for blocking apoptosis in the liver of younger *db/db* mice. At the 18th week of life, *db/db* mice displayed an almost threefold increase in the expression area of the Bad protein against the background of an unchanged expression of the Bcl-2 protein. The decrease in the Bcl-2/Bad staining area ratio in 18-week-old animals was due to the increase in the Bad expression area, which indicates the absence of antiapoptotic cell protection and creates conditions for activation of the mitochondrial pathway of apoptosis in the liver of male *db/db* mice with pronounced signs of obesity and DM2.
Key words: *db/db* mice; obesity; type 2 diabetes mellitus (DM2); liver; endothelial cells; hepatocytes; Bcl-2; Bad.

For citation: Michurina S.V., Ishchenko I.Yu., Arkhipov S.A., Cherepanova M.A., Vasendin D.V., Zavjalov E.L. Apoptosis in the liver of male *db/db* mice during the development of obesity and type 2 diabetes. *Vavilovskii Zhurnal Genetiki i Selektsii = Vavilov Journal of Genetics and Breeding*. 2020;24(4):435-440. DOI 10.18699/VJ20.43-o

Апоптоз в печени самцов мышей *db/db* при развитии ожирения и сахарного диабета 2-го типа

С.В. Мичурина[1], И.Ю. Ищенко[1] ✉, С.А. Архипов[1], М.А. Черепанова[1], Д.В. Васендин[3], Е.Л. Завьялов[2]

[1] Научно-исследовательский институт клинической и экспериментальной лимфологии – филиал Федерального исследовательского центра Институт цитологии и генетики Сибирского отделения Российской академии наук, Новосибирск, Россия
[2] Федеральный исследовательский центр Институт цитологии и генетики Сибирского отделения Российской академии наук, Новосибирск, Россия
[3] Сибирский государственный университет геосистем и технологий, Новосибирск, Россия
✉ e-mail: irenisch@mail.ru

Аннотация. Известно, что ожирение и сахарный диабет приводят к развитию метаболического синдрома и неалкогольной жировой болезни печени. В поддержании клеточного гомеостаза при неалкогольной жировой болезни печени принимают активное участие механизмы запрограммированной клеточной гибели. Белки семейства BCL-2 являются ключевым регулятором физиологического и патологического апоптоза. Используемые в исследовании гомозиготные самцы мышей линии BKS.Cg-*Dock7*^{m}*Lepr*^{db}/+/+/J (мыши *db/db*) характеризуются прогрессирующим ожирением и развитием сахарного диабета 2-го типа (СД2), выраженной гипергликемией с 4–8-й недели жизни и развитием органных поражений после 8–10-й недели. Целью работы было изучить экспрессию молекулярно-клеточных регуляторов апоптоза в клетках печени самцов мышей *db/db* на разных сроках развития ожирения и сахарного диабета (в возрасте 10 и 18 нед). Проведены иммуногистохимический анализ (с помощью непрямого авидин-биотинового пероксидазного метода) и морфометрическая оценка экспрессии антиапоптотического белка Bcl-2 и проапоптотического протеина Bad в клетках печени исследуемых животных на разных сроках развития ожирения и СД2. В печени исследуемых самцов в возрасте 10 нед установлено превышение значения площади окрашивания на белок Bcl-2 над бел-

ком Bad. Индекс соотношения площадей экспрессии Bcl-2/Bad у 10-недельных животных оказался в два раза выше по сравнению с 18-недельными особями, что свидетельствует о наличии условий для блокирования процессов апоптоза в печени мышей *db*/*db* более раннего возраста. На 18-й неделе жизни у самцов мышей *db*/*db* обнаружено почти трехкратное увеличение площади экспрессии белка Bad на фоне неизменившейся экспрессии белка Bcl-2. Снижение значения соотношения площадей окрашивания Bcl-2/Bad у 18-недельных животных произошло за счет роста площади экспрессии Bad, что подтверждает отсутствие антиапоптотической защиты клеток и создает условия для активации митохондриальной «ветви» апоптоза в печени самцов мышей *db*/*db* с выраженными признаками ожирения и СД2.
Ключевые слова: мыши *db*/*db*; ожирение; сахарный диабет 2-го типа; печень; эндотелиоциты; гепатоциты; Bcl-2; Bad.

Introduction

Mechanisms of programmed cell death are actively involved in maintaining cell homeostasis in the development of non-alcoholic fatty liver disease (NAFLD) (Schuppan, Schattenberg, 2013). Obesity and related metabolic disorders, including lipid accumulation in the liver and inflammation, play an important role in liver carcinogenesis. Recent data indicate that obesity and diabetes lead to the development of metabolic syndrome and NAFLD, which can progress in patients with this disease to non-alcoholic steatohepatitis, which includes the risk of cirrhosis and hepatocellular carcinoma (Shimizu et al., 2011). Proteins of the BCL-2 family are key regulators of physiological and pathological apoptosis. According to the modern model of apoptosis regulation, the ratio of the apoptosis regulator proteins Bcl-2, Bad and Bax determines the sensitivity of cells to the effects of apoptotic factors and is a "molecular switch" that determines whether tissue growth or atrophy will occur (Sun et al., 2015). Molecular features of the development of the mitochondrial pathway of apoptosis in the liver of male *db/db* mice in postnatal ontogenesis at different development stages of obesity and type 2 diabetes mellitus (DM2) have not yet been studied.

The aim of this research – to study the expression of apoptosis molecular cell regulators from the BCL-2 family proteins: the antiapoptotic protein Bcl-2 and the proapoptotic protein Bad in liver cells of male *db/db* mice at different stages of obesity and DM2 development (at the age of 10 and 18 weeks).

Materials and methods

The experiments were carried out in the SPF Vivarium of the Institute of Cytology and Genetics, SB RAS, on homozygous males of BKS.Cg-*Dock7*^{m}*+/+Lepr*^{db}/J mice (*db/db* mice). Homozygous individuals of this strain have a defect of the leptin receptor (spontaneous mutation *Lepr*^{db}) and are characterized by polyphagia, progressive obesity from 3–4 weeks of life, severe hyperglycemia from 4–8 weeks of life, the development of organ lesions after 8–10 weeks. Animals were stored in a room with a regular light cycle (14 h light/10 h darkness), a constant room temperature of 24 ± 2 °C and a relative humidity of 45 ± 10 %. The mice were kept on a standard food (Ssniff, Germany) and water *ad libitum*.

Studies were conducted on mice aged 10 (n = 7) and 18 (n = 7) weeks, which is comparable to 10 and 18 years of man age, respectively (Flurkey et al., 2006). Animals were sacrificed by cranio-cervical dislocation and liver samples were taken for light-optical and immunehistochemical studies. All experiments were performed in compliance with the principles of humanity and carried out in accordance with the "Rules for the Use of Experimental Animals" (the Annex to the order of the Ministry of Health of the USSR from 12.08.1977, No. 755) and the European Unity Directive (86/609/EEC). The study was approved by the local ethics committee (Protocol No. 128 of 15 March 2017).

The liver pieces were fixed in 10 % buffered formalin (BioVitrum, Russia) for 48 h, dehydrated in a series of alcohols of increasing concentration and enclosed in histomix (BioVitrum). The organ slices 3 μm in thickness were obtained using a LEICA RM2155 microtome (Germany) Liver preparations were stained with Mayer hematoxylin and eosin for light-optical examination.

An immunohistochemical study of the Bcl-2 and Bad protein expression was performed on liver paraffin sections using the indirect avidin-biotin-peroxidase method using the VectaStain Universal Elite ABC Kit (Vector Laboratories, Catalog Number PK-7200). At the last stage, immunohistochemical staining was carried out in a chromogenic substrate containing diaminobenzidine (the solution is prepared *ex tempore* from the components of the ImmPACT DAB kit, Vector Laboratories, Catalog Number SK-4105). Some sections were stained with Mayer hematoxilin, washed with distilled water and, after dehydration, mounted under the cover glass. To quantify the expression of Bcl-2 and Bad in the mouse liver, a computer-assisted morphometric analysis of digital photographs obtained using a LEICA DM 2500 microscope with a LEICA DFC425C video camera (Germany) at ×400 magnification was performed. Using the Image J software program, the average area of the staining zones on Bcl-2 and Bad was determined on digital images. The ratio of Bcl-2 expression area to Bad expression area was calculated.

Statistical processing of research results was carried out using Statistica 6.1 (serial number AXXR101E832903FA). To analyze the data obeying the normal distribution (the average staining area of Bcl-2 and Bad proteins), the arithmetic mean and standard error of the arithmetic mean were calculated; the significance of differences between the studied groups was established using Student's t-test. The significance of data differences other than the normal distribution (the ratio of Bcl-2 expression area to Bad expression area) was determined using the nonparametric Mann–Whitney test. Differences between the values compared were considered statistically significant at $p < 0.05$.

Results

In the liver of the male mice studied at the age of 10 weeks, stagnations in the interlobular veins, dilatation of lymphatic vessels and bile ducts were detected. Signs of protein dystrophy and lipid accumulations, mainly of small droplet nature,

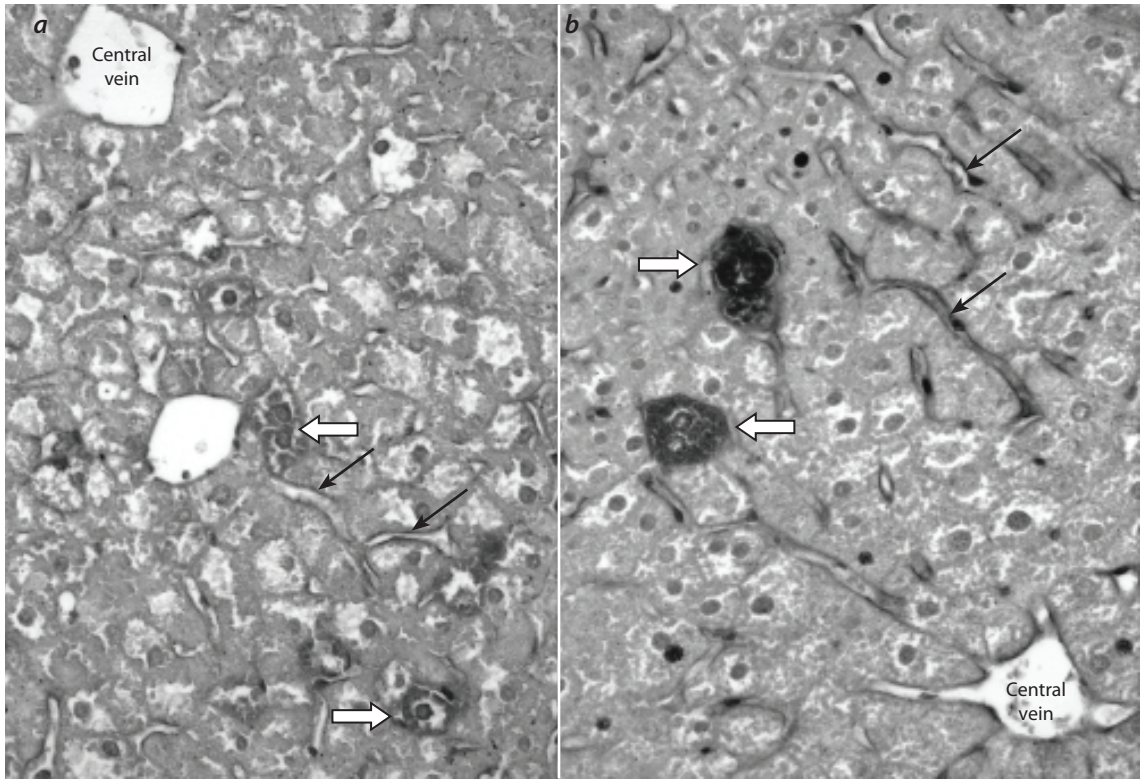

Fig. 1. The liver of *db/db* mice aged 10 weeks: *a* – poorly marked immunohistochemical staining for the proapoptotic protein Bad with subsequent Maier's hematoxylin staining; *b* – pronounced immunohistochemical staining for the antiapoptotic protein Bcl-2 with subsequent Maier's hematoxylin staining.

Here and in Fig. 3: black arrows point to immunohistochemically colored sinusoidal capillaries in the liver; white arrows point to immunohistochemically colored hepatocytes. Magnification is ×400.

were found in some hepatocytes and in groups of parenchymal cells located mainly in the intermediate zones of the hepatic lobules.

Immunohistochemically, a weak Bad-positive signal was identified in individual hepatocytes and in the heterogeneous population of sinusoidal cells of liver blood capillaries (Fig. 1, *a*) involved in the formation of the blood-lymph barrier in the liver, including endotheliocytes, Kupffer cells, Ito cells and Pit cells (Michurina et al., 2016a). At the same time, pronounced immunohistochemical staining was also observed in liver cells for the antiapoptotic protein Bcl-2. In the hepatic lobules, the marker studied was accumulated mainly in the endothelial cells of the lining of blood sinusoidal capillaries and in single hepatocytes (see Fig. 1, *b*).

Quantitative evaluation of the expression of the antiapoptotic protein Bcl-2 and the proapoptotic protein Bad showed an excess of the immunohistochemical staining area for the Bcl-2 protein over the value of this parameter for the Bad protein in the liver of *db/db* mice males aged 10 weeks (Fig. 2).

In the liver of male *db/db* mice at the age of 18 weeks, signs of nonalcoholic fatty liver disease (NAFLD) development were more pronounced than in animals aged 10 weeks. Diffuse accumulation of medium-sized and large lipid droplets was found in parenchymal cells of all hepatic lobule zones. It developed against the background of disturbances in microcirculation, intraorgan bile transport, a significant dilatation of blood and lymph vessels in the triad system and central veins.

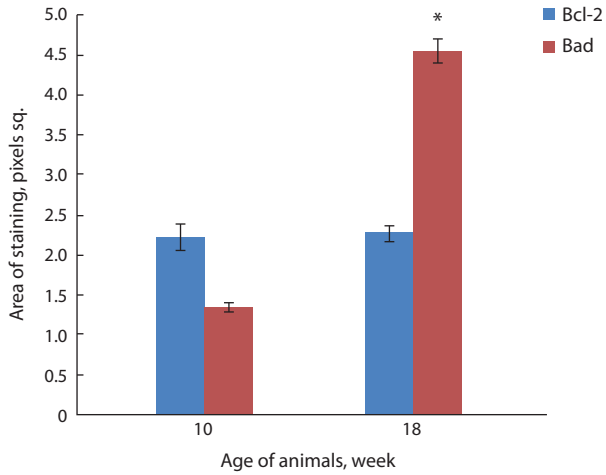

Fig. 2. Areas of Bcl-2 and Bad protein staining in the liver of *db/db* mice aged 10 and 18 weeks.

* The differences were significant between groups of "10 weeks" and "18 weeks" ($p < 0.05$).

The study of the expression of apoptosis molecular-cell regulators of BCL-2 family proteins in the liver of male *db/db* mice at the age of 18 weeks revealed a pronounced immunohistochemical staining for the proapoptotic protein Bad of endothelial cells of blood sinusoidal capillaries. A strong Bad-

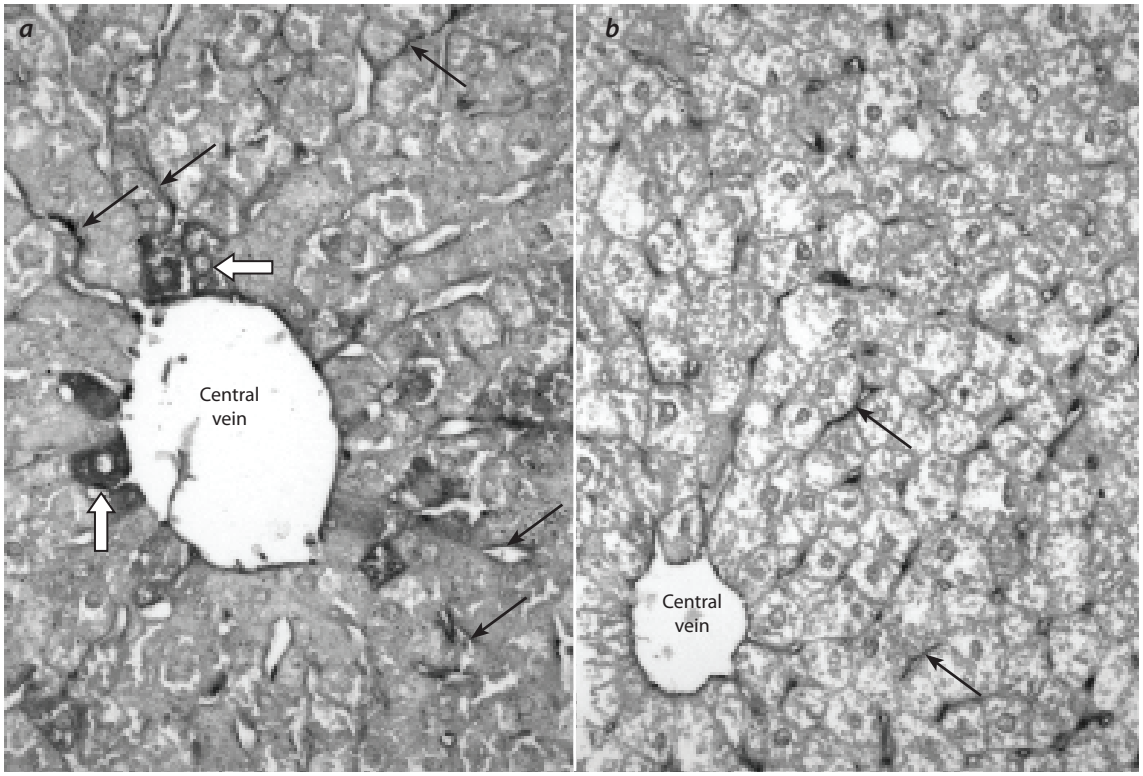

Fig. 3. The liver of *db/db* mice aged 18 weeks: *a* – pronounced immunohistochemical staining for the proapoptotic protein Bad with subsequent Maier's hematoxylin staining; *b* – weak immunohistochemical staining for the antiapoptotic protein Bcl-2 with subsequent Maier's hematoxylin staining.

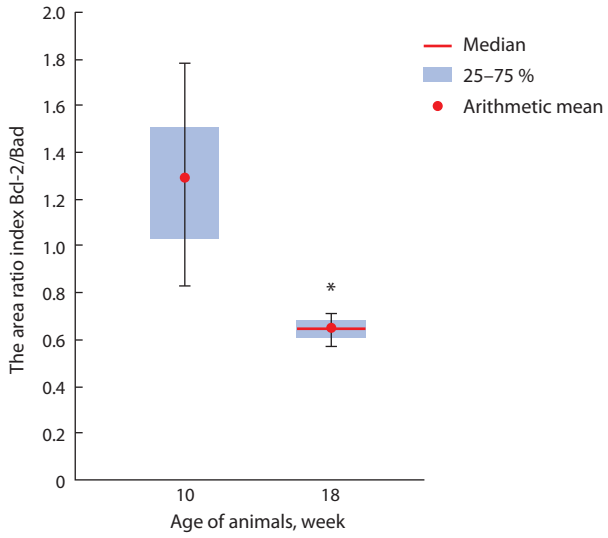

Fig. 4. The Bcl-2/Bad staining area ratio.

*The differences are significant between the groups "10 weeks" and "18 weeks" ($p < 0.05$).

positive signal was detected in hepatocytes located mainly in periportal zones and around central veins (Fig. 3, *a*) as well as in the ductal epithelium of triad bile ducts. At the same time, weak immunohistochemical staining for the antiapoptotic protein Bcl-2 was detected in cells of the blood-lymph barrier in the liver and in single hepatocytes of epy animals studied at the age of 18 weeks (see Fig. 3, *b*).

Morphometric analysis of the liver of 18-week-old animals showed an increase in the Bad protein expression area, compared to 10-week-old mice. At the same time, the staining Bcl-2 protein area did not change in comparison with the animals at the age of 10 weeks (see Fig. 2).

Evaluation of the ratio of Bcl-2/Bad expression areas revealed a significant decrease in this index in 18-week-old *db/db* mice compared to 10-week-old animals (Fig. 4), due to an increase, mainly, in the Bad expression area in the animals aged 18 weeks. Data obtained indicate the absence of antiapoptotic cell protection of organ cells, which creates conditions for activation of the mitochondrial pathway of apoptosis in liver cells of the *db/db* mice at the age of 18 weeks.

Discussion

It is known that the development of programmed cell death is influenced by posttranslational modifications of BCL-2 family proteins. One of the ways to regulate the activity of apoptosis-inducing proteins is the phosphorylation/dephosphorylation process, which affects their ability to form heterodimers with other members of the BCL-2 family proteins. According to current data, the induction of the antiapoptotic protein Bcl-2 expression causes the closure of mitochondrial membrane channels and prevents the release of the protease AIF (apoptosis inducing factor) and cytochrome C, thereby protecting the cell from apoptosis. At the same time, Bcl-2 blocks lipid peroxidation reactions in cell membranes, protecting cells from damage by free radicals and thus preventing the development of apoptosis (Chevalier et al., 2000; Paltsev, 2002; Mushkambarov, Kuznetsov, 2007; Dewanjee et al., 2015). We

had previously found that *db/db* mice were already obese by 10 weeks of age and had severe hyperglycemia with plasma glucose levels of 506 mg/dL (28.1 mmol/L) and higher. There were no significant differences in glucose, triglyceride, total cholesterol, ALT, or GGT levels in the *db/db* mice aged 10 and 18 weeks (Michurina et al., 2016b). At the same time, as was found in this study, the expression area of the antiapoptotic protein Bcl-2 exceeded the value of the imunohistochemical staining area of the proapoptotic protein Bad in the liver of the 10-week-old animals. Results obtained indicate the presence of antiapoptotic protection of liver cells at this stage of the NAFLD development.

We have previously identified ultrastructural disorders of the energy and protein-synthesis apparatus in liver cells, carbohydrate and fat metabolism disturbances in the liver of 18-week-old male *db/db* mice with DM2, which leads to the development of protein and fat dystrophy in hepatocytes (Michurina et al., 2016b).

Disorders of blood circulation and lymph flow in the *db/db* mouse liver lead to a disruption in the morphological organization of the blood-lymph barrier in the liver, and cause a decrease in LYVE-1 receptor expression on endothelial sinusoid cell membranes. Such morphological rearrangements contribute to the development of tissue hypoxia, oxidative stress and mitochondria damage, which are the inducers of cell death (Eckert et al., 2003; Michurina et al., 2016b). Under these conditions, the mitochondrial pathway of cell apoptosis is launched using the BCL-2 protein family. When the outer membrane of mitochondria is disturbed, a thermolabile factor is also released from the intermembrane space, catalyzing reactions with O_2 and leading to the development of oxidative stress. In this case, reactive oxygen species (ROS) are formed that destroy mitochondria and are powerful inducers of apoptosis (Kolesnikov et al., 1999; Dewanjee et al., 2015).

The development of microvesicular steatosis is also considered to be a consequence of severe mitochondrial dysfunction (Begriche et al., 2011). The same mitochondrial disorders are thought to be a common cause of small-bubble steatosis and apoptosis development in obese mice (Trak-Smayra et al., 2011).

In this study, we identified the greatest changes in the endothelial cells of the liver blood sinusoidal capillaries. We are just beginning to understand the complexity of the endothelial cell functions. It is now proven that these cells control liver regeneration as "a spatiotemporal rheostat". Dynamically regulating the angiopoietin-2 expression, they coordinate their own regeneration and proliferation of hepatocytes, support the restoration of connective tissue, and control the maturation and resting state of blood vessels (Hu et al., 2014). The endothelium acts as the first line of defense against invasion by pathogenic microorganisms, and also regulates vascular tone and permeability. Since damaged endotheliocytes can separate from their basement membrane and circulate freely in the blood, the possibility of detecting endothelial apoptosis *in vivo* was discussed. The degree of development of vascular injuries directly correlates with organ trauma in critically ill patients (Hutchins et al., 2013). The pronounced immunohistochemical staining revealed by us in the liver of the 18-week-old male *db/db* mice for the proapoptotic protein Bad of endothelial cells of the blood sinusoid capillaries with a low level of the antiapoptotic protein Bcl-2 expression in them indicates the development of a mitochondrial pathway of apoptosis in the cells of the blood-lymph barrier in the liver under NAFLD (Shimizu et al., 2011; Hutchins et al., 2013).

Since apoptosis is triggered through the inactivation of Bcl-2 upon its binding to the Bad protein, the increase in the proapoptotic Bad staining area established by us indicates the absence of antiapoptotic protection and the apoptosis development along the mitochondrial pathway in liver cells. This is also confirmed by a decrease in the Bcl-2/Bad liver expression area ratio in the male *db/db* mice at the 18th week of life.

Conclusion

Immunohistochemical analysis and morphometric evaluation of the expression of apoptosis molecular-cell regulators of BCL-2 family proteins – the antiapoptotic protein Bcl-2 and the proapoptotic protein Bad – in the liver cells of male *db*/*db* mice were carried out at different stages of obesity and type 2 diabetes mellitus development. An excess of the value of the Bcl-2 protein staining area over the Bad protein staining area was revealed in the liver of 10-week-old animals. The Bcl-2/Bad expression area ratio was twice as high in the 10-week-old animals as in the 18-week-old animals, indicating the presence of conditions for blocking apoptosis in the liver of younger mice. At the 18th week of life, mice displayed an almost threefold increase in the expression area of the Bad protein against the background of an unchanged expression of the Bcl-2 protein. The decrease in the ratio of Bcl-2/Bad staining areas in the 18-week-old animals was due to the increase in the Bad expression area. The obtained results indicate the absence of antiapoptotic cell protection and the creation of conditions for activation of the mitochondrial pathway of apoptosis in the liver of the male *db/db* mice with pronounced signs of obesity and DM2.

References

Begriche K., Massart J., Robin M.A., Borgne-Sanchez A., Fromenty B. Drug-induced toxicity on mitochondria and lipid metabolism: mechanistic diversity and deleterious consequences for the liver. *J. Hepatol*. 2011;54(4):773-794. DOI 10.1016/j.jhep.2010.11.006.

Chevalier R.L., Smith C.D., Wolstenholme J., Krajewski S., Reed J.C. Chronic ureteral obstruction in the rat suppresses renal tubular Bcl-2 and stimulates apoptosis. *Exp. Nephrol*. 2000;8(2):115-122. DOI 10.1159/000020657.

Dewanjee S., Dua T.K., Khanra R., Das S., Barma S., Joardar S., Bhattacharjee N., Zia-Ul-Haq M., Jaafar H.Z. Water spinach, Ipomoea aquatic (Convolvulaceae), ameliorates lead toxicity by inhibiting oxidative stress and apoptosis. *PLoS One*. 2015;10(10):e0139831. DOI 10.1371/journal.pone.0139831.

Eckert A., Keil U., Kressmann S., Schindowski K., Leutner S., Leutz S., Müller W.E. Effects of EGb 761 *Ginkgo biloba* extract on mitochondrial function and oxidative stress. *Pharmacopsychiatry*. 2003; 36(Suppl.1):S15-S23. DOI 10.1055/c-2003-40449.

Flurkey K., Currer J.M., Harrison D.E. Mouse models in aging research. In: Fox J.G., Barthold S.W., Davisson M.T., Newcomer C.E., Quimby F.W., Smith A.L. (Eds.). The Mouse in Biomedical Research. 2nd Edition. New York: Elsevier, 2006;3:637-672.

Hu J., Srivastava K., Wieland M., Runge A., Mogler C., Besemfelder E., Terhardt D., Vogel M.J., Cao L., Korn C., Bartels S., Thomas M., Augustin H.G. Endothelial cell-derived angiopoietin-2 controls liver regeneration as a spatiotemporal rheostat. *Science*. 2014;343(6169):416-419. DOI 10.1126/science.1244880.

Hutchins N.A., Chung C.S., Borgerding J.N., Ayala C.A., Ayala A. Kupffer cells protect liver sinusoidal endothelial cells from Fas-dependent apoptosis in sepsis by down-regulating gp130. *Am. J. Pathol*. 2013;182(3):742-754. DOI 10.1016/j.ajpath.2012.11.023.

Kolesnikov S.I., Semenyuk A.V., Grachev S.V. Toxicant Action Imprinting in Embryogenesis. Moscow, 1999. (in Russian)

Michurina S.V., Ishchenko I.Yu., Arkhipov S.A., Klimontov V.V., Rachkovskaya L.N., Konenkov V.I., Zavyalov E.L. Effects of melatonin, aluminum oxide, and polymethylsiloxane complex on the expression of LYVE-1 in the liver of mice with obesity and type 2 diabetes mellitus. *Bulletin of Experimental Biology and Medicine*. 2016a;162(2):269-272. DOI 10.1007/s10517-016-3592-y.

Michurina S.V., Ishenko I.J., Klimontov V.V., Archipov S.A., Myakina N.E., Cherepanova M.A., Zavjalov E.L., Koncevaya G.V., Konenkov V.I. Linagliptin alleviated fatty liver disease in diabetic *db/db* mice. *World J. Diabetes*. 2016b;7(19):534-546. DOI 10.4239/wjd.v7.i19.534.

Mushkambarov N.N., Kuznetsov S.L. Molecular Biology. Moscow, 2007. (in Russian)

Paltsev M.A. Molecular medicine and progress in basic sciences. *Vestnik Rossiyskoy Akademii Nauk = Herald of the Russian Academy of Sciences*. 2002;72(1):13-21. (in Russian)

Schuppan D., Schattenberg J.M. Non-alcoholic steatohepatitis: pathogenesis and novel therapeutic approaches. *J. Gastroenterol. Hepatol.* 2013;28(Suppl.1):68-76. DOI 10.1111/jgh.12212.

Shimizu M., Yasuda Y., Sakai H., Kubota M., Terakura D., Baba A., Ohno T., Kochi T., Tsurumi H., Tanaka T., Moriwaki H. Pitavastatin suppresses diethylnitrosamine-induced liver preneoplasms in male C57BL/KsJ-*db/db* obese mice. *BMC Cancer*. 2011;11:281. DOI 10.1186/1471-2407-11-281.

Sun D., Li S., Wu H., Zhang M., Zhang X., Wei L., Qin X., Gao E. Oncostatin M (OSM) protects against cardiac ischaemia/reperfusion injury in diabetic mice by regulating apoptosis, mitochondrial biogenesis and insulin sensitivity. *J. Cell. Mol. Med*. 2015;19(6):1296-1307. DOI 10.1111/jcmm.12501.

Trak-Smayra V., Paradis V., Massart J., Nasser S., Jebara V., Fromenty B. Pathology of the liver in obese and diabetic ob/ob and db/db mice fed a standard or high-calorie diet. *Int. J. Exp. Pathol*. 2011; 92(6):413-421. DOI 10.1111/j.1365-2613.2011.00793.x.

ORCID ID
E.L. Zavjalov orcid.org/0000-0002-9412-3874

Acknowledgements. Animal breeding was supported by budget project No. 0324-2019-0041 and is implemented using equipment of the Center for Genetic Resources of Laboratory Animals at ICG SB RAS, supported by the Ministry of Education and Science of Russia (the unique identifier of the project RFMEFI62117X0015).

Conflict of interest. The authors declare no conflict of interest.

Received September 24, 2019. Revised October 23, 2019. Accepted October 23, 2019. Published online March 24, 2020.

Вавиловский журнал генетики и селекции. 2020;24(4):441-445
DOI 10.18699/VJ20.636

Адаптация сульфофосфованилинового метода анализа общих липидов для различных биологических объектов на примере *Drosophila melanogaster*

М.А. Еремина ✉, Н.Е. Грунтенко

Федеральный исследовательский центр Институт цитологии и генетики Сибирского отделения Российской академии наук, Новосибирск, Россия
✉ e-mail: eremina@bionet.nsc.ru

Аннотация. Липидный обмен имеет решающее значение в физиологии. В последние десятилетия модельный объект *Drosophila melanogaster* активно используется в изучении фундаментальных вопросов метаболизма липидов и его нарушений, включая ожирение, а также в поиске терапевтических целей для лечения метаболических нарушений у человека. Быстрое и точное количественное определение содержания липидов – важный шаг в решении этих задач. Впервые метод количественного измерения общих липидов с использованием сульфофосфованилинового (СФВ) метода был описан Цольнером с коллегами в 1962 г., а адаптирован для насекомых Ван Генделем на самках желтолихорадочного комара *Aedes aegypti*. Преимущество этого метода по сравнению с традиционными гравиметрическим и хроматографическим методами анализа заключается в том, что он позволяет обходиться минимальным количеством биологического материала, не требует сложных манипуляций с образцом, является высокочувствительным, воспроизводимым и простым в реализации с минимальным набором оборудования. В настоящей работе описана модификация протокола Ван Генделя, позволяющая осуществлять адаптацию метода количественного определения общих липидов для различных организмов, на примере классической биологической модели *D. melanogaster*. В представленном протоколе адаптированы время реакции, объемы химических растворов и реагентов для проведения анализа образцов индивидуальных дрозофил. Данная работа является актуальной, так как описывает универсальную схему, согласно которой СФВ метод может быть адаптирован для количественного анализа содержания общих липидов у широкого спектра биологических объектов. Для проверки результативности модифицированного метода мы измерили содержание общих липидов у самок *D. melanogaster*, несущих гипоморфные мутации генов инсулинового сигнального каскада *dilp6* и *dfoxo*, по сравнению с линией дикого типа Canton-S и показали участие *dilp6*, но не *dfoxo* в регуляции жирового обмена. Полученные результаты подчеркивают эффективность колориметрического метода с использованием СФВ реакции и спектрофотометрии для количественного анализа содержания общих липидов.
Ключевые слова: *Drosophila melanogaster*; сульфофосфованилиновый метод; колориметрия; спектрофотометрия; общие липиды; жировой обмен; мутации $dilp^{641}$ и $dfoxo^{BG01018}$.

Для цитирования: Еремина М.А., Грунтенко Н.Е. Адаптация сульфофосфованилинового метода анализа общих липидов для различных биологических объектов на примере *Drosophila melanogaster*. *Вавиловский журнал генетики и селекции*. 2020;24(4):441-445. DOI 10.18699/VJ20.636

Adaptation of the sulfophosphovanillin method of analysis of total lipids for various biological objects as exemplified by *Drosophila melanogaster*

M.A. Eremina ✉, N.E. Gruntenko

Institute of Cytology and Genetics of Siberian Branch of the Russian Academy of Sciences, Novosibirsk, Russia
✉ e-mail: eremina@bionet.nsc.ru

Abstract. Lipid metabolism is crucial in physiology. In recent decades the model object *Drosophila melanogaster* has been actively used in the study of the fundamental issues of lipid metabolism and its disorders, including obesity, as well as in the search for therapeutic goals for the treatment of metabolic disorders in humans. Quick and accurate quantification of lipid content is an important step in solving these problems. For the first time the method of quantitative measurement of total lipids with the use of the sulfophosphovanillin (SPV) method was described by Zöllner and colleagues in 1962, and adapted for insects by Van Handel on females of the yellow fever mosquito *Aedes aegypti*. The advantages of this method compared to traditional gravimetric and chromatographic methods of analysis are the use of a small amount of biological material, lack of need for complex manipulations with the sample, its high sensitivity, reproducibility and simplicity of implementation with a minimum set of equipment. Here, a modification of the Van Handel protocol is described, which allows the method to be adapted for quantitative determination of total lipids for various organisms as exemplified a widely used model, *D. melanogaster*. To test the effectiveness of the modified

method, we measured the content of total lipids in *D. melanogaster* females carrying hypomorphic mutations of the *dilp6* and *dfoxo* insulin signaling pathway genes compared to the wild-type Canton-S line, and showed that *dilp6* took part in the regulation of fat metabolism, while *dfoxo* did not. The results obtained emphasize the effectiveness of the colorimetric method with the use of SPV reaction and spectrophotometry for the quantitative analysis of total lipids.
Key words: *Drosophila melanogaster*; sulfophosphovanillin method; colorimetry; spectrophotometry; total lipids; lipid metabolism; mutations $dilp^{641}$ and $dfoxo^{BG01018}$.

For citation: Eremina M.A., Gruntenko N.E. Adaptation of the sulfophosphovanillin method of analysis of total lipids for various biological objects as exemplified by *Drosophila melanogaster*. *Vavilovskii Zhurnal Genetiki i Selektsii = Vavilov Journal of Genetics and Breeding*. 2020;24(4):441-445. DOI 10.18699/VJ20.636 (in Russian)

Введение

Липидный обмен имеет решающее значение для выживания и размножения организмов, поскольку липиды формируют энергетический резерв организма и являются важными структурными компонентами клеточных мембран и сигнальными молекулами (Trinh, Boulianne, 2013). Для изучения механизмов регуляции метаболического обмена и его нарушений, включая ожирение, а также в поиске терапевтических целей для лечения метаболических нарушений у человека часто проводят исследования на различных животных моделях, от нематоды и дрозофилы до грызунов и приматов (Kleinert et al., 2018). *Drosophila melanogaster* подходит для моделирования метаболических заболеваний человека, поскольку, во-первых, большая часть генов и семейств генов, связанных с регуляцией углеводно-жирового метаболического пути, эволюционно консервативны у дрозофилы и человека; а во-вторых, дрозофила имеет менее сложный геном и меньшую избыточность генов, чем позвоночные, что дает значительные преимущества в изучении функций генов *in vivo* и определении новых компонентов пути (Liu, Huang, 2013; Álvarez-Rendón et al., 2018).

Консервативность распространяется и на функциональный уровень: жировое тело насекомого (аналог печени и белой жировой ткани млекопитающих) участвует в поглощении, запасании и обмене питательных веществ (Liu, Huang, 2013; Musselman, Kuhnlein, 2018). Содержание жира в организме мух может варьировать в широких пределах и служить чувствительным диагностическим критерием, указывающим на дисбаланс в метаболизме липидов (Hildebrandt et al., 2011). Быстрое и точное количественное определение уровня липидов очень важно при проведении исследований в этой сфере. К традиционным методам количественного определения липидов, как правило, относят гравиметрический или хроматографический методы анализа, недостатками которых считают сложность проведения, трудоемкость, использование большого количества исходного материала, что затрудняет выполнение небольших по объему анализируемого материала экспериментов (Anschau et al., 2017; Patel et al., 2019).

Ряд исследований доказывает, что колориметрический метод на основе сульфофосфованилиновой (СФВ) реакции является универсальным: применяется для определения содержания общих липидов и в спинномозговой жидкости, и в сыворотке и плазме крови человека, и в пищевых продуктах и экологических образцах (Park et al., 2016). Метод анализа общих липидов у насекомых впервые описан Ван Генделем (Van Handel, 1985) для самок желтолихорадочного комара *Aedes aegypti*. В настоящее время данный колориметрический метод используется для ряда других видов насекомых, в число которых входят сверчки *Gryllus bimaculatus* (Fukumura et al., 2018) и 15 представителей семейства жесткокрылых (Bozdoğan et al., 2016), а также модифицирован для эндопаразитоидов *Venturia canescens* (Foray et al., 2012), клещей *Ixodes ricinus* (Abdullah et al., 2018), рыб (Lu et al., 2008), простейших (Park et al., 2016) и хемолитотрофных микроорганизмов (Anschau et al., 2017). Стоит подчеркнуть, что метод, предложенный еще в 1962 г. (Zöllner et al., 1962; цит. по: Ростовцев, Резник, 1982), и сегодня не потерял актуальности и приобрел ряд модификаций, отвечающих современным целям и разнообразию объектов исследований.

Преимущество этого простейшего метода заключается в возможности анализа образцов малых объемов и в быстром количественном измерении содержания общих липидов (Park et al., 2016) с использованием минимального набора оборудования. Принцип метода основан на том, что СФВ реакция требует двойной связи углерод–углерод или свободных гидроксильных групп в липидных компонентах; концентрированная серная кислота вступает в реакцию с ненасыщенными липидами с образованием карбониевого аниона; фосфорная кислота вступает в реакцию с ванилином с образованием фосфатного эфира, приводя к увеличению реакционной способности карбонильной группы; карбониевый анион вступает в реакцию с карбонильной группой фосфованилина с образованием стабильного окрашенного комплекса (Knight et al., 1972). Интенсивность окрашивания может быть количественно определена путем измерения поглощения при 525–530 нм с использованием спектрофотометрических методов (Park et al., 2016).

Хотя колориметрический метод на примере количественного анализа содержания нейтральных липидов триглицеридов (90 % от всех липидов) был подвержен критике (Al-Anzi, Zinn, 2010), он показывает сходные результаты как с тонкослойной хроматографией, так и с колориметрическим анализом (Cheng et al., 2011; Tennessen et al., 2014; Byreddy et al., 2016).

Таким образом, возможность адаптировать этот простой и эффективный метод анализа для различных видов животных представляет несомненный интерес. В настоящей работе мы предлагаем протокол адаптации СФВ метода для количественной оценки содержания общих липидов у индивидуальных мух *D. melanogaster* и результаты применения этого метода при изучении содержания липидов у двух линий с мутациями генов инсулинового каскада. Для проверки эффективности метода мы исследовали содержание общих липидов у мух, несущих гипоморфные мутации генов инсулиноподобного пептида DILP6 ($dilp6^{41}$) и транскрипционного фактора dFOXO ($foxo^{BG01018}$). Мы

полагаем, что проведенное исследование позволит оценить участие данных генов в липидном обмене.

Материалы и методы

Реагенты

- Хлороформ (99.1 %) ХЧ (АО «База № 1 Химреактивов», Россия);
- метанол (99.5 %) ХЧ (ЗАО «Вектон», Россия);
- серная кислота (93.5–95.6 %) ОСЧ (ЗАО «Союзхимпром», Россия);
- ортофосфорная кислота (85 %) ОСЧ (ЗАО «Союзхимпром», Россия);
- ванилин кристаллический (ГОСТ 16599-71);
- рафинированное подсолнечное масло (ГОСТ 1129-2013).

Экспериментальные животные. Мухи содержались на стандартной питательной среде (агар-агар, 7 г/л; кукурузная мука, 50 г/л; сухие дрожжи, 18 г/л; сахар, 40 г/л) в инкубаторе (Sanyo, Япония) при температуре 25 °C, относительной влажности 50 %, 12-часовом световом дне. Для экспериментов имаго синхронизировали по вылету (мухи собирались в течение 3–4 ч). В работе были использованы три линии *D. melanogaster*: линия $dilp6^{41}$ с делецией 3′-области гена *phl*, 5′-области гена *dilp6*, захватывающей первый экзон и часть первого интрона (Rauschenbach et al., 2016); линия $foxo^{BG01018}$, несущая встройку P-элемента [GT1] в 5′-области гена *dfoxo*, приводящую к частичной потере функции гена (Dionne et al., 2006); и линия дикого типа Canton-S. Все линии получены из Bloomington Drosophila Stock Center.

Подготовка и хранение образцов. Для предотвращения ферментативной деградации липидов Ван Гендель рекомендует хранить насекомых при температуре –20 °C или ниже либо высушивать их при 90 °C для остановки ферментативной активности (Van Handel, 1985). Описана также возможность хранить насекомых в 70–95 % этаноле; при этом для предотвращения ферментативной деградации при хранении выше –20 °C рекомендуется измельчать насекомое (Lee, 2019). В настоящей работе мух замораживали в жидком азоте (–195.75 °C) и хранили при –80 °C. Во избежание влияния глазного пигмента на результаты измерений перед анализом мух декапитировали. В оригинальном методе (Van Handel, 1985) у самок рекомендуется удалять яичники либо не использовать в опытах оплодотворенных самок, так как липиды в яичниках запасаются для последующего развития потомства и не имеют установленной питательной ценности для мух. Но поскольку у дрозофил не представляется возможным извлечь яичники, не повредив при этом саму муху, в нашей работе мы постарались решить этот вопрос использованием для анализа неоплодотворенных самок. Также следует отметить, что количественное измерение общих липидов СФВ методом у мух с яичниками не препятствует обнаружению различий между линиями.

Колориметрический метод количественной оценки содержания общих липидов с использованием сульфофосфованилиновой реакции. Для получения фосфованилинового реагента к 120 мг ванилина добавляли 20 мл горячей воды и размешивали до полного растворения ванилина. Далее добавляли 80 мл H_3PO_4 до конечной концентрации 1.2 мг/мл.

Липидные стандарты, например триолеин (92860; Sigma), можно приобрести у поставщика химических веществ и разводить до нужной концентрации (Foray et al., 2012), однако в работе (Byreddy et al., 2016) указано, что триолеин дает слишком сильное окрашивание и не подходит в качестве стандарта. В качестве липидного стандарта исследователи в основном используют растительные масла (Van Handel, 1985; Park et al., 2016; Anschau et al., 2017). Известное количество стандарта вступает в реакцию с реагентами для получения калибровочной линии, линейные регрессии часто имеют значение R^2 0.95 или выше. В настоящей работе в качестве липидного стандарта использовали 0.1 % раствор рафинированного подсолнечного масла (ГОСТ 1129-2013) (0.919 кг/м^3). Для приготовления стандарта 10 мг масла растворяли в хлороформе до конечной концентрации 1 мг/мл.

Измерение концентрации общих липидов проводили посредством модифицированного для дрозофилы метода Ван Генделя (Van Handel, 1985). В связи с отличиями дрозофилы от комара *Ae. aegypti*, для которого разрабатывал свой метод Ван Гендель, в нашем протоколе были модифицированы время реакции, объемы химических растворов и реагентов для проведения анализа образцов индивидуальных дрозофил. Индивидуальную муху гомогенизировали в 100 мкл охлажденной смеси хлороформ-метанола (V/V), после чего образцы интенсивно встряхивали в течение 10 мин, далее 50 мкл супернантанта переносили в чистые пробирки и нагревали в микротермостате М-208 («Бис-Н», Россия) при 90 °C до полного испарения растворителя, добавляли 10 мкл H_2SO_4 и нагревали образцы при той же температуре 2 мин. Затем образцы охлаждали на льду и добавляли фосфованилиновый реагент до общего объема 1 мл. Инкубировали 15 мин при комнатной температуре в темноте до проявления розового окрашивания, стабильно сохранявшегося в течение 1 ч. Анализировали образцы в спектрофотометре Smart Spec Plus (Bio-Rad, США) при длине волны 525 нм против «холостого» образца, содержащего только фосфованилиновый реагент.

Для построения калибровочной линии Форей с коллегами (Foray et al., 2012) рекомендуют начинать с концентрации ниже ожидаемой в образце насекомого и заканчивать концентрацией выше ожидаемой. Калибровочную линию получали с использованием девяти разведений: 0, 1, 5, 10, 20, 40, 60, 80 и 100 мкг липидного стандарта в трех повторах. Далее процедуру выполняли согласно вышеописанному протоколу.

Статистический анализ. Расчет результатов проводили на основании данных калибровочной линии. Достоверность результатов оценивали с помощью *t*-критерия Стьюдента.

Результаты и обсуждение

Построение градуировочной кривой для определения содержания общих липидов у *D. melanogaster*

Посредством спектрофотометрического поглощения известных концентраций рафинированного подсолнечного масла при 525 нм получена градуировочная кривая (рис. 1). Установлена линейная регрессия: $y = 0.0023x + 0.0369$; $R^2 = 0.9971$.

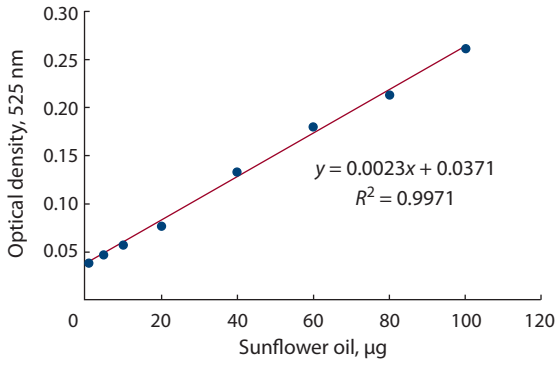

Fig. 1. Calibration line of the product of the sulfophosphovanillin reaction with sunflower oil dissolved in chloroform to the concentration 1 mg/ml.

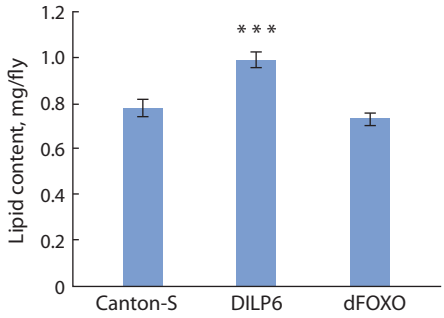

Fig. 2. The level of total lipids in 3-day-old *D. melanogaster* females of the wild-type line Canton-S and lines carrying hypomorphic mutations in the genes for insulin-like peptide DILP6 and transcription factor dFOXO.

Each value is an average of 16–20 measurements. Means ± SE are indicated. *** $p < 0.001$ – the significance of differences between mutant females with the mutation in the insulin-like peptide DILP6 gene ($dilp6^{41}$) and females of the Canton-S line.

Анализ образцов с известной концентрацией липидного стандарта показал, что метод является чувствительным и способен точно определять уровень общих липидов в диапазоне от 0 до 100 мкг.

Определение содержания общих липидов у самок *D. melanogaster* с гипоморфными мутациями генов инсулинового каскада *dilp6* и *dfoxo*

Известно, что инсулиновый сигнальный каскад дрозофилы включает шесть гомологов инсулина и инсулиноподобных факторов роста млекопитающих (DILPs1–6), которые связываются с единственным инсулиноподобным рецептором дрозофилы (dInR), активирующим инсулиновый каскад (Gruntenko, Rauschenbach, 2018), и два гомолога релаксина (DILPs7, 8) (Gontijo, Garelli, 2018). Стимуляция dInR через субстрат инсулиноподобного рецептора (CHICO, гомолог IRS1–4 млекопитающих) приводит к активации dAkt/PKB (гомолог протеинкиназы B), которая модулирует активность ряда белков, в частности транскрипционного фактора семейства Forkhead box class O, dFOXO (гомолог FOXO1, 3a и 4 у млекопитающих) (Álvarez-Rendón et al., 2018).

Ранее методом ПЦР в реальном времени было установлено двукратное снижение уровня экспрессии гена *dfoxo* (Gruntenko et al., 2016) и снижение в 13 раз уровня экспрессии гена *dilp6* (Еремина и др., 2019) в жировом теле (основном месте синтеза dFOXO и DILP6) у самок линий с мутацией $dilp6^{41}$ и $foxo^{BG01018}$ соответственно, по сравнению с уровнем экспрессии этих генов в жировом теле у самок линии дикого типа Canton-S. Кроме того, мы обнаружили, что уровень глюкозы и трегалозы – основного сахара насекомых, у самок обеих мутантных линий повышен по сравнению с контрольной линией Canton-S (Еремина и др., 2019). На основании этих данных мы предположили возможность участия генов *dilp6* и *dfoxo* в регуляции уровня жиров у дрозофилы. Для проверки этой гипотезы мы сравнили содержание общих липидов у самок *D. melanogaster* с мутациями $dilp6^{41}$ и $foxo^{BG01018}$, а также у самок контрольной линии Canton-S с помощью СФВ метода. Результаты проведенных измерений представлены на рис. 2. Очевидно, что у мутантных самок линии $dilp6^{41}$ уровень общих липидов повышен по сравнению с самками дикого типа (различия достоверны при $p < 0.001$), однако уровень общих липидов у самок линии $foxo^{BG01018}$ не отличается от такового у самок дикого типа Canton-S.

В статье (Murillo-Maldonado et al., 2011) говорится об увеличении содержания общих липидов у линий с частичной потерей функции генов инсулинового каскада *PKB*, *dInR* и *chico*. Кроме того, авторы определили содержание углеводов у этих линий и продемонстрировали , что лишь у небольшого числа линий наблюдались значительные изменения. Так, гетероаллельная комбинация $InR^{3T5/E19}$ приводила к значительному увеличению содержания углеводов, тогда как для $PKB^{1/3}$ и $chico^{1/1}$ существенных изменений не наблюдалось. Ранее нами было выявлено участие генов *dilp6* и *dfoxo* в регуляции углеводного обмена, сопровождающееся повышением уровня глюкозы и трегалозы у гипоморфных мутантов $dilp6^{41}$ и $foxo^{BG01018}$ (Еремина и др., 2019). Однако оставалось невыясненным, участвуют ли эти гены в регуляции липидного обмена. В настоящей работе с помощью быстрого метода с использованием сульфофосфованилиновой реакции мы показали, что в регуляции липидного обмена принимает участие *dilp6*, но не *dfoxo*. Наши результаты согласуются с результатами Мурилло-Мальдонадо с коллегами (Murillo-Maldonado et al., 2011) и свидетельствуют о том, что гены инсулинового сигнального каскада могут влиять либо только на углеводный обмен, как в случае *dfoxo*, либо только на липидный обмен, как в случае *PKB* и *chico,* либо и на углеводный, и на липидный, как в случае *dilp6* и *dInR*. Возможные механизмы этого влияния требуют дальнейшего изучения.

Заключение

Полученные данные демонстрируют высокую эффективность и чувствительность колориметрического метода с использованием сульфофосфованилиновой реакции для определения уровня общих липидов, в том числе в низких концентрациях. Проведенный анализ содержания общих липидов у самок *D. melanogaster* с гипоморфными мутациями генов инсулинового каскада это подтверждает, демонстрируя участие гена *dilp6*, но не *dfoxo* в регуляции жирового обмена. Таким образом, предложенный нами

протокол модификации колориметрического метода анализа содержания общих липидов с использованием спектрофотометрии может быть успешно применен при изучении механизмов жирового обмена у широкого спектра биологических объектов.

Список литературы / References

Еремина М.А., Карпова Е.К., Раушенбах И.Ю., Пирожкова Д.С., Андреенкова О.В., Грунтенко Н.Е. Влияние мутаций генов инсулинового сигнального каскада на изменение уровня углеводов у самок *Drosophila melanogaster* при тепловом стрессе. *Генетика*. 2019;55(4):485-488. DOI 10.1134/S0016675819030068.
[Eremina M.A., Karpova E.K., Rauschenbach I.Yu., Pirozhkova D.S., Andreenkova O.V., Gruntenko N.E. Mutations in the insulin signaling pathway genes affect carbohydrate level under heat stress in *Drosophila melanogaster* females. *Russ. J. Genet.* 2019;55(4):519-521. DOI 10.1134/S1022795419030050.]

Ростовцев В.Р., Резник Г.Е. Количественное определение липидных фракций в крови. *Лаб. дело*. 1982;4:26-29.
[Rostovtsev V.N., Reznik G.E. Quantification of lipid fractions in blood. *Laboratornoe Delo = Laboratory Science.* 1982;4:26-29. (in Russian)]

Abdullah S., Davies S., Wall R. Spectrophotometric analysis of lipid used to examine the phenology of the tick *Ixodes ricinus*. *Parasit Vectors*. 2018;11:523. DOI 10.1186/s130-71-018-3102-3.

Al-Anzi B., Zinn K. Colorimetric measurement of triglycerides cannot provide an accurate measure of stored fat content in *Drosophila. PLoS One.* 2010;5(8):e12353. DOI 10.1371/journal.pone.0012353.

Álvarez-Rendón J.P., Salceda R., Riesgo-Escovar J.R. *Drosophila melanogaster* as a model for diabetes type 2 progression. *BioMed. Res. Int.* 2018;2018:1417528. DOI 10.1155/2018/1417528.

Anschau A., Caruso C.S., Kuhn R.C., Franco T.T. Validation of the sulfo-phospho-vanillin (spv) method for the determination of lipid content in oleaginous microorganisms. *Braz. J. Chem. Eng.* 2017;34(1):19-27. DOI 10.1590/0104-6632.20170341s20140222.

Bozdoğan H., Erbey M., Aksoy H.A. Total amount of protein, lipid and carbohydrate of some adult species belong to curculionidae family (Coleoptera: Curculionidae). *J. Entomol. Zool. Stud.* 2016;4(5):242-248.

Byreddy A.R., Gupta A., Barrow C.J., Puri M. A quick colorimetric method for total lipid quantification in microalgae. *J. Microbiol. Meth.* 2016;125:28-32.

Cheng Y.S., Zheng Y., VanderGheynst J.S. Rapid quantitative analysis of lipids using a colorimetric method in a microplate format. *Lipids.* 2011;46(1):95-103. DOI 10.1007/s11745-010-3494-0.

Dionne M.S., Pham L.N., Shirasu-Hiza M., Schneider D.S. Akt and FOXO dysregulation contribute to infection-induced wasting in *Drosophila*. *Curr. Biol.* 2006;16:1977-1985.

Foray V., Pelisson P.-F., Venner M.C.B., Desouhant E., Venner S., Menu F., Giron D., Rey B. A handbook for uncovering the complete energetic budget in insects: the van Handel's method (1985) revisited. *Physiol. Entomol.* 2012;37:295-302. DOI 10.1111/j.1365-3032.2012.00831.x.

Fukumura K., Konuma T., Tsukamoto Y., Nagata S. Adipokinetic hormone signaling determines dietary fatty acid preference through maintenance of hemolymph fatty acid composition in the cricket *Gryllus bimaculatus*. *Sci. Rep.* 2018;8:4737. DOI 10.1038/s41598-018-22987-2.

Gontijo A.M., Garelli A. The biology and evolution of the Dilp8-Lgr3 pathway: a relaxin-like pathway coupling tissue growth and developmental timing control. *Mech. Dev*. 2018;154:44-50. DOI 10.1016/j.mod.2018.04.005.

Gruntenko N.E., Adonyeva N.V., Burdina E.V., Karpova E.K., Andreenkova O.V., Gladkikh D.V., Ilinsky Y.Y., Rauschenbach I.Yu. The impact of FOXO on dopamine and octopamine metabolism in *Drosophila* under normal and heat stress conditions. *Biol. Open.* 2016;5:1706-1711. DOI 10.1242/bio.022038.

Gruntenko N.E., Rauschenbach I.Y. The role of insulin signalling in the endocrine stress response in *Drosophila melanogaster*: a minireview. *Gen. Comp. Endocrinol*. 2018;258:134-139. DOI 10.1016/j.ygcen.2017.05.019.

Hildebrandt A., Bickmeyer I., Kühnlein R.P. Reliable *Drosophila* body fat quantification by a coupled colorimetric assay. *PLoS One.* 2011;6(9):e23796. DOI 10.1371/journal.pone.0023796.

Kleinert M., Clemmensen C., Hofmann S.M., Moore M.C., Renner S., Woods S.C., Huypens P., Beckers J., de Angelis M.H., Schürmann A., Bakhti M., Klingenspor M., Heiman M., Cherrington A.D., Ristow M., Lickert H., Wolf E., Havel P.J., Müller T.D., Tschöp M.H. Animal models of obesity and diabetes mellitus. *Nat. Rev. Endocrinol.* 2018;14(3):140-162. DOI 10.1038/nrendo.2017.161.

Knight J.A., Anderson S., Rawle J.M. Chemical basis of the sulfo-phospho-vanillin reaction for estimating total serum lipids. *Clin. Chem.* 1972;18(3):199-202.

Lee C.L. What we can learn from the energetic levels of insects: a guide and review. *Ann. Entomol. Soc. Am.* 2019;112(3):220-226. DOI 10.1093/aesa/say051.

Liu Z., Huang X. Lipid metabolism in *Drosophila*: development and disease. *Acta Biochim. Biophys. Sin. (Shanghai)*. 2013;45(1):44-50. DOI 10.1093/abbs/gms105.

Lu Y., Ludsin S.A., Fanslow D.L., Pothoven S.A. Comparison of three microquantity techniques for measuring total lipids in fish. *Can. J. Fish. Aquat. Sci.* 2008;65:2233-2241. DOI 10.1139/F08-135.

Murillo-Maldonado J.M., Sánchez-Chávez G., Salgado L.M., Salceda R., Riesgo-Escovar J.R. *Drosophila* insulin pathway mutants affect visual physiology and brain function besides growth, lipid, and carbohydrate metabolism. *Diabetes.* 2011;60(5):1632-1636. DOI 10.2337/db10-1288.

Musselman L.P., Kühnlein R.P. *Drosophila* as a model to study obesity and metabolic disease. *J. Exp. Biol.* 2018;221(Suppl.1):jeb163881. DOI 10.1242/jeb.163881.

Park J., Jeong H.J., Yoon E.Y., Moon S.J. Easy and rapid quantification of lipid contents of marine dinoflagellates using the sulpho-phospho-vanillin method. *Algae.* 2016;31(4):391-401. DOI 10.4490/algae.2016.31.12.7.

Patel A., Antonopoulou I., Enman J., Rova U., Christakopoulos P., Matsakas L. Lipids detection and quantification in oleaginous microorganisms: an overview of the current state of the art. *BMC Chem. Eng.* 2019;1:13. DOI 10.1186/s42480-019-0013-9.

Rauschenbach I.Yu., Karpova E.K., Burdina E.V., Adonyeva N.V., Bykov R.A., Ilinsky Y.Y., Menshanov P.N., Gruntenko N.E. Insulin-like peptide DILP6 regulates juvenile hormone and dopamine metabolism in *Drosophila* females. *Gen. Comp. Endocrinol.* 2016;243:1-9. DOI 10.1016/j.ygcen.2016.11.004 0016-6480.

Tennessen J.M., Barry W.E., Cox J., Thummel C.S. Methods for studying metabolism in *Drosophila*. *Methods*. 2014;68(1):105-115. DOI 10.1016/j.ymeth.2014.02.034.

Trinh I., Boulianne G.L. Modeling obesity and its associated disorders in *Drosophila*. *Physiology.* 2013;28:117-124. DOI 10.1152/physiol.00025.2012.

Van Handel E. Rapid determination of total lipids in mosquitoes. *J. Am. Mosq. Control Assoc.* 1985;1:302-304.

ORCID ID
M.A. Eremina orcid.org/0000-0001-6136-6928
N.E. Gruntenko orcid.org/0000-0003-3272-1518

Acknowledgements. This work was supported by State Budgeted Project 0324-2019-0041 and the Russian Foundation for Basic Research, project 20-04-00579.

Conflict of interest. The authors declare no conflict of interest.

Received April 08, 2020. Revised May 22, 2020. Accepted May 22, 2020.

Прием статей через электронную редакцию на сайте http://vavilov.elpub.ru/index.php/jour
Предварительно нужно зарегистрироваться как автору, затем в правом верхнем углу страницы выбрать «Отправить рукопись». После завершения загрузки материалов обязательно выбрать опцию «Отправить письмо», в этом случае редакция автоматически будет уведомлена о получении новой рукописи.

«Вавиловский журнал генетики и селекции»/"Vavilov Journal of Genetics and Breeding"
до 2011 г. выходил под названием «Информационный вестник ВОГиС»/
"The Herald of Vavilov Society for Geneticists and Breeding Scientists".

Регистрационное свидетельство ПИ № ФС77-45870 выдано Федеральной службой по надзору в сфере связи, информационных технологий и массовых коммуникаций 20 июля 2011 г.

«Вавиловский журнал генетики и селекции» включен ВАК Минобрнауки России в Перечень рецензируемых научных изданий, в которых должны быть опубликованы основные результаты диссертаций на соискание ученой степени кандидата наук, на соискание ученой степени доктора наук, Российский индекс научного цитирования, ВИНИТИ, базы данных Emerging Sources Citation Index (Web of Science), Zoological Record (Web of Science), Scopus, Ebsco, DOAJ, Ulrich's Periodicals Directory, Google Scholar, Russian Science Citation Index на платформе Web of Science, каталог научных ресурсов открытого доступа ROAD.

Открытый доступ к полным текстам:
на сайте ИЦиГ СО РАН – bionet.nsc.ru/vogis/
платформе Elpub – vavilov.elpub.ru/index.php/jour
платформе Научной электронной библиотеки – elibrary.ru/title_about.asp?id=32440

Подписку на «Вавиловский журнал генетики и селекции» можно оформить в любом почтовом отделении России. Индекс издания 42153 по каталогу «Пресса России».

✉ e-mail: vavilov_journal@bionet.nsc.ru

Издатель: Федеральное государственное бюджетное научное учреждение
«Федеральный исследовательский центр Институт цитологии и генетики
Сибирского отделения Российской академии наук»,
проспект Академика Лаврентьева, 10, Новосибирск, 630090.
Адрес редакции: проспект Академика Лаврентьева, 10, Новосибирск, 630090.
Секретарь по организационным вопросам С.В. Зубова. Тел.: (383)3634977.
Издание подготовлено информационно-издательским отделом ИЦиГ СО РАН. Тел.: (383)3634963*5218.
Начальник отдела: Т.Ф. Чалкова. Редакторы: В.Д. Ахметова, И.Ю. Ануфриева. Дизайн: А.В. Харкевич.
Компьютерная графика и верстка: Т.Б. Коняхина, О.Н. Савватеева.

Подписано в печать 20.06.2020. Выход в свет 30.06.2020. Формат 60 × 84 $^1/_8$. Усл. печ. л. 13.95.
Уч.-изд. л. 16.2. Тираж 150 экз. (1-й завод 1–50 экз.). Заказ № 70. Цена свободная.

Отпечатано в типографии ФГУП «Издательство СО РАН», Морской проспект, 2, Новосибирск, 630090.